Thesis submitted for the degree of

Doctor of Philosophy

at the University of Leicester

by

Angela Tracy Clark

Department of Biochemistry

University of Leicester

January 2003

ProQuest LLC
789 East Eisenhower Parkway
P.O. Box 1346
Ann Arbor, MI 48106-1346

ACKNOWLEDGEMENTS

My biggest thanks go to my supervisor Graham Belsham, at IAH, Pirbright. Without his guidance and encouragement this Ph.D. would have been impossible.

I am also very grateful to Anne Willis, my supervisor from University of Leicester, for her valuable suggestions. Thanks must go to Toru Inoue for being such a pleasure to work with during our collaboration. Thanks too for the HCV IRES constructs kindly provided by Professor Dave Rowlands and Sven Enterlein. I am also grateful to Graham Conn for performing the RNA melting curves.

I appreciate all the help given to me by Pirbright staff during my Ph.D. especially members of Graham's lab and the picornavirus group (past and present).
In particular, to Wen Robertson, Natalie Ross-Smith, Yiannis Stassinopoulos and Louisa Chard for being so helpful.
Big thanks to Kat and Jude for their tremendous support (and silliness!).

A huge shout out to The Pendelians. I've never met a lovelier bunch of people and I've loved living with you guys. Also to the rest of the Durham lot for their support.

Enormous thanks have to go to my family – Mum, Dad, Paul, Chris (and Sasha!) - for always being there for me. Your faith in me means so much.

Angela Clark

Structure and Function Analysis of Picornavirus Internal Ribosome Entry Site Elements

Picornaviruses have a single-stranded, positive-sense RNA genome. An internal ribosome entry site (IRES) situated within the 5' untranslated region of the genome mediates cap-independent translation of the picornavirus RNA. In an attempt to further understand the mechanism of IRES-mediated translation, it was decided to investigate the role of several nucleotides within the encephalomyocarditis virus IRES which are absolutely conserved among all cardiovirus and aphthovirus IRES elements and in close proximity to the binding site of the translation initiation factor, eIF4GI. Four nucleotides within the J domain were randomised to generate a pool of mutant IRES elements containing up to 256 different sequences. Analysis of this pool, using a cell selection system to isolate functional IRES elements, revealed that the four nucleotides were essential for IRES activity. Furthermore it was shown that mutations at these nucleotides severely affected the binding of eIF4GI and eIF4A to the IRES. A clear correlation was seen between the activity of the mutant IRES element and its ability to bind eIF4GI/ eIF4A. This strongly suggests that the binding of eIF4GI to the IRES is functionally relevant *in vivo*.

It was also shown that the IRES elements from several different hepatitis C virus genotypes could be used within the cell selection system. This is particularly useful since the analysis of HCV within cells is currently restricted.

Finally, the role of residue 20 within the swine vesicular disease virus 2A protease was investigated. This residue is known to affect translation of the picornavirus RNA and virus virulence. To analyse the role of residue 20 to the function of 2A, this residue was substituted for each of the 20 amino acids. This revealed that amino acid substitutions were reasonably well tolerated with the exception of proline.

LIST OF CONTENTS

CHAPTER 1 cont...

CHAPTER 1 cont...

CHAPTER 3 cont...

LIST OF FIGURES

LIST OF FIGURES cont....

Chapter 4:

Chapter 5:

LIST OF FIGURES cont....

Chapter 6:

LIST OF TABLES

ABBREVIATIONS

A	adenine
A site of ribosome	amino acyl-tRNA site
ALF	automated laser fluorescence
BiP	immunoglobulin heavy-chain binding protein
BSA	bovine serum albumin
C	cytosine
C-terminus	Carboxy-terminus
CaMV	cauliflower mosaic virus
CAT	chloramphenicol acetyl transferase
CB4	coxsackievirus B4
CrPV	cricket paralysis virus
DMEM	Dulbecco's Modified Eagles media
DNA	deoxyribonucleic acid
eEF	eukaryotic elongation factor
eIF	eukaryotic initiation factor
EMCV	encephalomyocarditis virus
eRF	eukaryotic release factor
FCS	foetal calf serum
FMDV	foot-and-mouth disease virus
G	guanine
GDP	guanosine diphosphate
GTP	guanosine triphosphate
GUS	B-glucuronidase

HAV	hepatitis A virus
HCV	hepatitis C virus
HOOK	(cistron or protein) modified single chain antibody containing a transmembrane domain, a membrane signal, a haemagglutinin (HA) epitope and a c-myc epitope
HRV	human rhinovirus
IGR	intergenic region
Ig	immunoglobulin
IRES	internal ribosome entry site
LB	Luria-Bertani media
L protein	leader protein
LUC	luciferase
Met	methionine
MPC	magnetic particle concentrator
N-terminus	amino-terminus
nt	nucleotide/s
ORF	open reading frame
P site of ribosome	peptidyl-tRNA site
PABP	poly(A) binding protein
PCBP	poly(C) binding protein
PCR	polymerase chain reaction
PKR	double-stranded-RNA-dependent protein kinase
PSIV	*Plautia stali* intestinal virus
PTB	polypyrimidine tract binding protein
PV	poliovirus

RhPV	*Rhopalosiphum padi* virus
RNA	ribonucleic acid
rpm	revolutions per minute
RRF	ribosome recycling factor
rrl	rabbit reticulocyte lysate
RT	reverse transcriptase
RXB	GUS/ HOOK vector with short linker sequence between the 2 cistrons
SCE	selected cell extract
SDS-PAGE	sodium dodecyl sulphate –polyacrylamide gel electrophoresis
SVDV	swine vesicular disease virus
[J1	infectious cDNA of a virulent strain of SVDV
00	infectious cDNA of an avirulent strain of SVDV]
TCE	total cell extract
T	thymine
TMEV	Theiler's murine encephalomyelitis virus
TNT	coupled transcription/ translation *in vitro* reaction
U	uracil
unr	Upstream of ras
uORF	upstream open reading frame
UTR	untranslated region
UV	ultra violet
wt	wild-type
4E-BP	eIF4E-binding protein

CHAPTER 1

Introduction

1.1 Picornaviruses

The *Picornaviridae* family of viruses contains many well known disease-causing agents of both humans and animals. For example, foot-and-mouth disease virus (FMDV) causes one of the most economically important diseases of livestock as was highlighted in the recent British outbreak. Many picornaviruses are relevant to human health such as poliovirus (PV) and rhinoviruses which cause poliomyelitis and the common cold, respectively. There are currently nine genera within the family and these are listed in Table 1. The viruses are non-enveloped, small icosahedral particles and have a single-stranded, positive sense RNA genome of approximately 8000 nucleotides. The genome contains a single open reading frame (ORF) which encodes a polyprotein that is proteolytically cleaved by virus-encoded proteases to produce the mature viral proteins. The RNA genome also contains a 5' and 3' untranslated region (UTR) plus a poly(A) tail. In the majority of the genera, the 5'UTR has been shown to contain an internal ribosome entry site (IRES). As detailed below, this element allows the viral RNA to be translated cap-independently (for a review see Belsham & Jackson, 2000). This is essential since, unlike eukaryotic mRNAs, the viral RNA does not possess a cap-structure at the 5' end. The 3'UTR has been suggested to be involved in viral replication (Spector & Baltimore, 1974; Sarnow *et al.*, 1986; Sarnow, 1989a; Rohll *et al.*, 1995). In addition, both the poly(A) tail and the 3'UTR have both been shown to stimulate translation of

Genus	Representative species
Aphthovirus	Foot-and-mouth disease virus (FMDV)
	Equine rhinitis A virus (ERAV)
Cardiovirus	Encephalomyocarditis virus (EMCV)
	Theiler's murine encephalomyelitis virus (TMEV)
Enterovirus	Poliovirus (PV)
	Coxsackievirus
	Swine vesicular disease virus (SVDV)
Hepatovirus	Human hepatitis A virus (HAV)
Parechovirus	Human parechovirus 1 (HpeV1)
Rhinovirus	Human rhinovirus (common cold)
Teschovirus	Porcine teschovirus-1 Talfan (PTV-1)
Kobuvirus	Aichi virus
Erbovirus	Equine rhinitis B virus

Table 1: The genera of the *Picornaviridae* family

the viral RNA (Bergamini *et al.*, 2000; Lopez de Quinto *et al.*, 2002).

1.1.1 Infectious Cycle

The infectious cycle of picornaviruses is composed of several stages which are described in detail below. The first of these is the interaction of the virion with one or more cellular receptors on the cell surface to mediate cell entry. Subsequently the RNA genome is uncoated and passes through a membrane into the cytoplasm. The viral RNA is translated to produce the viral proteins required for replication and encapsidation. RNA replication then takes place to produce progeny RNA molecules. The processes of RNA translation and replication cannot occur simultaneously on the same RNA molecule and therefore some event must occur to trigger the switch from translation to replication. Both processes occur entirely within the cytoplasm. After synthesis of huge amounts of genomic RNA, encapsidation takes place to produce progeny virions which are then released from the cell.

1.1.1a Cell Entry

The virions of picornaviruses are icosahedral and very small, approximately 30nm in diameter. High resolution structures of the virions have been determined for several genera (e.g. Hogle *et al.*, 1985; Rossmann *et al.*, 1985; Luo *et al.*, 1987; Acharya *et al.*, 1989). There are four structural proteins 1A, 1B, 1C and 1D (also known as VP4, VP2, VP3 and VP1, respectively) present in the capsid. Sixty copies of these four proteins make up one capsid with the carboxy termini of 1B, 1C and 1D exposed on the outer surface. Protein 1A and the amino termini of 1B, 1C and 1D

(which form an extensive network) are internal. The majority of rhinoviruses and enteroviruses bind to cellular receptors which belong to the immunoglobin superfamily (e.g. ICAM-1, the coxsackie-adenovirus receptor and the poliovirus receptor) (Greve *et al.*, 1989; Mendelsohn *et al.*, 1989; Staunton *et al.*, 1989; Bergelson *et al.*, 1997). The binding site lies within a depression called the "canyon" which lies at the 5-fold axis of symmetry. Binding to the canyon makes the virus unstable and subsequently triggers uncoating (Oliveira *et al.*, 1993). This allows viral RNA to be externalised and enter the cell. Sometimes a co-receptor is required for virus entry into cells (for example, Shafren *et al.*, 1997). A model of how the RNA enters the cell has been proposed (Belnap *et al.*, 2000) but the exact details remain unclear.

In contrast, FMDV and several other entero-/ rhinoviruses bind to receptors which do not belong to the immunoglobin superfamily. In these cases, binding to the receptor does not occur at a "canyon" and does not initiate the uncoating process. For example, the FMDV virion does not possess a canyon and it binds to integrins through interaction with an RGD motif within a loop of VP1 (Berinstein *et al.*, 1995; Jackson *et al.*, 2000; Jackson *et al.*, 2002). This binding does not cause viral instability. Instead, the virus is thought to enter the cell through receptor-mediated endocytosis. The FMDV virion is very acid labile and consequently uncoats within endosomes due to a decrease in pH (Burroughs *et al.*, 1971; Curry *et al.*, 1995; Miller *et al.*, 2001).

1.1.1b Translation of Viral Proteins

The viral RNA is translated by a cap-independent IRES-mediated mechanism. This differs from the cap-dependent mechanism by which most eukaryotic mRNAs are

translated as described below (Section 1.2). The single ORF within the viral RNA encodes a polyprotein which is co-translationally and post-translationally cleaved by virally encoded proteases to produce the mature viral proteins (shown in Figure 1). The primary cleavage occurs in *cis*. For entero- and rhinoviruses, the first cleavage event occurs between P1 and P2 and is mediated by the 2A protease. The 2A protease belongs to the trypsin-like subgroup of serine proteases but the active site nucleophile is a cysteine not serine (Bazan & Fletterick, 1988). However, the 2A proteins differ greatly among all picornaviruses and is not a recognisable protease in the other genera. Despite this, the 2A protein from cardio- and aphthoviruses can generate its own cleavage from the viral polyprotein by inducing cleavage at the 2A/2B junction. The mechanism for this reaction remains unclear and it is interesting to note that cardiovirus 2A sequence is far longer than the aphthovirus sequence (150 amino acids compared to 18 amino acids). However, only the last 19 amino acids of the cardiovirus 2A are required for this cleavage event to occur (Donnelly *et al.*, 1997). The 2A protein from parechoviruses, hepatoviruses and kobuviruses are thought not to be involved in polyprotein processing (Jia *et al.*, 1993; Schultheiss *et al.*, 1995; Yamashita *et al.*, 1998).

All other polyprotein cleavage events are mediated by the 3C protease with two exceptions. The first of these is the cleavage of 1AB (VP0) which is linked to encapsidation. The mechanism of this cleavage remains unidentified. The second exception is that the aphthoviruses encode a leader (L) protease at the start of the polyprotein. The L protease is a papain-like cysteine proteinase (Gorbalenya *et al.*, 1991; Guarne *et al.*, 1998) which catalyses its own release from the polyprotein. The picornavirus 3C proteases are larger than the enterovirus 2A protease but also belong to

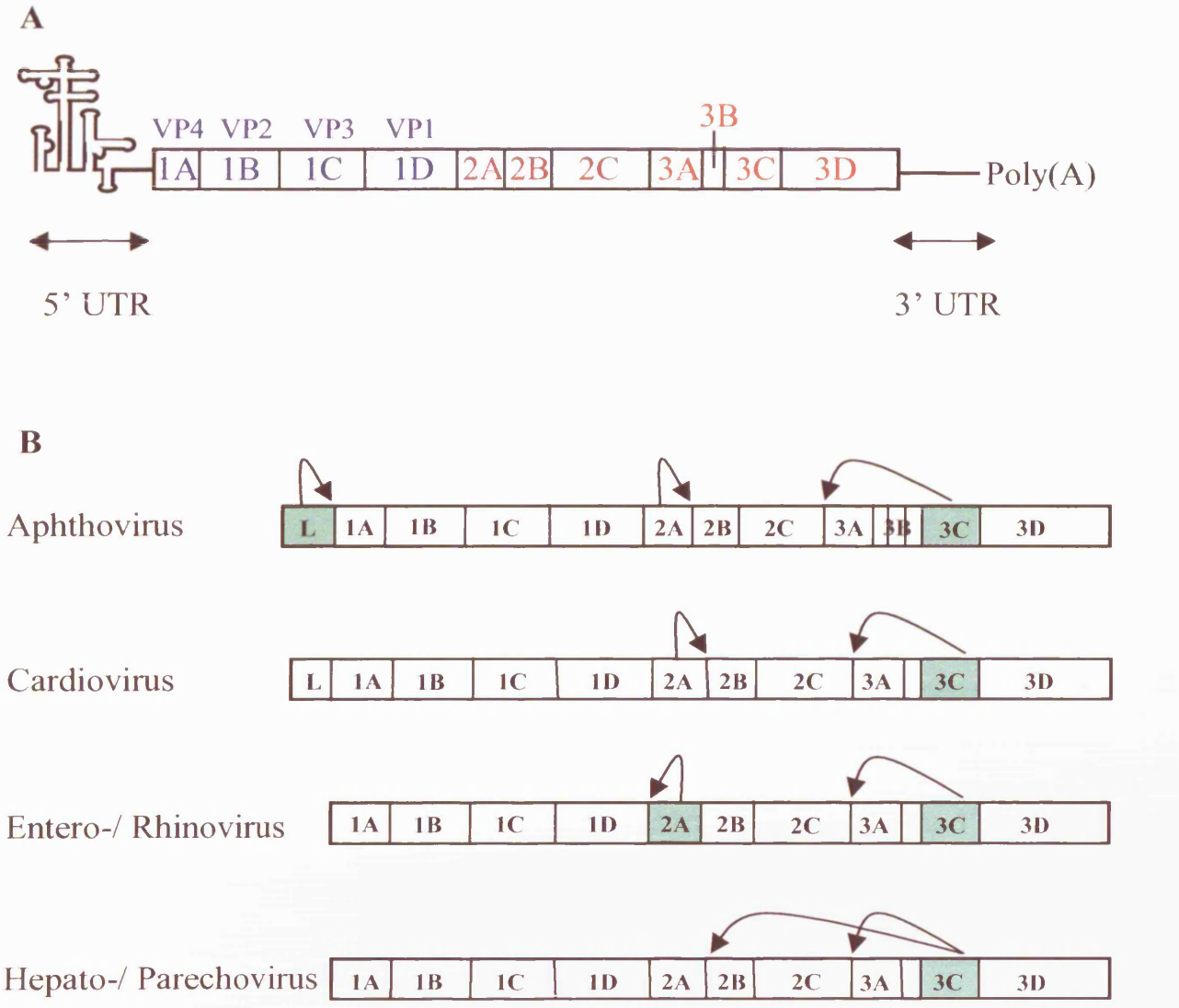

Figure 1: The typical picornavirus genome is shown in panel A. One large open reading frame encodes a polyprotein. The proteins in blue lettering are the structural proteins. The polyprotein is proteolytically cleaved by virus encoded proteases. Panel B shows the primary cleavages. The remaining cleavages are mediated by $3C^{pro}$ (except at the 1A/1B junction which is cleaved during encapsidation). Proteases are shown in green.

the trypsin-like subgroup of serine proteases in which the active site nucleophile is a cysteine not serine (Bazan & Fletterick, 1988). Polyprotein processing results in the release of the mature viral proteins (of which there are 10 or more) but, in addition, there are several intermediates such as 3CD that have a role in the virus growth cycle. The non-structural proteins produced have a diverse set of roles but are primarily involved in the RNA replication process.

1.1.1c RNA Replication

RNA replication occurs in two steps: the synthesis of negative sense strands from the genome RNA template followed by synthesis of positive strand RNA from the negative strand templates. Synthesis of the viral RNA is directed by the virus encoded RNA-dependent RNA polymerase, $3D^{pol}$, and occurs within membrane-associated replication complexes. The viral protein 3B (also called VPg) is attached to the 5' end of the picornavirus genome and is uridylylated by $3D^{pol}$. It can then act as a primer for RNA synthesis (Paul *et al.*, 1998). The replication of poliovirus is the most studied of the picornaviruses. Within the 5' UTR of the PV genome (upstream of the IRES) is a sequence involved in replication called the cloverleaf, which forms a ribonucleoprotein complex with the viral precursor $3CD^{pro}$ in the presence of either viral 3AB or a cellular poly(C) binding protein, PCBP. This complex is involved in *trans* for positive strand RNA synthesis (Andino *et al.*, 1990; Andino *et al.*, 1993; Xiang *et al.*, 1995; Gamarnik & Andino, 1997; Parsley *et al.*, 1997). Recently, it has been proposed that the complex is also involved in *cis* for circularization of the genome (through protein-protein interactions) to enable negative strand synthesis (Barton *et al.*, 2001; Herold & Andino, 2001; Lyons *et al.*, 2001). Sequences within the 3' UTR have also been

implicated in replication (Spector & Baltimore, 1974; Sarnow *et al.*, 1986; Sarnow 1989a; Rohll *et al.*, 1995) as have sequences within the PV IRES element (Borman *et al.*, 1994).

Moreover, PV replication has been shown to require a *cis*-acting replication element (*cre*) situated within the coding sequence (Goodfellow *et al.*, 2000). This *cre* appears to be involved in negative strand synthesis and is thought to be the template for the uridylylation of VPg (Paul *et al.*, 2000; Rieder *et al.*, 2000). The replication mechanism for other genera of picornaviruses may well differ from that of PV since they do not all possess a cloverleaf structure at the 5' end. However, *cis*-replication elements have been found within many of the genera and therefore there may be a shared mechanism for the uridylylation of VPg (McKnight & Lemon, 1998; Lobert *et al.*, 1999; Gerber *et al.*, 2001; Mason *et al.*, 2002).

1.1.1d Translation to Replication Switch

At some point there is a switch from translation to RNA replication as the two processes cannot occur on the same RNA molecule (Gamarnik & Andino, 1998; Barton *et al.*, 1999). One possible mechanism of this switch has been suggested for PV which involves the cloverleaf structure in the 5'UTR (Gamarnik & Andino, 1998). Binding of PCBP to the cloverleaf seems to increase viral translation but binding of 3CD inhibits viral translation and up-regulates viral replication. Therefore, 3CD binding could act as the trigger to switch to replication. PCBP also binds to the PV IRES and stimulates PV-translation (Blyn *et al.*, 1996; Blyn *et al.*, 1997). It has been suggested that 3CD binding to the cloverleaf increases the affinity of PCBP to the

cloverleaf but does not affect its binding to the IRES (Gamarnik & Andino, 2000). This means that, in the presence of 3CD, PCBP would preferentially bind to the cloverleaf and inhibit translation. There is however, uncertainty about this mechanism due to the fact that PCBP is present at sufficiently high cytoplasmic concentrations (100nM in HeLa cells) to bind to both the cloverleaf and IRES structures.

Other possible mechanisms have been proposed that involve cleavage of cellular proteins by virus encoded proteases. For example, the polypyrimidine tract-binding protein (PTB) is cleaved in several places by the 3C protease during PV-infection (Back *et al.*, 2002). PTB has been shown to bind to the PV IRES and to stimulate IRES activity (Hellen *et al.*, 1994a; Hunt & Jackson, 1999). The cleavage products were shown to inhibit PV translation and therefore this cleavage could act as a switch to allow replication to occur. Clearly there is a need to clarify and identify which mechanisms are involved in determining when replication can commence.

1.1.1e Encapsidation

The final step in virus infection is the assembly of virions. The first assembly intermediate is a protomer which is formed of one molecule of each of the four structural proteins (1A-1D). The proteins 1A and 1B are present as the precursor 1AB since no cleavage at the 1A/1B junction has yet taken place. Five protomers are thought to assemble into the next assembly intermediate, a 14S pentamer. The cleavage of the P1 protein into each of the structural proteins occurs slowly and these cleavages may trigger 14S pentamer formation. The 14S pentamers in turn associate to form an immature virion. The mature virion is generated when the viral RNA is

packaged into the protein shells and 1AB is cleaved. The cleavage of 1AB is simultaneous with RNA packaging but the mechanism responsible for the cleavage has yet to be identified. There is some speculation that the catalysis is mediated by a residue present in 1B and a nucleotide of the RNA (hence the linkage between the two processes) (Arnold *et al.*, 1987; Hindiyeh *et al.*, 1999).

1.1.2 Effect of Picornavirus Infection on Host Cell

When picornaviruses infect cells, a variety of effects are seen within the host cell. One of these is a rapid inhibition of host cell protein synthesis (as described in detail in Section 1.2.2). This inhibition occurs within 1 to 3hr within PV-, FMDV- and rhinovirus-infected cells (Etchison *et al.*, 1982; Etchison & Fout, 1985; Devaney *et al.*, 1988). Translation is also inhibited in cells infected with the cardiovirus EMCV but this occurs later in infection (Jen & Thach, 1982). Interestingly, no such inhibition is seen within cells during hepatitis A virus (HAV) or parechovirus infection. Host cell transcription and nucleo-cytoplasmic trafficking have been shown to be affected within PV-infected cells (Clark *et al.*, 1993; Yalamanchili *et al.*, 1997; Belov *et al.*, 2000; Gustin & Sarnow, 2001). Both of these effects are thought to be caused (at least in part) by virus-induced cleavage of cellular proteins. For example, the PV 3C protease is known to cleave a transcription factor called CREB (Yalamanchili *et al.*, 1997). There is also an inhibition of cellular protein secretion by the PV proteins 2B and 3A (Doedens & Kirkegaard, 1995).

Significant alterations in membrane arrangements have been observed in PV and HAV infected cells (Bienz *et al.*, 1983; Klinger *et al.*, 2001). This is due to the

formation of virus-induced vesicles from the endoplasmic reticulum and these are involved in viral replication (Suhy *et al.*, 2000; Rust *et al.*, 2001). The virus precursor protein 2BC is involved in the formation of these vesicles (Bienz *et al.*, 1983; Cho *et al.*, 1994; Teterina *et al.*, 1997; Suhy *et al.*, 2000). Cell death via apoptosis is sometimes induced in PV-infected cells but only in particular cell types and under certain conditions (Tolskaya *et al.*, 1995; Agol *et al.*, 1998; Agol *et al.*, 2000). The viral proteins 2A and 3C are responsible for this apoptotic response (Barco *et al.*, 2000; Goldstaub *et al.*, 2000). The exact mechanism by which this occurs is uncertain but the 2A protease inhibits cellular protein synthesis and therefore may induce apoptosis indirectly. The ability to induce apoptosis has been seen in other enterovirus infections such as coxsackievirus B3 (Carthy *et al.*, 1998), enterovirus 71 (Kuo *et al.*, 2002) and also for the cardiovirus, TMEV (Jelachich & Lipton, 1999). However, later in PV infection there is expression of an anti-apoptotic activity. This means that in the middle of the infectious cycle (when progeny virus are being formed), apoptosis is halted and cytopathic effects (CPE) can be seen (Tolskaya *et al.*, 1995; Agol *et al.*, 2000). It has been determined that the viral proteins 2B and 3A inhibit tumour necrosis factor-induced apoptosis (Neznanov *et al.*, 2001).

1.2 Translation in Picornavirus-Infected Cells

In order to describe how picornavirus infection inhibits host cell protein synthesis, it is necessary to first introduce translation within uninfected eukaryotic cells. The mechanism of picornavirus IRES-mediated translation will then be explained.

1.2.1 Translation within Uninfected Cells

Eukaryotic cellular mRNAs are monocistronic and possess a m^7G-cap structure at the 5' end. Translation initiation on the majority of eukaryotic mRNAs is cap-dependent (shown schematically in Figure 2) (for reviews see Hershey & Merrick, 2000). Briefly, the small (40S) ribosome subunit binds to the 5' end of the mRNA through an indirect interaction (via eIF4F) with the cap-structure. It then scans along the 5' untranslated region (5' UTR) of the mRNA until the initiation codon is recognised. The translation initiation codon is almost invariably AUG which encodes for the amino acid methionine (Met). When the 40S ribosome reaches the AUG codon, base-pairing will occur between the AUG codon and the anti-codon of the initiator tRNA. The large (60S) ribosomal subunit then binds and peptide synthesis begins.

The 40S ribosome subunit initially forms a 43S preinitiation complex by binding initiation factor 3 (eIF3) and a ternary complex consisting of eIF2 associated with the initiator tRNA (Met-$tRNA_i$) and GTP. This complex then binds to the 5' cap of the mRNA via an interaction with the cap binding complex, eIF4F (for a review see Gingras *et al.*, 1999). The cap-binding complex is formed of 3 subunits: eIF4E, eIF4G and eIF4A. The protein eIF4E binds directly to the cap structure of the mRNA. eIF4A is an ATP-dependent RNA helicase and is thought to unwind any secondary structure present in the 5'UTR to enable the 40S ribosome subunit to bind (Grifo *et al.*, 1983). Its helicase activity is stimulated by the factors eIF4B and eIF4H (Jaramillo *et al.*, 1991; Richter-Cook *et al.*, 1998). The third subunit eIF4G contains binding sites for many proteins and is thought to act as a bridge, indirectly linking the 40S ribosome

Formation of 43S preinitiation complex:

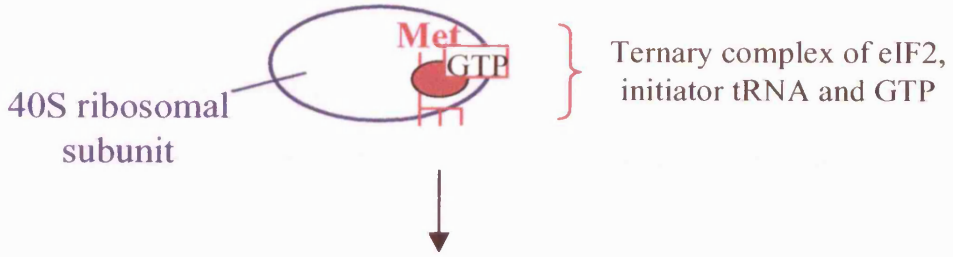

Binding of 43S complex to the 5' cap structure of the mRNA:

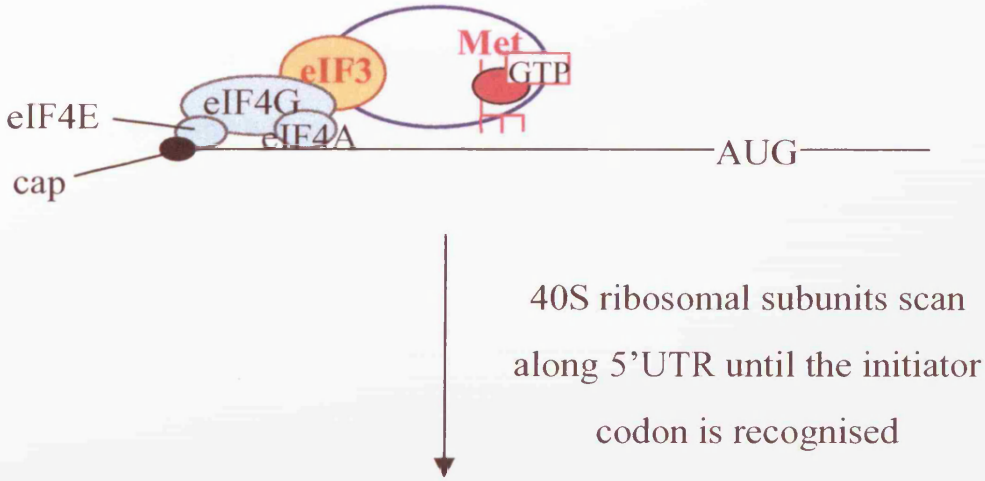

Formation of the 48S preinitiation complex:

Figure 2: Translation initiation within eukaryotic cells. This diagram shows the outline of the pathway but many additional factors are required as described in the text. Once the 48S complex has been formed, there is GTP hydrolysis and a dissociation of factors to allow the 60S ribosomal subunit to bind. The 80S ribosome is then formed and peptide synthesis begins.

subunit to the mRNA through its interaction with both eIF4E (which is bound to the cap) and eIF3 (bound to the 40S subunit) (shown schematically in Figure 3). Once associated with the mRNA, the ribosome moves along the 5' untranslated region (5' UTR) by a mechanism called scanning, with the help of factors eIF1 and eIF1A, until it recognises the initiation codon, AUG (for reviews of scanning refer to Kozak, 1989; Kozak, 1999).

Most eukaryotic mRNAs have a short 5'UTR (about 50 to 100 nucleotides (nt) long) and in the majority of cases, the initiation codon is the first AUG codon reached by the scanning ribosome which is in a favourable context. A consensus sequence for initiation has been identified as GCCGCCA/GCCAUGG (Kozak, 1987a). If the sequence surrounding the 5' proximal AUG codon is in poor context, the ribosome may continue scanning until it reaches a downstream AUG codon in a better context. This is called leaky scanning and is described in more detail in Section 1.4.1. The length of the 5' UTR and the presence of secondary structure can also affect translational efficiency. Shortening of the 5'UTR to as little as 3 nt-long inhibits translation initiation but increasing the length can stimulate translation (Kozak, 1991a; Kozak, 1991b). The eIF4A helicase can remove a certain extent of secondary structure present within the 5' UTR but strong secondary structures, such as a stable hairpin, inhibit translation. It is likely that they inhibit movement of the scanning 40S ribosomes. There are two exceptions to this observation. The first is that a stable hairpin placed in close proximity to the initiation codon (about 12nt downstream) can stimulate translation (Merrick, 1992). It is thought that it causes a pause in scanning which helps position the 40S ribosome at the initiation codon. Additionally, relatively

weak secondary structures can inhibit initiation when placed in close proximity to the cap structure (Lawson *et al.*, 1986).

When the scanning ribosome has reached the initiation codon, the initiation codon and the anti-codon of the Met-tRNA$_i$ base-pair. This results in a 48S preinitiation complex. Subsequently, there is a dissociation of initiation factors from the 40S subunit to enable the 60S ribosome subunit to bind. This requires two additional factors called eIF5 and eIF5B and also the hydrolysis of GTP. After this, the 60S ribosome subunit joins and the 80S ribosome is formed. The initiator tRNA will be positioned in the peptidyl-tRNA site (the P site) of the ribosome and peptide synthesis can begin. As indicated above, there are many translation factors involved in initiation and below is a summary of some of the most prominent factors:

<u>eIF4E</u>

eIF4E is a small protein (24kDa) which is highly conserved in eukaryotes to the extent that mammalian eIF4E can substitute for yeast eIF4E (Altmann *et al.*, 1989). Through structure analysis it is known that the cap binds to a hydrophobic cleft in the inner surface of eIF4E (Marcotrigiano *et al.*, 1997; Matsuo *et al.*, 1997). The binding site for eIF4G is on the opposite, dorsal side which is also where the translation inhibitors called eIF4E-binding proteins (4E-BPs) bind. eIF4E binds to the cap-structure of the mRNA with more affinity when it is part of the eIF4F complex, rather than alone (Haghighat & Sonenberg, 1997). Evidence suggests that the binding of eIF4G to eIF4E stabilises conformational changes that occur within eIF4E upon binding of the cap and that eIF4G does not increase cap-binding through its interaction with the mRNA directly (von der Haar *et al.*, 2000).

eIF4E has an important role in translational control and hence cell growth. It is the least abundant of the initiation factors and thought to be the limiting factor for translation initiation (Duncan *et al.*, 1987). Overexpression of eIF4E causes transformation within cells (reviewed in Sonenberg, 1996). The binding of the translation inhibitor, 4E-BP, is mutually exclusive to the binding of eIF4G and therefore this inhibits assembly of the eIF4F complex. Consequently the association of 4E-BP with eIF4E inhibits cap-dependent translation (Pause *et al.*, 1994a; Haghighat *et al.*, 1995). 4E-BP can be phosphorylated at several residues and its phosphorylation state determines its affinity for eIF4E (Pause *et al.*, 1994a; Fadden *et al.*, 1997; Heesom *et al.*, 1998). Hyper-phosphorylation leads to dissociation from eIF4E and hence increased translation rates (Pause *et al.*, 1994a). This phosphorylation is induced by many external stimuli including insulin, growth factors and cytokines (reviewed in Gingras *et al.*, 1999). In contrast, other stimuli such as serum starvation and heat shock mediate hypo-phosphorylation of 4E-BP1. eIF4E is also phosphorylated itself by the serine/threonine kinase Mnk-1 (Waskiewicz *et al.*, 1999). This phosphorylation increases the affinity of eIF4E for the cap structure (Minich *et al.*, 1994). For this reason it has been suggested that eIF4E phosphorylation could act to clamp the bound mRNA in place. Again the phosphorylation of eIF4E is modulated by external stimuli such as heat shock or viral infection.

eIF4A

eIF4A is the prototype of the DEAD box family of putative RNA helicases. This family is named after the conserved DEAD box motif which is involved in ATP hydrolysis that is essential for helicase activity. There are in fact nine highly conserved

motifs in the DEAD box family which include the SAT sequence involved in RNA helicase activity and a motif which binds to the RNA in an ATP-dependent manner (the HRIGRXXR) (Pause & Sonenberg, 1992; Pause *et al.*, 1993). The crystal structure of eIF4A has been determined which provides suggestions as to the exact mechanism by which these helicases function (Benz *et al.*, 1999; Johnson & McKay, 1999; Caruthers *et al.*, 2000).

eIF4A is 50kDa in size and has an RNA-dependent ATPase activity (Grifo *et al.*, 1983). On its own, eIF4A has a low bidirectional RNA helicase activity but this is stimulated by the factors eIF4B and eIF4H (Rozen *et al.*, 1990; Jaramillo *et al.*, 1991; Richter-Cook *et al.*, 1998; Rogers *et al.*, 1999). Any secondary structure present in the 5'UTR is thought to be unwound by eIF4A and this facilitates ribosome binding (Rogers *et al.*, 1999; Svitkin *et al.*, 2001a). Interestingly, eIF4A is the most abundant of the translation factors with about three copies per ribosome. *In vitro* translation systems require free eIF4A and also eIF4A present within the eIF4F complex (Grifo *et al.*, 1983). From characterisation of dominant negative mutants of eIF4A it appears that eIF4A functions primarily as part of the eIF4F complex and free eIF4A is required for recycling through eIF4F (Pause *et al.*, 1994b).

Three isoforms of eIF4A have been identified called eIF4AI, eIF4AII and eIF4AIII. In mammalian cells, eIF4AI and eIF4AII have 91% identity at the amino acid level (Nielsen & Trachsel, 1988). They are both cytoplasmic and interact with eIF4G (Conroy *et al.*, 1990). The third isoform however is predominantly nuclear and appears to be functionally different (Li *et al.*, 1999; Holzmann *et al.*, 2000). It has only 65% amino acid identity and actually inhibits translation initiation (Li *et al.*, 1999).

eIF4G contains two binding sites for eIF4A (see below) but eIF4AIII only binds at the one site, in the central domain of eIF4G. This appears to inhibit binding of eIF4AI to eIF4G.

eIF4G

This factor serves as a scaffolding molecule, interacting with several members of the translational machinery (shown in Figure 2). Mammalian eIF4G can be considered as being comprised of three parts. The N-terminal third contains the binding sites for eIF4E and the poly(A) binding protein (PABP) (Lamphear *et al.*, 1995; Mader *et al.*, 1995; Imataka *et al.*, 1998). The middle domain, is highly conserved between humans, yeast and plants, it contains overlapping binding sites for eIF4A, eIF3 and also an RNA-binding domain (Imataka & Sonenberg, 1997; Goyer *et al.*, 1993; Pestova *et al.*, 1996a; further defined in Morino *et al.*, 2000). The crystal structure of the middle portion revealed a crescent-shaped HEAT repeat domain that is present in many other proteins involved in assembling large multisubunit complexes (Marcotrigiano *et al.*, 2001). The binding sites for eIF4A and RNA in this central portion were shown to be adjacent and partially overlapping. The C-terminal region of eIF4G contains an additional eIF4A binding site and the binding site of Mnk-1 (Lamphear *et al.*, 1995; Imataka & Sonenberg, 1997; Pyronnet *et al.*, 1999).

As a result of these many interactions, eIF4G has several functions in translation initiation. The interaction of eIF4G with eIF4E and eIF3 allows the 40S ribosome subunit to associate with the 5' cap structure. Additionally, the affinity of eIF4E for the cap structure and the helicase activity of eIF4A are both higher when present as part of the eIF4F complex (Rozen *et al.*, 1990; Haghighat & Sonenberg,

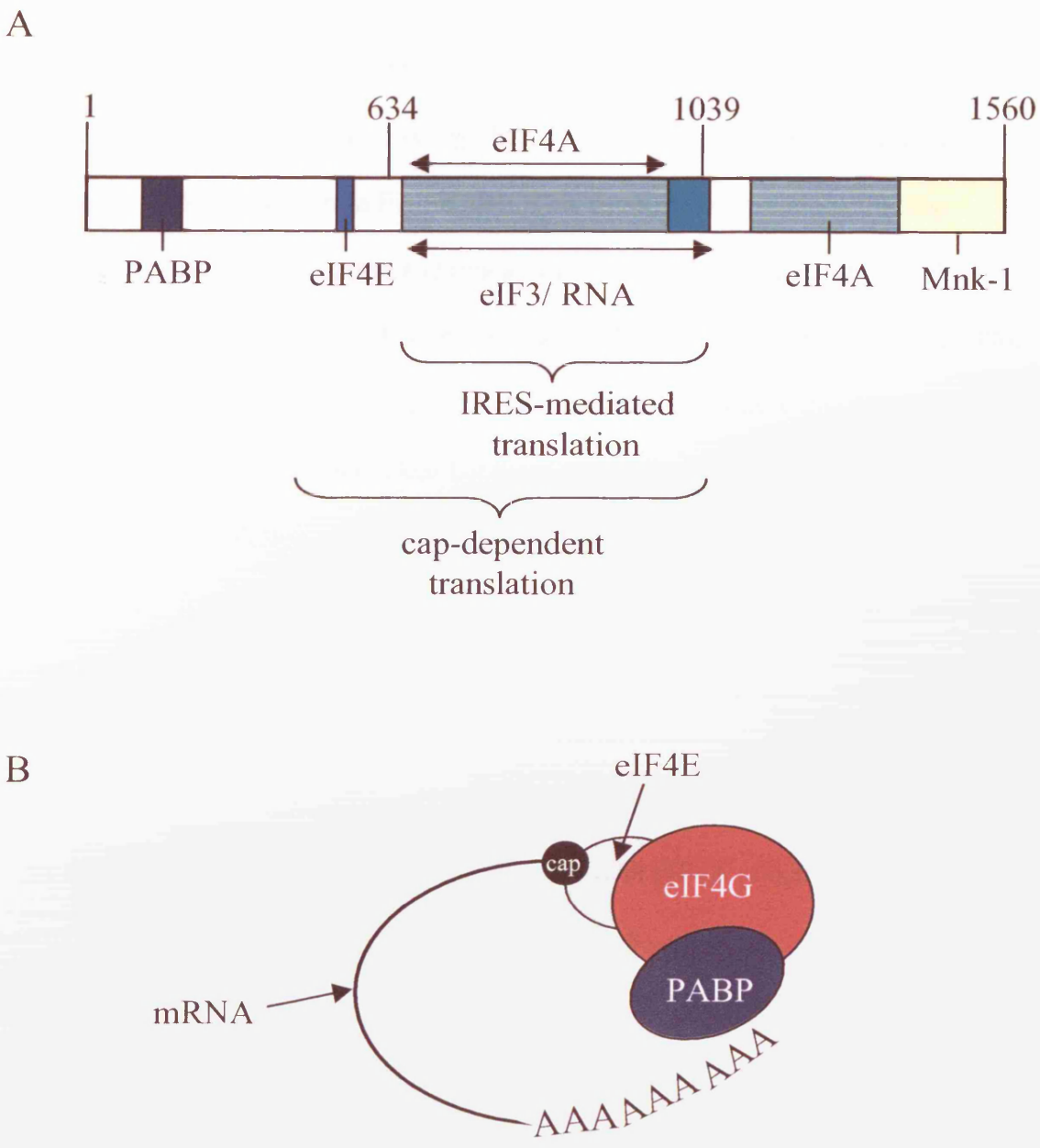

Figure 3: The eukaryotic translation factor eIF4G acts as a scaffolding molecule. Panel A shows the three functional domains of eIF4G and the position of the protein binding sites (based on a Figure from Morino *et al.*, 2000). Panel B shows the proposed model for poly(A) stimulated translation in which the mRNA is circularized through eIF4E-eIF4G-PABP interactions.

1997). eIF4G also recruits the Mnk-1 kinase to phosphorylate eIF4E (Pyronnet *et al.*, 1999). The PABP binding site present within the N-terminal region of both yeast and mammalian eIF4G allows the mRNA being translated to circularise. The 5' cap structure and the 3' poly(A) tail link together via an eIF4E-eIF4G-PABP interaction (Wells *et al.*, 1998; as shown in Figure 3B). This supports observations that the poly(A) tail stimulates translation and that a synergistic effect is seen when both the cap-structure and the poly(A) tail are present on a mRNA (Munroe & Jacobson, 1990; Gallie, 1991; Tarun & Sachs, 1995). The exact mechanism of how this circularization stimulates translation remains unclear but there are several possibilities. It could help the recycling of translation factors from one round of translation to the next (see Section 1.5.2). It could also act as a selection process as only full-length mRNAs will possess both a cap-structure and poly(A) tail. Furthermore, it is possible that PABP binding may induce a change in eIF4G which could increase its affinity for other factors and thereby increase 40S ribosome subunit recruitment. The human PABP-binding protein (PAIP-1) is also known to interact with eIF4A which could reinforce the interaction of PABP with eIF4G (Craig *et al.*, 1998).

As explained in detail later, the majority of picornavirus IRES elements only require the middle third of eIF4G for cap-independent translation and this region binds directly to the RNA (Pestova *et al.*, 1996a). This region is also sufficient for, or even stimulatory to, translation of uncapped RNAs in reticulocyte lysate (Ohlmann *et al.*, 1995; Ohlmann *et al.*, 1996; De Gregorio *et al.*, 1998). There is some controversy about the minimal core of eIF4G required for cap-dependent translation (detailed in Section 1.2.2). Nonetheless, it is clear that intact eIF4G is more efficient at mediating cap-dependent translation than a portion of eIF4G lacking the amino-terminal region

(in terms of concentration required for maximum translation) (Ali *et al.*, 2001). The C-terminal third of eIF4G is non-essential for translation and has been suggested to act as a modulatory region (Morino *et al.*, 2000). The relevance of the second binding site of eIF4A within the C-terminal domain remains to be clarified. Interestingly, the C-terminal eIF4A binding site is not present in yeast, suggesting that it is not necessary for the function of eIF4G in translation. Furthermore, it seems that only one eIF4A molecule binds to eIF4G at any time *in vivo* (Li *et al.*, 2001). Also, the translation inhibitor eIF4AIII binds to the eIF4A site in the middle region of eIF4G and inhibits binding of eIF4AI to eIF4G (Li *et al.*, 1999) which again indicates that only one molecule of eIF4A binds at one time. It is possible that one molecule of eIF4A binds to both sites (through different binding sites on eIF4A).

There are two homologs of eIF4G: eIF4GI and eIF4GII which are functionally identical and have about 40% sequence similarity (Yan *et al.*, 1992; Gradi *et al.*, 1998a; Imataka *et al.*, 1998). The conserved middle domain containing the eIF4A and RNA binding sites are 88% identical. A difference in the roles of these two isoforms has yet to be determined. There are also two distant orthologs of eIF4G called DAP5 and PAIP (Imataka *et al.*, 1997; Shaughnessy *et al.*, 1997; Yamanaka *et al.*, 1997; Craig *et al.*, 1998). PAIP resembles the middle portion of eIF4G and contains a PABP binding site within its C-terminus. As mentioned above, it seems to be involved in poly(A) tail stimulated translation (Craig *et al.*, 1998). In contrast, the protein DAP5 is a translation inhibitor (Imataka *et al.*, 1997). It resembles the C-terminal two thirds of eIF4G and is able to bind eIF4A and recruit 40S ribosome subunits. Therefore, it may act as a competitor to eIF4G and sequester these factors.

eIF1 and eIF1A

Before translation initiation can commence, there has to be a pool of free 40S ribosome subunits which requires the dissociation of 80S ribosomes. The factors eIF1A and eIF3 promote this dissociation although the mechanism by which this occurs is uncertain (Thomas *et al.*, 1980; Chaudhuri *et al.*, 1999). eIF1A is also required for efficient formation of 48S preinitiation complexes *in vitro* along with factor eIF1 (Pestova *et al.*, 1998a). Little is known about the actual mechanism of how they function but they are either involved in the scanning of the 43S preinitiation complex and/ or in the binding of the complex to the initiation codon. However, the two factors are known to act together. On its own eIF1 only weakly stimulates 40S ribosome binding to the initiation codon and eIF1A has no effect at all.

Both these factors are small (eIF1 is 13.5 kDa and eIF1A is 19kDa) and high-resolution structures have been determined (Fletcher *et al.*, 1999; Battiste *et al.*, 2000). eIF1A has an RNA binding site which is large and essential for scanning. Eukaryotic eIF1A is very similar to the initiation factor IF1 in prokaryotes (Kyrpides & Woese, 1998; reviewed in Roll-Mecak *et al.*, 2001). Additionally, eIF1A has been shown to interact with eIF5B which has high sequence similarity to prokaryotic IF2 (Choi *et al.*, 2000). By comparison to their prokaryotic orthologs, it has been suggested that eIF1A and eIF5B bind to the amino acyl-tRNA (A) site of the ribosome and stabilize the binding of the Met-tRNAi to the ribosomal peptidyl-tRNA (P) site (Choi *et al.*, 2000; Roll-Mecak *et al.*, 2001). Yeast eIF1 is a subunit of the multi-subunit factor, eIF3 (Naranda *et al.*, 1996). Human eIF1 is 62% similar to the yeast eIF1 and it is found to associate with eIF3 (Fletcher *et al.*, 1999). This may account for how eIF1 is recruited to the 40S ribosome subunit.

eIF2

This factor forms a ternary complex with GTP and Met-tRNA$_i$. It recognises and selects the Met-tRNA$_i$ from the pool of tRNAs. It is formed from 3 subunits: α, β and γ. The N-terminal fragment of the α subunit and a zinc-finger motif within the β subunit are thought to be involved in recognition of the initiation codon. The β subunit also contains binding sites for eIF2B, eIF5 and RNA (Asano *et al.*, 1999; Laurino *et al.*, 1999). The GTPase activity of eIF2 is located within the γ subunit to which both GTP and Met-tRNA$_i$ bind.

When recognition of the initiation codon occurs, GTP is hydrolysed to GDP. In order to bind Met-tRNA$_i$, eIF2 needs to be complexed with GTP and therefore a guanylate exchange reaction catalysed by eIF2B is necessary. This step is a major target for translational control since phosphorylation of the α subunit of eIF2 prevents this guanylate reaction occurring. eIF2α is known to be phosphorylated during stress conditions by four different kinases (e.g. PKR) at Ser-51. When phosphorylated, it binds more tightly to eIF2B and the GDP is not converted to GTP. Therefore, it acts as a competitive inhibitor of eIF2B and sequesters eIF2B which is present in much lower concentrations than eIF2α (Oldfield *et al.*, 1994). Furthermore, eIF2B activity itself is thought to be controlled by phosphorylation (Welsh & Proud, 1993; Singh *et al.*, 1994).

eIF3

This factor is the largest of the initiation factors (approximately 600 kDa in mammalian cells) and is composed of at least 11 subunits (5 in yeast). It is thought to be involved in the dissociation of 80S ribosomes into its subunits that is essential for

translation initiation to start (Goss *et al.*, 1988). Additionally, it is required for binding of the 43S preinitiation complexes to mRNAs (Pestova *et al.*, 1998a). The subunits of eIF3 interact with many of the translation factors and may be responsible for recruiting these factors in close proximity to the 40S ribosome subunits. At least four of its subunits are known to bind RNA. One or more of the subunits of eIF3 interact with eIF4G but the subunit/s responsible for the interaction have not yet been determined. Evidence also suggests eIF3 binds to eIF1, eIF5 and eIF4B (Methot *et al.*, 1996; Bandyopadhyay & Maitra, 1999; Fletcher *et al.*, 1999).

eIF5 and eIF5B

Both eIF5 and eIF5B are required for the formation of 80S ribosomes after the 48S preinitiation complex has been formed. eIF5 was isolated first and shown to be required for stimulating hydrolysis of eIF2-bound GTP (Chakrabarti & Maitra, 1991). This triggers dissociation of the initiation factors from the 40S ribosomal subunits by an unknown mechanism. However, eIF5 alone is not sufficient for formation of active 80S ribosomes *in vitro* (Pestova *et al.*, 2000). eIF5B was found to be required in combination with eIF5 for joining of the two ribosome subunits in the presence of other factors such as eIF1, eIF1A, eIF2 and eIF3 (Pestova *et al.*, 2000). It is thought that eIF5 stimulates the hydrolysis of eIF2-bound GTP as, although eIF5B is a GTPase, eIF5B does not stimulate hydrolysis of the eIF2-bound GTP in the presence of eIF1 and eIF3. Rather it seems that eIF5B is responsible for hydrolysis of GTP bound to itself and that this reaction is important for eIF5B release from the ribosome. This stems from experimental data showing that recombinant eIF5B was found associated with 80S ribosomes that were formed in the presence of GMP-PNP (a nonhydrolyzable analogue of GTP) but not in the presence of GTP (Pestova *et al.*, 2000). Other factors

such as eIF1, eIF2 and eIF3 were displaced from the 80S ribosomes in the presence of GMP-PNP so hydrolysis of GTP bound to eIF5B is not required for their displacement.

eIF5 is 49kDa and interacts with eIF2 and eIF3 (Chakrabarti & Maitra, 1991). It is possible that eIF5 may in fact form a complex with eIF1, eIF3, and eIF2/GTP/Met-tRNAi and that this complex may bind to the ribosome in one step (Asano *et al.*, 2000). The ability of eIF5 to stimulate the GTPase activity of eIF2 is only induced when eIF2 is associated with the 40S subunit. eIF5B is a larger protein of 175kDa and as discussed before it is an eukaryotic ortholog of the prokaryotic protein IF2. The GTPase activity of eIF5B is greatly stimulated by the ribosomal subunits (Pestova *et al.*, 2000). It is still unclear how eIF5B facilitates formation of 80S ribosomes.

1.2.2 Inhibition of Host Cell Protein Synthesis

As mentioned previously, the majority of picornaviruses shutoff host cell translation. There are two main mechanisms by which this can occur. Within cells infected with either FMDV, an enterovirus or a rhinovirus, host-cell shutoff occurs rapidly and is mediated by the cleavage of eIF4G by viral proteases (Etchison *et al.*, 1982; Devaney *et al.*, 1988). In contrast, the inhibition of host cell translation within EMCV-infected cells occurs later in infection and does not involve cleavage of eIF4G (Jen & Thach, 1982).

1.2.2a Cleavage of Translation Factors by Viral Proteases

The cleavage of eIF4G is induced by the 2A protease within cells infected with

entero- or rhinoviruses. In FMDV-infected cells, the leader protease (L) mediates this cleavage. Both proteases cleave eIF4G within the N-terminal third and therefore the region containing the eIF4E-binding site and the PABP-binding site is separated from the remainder of the molecule (Lamphear *et al.*, 1995). This cleavage was thought to inhibit host cell translation, however, exceptions to the correlation of eIF4G cleavage and host cell shutoff have been observed. Within cells infected with PV, the use of virus replication inhibitors (such as guanidine) resulted in the cleavage of nearly all eIF4G but only 70% of host protein synthesis was inhibited (Bonneau & Sonenberg, 1987). Additionally, there was a time delay of 20 to 30 minutes between the cleavage of eIF4G and protein synthesis inhibition (Etchison *et al.*, 1982). However, these anomalies were explained when the functional homolog eIF4GII was isolated and shown to be cleaved more slowly in PV-infected cells than eIF4GI (Gradi *et al.*, 1998b). Cleavage of eIF4GII is required for complete inhibition of host protein synthesis.

In vitro experiments reinforced the theory that cleavage of eIF4G rendered eIF4F inactive for cap-dependent translation. The formation of 48S preinitiation complexes on globin mRNA was severely diminished if a fragment of eIF4G lacking the N-terminal region was used (Morino *et al.*, 2000). More recent evidence contradicts this and suggests that the C-terminal two-thirds of eIF4G are sufficient to mediate cap-dependent translation (Ali *et al.*, 2001a). This was demonstrated using an *in vitro* assay in which rabbit reticulocyte lysate (rrl) was depleted of endogenous eIF4G. Recombinant p100 (corresponding to the C-terminal two-thirds of eIF4G) supported translation of capped mRNAs within the eIF4G-depleted rrl. Nevertheless, the concentration of p100 required for maximum translation was very high

(approximately four times the amount of eIF4G present within rrl). Therefore, it is evident that the picornavirus IRES element outcompetes the capped mRNAs for the limiting amount of p100. Of course, IRES-mediated translation is not affected by eIF4G cleavage as it only requires the middle third of eIF4G (Pestova *et al.*, 1996a). The notable exception to this is HAV which requires intact eIF4G for viral translation (Borman & Kean, 1997).

The binding of eIF4E to eIF4G renders eIF4G more susceptible for cleavage (Haghighat *et al.*, 1996; Haghighat & Sonenberg, 1997). However, the actual mechanism for cleavage of eIF4G by the 2A and L proteases is controversial. One possible scenario is that 2A activates a latent cellular protease which then cleaves eIF4G. This could lead to an amplification effect. Evidence in support of this theory is that the predominant eIF4G cleavage activity within PV-infected cells has been reported as being distinct from PV 2A (Lloyd *et al.*, 1986; Bovee *et al.*, 1998a). Furthermore, eIF4G cleavage has been observed in PV and FMDV-infected cells in which the levels of 2A and L are undetectable (due to inhibition of virus replication using guanidine treatment) (Bonneau & Sonenberg, 1987; Belsham *et al.*, 2000). Notwithstanding this, there is *in vitro* data indicating that eIF4G is cleaved directly by the 2A and L proteases (Lamphear *et al.*, 1993; Liebig *et al.*, 1993; Kirchweger *et al.*, 1994; Haghighat *et al.*, 1996). Recently, experiments using a thermosensitive mutant of the HRV 2A protease strongly suggested that both eIF4GI and eIF4GII are directly cleaved by 2A (Liebig *et al.*, 2002). In contrast to this, the concentration of PV 2A protease required for efficient cleavage was reported as being much higher than the concentration present *in vivo* (Bovee *et al.*, 1998b). However, more recently the direct cleavage of eIF4G by the 2A and L proteases *in vitro* was demonstrated to be more

efficient when the proteases were being translated at the same time (Glaser & Skern, 2000). Further complications arose when it was reported that that even if the 2A protease cleaves eIF4G directly, there are additional cellular proteases which mediate cleavage of eIF4G (Zamora *et al.*, 2002). Using column purification techniques, differing cleavage products of eIF4G were identified and a second cleavage site was found to lie about 40 residues upstream of the 2A cleavage site. This study also proposed that caspases were involved in the eIF4G cleavage within PV-infected cells although this had previously been shown not to be the case (Roberts *et al.*, 2000).

In addition to eIF4G cleavage, picornaviral proteases are known to cleave other cellular proteins also affecting host cell translation. For example, PABP is known to be cleaved within enterovirus-infected cells and this is thought to contribute to the inhibition of host cell protein synthesis (Joachims *et al.*, 1999; Kerekatte *et al.*, 1999). As mentioned in Section 1.2.1, PABP allows circularization of the mRNA being translated and thus stimulates translation. There is also evidence that PABP may stimulate 80S ribosome formation and has a role in mRNA stability (Sachs & Davis, 1989; Hoshino *et al.*, 1999a). PABP is cleaved at multiple sites within the highly conserved C-terminal domain by the enterovirus 2A and 3C proteases. Ribosome-associated PABP seems to be preferentially cleaved rather than free PABP (Kuyumcu-Martinez *et al.*, 2002). Yet cleavage of PABP occurs slowly and is unlikely to be responsible for the majority of host cell translation inhibition.

The FMDV 3C protease has been shown to cleave eIF4G and eIF4AI (Belsham *et al.*, 2000). The 3C-mediated cleavage site within eIF4G is distinct from the L-mediated cleavage site and a degradation of the primary cleavage products (from the L-

mediated cleavage) is observed. Furthermore, the cleavage of eIF4A by 3C separates the critical regions required for helicase activity (Li *et al.*, 2001). However, these cleavages occur late in infection (about 3 hours post infection) and are co-incident with a decrease in viral RNA translation (Belsham *et al.*, 2000). Therefore, these cleavages occur too late to be relevant to the shutoff of host cell translation.

1.2.2b Inhibition of Host Cell Protein Synthesis in EMCV-Infected Cells

A second mechanism for translation inhibition is used by cardioviruses. This involves dephosphorylation of 4E-BP1. As mentioned before 4E-BP1 is a translation regulator and, when unphosphorylated, binds to eIF4E. This binding is mutually exclusive to binding of eIF4G and therefore leads to inhibition of cap-dependent translation (Pause *et al.*, 1994a; Haghighat *et al.*, 1995). A clear correlation has been demonstrated between dephosphorylation of 4E-BP1 and translation inhibition in EMCV-infected Krebs-II ascites cells (Gingras *et al.*, 1996). Dephosphorylation of 4E-BP1 has also been observed in PV-infected cells but is unlikely to be relevant to host cell shutoff as it occurs much later in infection after the cleavage of eIF4G (Gingras *et al.*, 1996). The actual mechanism by which this dephosphorylation occurs remains unknown. EMCV infection also leads to a change in intracellular ion concentrations which has been suggested to selectively inhibit host cell protein synthesis (Carrasco & Smith, 1976; Alonso & Carrasco, 1981). A number of other translation factors such as eIF4E and eIF2α have been reported to be phosphorylated during picornavirus infection but the importance of this to host cell shutoff remains undefined (Black *et al.*, 1989; Kleijn *et al.*, 1996).

1.2.3 IRES-Mediated Translation of Picornavirus Proteins

There are at least three different classes of picornavirus IRES elements that vary in both structure and function, discussed below. The mechanism of picornavirus IRES-mediated translation requires canonical translation factors. Other cellular *trans*-acting factors have also been identified.

1.2.3a The Three Groups of Picornavirus IRES Elements

Three classes of picornavirus IRES elements have been identified to date. These are: (1) the entero-and rhinovirus IRES elements; (2) the cardio- and aphthovirus IRES elements and (3) the hepatitis A IRES element. The newly characterised teschovirus IRES seems to belong to a fourth group as it has unique qualities (Kaku *et al.*, 2002). There is little conservation within the primary sequence of the different IRES elements. In addition, the different classes of IRES elements vary both in their secondary structure (shown in Figure 4) and in mechanism. The only common features between the IRES elements from the first three well characterised groups are that they are a similar length (approximately 450nt) and contain a Yn-Xm-AUG motif at the 3' border (Pestova *et al.*, 1991; Belsham & Jackson, 2000). Yn is a polypyrimidine tract (of 12 to 15 residues), followed by a spacer element of 14 to 22 nt (Xm) and an AUG codon which allows ribosome entry. In contrast, the teschovirus IRES lacks a significant pyrimidine tract and is smaller (at most 405nt long) (Kaku *et al.*, 2002). Early mutagenesis experiments suggested the pyrimidine tract was essential for picornavirus IRES activity but more recently it was shown that an EMCV IRES containing a poly-purine tract in place of the polypyrimidine tract was clearly

1) Entero/ and Rhinoviruses

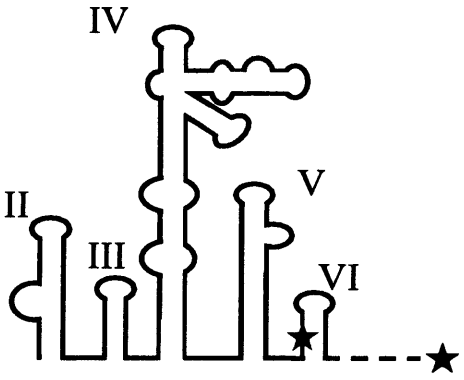

2) Cardio/ and Aphthoviruses

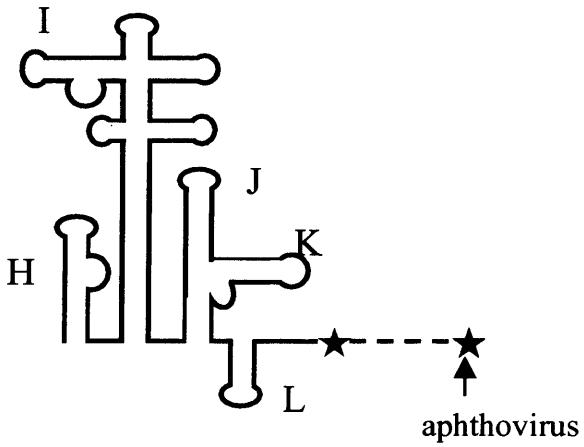

3) Hepatitis A virus

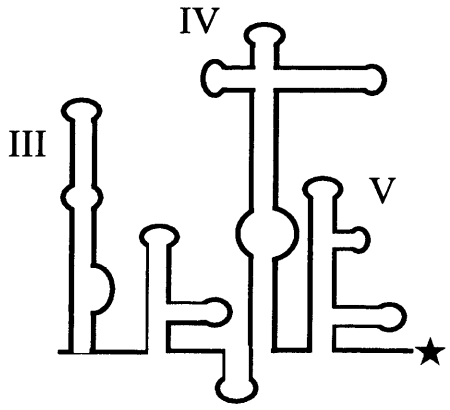

Figure 4: Schematic diagram of the predicted secondary structure of the picornavirus IRES elements. The polypyrimidine tract is shown in red. About 20nt downstream of this tract is the putative ribosome entry site, marked by an orange star. Translation initiation occurs at this AUG for several picornaviral IRES elements. The exceptions are aphtho-, entero- and rhinoviruses. For these viruses, the initiation codon is further downstream, shown by a blue star.

functional (Kuhn *et al.*, 1990; Pestova *et al.*, 1991; Nicholson *et al.*, 1991; Kaminski *et al.*, 1994).

Group 1 IRES Elements

The predicted secondary structure of the IRES element from entero- and rhinoviruses is shown in Figure 4. The 5'UTR contains six structural domains and domains II to VI have been shown to be essential for IRES activity (Nicholson *et al.*, 1991). Domain I is the cloverleaf structure involved in viral replication. As mentioned previously, the ribosome enters at the 3' border of the IRES. However, PV translation initiation occurs further along at an initiation codon approximately 150nt downstream. It is possible that the ribosome scans from the point at which it enters on the viral RNA to the initiation site (Hellen *et al.*, 1994b). However, another study showed that when the context of the upstream AUG codon (at the 3' border of the IRES) was optimised, many ribosomes still initiated translation at the authentic initiation codon downstream (Pestova *et al.*, 1994), suggesting factors other than the codon context are important.

The entero- and rhinoviruses IRES elements do not function effectively in rrl. There is little translation observed and aberrant initiation occurs (Brown & Ehrenfeld, 1979; Dorner *et al.*, 1984). However, efficient IRES activity can be seen when the rrl is supplemented with cytoplasmic extracts from HeLa cells. This indicates that these elements require proteins in addition to the canonical translation factors to function and these are called *trans*-acting factors.

Group 2 IRES Elements

The predicted secondary structure of the IRES elements from aphtho- and cardioviruses shown in Figure 4 (based on Pilipenko *et al.*, 1989; Duke *et al.*, 1992). It should be noted that an alternative structure has been proposed for the EMCV IRES (Palmenberg & Sgro, 1997). In this model, domain I is separated into 3 different sub-domains.

In contrast to Group 1, the Group 2 IRES elements function very efficiently in rrl. This means that any *trans*-acting factors required for maximum IRES activity must be present at a sufficient concentration within rrl. Another difference to the entero-/ rhinovirus IRES elements is that EMCV translation initiation occurs at the same AUG codon at which the ribosome enters, near the 3' border of the IRES (Kaminski *et al.*, 1990). The scenario for FMDV is slightly different again in that it possesses two initiation codons (Sanger *et al.*, 1987). The first of these is the AUG codon at the 3' border of the IRES and the second is 84 nucleotides downstream, in-frame. As a result, two forms of the leader protein are produced called Lab and Lb. Lb is a truncated version of Lab, lacking an N-terminal region, but both possess the same protease activity. Approximately 75% of ribosomes initiate at the second AUG and so more Lb is produced than Lab (Sanger *et al.*, 1987). The exact ratio of Lb to Lab expressed varies between strains.

The mechanism by which more translation initiation occurs at the second AUG is unclear. One hypothesis is that the ribosomes enter very close to the Lab start site but because of the poor context of the AUG codon at the Lab start site, the majority of

ribosomes scan downstream to reach the second AUG codon that has a more favourable context (Belsham, 1992). This model was based on the observation that ribosomes initiated translation at additional AUG codons placed between the Lab and Lb start sites. However, there is conflicting experimental data that suggests not all the ribosomes enter the IRES element at the Lab initiation site. For instance, experiments in which the context of the Lab AUG codon was improved increased the efficiency of initiation occurring at the Lab site but had no effect on the level of initiation occurring at the Lb site (Lopez de Quinto & Martinez-Salas, 1999). This is consistent with an *in vitro* assay in which ribosome scanning between the Lab and Lb initiation codons was inhibited and yet translation initiation at the downstream AUG was only decreased to a limited extent (Poyry *et al.*, 2001). A second hypothesis is that the majority of ribosomes scan along to the Lb site but a small proportion of ribosomes reach it by another mechanism, possibly by ribosome shunting.

The parechovirus IRES is considered to belong to the aphtho- and cardiovirus group as it has a very similar predicted secondary structure (Nateri *et al.*, 2000). Domains I, J and K were shown to be fundamentally important for parechovirus IRES activity, the same as for aphtho- and cardiovirus IRES elements. Nonetheless, the parechovirus IRES differs in that domains H and L do not significantly affect IRES activity.

Group 3 IRES Elements

The third group of picornaviral IRES elements consists of the HAV IRES. Initially, the HAV IRES was identified as having a similar secondary structure to the

Group 2 IRES elements (Brown *et al.*, 1991; Brown *et al.*, 1994) but further characterisation has revealed that the HAV IRES has several differences. It has the lowest activity of all the picornavirus IRES elements *in vitro* and in a variety of cell types (Borman *et al.*, 1995; Borman *et al.*, 1997). Similar to Group 1 IRES elements, the HAV IRES does not function effectively in rrl. In contrast to Group 1 IRES elements, this activity is corrected by the addition of cytoplasmic liver extract, not cytoplasmic HeLa cell extract (Glass & Summers, 1993). This indicates the HAV IRES requires different *trans*-acting factors for maximum activity

1.2.3b Role of Canonical Proteins in Picornavirus IRES-Mediated Translation

A lot of research has been done to determine the mechanism used by picornavirus IRES elements. Surprisingly, picornavirus IRES-mediated translation uses many of the same factors as cap-dependent translation (shown in Figure 5). This has been demonstrated by the fact that eIF2, eIF3 and eIF4F are essential for 40S ribosome recruitment to the EMCV and FMDV IRES in an *in vitro* ribosome binding assay (Pestova *et al.*, 1996b; Pilipenko *et al.*, 2000). The factor eIF4B stimulates EMCV translation initiation, as does PTB to a lesser extent (Pestova *et al.*, 1996b). Further analysis showed that eIF4G binds directly to the IRES element and the complex eIF4F can be substituted for the middle third of eIF4G and eIF4A for ribosome recruitment to occur on the EMCV IRES (Pestova *et al.*, 1996a). The binding site for eIF4G is within the J-K domains of the cardio- and aphthovirus IRES elements (Kolupaeva *et al.*, 1998; Lopez de Quinto & Martinez-Salas, 2000; Saleh *et al.*, 2001; Stassinopoulos & Belsham, 2001). The presence of eIF4A stimulates binding of the central portion of eIF4G to the IRES (Lomakin *et al.*, 2000; Pilipenko *et*

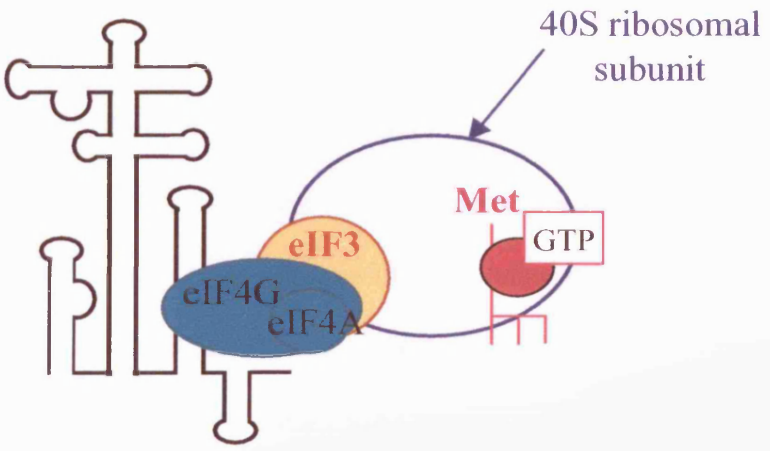

Figure 5: Model of ribosome recruitment by the EMCV/ FMDV IRES elements. The EMCV/ FMDV IRES elements require canonical translation factors for activity and it is believed that the IRES recruits 43S preinitiation complexes through its interaction with eIF4G.

al., 2000). Indeed, eIF4A has been shown to be essential for IRES-mediated translation as dominant negative mutants of eIF4A inhibit translation from picornavirus IRES elements (Pause *et al.*, 1994b; Svitkin *et al.*, 2001a).

The HAV IRES is unique in that it requires intact eIF4F for activity and is inhibited by cleavage of eIF4G by the viral proteases, 2A and L (Whetter *et al.*, 1994; Borman *et al.*, 1995). Moreover, addition of a cap analogue or 4E-BP inhibits HAV translation (Brown *et al.*, 1994; Ali *et al.*, 2001; Borman *et al.*, 2001). This suggests that HAV IRES activity requires eIF4G to be associated with eIF4E. This could either be due to a direct interaction between eIF4E and the HAV IRES. Alternatively, it could be that the binding of eIF4E to eIF4G changes the conformation of eIF4G so that it promotes binding to the HAV IRES (Ali *et al.*, 2001b).

It is assumed that the PV and HRV IRES elements require similar canonical factors to the cardio- and aphthovirus IRES elements although they clearly require additional *trans*-acting factors. This is reinforced by the observation that the dominant-negative form of eIF4A strongly inhibits PV IRES-mediated translation (Pause *et al.*, 1994b; Svitkin *et al.*, 2001a) but the binding site for eIF4G within entero-/rhinovirus IRES elements has yet to be determined. Recently, the binding site for eIF4B has been mapped within the PV IRES and lies within domain V although sequences within domain VI also seem to be important to some extent (Ochs *et al.*, 2002). This is similar to the binding site of eIF4B within the FMDV and EMCV IRES elements which also lies at the 3' end of the IRES (Meyer *et al.*, 1995; Kolupaeva *et al.*, 1998; Lopez de Quinto *et al.*, 2001). Indeed, the interactions of the IRES with canonical translation factors appear to be clustered around the 3' end of the IRES as a subunit of the factor

eIF3 has recently been shown to interact with domain 5 of the FMDV IRES (Lopez de Quinto *et al.*, 2001).

PABP may also play a role in picornavirus translation since the poly(A) tail at the 3' end of the RNA genome has been shown to stimulate IRES-mediated translation (Bergamini *et al.*, 2000). This stimulation is mediated through PABP interaction with eIF4G (as for cellular mRNAs) (Michel *et al.*, 2001; Svitkin *et al.*, 2001b). Hence, PABP-mediated stimulation may be relevant in the first few rounds of translation within FMDV, enterovirus and rhinovirus-infected cells before eIF4G cleavage which abrogates poly(A) tail-mediated stimulation. On the other hand, PABP-mediated stimulation may be involved throughout the EMCV infectious cycle, as there is no cleavage of eIF4G.

1.2.3c Role of *Trans*-Acting Factors in Picornavirus IRES-Mediated Translation

As previously discussed, several *trans*-acting factors have been identified which are either essential or stimulatory to picornavirus IRES activity. The different picornavirus IRES elements display varying translational efficiencies within rrl and within different cell types (Borman *et al.*, 1995; Borman *et al.*, 1997; Roberts *et al.*, 1998). It has been suggested that IRES activity may affect virus tropism and therefore the identification of *trans*-acting factors is valuable. The activity of the PV IRES is stimulated by the La autoantigen, PCBP and PTB as described below.

La is involved in the initiation and termination of RNA polymerase III transcription within uninfected cells. It has also been found associated with various

small RNA molecules. Within rrl, La has been shown to stimulate PV IRES activity and increase the selection of the correct initiation codon (Meerovitch *et al.*, 1993). La is predominantly distributed within the nucleus but during PV-infection the viral protease 3C cleaves La and a truncated La protein, still capable of stimulating PV RNA translation, accumulates in the cytoplasm (Shiroki *et al.*, 1999). Initially it appeared that the level of La required for PV IRES stimulation was higher than the *in vivo* concentration of La but this redistribution may increase the localised intracellular concentration of La.

PCBP is a KH domain RNA binding protein and its putative function is mediating mRNA stability. Interestingly, PCBP has been implicated in several aspects of PV infection. As discussed before, PCBP binds to the cloverleaf structure within the 5' UTR which is involved in RNA replication. This interaction has also been shown to be involved in viral RNA stability (Murray *et al.*, 2001). In addition PCBP greatly stimulates PV and rhinovirus IRES activity (Blyn *et al.*, 1996; Blyn *et al.*, 1997; Walter *et al.*, 1999). It is important to note that PCBP also binds to the FMDV and EMCV IRES elements but has no effect on their activity (Walter *et al.*, 1999; Stassinopoulos & Belsham, 2001).

It has been shown that PTB stimulates the activity of the HRV and PV IRES elements (Borman *et al.*, 1993; Hunt & Jackson, 1999). PTB binds to multiple sites within the PV IRES (Hellen *et al.*, 1994a). A complex consisting the unr protein (named from Upstream of ras) and the unr-interacting protein was found to act synergistically with PTB to stimulate HRV activity (Hunt *et al.*, 1999). Interestingly this complex had no effect on PV IRES activity. PTB also binds to both the EMCV

and FMDV IRES (Kolupaeva *et al.*, 1996). This stimulates FMDV IRES activity but has little effect on the activity of the EMCV IRES (Pestova *et al.*, 1996b; Niepmann *et al.*, 1997; Kaminski & Jackson, 1998; Pilipenko *et al.*, 2000). A novel *trans*-acting factor has been identified for the FMDV IRES, called $ITAF_{45}$, which is a proliferation-dependent protein (Pilipenko *et al*, 2000). This protein is distributed throughout the cytoplasm at specific points in the cell cycle (metaphase to telophase) and is therefore likely to stimulate the activity of the FMDV IRES at these points in the cell cycle.

The common feature between these *trans*-acting factors is that they are RNA binding proteins. In particular, the majority, contain several RNA binding motifs. They therefore have the potential to interact with multiple sites within the IRES. For this reason, it is plausible that they are involved in the formation or stability of the tertiary structure of the IRES element. They can be thought of as RNA chaperones which ensure the IRES folds correctly. The best evidence of this is for PTB. PTB is a homodimer and each monomer has 4 putative RNA binding domains. Multiple PTB binding sites have been mapped within the PV, FMDV and EMCV IRES elements (Hellen *et al.*, 1994a; Kolupaeva *et al.*, 1996). Consistent with the idea that PTB is an RNA chaperone, it was discovered that the activity of an EMCV IRES mutant became dependent on PTB (Kaminski *et al.*, 1995). This mutant contained an extra A in an A bulge between the J and K domains which probably led to a distortion of the IRES. Presumably, PTB was essential for the activity of this mutant as it ensured correct folding of the IRES.

1.2.3d Role of Viral Proteins in Picornavirus IRES Activity

None of the virus encoded proteins are essential for viral translation. Nonetheless, the presence of the enterovirus 2A or the FMDV L protease has been noted to stimulate IRES activity. Within mouse neuroblastoma cells and rrl, the viral proteases significantly stimulated the activity of enterovirus and rhinovirus IRES elements (Borman *et al.*, 1995; Borman *et al.*, 1997). Only modest stimulation was observed for the EMCV and FMDV IRES but the level of stimulation increased in other cell types (Roberts *et al.*, 1998). Generally, it appears that the level of stimulation is greatest in cells in which the IRES elements have a low activity (Roberts *et al.*, 1998).

One possible reason for this activation could be that the cleavage of eIF4G by the viral proteases inhibits cap-dependent translation and therefore provides a greater pool of available translation machinery. However, there are several lines of evidence against this. For example, the addition of 4E-BP inhibits cap-dependent translation but does not increase IRES activity (Roberts *et al.*, 1998). Additionally, IRES stimulation by the 2A protease has been reported in cells in which cap-dependent translation was not significantly inhibited (Hambidge & Sarnow, 1992). The main cleavage product of eIF4G does not directly stimulate IRES activity either (Roberts *et al.*, 1998). Therefore, it may be that the viral proteases cleave another cellular protein and this in some way activates the viral IRES.

1.2.3e Tertiary Structure of the Picornavirus IRES Element

The tertiary structure of the picornavirus IRES elements is believed to be essential for activity. This hypothesis has been reinforced by the idea of *trans*-acting factors such as PTB acting as RNA chaperones. Furthermore, within Group 1 and 2 IRES elements, a GNRA tetraloop is absolutely conserved and this motif has been implicated as being involved in RNA tertiary interactions (e.g. Costa & Michel, 1995). Mutations within this motif have reinforced the idea that the GNRA tetraloop is critical for IRES activity (Lopez de Quinto & Martinez-Salas, 1997; Roberts & Belsham, 1997; Robertson *et al.*, 1999). Additionally, defective picornaviral IRES elements can be complemented in *trans* by co-expression with a functional IRES element (Stone *et al.*, 1993; Drew & Belsham, 1994; van der Velden *et al.*, 1995; Roberts & Belsham, 1997). This suggests RNA:RNA interactions are taking place. Long-range RNA: RNA interactions have been shown to occur within the FMDV IRES *in vitro* (Ramos & Martinez-Salas, 1999). The overall tertiary structure of the FMDV IRES has been visualized using electron microscopy but unfortunately these experiments provided very low resolution data (Beales *et al.*, 2001). The large size of the IRES elements is problematic for X-ray crystallography and the largest RNA molecule determined in this way is only 160nt long (Cate *et al.*, 1996). Consequently the tertiary structure of the picornavirus IRES elements remains largely unexplored. However, the tertiary structure of several small regions of the non-picornavirus, hepatitis C virus (HCV) IRES have been determined by both NMR and cystallography (Klinck *et al.*, 2000; Collier *et al.*, 2002; Kieft *et al.*, 2002). Possibly the same approach could be used to investigate the three-dimensional shape of various functional domains of the picornavirus IRES elements.

1.3 Other IRES Elements

1.3.1 Viral IRES Elements

Several viruses other than picornaviruses are now known to contain IRES elements. These include hepaciviruses, pestiviruses, retroviruses, lentiviruses and insect RNA viruses (Reynolds *et al.*, 1995; Pestova *et al.*, 1998b; Berlioz & Darlix, 1995; Ohlmann *et al.*, 2000; Wilson *et al.*, 2000a). There is a lot of variation between all the different IRES elements although the IRES elements of hepaciviruses and pestiviruses are very similar as they belong to the same family (*Flaviviridae*). The best characterised IRES (other than picornavirus IRES elements) is the HCV IRES. It differs greatly from the picornaviral IRES elements both in function since it does not require eIF4G and also in structure. The IRES element lying within the intergenic region of the genome of cricket paralysis virus (an insect RNA virus) is again very different. This IRES is capable of recruiting ribosomes directly in the absence of any translation factors. Indeed, the genome from the closely related *Plautia stali* intestinal virus contains an IRES which is able to initiate translation without initiator Met-tRNA$_i$. The translation initiation mechanisms used by these IRES elements are described in detail below:

1.3.1a HCV IRES

The secondary structure of HCV has been well characterised and contains 4 highly structured domains (shown in Figure 23 in Chapter 5) (Brown *et al.*, 1992; Honda *et al.*, 1999). This structure is very similar to the IRES elements from the

pestivirus genus including bovine viral diarrhea virus (BVDV) and classical swine fever virus (CSFV) although they have low sequence identity (Brown *et al.*, 1992; Wang *et al.*, 1995; Honda *et al.*, 1999). The first domain (nt 1-40 of the 5' UTR) of the HCV IRES is thought to be unnecessary for the activity of the IRES (Rijnbrand *et al.*, 1995; Honda *et al.*, 1996; Reynolds *et al.*, 1996). Translation initiation occurs at the 3' border at nucleotide 342 (Reynolds *et al.*, 1996). Therefore, the HCV IRES element is significantly smaller than the picornavirus IRES elements (with the exception of teschoviruses). However, sequences immediately downstream of this AUG, within the open reading frame of the core protein have been shown to be important for efficient IRES-driven translation (Reynolds *et al.*, 1995; Honda *et al.*, 1996; Lu & Wimmer, 1996). The involvement of the coding sequence is now believed to be due to a requirement for a lack of secondary structure immediately downstream of the initiation site (Rijnbrand *et al.*, 2001). A highly conserved pseudoknot just upstream of the initiation codon has been shown to be critical for IRES function (Wang *et al.*, 1995).

The HCV IRES differs significantly from picornavirus elements in that eIF4G, eIF4B and eIF4A are not required for recruitment of the 43S preinitiation complex (Pestova *et al.*, 1998b). Indeed translation initiation on the HCV IRES is unaffected by dominant negative mutants of eIF4A which block cap-dependent translation and picornavirus IRES-directed translation initiation (Pause *et al.*, 1994b; Pestova *et al.*, 1998b). The factor eIF3 stimulates, but is not essential for, 43S ribosomal binding to the HCV IRES (Pestova *et al.*, 1998b). However, eIF3 is required for formation of 80S ribosomes at the initiation codon (in addition to eIF5, eIF5B and GTP). eIF3 binds directly to domain III of the HCV IRES and is thought to stabilise the interaction of the 40S ribosome subunit with the IRES (Sizova *et al.*, 1998). Nonetheless, it appears that

the high affinity of the 40S ribosome subunit for the IRES drives the formation of the 48S preinitiation complex (Kieft *et al.*, 2001). The 40S ribosome subunit binds directly to the HCV IRES at multiple points (Pestova *et al.*, 1998b; Kolupaeva *et al.*, 2000). This binding induces a conformational change in the 40S ribosome subunit (Spahn *et al.*, 2001a). The 40S ribosome binding sites lie within domain III and IV and involve nucleotides which are critical for IRES activity such as a highly conserved GGG triplet in stem loop of IIId and the pseudoknot (Wang *et al.*, 1995; Buratti *et al.*, 1998; Jubin *et al.*, 2000). The ribosomal S9 protein binds directly to the HCV IRES but is not thought to be the sole determinant for the binding of the 40S ribosome subunit to the IRES (Pestova *et al.*, 1998b; Kolupaeva *et al.*, 2000). Ribosome recruitment depends on the tertiary structure of the IRES (Kieft *et al.*, 2001) as does the binding of S9 ribosomal protein (Odreman-Macchioli *et al.*, 2000). This is the only evidence to date that the tertiary structure of an IRES element affects protein interactions. Other proteins such as PTB, La and heterogeneous nuclear ribonucleoprotein L (hnRNP L) have been shown to bind to the HCV IRES (Ali & Siddiqui, 1995; Ali & Siddiqui, 1997; Hahm *et al.*, 1998). PTB and La stimulate IRES activity (Ali *et al.*, 2000; Anwar *et al.*, 2000). The factors eIF2Bγ and eIF2γ have also been suggested to be cofactors for HCV IRES-mediated translation (Kruger *et al.*, 2000).

1.3.1b Insect RNA Virus IRES Elements

Cricket paralysis-like viruses are a group of positive sense viruses that infect insects. Examples include cricket paralysis virus (CrPV), *Plautia stali* intestinal virus (PSIV) and *Rhopalosiphum padi* virus (RhPV). They have a dicistronic genome in which the first cistron encodes a polyprotein containing the non-structural proteins and

the second cistron encodes a polyprotein which is processed to the structural proteins (that are remarkably similar to the picornavirus capsid proteins). The 5' and intergenic untranslated regions are both long, about 500nt, and have been reported to contain IRES elements (Sasaki & Nakashima, 1999; Domier *et al.*, 2000; Wilson *et al.*, 2000a; Woolaway *et al.*, 2001).

The IRES located within the intergenic space (the IGR IRES) mediates translation of the second ORF elements and is very short, about 180nt-long. It has three domains and contains 3 conserved pseudoknots, one of which is known to be important for IRES activity (Sasaki & Nakashima, 2000; Kanamori & Nakashima, 2001). The IGR IRES has attracted a lot of interest as it initiates translation at a codon which does not encode methionine. The PSIV IRES initiates translation at a CAA codon (encoding glutamine), the RhPV intergenic IRES uses CCU (encoding proline) and the CrPV intergenic IRES initiates at GCU (encoding alanine) (Sasaki & Nakashima, 1999; Domier *et al.*, 2000; Wilson *et al.*, 2000a). This is very unusual as the initiation codon in eukaryotes is almost always AUG and the known exceptions only differ from AUG by one nucleotide which can still be recognised by Met-tRNAi. Translation initiation of the second ORF occurs without the initiator tRNA, eIF2 or GTP (Sasaki & Nakashima, 2000; reviewed in McCarthy, 2000; RajBhandary, 2000). *In vitro* ribosome binding assays confirm that the CrPV IGR IRES element does not require any translation initiation factors for 80S ribosome formation (Wilson *et al.*, 2000b). The first codon GCU is located within the A site of the ribosome and a triplet CCU, which forms the functionally-relevant pseudoknot, is positioned in the ribosomal P site. Therefore, it is possible that the mechanism of translation initiation is similar to translation elongation (described in Section 1.5.1) and that the IGR IRES is a

molecular mimic of the initiator tRNA. Domains 1 and 2, which associate directly with the 40S ribosome subunits, are closely associated with one another because of pseudoknot formation. Domain 3, containing the pseudoknot important for IRES activity, is thought to be located more externally and may mimic tRNA, allowing the initiation of peptide synthesis (Kanamori & Nakashima, 2001).

The IRES elements present within the 5'UTRs of cricket paralysis-like viruses are known initiate at conventional AUG codons and are not so well characterised. It is interesting to note that the RhPV 5' UTR IRES and the CrPV IGR-IRES both function in insect, mammalian and plant *in vitro* translation systems (Wilson *et al.*, 2000a; Woolaway *et al.*, 2001). This means these elements have the potential to be used in plant or insect expression systems. One possible reason for the use of two separate IRES elements within the cricket paralysis-like virus genomes could be to allow differential expression. In fact the second ORF (encoding the structural proteins) is expressed at higher amounts than the first ORF (Moore *et al.*, 1981)

1.3.2 Cellular IRES Elements

1.3.2a Identification of Cellular IRES Elements

The mRNA encoding BiP, the immunoglobin binding protein, was the first cellular mRNA found to contain an IRES element (Sarnow, 1989b). It was discovered because BiP was still translated within PV-infected cells in which cap-dependent translation was inhibited. Since then many cellular IRES elements have been identified (listed in database http://www.rangueil.inserm.fr/IRESdatabase). These mRNAs

encode proteins which are involved in many cellular processes such as differentiation (e.g. PDGF2), development (e.g. *Drosophila antennapedia*), cell growth/ transformation (e.g. c-myc) and apoptosis (e.g. X-linked inhibitor of apoptosis). The vast majority of these have been identified due to their activity in dicistronic assays. Within these assays, the putative IRES elements are placed between two cistrons. The translation of the upstream cistron is cap-dependent but translation of the second, downstream cistron is dependent on the presence of a functional IRES element in the intergenic region. Criticism of this assay has arisen, as care must be taken to ensure the dicistronic mRNA is complete and has not been broken to yield monocistronic constructs (e.g. Kozak, 2001a). This could occur if a cryptic splice site or a promoter sequence was present within the putative IRES element.

An alternative method in which to isolate cellular mRNAs containing IRES elements has been successfully used (Johannes & Sarnow, 1998; Johannes *et al.*, 1999). This involves identification of cellular mRNAs which, like BiP, are translated in PV-infected cells in which cap-dependent translation is inhibited. These mRNAs will still be associated with the polysomes within PV-infected cells and therefore can be isolated. This technique has been coupled with cDNA microarray technology to identify the mRNAs isolated (Johannes *et al.*, 1999). It was found that 200 out of the 7000 analysed mRNAs were still associated with polysomes in PV infected cells in which most of eIF4G (both isoforms) was cleaved. One disadvantage of this system is that it also isolates mRNAs which do not possess an IRES element but can still be translated at low concentrations of eIF4G. For example, translation of vaccinia virus mRNAs and adenovirus late mRNAs have a low requirement for eIF4F although they do not contain an IRES element (Dolph *et al.*, 1990; Schneider, 1995; Mulder *et al.*,

1998). Also, it would exclude the HAV IRES which requires intact eIF4G for activity. Despite this, several novel IRES elements such as Pim-1 and Cyr-61 (involved in angiogenesis and transcription, respectively) were identified in addition to IRES elements already isolated from previous studies.

1.3.2b Structure of cellular IRES elements

Initially a common structural feature was discovered within cellular IRES elements (Le & Maizel, 1997). The motif consisted of a Y-shaped double-hairpin structure and a small hairpin but this has not been shown to be essential for IRES activity. The structures of cellular IRES elements seem to differ significantly from those of viral origin. Viral IRES elements have quite clearly defined boundaries. In contrast, the boundaries of cellular IRES elements are often difficult to define. In addition, the IRES elements from several cellular mRNAs such as BiP, c-myc and VEGF possess "modules" capable of IRES activity (Yang & Sarnow, 1997; Stoneley *et al.*, 1998; Huez *et al.*, 1998). These short sequences are not overlapping and no common motif has been identified, suggesting that many sequences may act as modular IRES elements. This has prompted large-scale screening of short, random oligonucleotide sequences for IRES activity (Venkatesan & Dasgupta, 2001; Owens *et al.*, 2001). These screens have proved successful and four novel IRES modules have been identified. The best-characterised IRES module is a 9-nucleotide sequence present within the Gtx IRES (Chappell *et al.*, 2000a). When multiple copies of this 9 nucleotide sequence were linked together the IRES activity increased significantly (10 copies linked together increased activity by about 500-fold). The IRES module is 100% complementary to part of the 18S ribosomal RNA and so probably functions like

a prokaryotic Shine-Dalgarno sequence. This has been emphasised by the fact that the 9-nt sequence could be crosslinked to ribosomes presumably through its interaction with 18S rRNA (Hu *et al.*, 1999). Sequence similarity to the 18S rRNA has also been noted in other cellular IRES elements although their ability to act as a module with IRES activity has yet to be determined (Bernstein *et al.*, 1997; Gan *et al.*, 1998). However, it is likely that other methods for ribosome recruitment may be utilised by cellular IRES elements such as protein interactions.

1.3.2c Protein Requirements of Cellular IRES Elements

Little is known about the role of canonical translation factors in internal initiation by cellular IRES elements. The only indication that they are involved is that overexpression of eIF4G in cultured cells stimulates the activity of the IRES present in the mRNA encoding ornithine decarboxylase (Hayashi *et al.*, 2000). Also, the apoptotic initiation factor DAP5 stimulates IRES-mediated translation of several cellular IRES elements which are expressed during apoptosis such as DAP5 and c-myc (Henis-Korenblit *et al.*, 2000; Henis-Korenblit *et al.*, 2002). The involvement of non-canonical, *trans*-acting factors has been studied in more depth. The protein La stimulates the IRES-mediated translation of the X-linked inhibitor of apoptosis (XIAP) and BiP (Holcik & Korneluk, 2000; Kim *et al.*, 2001). PTB and unr have been identified as *trans*-acting factors for IRES-mediated translation of apoptotic protease-activating factor 1 (apaf-1) (Mitchell *et al.*, 2001). Interestingly, PTB appears to inhibit the activity of the BiP IRES (Kim *et al.*, 2000). The IRES in the PDGF2 mRNA has been shown to interact with the protein hnRNP C (Sella *et al.*, 1999). To date, the exact role of these *trans*-acting factors is unclear. Yet, it should be noted that

the proteins hnRNP C, PTB and La are predominantly localised to the nucleus. This is particularly interesting as several cellular IRES elements require a nuclear event before they are active (Stoneley *et al.*, 2000a). The exact reason for this is undetermined.

1.3.2d Expression of Cellular IRES Elements

It is important to remember that cellular mRNAs containing an IRES element will also possess a cap structure at the 5' end. This allows the protein to be produced cap-dependently as well as cap-independently (Henis-Korenblit *et al.*, 2000; Cornelis *et al.*, 2000). The protein produced by these two means may differ. For example, two isoforms of the PITSLRE protein kinase are produced (p100 and p58) from the combination of cap-dependent translation and IRES-mediated translation (Cornelis *et al.*, 2000). Another advantage of a cellular mRNA possessing an IRES is that it allows expression of the protein at times when cap-dependent translation is inhibited. The IRES-mediated translation of several cellular proteins is stimulated during apoptosis and specific phases of the cell cycle, when the level of cap-dependent translation is low (Coldwell *et al.*, 2000; Cornelis *et al.*, 2000; Henis-Korenblit *et al.*, 2000; Pyronnet *et al.*, 2000; Stoneley *et al.*, 2000b). Other stress conditions such as hypoxia, amino acid deprivation and γ-radiation can also activate several cellular IRES elements (Stein *et al.*, 1998; Holcik *et al.*, 2000; Fernandez *et al.*, 2001). Both eIF4G and DAP5 (an isoform of eIF4G involved in apoptosis) were reported to contain IRES elements (Gan & Rhoads., 1996; Gan *et al.*, 1998; Henis-Korenblit *et al.*, 2000). This would allow translation of eIF4G and its isoforms in conditions when cap-dependent translation is inhibited. However, recent evidence has thrown doubt on whether eIF4G does actually contain an IRES element since there is a promoter sequence present within the putative

IRES element which could explain the results from previous experiments (Han & Zhang, 2002). Nevertheless, this does not explain why the eIF4GI mRNA was found to be associated with polysomes within PV-infected cells when cap-dependent translation was inhibited (Johannes & Sarnow, 1998).

Links between abnormal IRES activity and disease have been reported. For example, a point mutation within the c-myc IRES was shown to increase the activity of the IRES and this mutant IRES could be detected in samples from people suffering from multiple myeloma (Paulin *et al.*, 1996; Paulin *et al.*, 1998; Chappell *et al.*, 2000b). Obviously, the translation control of all proto-oncogenes and growth factors is carefully regulated and understanding the IRES-mediated expression of such proteins is of great importance.

1.4 Other Mechanisms for Translation Initiation

1.4.1 Leaky Scanning

Leaky scanning occurs when the first AUG codon encountered by the scanning ribosome is in poor context. Consequently, some ribosomes will continue scanning and initiate translation at a downstream AUG which is in a better context. The result of this is that two protein products will be produced. If the two AUG codons are in-frame with one another, the two proteins will be identical except that one protein will have an extra amino-terminal region. However, if the second AUG codon is not in-frame with the first, the two proteins will be completely different. Upstream AUG codons usually decrease the level of translation initiation at a downstream initiation

codon. One example of leaky scanning is the translation of the hepatitis B virus polymerase (P) gene. The P protein is translated from a bicistronic pregenomic RNA and its ORF overlaps the core (C) protein ORF. The initiation codon of the P protein is preceded by the C initiation codon and 3 other AUGs that are in different reading frames. The leaky scanning on AUGs in poor context is one mechanism by which the P protein is translated (Lin & Lo, 1992; Fouillot *et al.*, 1993; Hwang & Su, 1998).

1.4.2 Ribosome Shunting

Ribosome shunting essentially means discontinuous scanning. The 40S ribosome subunit is recruited to the 5' end of the mRNA in a cap-dependent manner but is then translocated to a downstream AUG codon. Ribosome shunting has been described to occur on the mRNA encoding mammalian heat shock protein 70 (Hsp70) and various viral mRNAs such as adenovirus late mRNAs, cauliflower mosaic virus 35S mRNA and Sendai virus Y mRNA (Futterer *et al.*, 1993; Yueh & Schneider, 1996; Curran & Kolakofsky, 1998). The best characterised examples of ribosome shunting are of the adenovirus late mRNAs and cauliflower mosaic virus 35S mRNA which use two distinct mechanisms.

Ribosome shunting within the adenovirus late mRNAs allows selective translation of adenovirus late proteins (Yueh & Schneider, 1996). Adenoviruses inhibit cap-dependent translation by inhibiting phosphorylation of eIF4E and this prevents expression of host cell proteins and early adenovirus proteins late in infection (Zhang *et al.*, 1994). The adenovirus late mRNAs contain a tripartite leader with a short unstructured region at the 5'end followed by several stable hairpin structures. These

hairpin structures contain elements necessary for ribosome shunting. There are three conserved elements which show complementarity to the RNA strands of a hairpin in the 18S rRNA and these are involved in the shunting process (Yueh & Schneider, 2000). A similar element is present within Hsp70 mRNA (Yueh & Schneider, 2000). However, the exact mechanism used still remains to be elucidated. One proposed model is that the 40S ribosome subunits are recruited to the 5' end of the mRNA by the cap structure but during scanning the presence of the hairpins within the tripartite leader causes the ribosomes to fall off the mRNA. The shunting element will then rebind the 40S subunits either through a direct interaction with 18S rRNA or indirectly via translation factors. An alternative model suggests that the ribosomes do not fall off the mRNA but rather get halted by the hairpin structures. Tethered to the mRNA, they could interact with the shunting elements (Schneider, 2000). It is unclear how the 40S ribosome subunits are translocated.

Ribosome shunting in cauliflower mosaic virus (CaMV) 35S RNA occurs by a different mechanism and has a different function. The CaMV leader is 600 nucleotides long. It contains 6 to 7 small ORFs and a stable hairpin structure. The presence of the stable secondary structure and the ORFs should inhibit translation but it appears that the scanning 40S ribosomes are shunted across the hairpin structure. The shunting element in the CaMV RNA comprises a short upstream ORF followed by a downstream stable hairpin structure (Dominguez *et al.*, 1998; Hemmings-Mieszczak *et al.*, 1998). The integrity of the short upstream ORF is important for CaMV infectivity (Poogin *et al.*, 2001). Again, the actual mechanism of shunting is still to be elucidated.

1.4.3 Reinitiation

Eukaryotic mRNAs normally contain a single ORF but there are many examples of mRNAs which contain short upstream ORFs (uORFs). When the uORF is non-overlapping with the main ORF, reinitiation can occur. This means that the uORF is translated but after termination the ribosome resumes scanning and initiates at the downstream AUG. Obviously, the efficiency of reinitiation will determine if the presence of upstream ORFs is inhibitory or not to the translation of the main ORF.

One factor which is important in determining reinitiation efficiency is the distance between the stop codon of the uORF and the downstream AUG. Reinitiation becomes more efficient as this distance is increased (Kozak, 1987b). Presumably a longer distance gives the post-termination ribosome more time to re-acquire the translation factors need for reinitiation. As expected, the factor eIF2 is known to be important since the ribosome will need to re-acquire the ternary complex of eIF2/GTP/Met-tRNA$_i$ before reinitiation can occur (Hinnebusch, 1997). In addition, a decrease in reinitiation efficiency is seen when the length of the uORF is increased (Luukkonen *et al.*, 1995; Hwang & Su, 1998; Kozak, 2001b). This is thought to be due to the fact that the longer the elongation phase of translation continues the greater chance that necessary initiation factors are lost. Consistent with this theory, a decrease in reinitiation was observed when a pseudoknot structure was placed within an uORF in a construct capable of reinitiation (Kozak, 2001b). The pseudoknot will have caused a pause in elongation. However, a pseudoknot placed within the main ORF did not affect its translation. The sequence surrounding the stop codon of the uORF has also been shown to be important in determining reinitiation, at least in yeast (Grant &

Hinnenbusch, 1994). Ribosomes are not able to reinitiate translation at an AUG codon upstream of the uORF stop codon (Kozak, 2001b).

1.5 Translation Elongation and Termination

So far, this introduction has discussed mechanisms for translation initiation. However, there are two more processes involved in translation: elongation and termination. A brief summary of both steps is given below:

1.5.1 Elongation

At the end of initiation, the 80S ribosomes have been formed and the initiator tRNA is positioned at the ribosomal P site. The process of elongation is cyclic and one amino acid is added to the growing polypeptide chain per cycle (shown schematically in Figure 6) (reviewed in Merrick & Nyborg, 2000). The sequence of codons in the mRNA determines the sequence of aminoacylated-tRNAs added to the nascent peptide chain. In contrast to translation initiation, there is a high level of conservation between the mechanism used for translation elongation in prokaryotes and eukaryotes. Three elongation factors are involved in both which are called EF1A, EF1B and EF2 within prokaryotes and eEF1A, eEF1B and eEF2 within eukaryotes.

At the start of a cycle of elongation, the next codon to be translated is exposed on the A site of the ribosome. Aminoacylated-tRNAs (aa-tRNAs) form ternary complexes with EF1A:GTP and enter the A site where they are tested as to whether the anticodon of the tRNA base pairs with the exposed codon. If base pairing does occur,

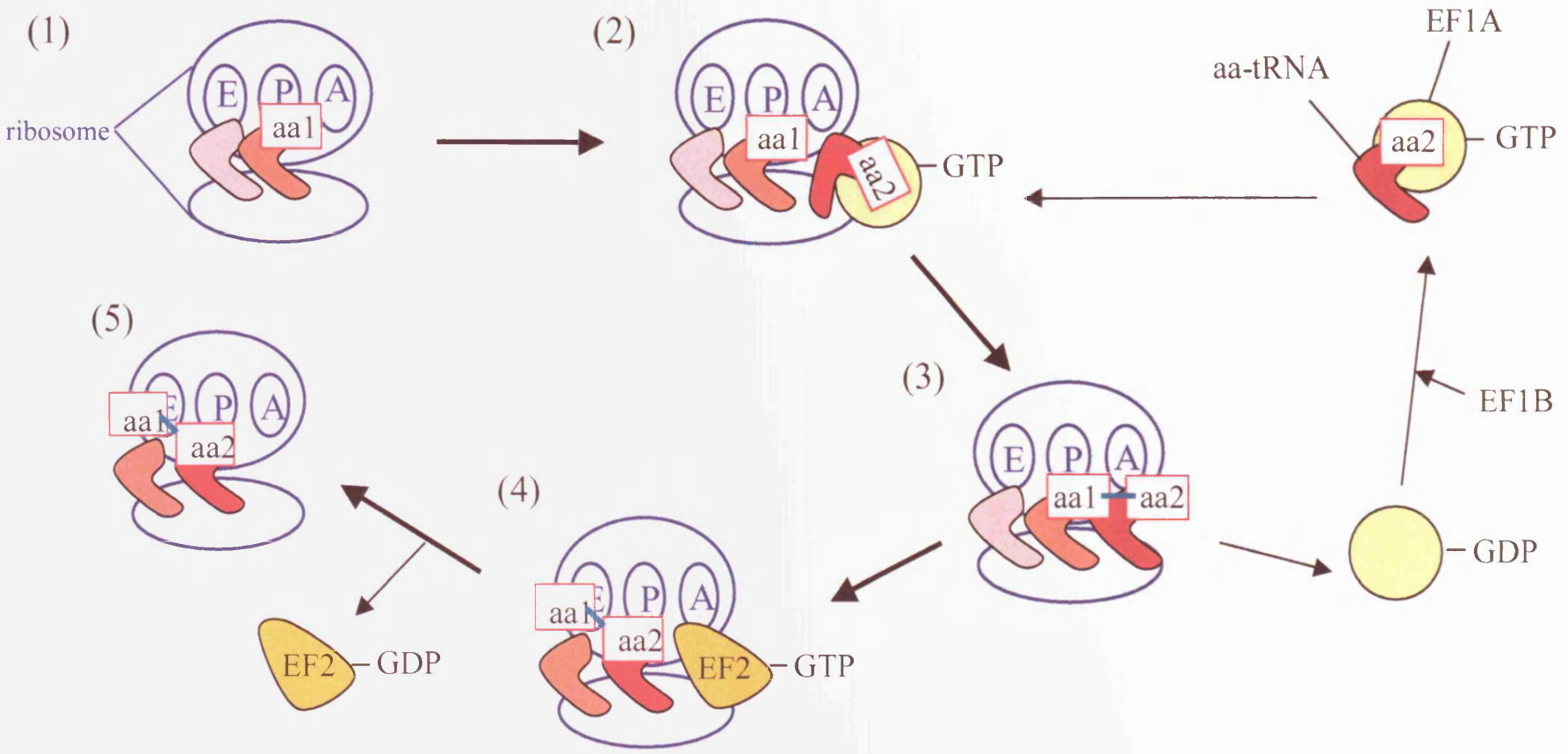

Figure 6: One cycle of translation elongation. See text for details. Factor EF1-GTP recruits the amino acyl-tRNA to the A site of the ribosome (2). GTP hydrolysis occurs and EF1 is released. A peptide bond is then formed between the incoming amino acid and the nascent peptide chain (3). Factor EF2-GTP moves the tRNA along into the P site and is released as EF2-GDP (3 and 4).

the ternary complex is brought into contact with the GTPase activating centre of the ribosome and EF1A:GDP is released from the ribosome. When EF1A:GDP is released, the 3' end of the aa-tRNA enters the A site on the large ribosome subunit and a peptide bond is formed between the incoming amino acid and the growing peptide chain (situated in the P site), catalysed by the peptidyl transferase centre of the ribosome. At this point the incoming tRNA is attached to the peptide chain in the P site but is still situated in the A site. An aa-tRNA from the previous cycle of translation initiation remains in the P site and will be deacylated. The factor EF2:GTP is responsible for moving the incoming tRNA into the P site and moving the recently deacylated tRNA into the exit site of the ribosome. This also exposes the next codon to be translated at the A site and ensures that the ribosome moves along the RNA by exactly 3 nucleotides. This process is GTP dependent. EF2:GTP comes into contact with the GTPase activating centre of the ribosome and is released as EF2:GDP. The elongation factor, EF1B is responsible for facilitating the guanine nucleotide exchange of EF1A:GDP into active EF1A:GTP.

To offer insight into how the elongation factors functions, the structures the prokaryotic factors have been determined and work has started to elucidate the structures of the eukaryotic factors (for a review see Andersen & Nyborg, 2001). In addition, the structures of prokaryotic and eukaryotic ribosomes have been studied in detail. Cryo-EM reconstructions show the ribosome bound to tRNA, EF1A and EF2 (Stark *et al.*, 1997a; Stark *et al.*, 1997b; Agrawal *et al.*, 1998; Agrawal *et al.*, 2000). A crystal structure of the entire prokaryotic ribosome, containing bound tRNAs has been determined to 5.5 Å resolution (Yusupov *et al.*, 2001). It appears that the interface between the ribosome subunits, where the tRNAs bind, largely consists of rRNA rather

than protein (also suggested by Green & Noller, 1997). This confirms reports that the catalytic peptidyl-transferase centre within prokaryotic ribosomes consists of RNA (Nissen *et al.*, 2000). Additionally, it has been shown that the tRNAs bind close to the bridges which link together the two ribosomal subunits (Yusupov *et al.*, 2001). It is believed that tRNA translocation (mediated by EF2) results in movement at the subunit interface. The structure of the complete yeast ribosome has been determined to a 15 Å resolution and this revealed that although there are differences to the prokaryotic ribosome, there are also many similarities (Spahn *et al.*, 2001b). Therefore, prokaryotes and eukaryotes may share a common mechanism for translation elongation.

1.5.2 Termination

The final step of translation is the recognition of the stop codon and translation termination (reviewed in Welch *et al.*, 2000; Ehrenberg & Tenson, 2002). There are 3 codons that signal translation termination: UAG, UAA and UGA. Like elongation, translation termination proceeds with the help of a small number of protein factors. These are called class I and class II release factors. In eukaryotes there is one class I release factor (eRF1) that recognises all three stop codons but in prokaryotes there are two release factors called RF1 and RF2. Protein RF1 mediates termination at codons UAA and UAG whilst RF2 recognises codons UAA and UGA.

The recognition of the stop codon by the class I release factor occurs in the A site of the ribosome. The factor then induces cleavage of the ester bond connecting the peptide chain to the tRNA in the P-site of the ribosome. Recognition of the stop codon

has to be very accurate so that termination does not occur at any other codons and prematurely abort translation. Premature translation termination has been linked to many inherited diseases and therefore is a target for treatment of these diseases (see review Maquat, 2000). The average error rate of stop codon recognition is very low (10^{-5}) but the actual mechanism by which this precise recognition occurs is unclear. What is known is that a sequence of 3 amino acids (PAT in RF1 or SPF in RF2) within the prokaryotic release factors determines which two of the three stop codons the factor recognises (Ito *et al.*, 2000). Also it is known that proof-reading is not used to ensure a low error rate (Freistroffer *et al.*, 2000). The context of the stop codon, especially the nucleotide immediately downstream of the stop codon, has proved to be very important in determining if termination occurs (McCaughan *et al.*, 1995). The sequence required for optimum translation termination in eukaryotes is UAA(A/G) and UGA(A/G) (Brown *et al.*, 1990).

The peptidyl transferase centre of the ribosome is thought to carry out the cleavage of the peptide chain from the tRNA which is induced by the class I release factors. In support of this, the cleavage can occur in the absence of any release factors (and is stimulated by several situations such as high pH or organic solvents) (Caskey *et al.*, 1971). It may be that recognition of the stop codon by the release factor causes a conformational change which induces the peptidyl transferase centre to cleave the peptide bond. Present among all class I release factors is a short 3 amino acid sequence (GGQ) which appears to be critical for inducing cleavage. The role of the class II release factors (eRF3 in eukaryotes and RF3 in prokaryotes) is to facilitate the removal of the class I factor after the cleavage (Zavialov *et al.*, 2001).

There is some speculation that the release factors mimic tRNAs. This has stemmed from the fact that the class I release factors enter the A site of the ribosome and bring about cleavage of the peptide chain by the peptidyl transferase centre of the ribosome. The sequence GGQ has been suggested to mimic the 3' end of the tRNA where the amino acid binds and the SPF motif in RF1 (or PAT in RF2) could mimic the tRNA anticodon. This theory has been fuelled by the determination of the structure of these factors (Song *et al.*, 2000; Vestergaard *et al.*, 2001). Nonetheless, the theory remains to be proven beyond speculation (for reviews see Nakamura *et al.*, 2001; Ehrenberg & Tenson, 2002).

Some *trans*-acting factors have been identified as having a role in translation termination. For example, three Upf proteins, which form a complex, have been found to affect translation termination (Weng *et al.*, 1996a; Weng *et al.*, 1996b; Czaplinski *et al.*, 1998). Upf1p, in particular, has been shown to interact with eRF1 and eERF3 (Czaplinski *et al.*, 1998).

Translation termination can be considered as the second to last step of translation as ribosome recycling occurs after cleavage of the peptide chain from the tRNA. The ribosome recycling factor (RRF) is involved in this step. To date, RRF and ribosome recycling have been studied in detail only in the prokaryotic system. Fast recycling has been shown to require both RF3 and RRF (Freistroffer *et al.*, 1997; Pavlov *et al.*, 1997). The structure determination of RRF also suggests that it may function as a tRNA mimic (Semler *et al.*, 1999) but this has since been disproved (Karimi *et al.*, 1999). It appears that RRF and EF-2 mediate dissociation of the ribosomal subunits through GTP hydrolysis and that IF3 removes the deacylated tRNA

from the P site of the 30S particle (Karimi *et al.*, 1999). It is interesting to note that eRF3 interacts with PABP (Hoshino *et al.*, 1999b). This may serve to strengthen the circularisation of the mRNA (through the PABP-eIF4G interaction) and aid recycling of the terminating ribosomes onto the same transcript.

1.6 Project Aims

The picornavirus IRES elements are the most extensively studied of all the IRES elements identified to date. Knowledge of the proteins which interact with the picornavirus IRES elements has increased significantly within the last five years. For instance, it is clear that the translation initiation factor eIF4G interacts with the J-K domain of cardio- and aphthovirus IRES elements (Kolupaeva *et al.*, 1998; Lopez de Quinto & Martinez-Salas, 2000; Saleh *et al.*, 2001; Stassinopoulos & Belsham, 2001). This is thought to be how picornavirus IRES elements recruit 40S ribosome subunits. Several *trans*-acting factors have also been identified which are thought to act by stabilising the tertiary structure of the picornavirus IRES element.

Nonetheless, there are still several aspects of picornavirus RNA translation which are unclear. One example is that many of the protein interactions have been characterised using *in vitro* assays. Therefore, many have yet to be shown to be functionally relevant *in vivo*. Additionally, within each of the 3 main groups of picornavirus IRES elements there are many nucleotides which are highly conserved. It is likely that these nucleotides have been conserved for a reason since the evolutionary rate of viral genomes is relatively fast and yet the role of most of the nucleotides is unknown. The top of stem-loop I and the J - K domains of the cardio-

and aphthovirus IRES elements show high sequence conservation. The first aim of this thesis was to analyse the role of four such conserved nucleotides within domain J of the EMCV IRES element. A cell selection system was used to isolate functional IRES elements with mutations at these four nucleotides from a pool of mutants containing up to 256 possible sequences. This system allows selection of transfected cells expressing mRNAs containing a functional IRES element. The four conserved nucleotides studied are positioned close to the eIF4G binding site and therefore it was investigated if eIF4GI binding was affected by mutations at these positions. This was done using an *in vitro* bead-IRES-protein binding assay. Additionally, it was shown that the IRES element from HCV was suitable for use in the cell selection system described above. This is of interest as the IRES elements from picornaviruses and HCV differ considerably both in function and structure.

Another topic which was investigated in this thesis was the 2A protease of the enterovirus, SVDV. This is because the 2A protease from entero- and rhinoviruses (in addition to the FMDV L protease) has been shown to have two important roles in picornavirus RNA translation. The first is that it inhibits the cap-dependent translation of host cell proteins which is likely to suppress the anti-viral response of the host cell and to make the translational machinery available for translation of viral RNA. Additionally, the 2A protease stimulates the activity of the IRES element. Residue 20 of the SVDV 2A protease has been shown to be involved in both protease function and in virus virulence (Kanno *et al.*, 1999; Sakoda *et al.*, 2001). In this study, the role of this residue was further investigated by substituting residue 20 for each of the 20 amino acids and analysing the activities of the mutant 2A proteases.

CHAPTER 2

Materials and Methods

2.1 Agarose Gel Electrophoresis

DNA samples were run on 1% agarose gels in TAE buffer (final concentrations: 40mM Tris, 1.14ml/l glacial acetic acid and 1mM EDTA pH 8.0) using ethidium bromide as stain (1μg/ml, Promega). The DNA was viewed under UV illumination and recorded using Gel Doc, BIO-Rad.

RNA samples were run on 1% agarose gels in TBE buffer (final concentrations: 0.1M Tris, 0.1M Boric acid and 5mM EDTA pH 8.0) with ethidium bromide and viewed under UV illumination as above.

2.2 Polymerase Chain Reaction (PCR)

Polymerase chain reactions were carried out using *Taq* DNA polymerase (Roche) unless specified otherwise. Reactions were set up containing approximately 10ng of template DNA, 1μl of mixed dNTPs (Promega, 10mM), 20pmol of each primer (MWG-Biotech or Invitrogen), 5μl of 10x PCR buffer (Roche) and made up to a total reaction volume of 50μl with mQ H_2O. The reactions were initially heated (94°C for 5min) and then *Taq* DNA polymerase (2.5 units, Roche) was added.

The following programme was used:

Step	Temperature	Time	No. of cycles
1-Hot Start (before polymerase added)	94°C	5min	1
2-Denaturing	94°C	45s	x 30
Annealing	varied	45s	
Elongation	72°C	2min	
3- Elongation	72°C	10min	1

For some applications, a proof-reading polymerase, *Pfu*, was used instead of *Taq*. In these cases, the reactions were carried out as above except *Pfu* reaction buffer and 1.5 units of *Pfu* were substituted (Promega).

2.3 DNA Fragment Purification by Low Melting Point Agarose Gel

DNA fragments were separated on a 1% low melting point agarose gel in TAE buffer. Following electrophoresis, the DNA was viewed under UV light and the desired bands excised. The GFX purification kit (Amersham Biosciences Inc) was used to extract the DNA according to the manufacturer's protocol. The DNA was eluted in 50µl mQ H_2O.

2.4 DNA Purification by Phenol:Chloroform Extraction and Alcohol Precipitation

An equal volume of phenol/chloroform/isoamyl alcohol mixture (Invitrogen) was added to the solution containing DNA. This mixture was vortexed for 30s and centrifuged at 14000rpm for 2min. The upper, aqueous layer was transferred to a fresh microfuge tube and 2.5 volumes of ethanol (100%) and 0.1 volumes of sodium acetate (2M, pH 4.5) were then added. If the amount of DNA present was small, 20μg of glycogen (Roche) was added at this point to act as a carrier. The tubes were kept at –20°C for at least 30min. After this, the tubes were centrifuged at 14000rpm for 10min. The supernatant was carefully removed and 1ml of 70% ethanol was added. The tubes were spun at 14000rpm for 5min and again the supernatant was removed. The pellet was air dried for 5min and resuspended in an appropriate volume of mQ H_2O.

2.5 Ligations

A 1:3 molar ratio of vector:insert DNA was used in a reaction mixture containing 2μl of ligase 10x buffer, 3 units T4 DNA ligase (Promega) and made up to a total volume of 20μl with mQ H_2O. The reactions were incubated overnight at 14°C.

2.6 Competent *E.coli* Cells

E.coli DH5α were grown in Luria-Bertani media (10% (w/v) tryptone, 5% yeast extract, 10% NaCl, 20ml) to an OD of 0.2-0.3 at 600 nm and then centrifuged at 3000rpm for 5min. The cells were resuspended in a solution containing 100mM $CaCl_2$ and 10mM Tris pH 7.5 (20ml) and left on ice for 20min before centrifugation

(3000rpm for 5min). The cells were resuspended in a solution containing 100mM $CaCl_2$ and 10mM Tris pH 7.5 (1 ml).

2.7 Transformation of *E.coli*

Ligation mix DNA or mini-prep DNA (5µl) was added to competent DH5α cells (100µl) and incubated on ice for 10min. The mixture was heat shocked at 37°C for 5min and 1ml Luria-Bertani media (LB) was added. Then the samples were incubated at 37°C for 1hr. The resulting cells were either plated out on LB agar plates containing ampicillin or grown overnight in LB media containing ampicillin (for plasmid DNA preps). If the cells were to be plated, the samples were spun at 14000rpm for 1min and 1ml of supernatant was removed. The pellet was resuspended in the remaining 100µl of solution and spread.

2.8 Plasmid DNA Preps

For mini-preps, 5ml of LB media containing ampicillin (100µg/ml) was inoculated with a single colony and incubated at 37°C overnight. Plasmid DNA was extracted using the Promega Wizard mini-prep kit. For maxi-preps, 200ml of LB broth containing ampicillin (100µg/ml) was inoculated with an aliquot of transformed DH5α and grown-up overnight at 37°C. The RPM-1G (BIO-101) kit was used to extract the plasmid DNA. Midi-preps were carried out with 50ml of overnight culture of transformed DH5α using the Qiagen midi-prep kit, following manufacturer's recommendations. All DNA concentrations were calculated by measuring the OD at 260nm and using the following formula:

A_{260} x dilution factor x 50 = concentration (μg/ml)

2.9 Tissue Culture

COS-7 (green monkey kidney cells) and BHK-38 (baby hamster kidney) cells were grown in Dulbeccos Modified Eagles Media (DMEM) media with Hepes supplemented with 10% foetal calf serum (FCS), glutamine (2mM final concentration), penicillin and streptomycin (both 1μg/l). To set up 35mm dishes for transfection, the cells in a 75cm^3 flask were detached using versene-trypsin (20ml). The separated cells were centrifuged at 1500rpm for 2min and the resulting pellet was resuspended in 10ml of fresh media. For COS cells, this suspension was diluted 1 in 5 and 2ml was used per dish. For BHK cells, the cell suspension was diluted 1 in 7 and 2ml was used per dish. The dishes were left overnight at 37°C (in an incubator with humidity and 5% CO_2) to allow the cells to attach.

2.10 Transient Expression Assay

COS-7 cells or BHK-38 cells (approximately 75% confluent, 35-mm dishes) were infected with a recombinant vaccinia virus, vTF7-3, for 1 hr (approximately 5-10 plaque forming units per cell was used, the exact amount used was optimised for maximum reporter gene expression as determined by a luciferase assay as described in Section 2.11). Vaccinia virus vTF7-3 expresses T7 RNA polymerase (Fuerst *et al.*, 1986). During the incubation step, Lipofectin (8μl, Invitrogen) was mixed with Optimem (192μl, Invitrogen) and incubated at room temperature for approximately 45min. The DNA to be transfected (2.5μg unless otherwise stated) was diluted in

200µl mQ H_2O in bijoux tubes and then 200µl of the Lipofectin mix was added. This mix was incubated at room temperature for approximately 20min. When the vaccinia incubation step was complete, the cells were washed with serum-free DMEM (2ml). All media was removed and 400µl of the DNA/Lipofectin mix was added. The cells were then incubated at 37°C for 4-6 hours in a 5% CO_2 incubator to allow transfection to occur. They were shaken every 30min to ensure the cells did not dry out. Then DMEM media with Hepes containing 10% FCS was added. About 20h after the start of transfection, the cells were harvested. For total cell extracts, the cells were harvested in buffer C (50mM Tris pH 8.0, 0.12M NaCl, 0.5% NP40, 400µl). The cell debris was pelleted by centrifugation at 14000rpm for 5min. Otherwise the cells were harvested for use in the selection system as described in Chapter 3.

2.11 Luciferase Assay

Expression of the luciferase reporter gene was measured using a luciferase assay kit (Promega). The luciferase assay substrate was reconstituted according to manufacturer's instructions (Promega). Then an aliquot of cellular extract (10µl) was added to the luciferase substrate (100µl), mixed gently and a luminometer (Bio-orbit) was used to measure the luminescence activity.

2.12 SDS-PAGE and Western Blots

Proteins were analysed using SDS-PAGE and western blot analysis. SDS-PAGE was carried out as described previously (Laemmli, 1970). 10% polyacrylamide mini-gels (Biorad mini-Protean system II or III) were used unless

stated otherwise. The gels were run at 200V. The gels were either stained directly or used for western blots.

If the gels were to be stained, a Coomassie blue stain was used. The gel was then destained in 20% methanol/ 7.5% glacial acetic acid and dried under vacuum at 80°C.

Western blot analysis was used to detect specific proteins. After SDS-PAGE the proteins were blotted onto an Immobilon P membrane (Millipore) using the Biorad mini-Protean system set at 100V, 400mA for 90min and using a transfer buffer containing 20% methanol, 25mM Tris and 190mM Glycine (final concentrations). The membrane was blocked overnight with 5% Marvel (w/v) in 1xTBS-TWEEN (containing 20mM Tris-Cl pH7.6, 14mM NaCl and 0.1% Tween20). The membrane was then incubated with the appropriate primary antibody (see Table 2 for details of all the antibodies used) in 5ml of 5% Marvel solution for 1hr with constant shaking. It was then washed in 1x TBS-TWEEN to remove any unbound antibody (two 30s and two 10min washes). The appropriate peroxidase-labeled secondary antibody (Amersham Biosciences, diluted 1:1600 in Marvel) was incubated with the membrane for 1hr with constant shaking. Washing steps were then carried out again with 1xTBS-Tween solution (2x 30s and 2x 10min). The proteins were visualised by chemiluminescence using the reagents Supersignal (Pierce) or ECL plus (Amersham Biosciences).

Antibody	Spp	Dilution	Manufacturer or Reference
α-myc (9E10)	mouse	1:1000	Santa Cruz Biotech; Roche
α-β-glucuronidase (GUS)	rabbit	1:5000	5 Prime → 3 Prime, Inc
α-actin	rabbit	1:1000	Sigma
α-eIF4GI (C-terminal)	sheep	1:1000	Li *et al.*, 2001a
α-4A (N-terminal)	sheep	1:1000	Li *et al.*, 2001a
α-LUC	rabbit	1:1000	Promega
α-CAT	rabbit	1:3000	5 Prime → 3 Prime, Inc

Table 2: List of all the antibodies used for Western blot analysis. The species of animal the antibodies were raised in are shown as are the dilutions the antibodies were used for Western blot analysis.

2.13 *In Vitro* Transcription/ Translation Reactions

Transcription/translation coupled reactions (TNTs) were set up with T7 Quick Coupled Transcription/ Translation lysate (Promega, 6.5µl), 0.5µg plasmid DNA, [^{35}S]- Methionine (10µCi) and made up to a final volume of 10µl with mQ H_2O. The reactions were incubated at 30°C for 1 hr. An aliquot (3µl) was mixed with SDS sample buffer and dithiothreitol (DTT) (New England Biolabs) and heated at 95°C for 5min. The proteins present in the aliquot were analysed using SDS-PAGE. Large 10% polyacrylamide gels were run at 250V, stained with Coomassie blue stain and then destained in 20% methanol/ 7.5% glacial acetic acid. The gels were dried under vacuum at 80°C and then used for autoradioraphy. In some cases, phosphoimager screening (Personal molecular imager FX/ BIO-Rad) was also carried out for quantification of the proteins produced using Quantity One software.

2.14 DNA Sequencing

An ALFexpress DNA Sequencer (Amersham Biosciences) was used for automated sequencing. The reactions were set up using the AutoRead Sequencing kit as described by the manufacturer (Amersham Biosciences). Plasmid DNA (10µg in a 32µl volume) was denatured by adding 8µl NaOH (2M) and incubating at room temperature for 10min. Then 7µl NaAc (3M), 4µl mQ H_2O and 120µl 100% ethanol were added. After mixing, the samples were left at –20°C for at least 15min. The DNA was then pelleted by centrifugation at 14000rpm for 15min at 4°C. The pellet was then washed in 70% ethanol (70µl) and centrifuged at 14000rpm for a further 10min at 4°C. The supernatant was carefully removed and the pellet was air-dried for

5min. Then 2μl annealing buffer and 2μl of Cy5-labeled primer (20pmol, MWG-Biotech) were added and heated at 65°C for 5min. The sequences of the Cy5 primers used are listed in Table 3. The tubes were transferred to 37°C for 10min and then allowed to cool at room temperature for a further 5min to ensure that the primer had annealed to the single stranded DNA. Extension buffer (1μl, supplied in kit), DMSO (3μl) and T7 DNA polymerase (diluted 1:1 in enzyme dilution buffer, 8 units) were added. Meanwhile, tubes were set up containing 2.5μl of the appropriate nucleotide mix (either A, C, G or T mix). These tubes were heated to 37°C and then 4.5μl of the reaction mix was added. These reactions were allowed to proceed for 5min and then stop buffer was added (5μl). After mixing, the tubes were either stored at –20°C or loaded immediately onto a sequencing gel.

The samples were run on polyacrylamide sequencing gels (using Sequa gel reagents from Amersham Biosciences) using 0.5xTBE buffer (Amersham Biosciences). Prior to loading, the sequencing reactions were heated to 95°C for 3min. After the samples were loaded, the gels were run for 840min at 1600V.

Cy5-labeled primer (anneals to sequence within)	Direction	Sequence
HOOK ORF	reverse	5' GTCACCAGTGGAACCTG 3'
GUS (β-glucuronidase) ORF	forward	5' GGGAGGCAAACAATGAATCA 3'
SP64poly(A)	forward	5' TAGGCTTGTACATATTGTCG 3'

Table 3: The Cy5-labeled primers used in DNA sequencing.

CHAPTER 3

Use of a Cell Selection System to Identify Functional IRES Elements: Analysis of Conserved Nucleotides within the J Domain of the EMCV IRES Element

3.1 Introduction and Aims

Previously, a system was devised in our laboratory to select IRES elements which are functional within cells (Robertson *et al.*, 1999). Dicistronic mRNAs are frequently used to assay for sequences that act as IRES elements and this system utilises dicistronic constructs which contain an upstream β-glucuronidase (GUS) open reading frame (ORF) and a downstream HOOK ORF (shown in Figure 7A) The putative IRES sequence is placed between the two cistrons. Translation of the upstream cistron, GUS, is cap-dependent but translation of the downstream cistron, HOOK, is negligible without the presence of an IRES element immediately upstream. The HOOK ORF encodes a single chain antibody (sFv) modified to contain a transmembrane domain, a membrane signal, a haemagglutinin (HA) epitope and a c-myc epitope. Within the system, the dicistronic mRNAs are transiently expressed in mammalian cells using a recombinant vaccinia virus which expresses T7 RNA polymerase (Fuerst *et al.*, 1986). If a functional IRES is present within the mRNA, HOOK will be expressed and targeted to the plasma membrane. Therefore, at the cell surface the c-myc epitope is displayed which can be recognised by an anti-myc monoclonal antibody (9E10). This, in turn, is recognised by anti-mouse IgG-coated

Figure 7:

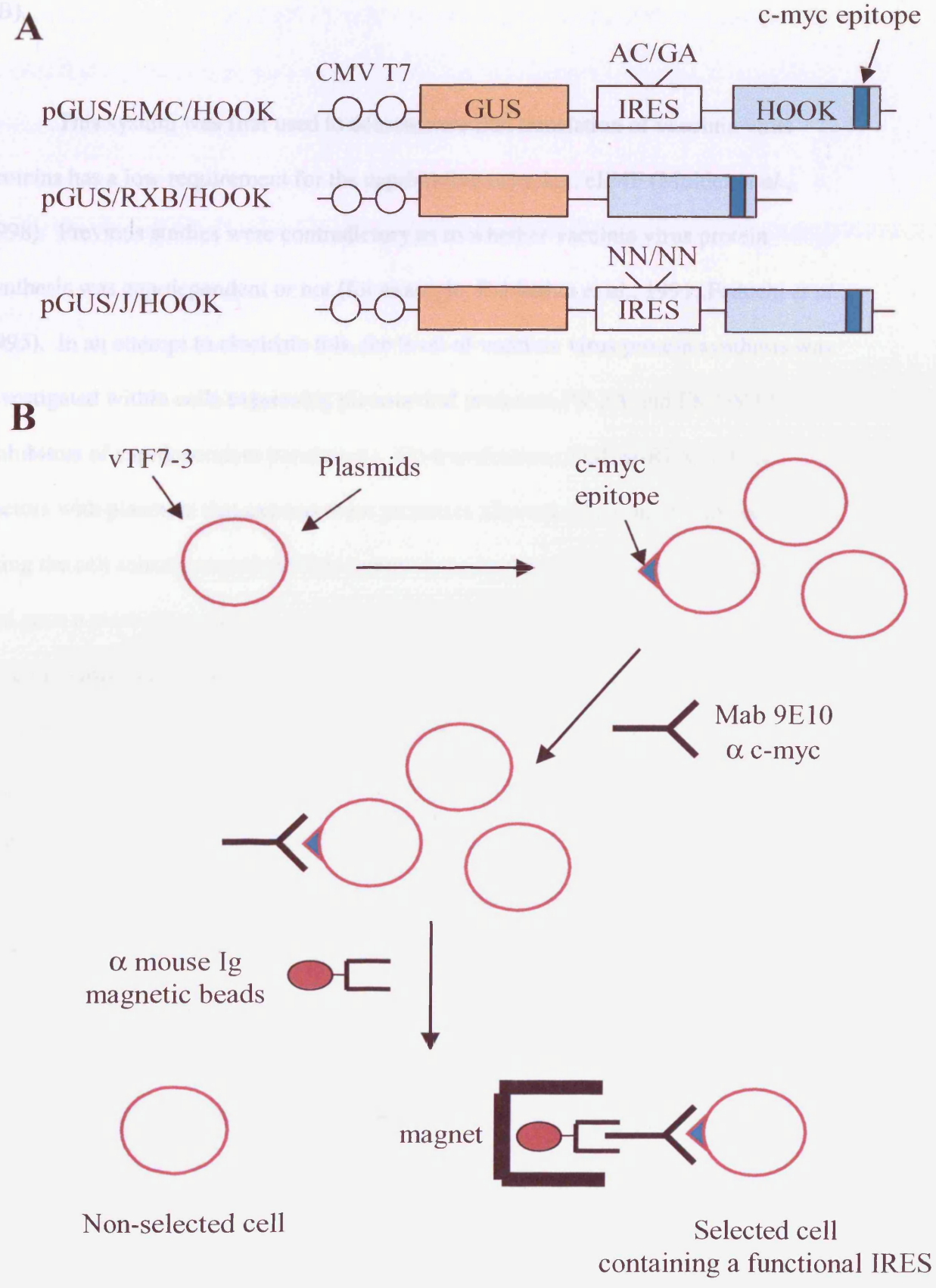
A
c-myc epitope
AC/GA
CMV T7
pGUS/EMC/HOOK
GUS
IRES
HOOK
pGUS/RXB/HOOK
NN/NN
pGUS/J/HOOK
IRES
B
vTF7-3
Plasmids
c-myc
epitope
Mab 9E10
α c-myc
α mouse Ig
magnetic beads
magnet
Non-selected cell
Selected cell
containing a functional IRES

magnetic beads. Therefore, cells that express a dicistronic mRNA containing a functional IRES can be selected using a magnet (shown diagrammatically in Figure 7B).

This system was first used to demonstrate that translation of vaccinia virus proteins has a low requirement for the cap-binding complex, eIF4F (Mulder *et al.*, 1998). Previous studies were contradictory as to whether vaccinia virus protein synthesis was cap-dependent or not (for example, Bablanian *et al.*, 1991; Feduchi *et al.*, 1995). In an attempt to elucidate this, the level of vaccinia virus protein synthesis was investigated within cells expressing picornaviral proteases PV 2A and FMDV Lb (inhibitors of cap-dependent translation). Co-transfection of GUS/IRES/HOOK vectors with plasmids that express these proteases allowed selection of transfected cells using the cell selection system. This removed the background of non-transfected cells and gave a more accurate depiction of whether the picornavirus proteases inhibited vaccinia virus translation. The outcome was that while expression of the GUS reporter sequence required intact eIF4F, the synthesis of vaccinia virus proteins had a low requirement for intact eIF4F. This is consistent with experiments using temperature sensitive vaccinia virus mutants. These mutants expressed a capping enzyme which was defective at capping vaccinia RNAs at the nonpermissive temperature and yet the level of protein synthesis of the viral proteins was not significantly altered (Hassett *et al.*, 1997). Additionally, vaccinia virus mRNAs have short, unstructured 5' UTRs analogous to adenovirus late mRNAs which also have a low requirement for eIF4F for initiation of translation (Dolph *et al.*, 1990; Schneider, 1995).

The cell selection system has also been used to isolate functional IRES elements from a large pool of mutant encephalomyocarditis virus (EMCV) IRES elements (Robertson *et al.*, 1999). An RNA tetraloop fitting the GNRA consensus (where R is a purine) is present within a structure containing a 4-way junction in the apical region of the I domain of cardio- and aphthovirus IRES elements. These tetraloops are believed to be involved in RNA:RNA and RNA:protein interactions. It was known that a single point mutation within this motif (GCGA to GCGC) abolished IRES function (Roberts & Belsham, 1997). To further investigate the general importance of this region for IRES function, the EMCV IRES tetraloop (with the wt sequence of GCGA) was randomised to NNNN. Thereby a pool of up to 256 different mutants was created and this pool was used in the cell selection system. This revealed that the GNRA tetraloop was critical for IRES activity. All functional IRES elements had a tetraloop with a 3' A residue. The majority (75%) of the functional IRES elements recovered from the selection system contained sequences which fitted a RNRA consensus and all contained a purine either at the first or third position of the tetraloop. Non-functional IRES elements were identified which had sequences such as YCYA tetraloops (where Y is a pyrimidine) or no A residue at the fourth base position. This study demonstrated that the selection system could be successfully used to screen a large number of IRES elements for activity. Previous mutagenesis experiments also determined the importance of the GNRA tetraloop (Lopez de Quinto & Martinez-Salas, 1997; Roberts & Belsham, 1997). Nonetheless, this selection system allowed a more extensive examination since only a minority of possible sequences had been investigated in the other studies. The selection system described here has the advantage that a very large number of mutations can be generated and then screened simultaneously.

The importance of the GNRA tetraloop is implied through its conservation in both cardio-/aphthoviruses and entero-/rhinovirus IRES elements. Within each group of IRES elements (i.e. the cardio-/aphthovirus group or the entero-/rhinovirus group) there are certain bases that are absolutely conserved. The conserved bases of the cardio-/aphthovirus group are mainly clustered into the top of domain I and the J/K domains (Figure 8). The role of the majority of these nt remains unclear but the importance of these three domains for IRES activity was highlighted by Duke *et al.* in 1992. Deletions within these three domains significantly reduced translational activity. Further studies have revealed that deletion of the entire J and K domains or even just part of the J domain abolishes IRES activity (Drew & Belsham, 1994; Roberts & Belsham, 1997). One explanation for this finding was the discovery that eIF4G binds within the J and K domains (Kolupaeva *et al.*, 1998, Stassinopoulos & Belsham, 2001; Lopez de Quinto & Martinez-Salas, 2000 and Saleh *et al.*, 2001). In chemical and enzymatic footprinting experiments with the EMCV IRES and eIF4G, the main site of protection was found to be at the J and K domain junction and to contain the oligo(A) loop (Kolupaeva *et al.*, 1998). Interestingly, this loop is conserved within many cardio-/aphthovirus IRES elements and had previously been determined to be critical for IRES activity (Hoffmann & Palmenberg, 1995). However, the oligo(A) loop is not the sole determinant for eIF4G binding as mutant IRES elements which contained this loop in a different structural context were unable to bind eIF4G (Kolupaeva *et al.*, 1998). A more detailed review of the literature concerning the interaction of eIF4G to the J and K domains is given in Chapter 4.

Figure 8: The sequence and predicted secondary structure of the EMCV IRES (adapted from Belsham & Jackson, 2000). The nucleotides shown in black boxes are conserved among all members of the cardio-aphthovirus group and are mainly clustered into the top of domain I and within the J-K domains. Part of the J domain is shown enlarged and the nt targeted for mutagenesis (nt 704-705 and nt 723-724) are shown in orange. These 4 nt were randomised using mutagenesis and the resulting pool of mutants was analysed using a selection system for functional IRES elements.

Figure 8

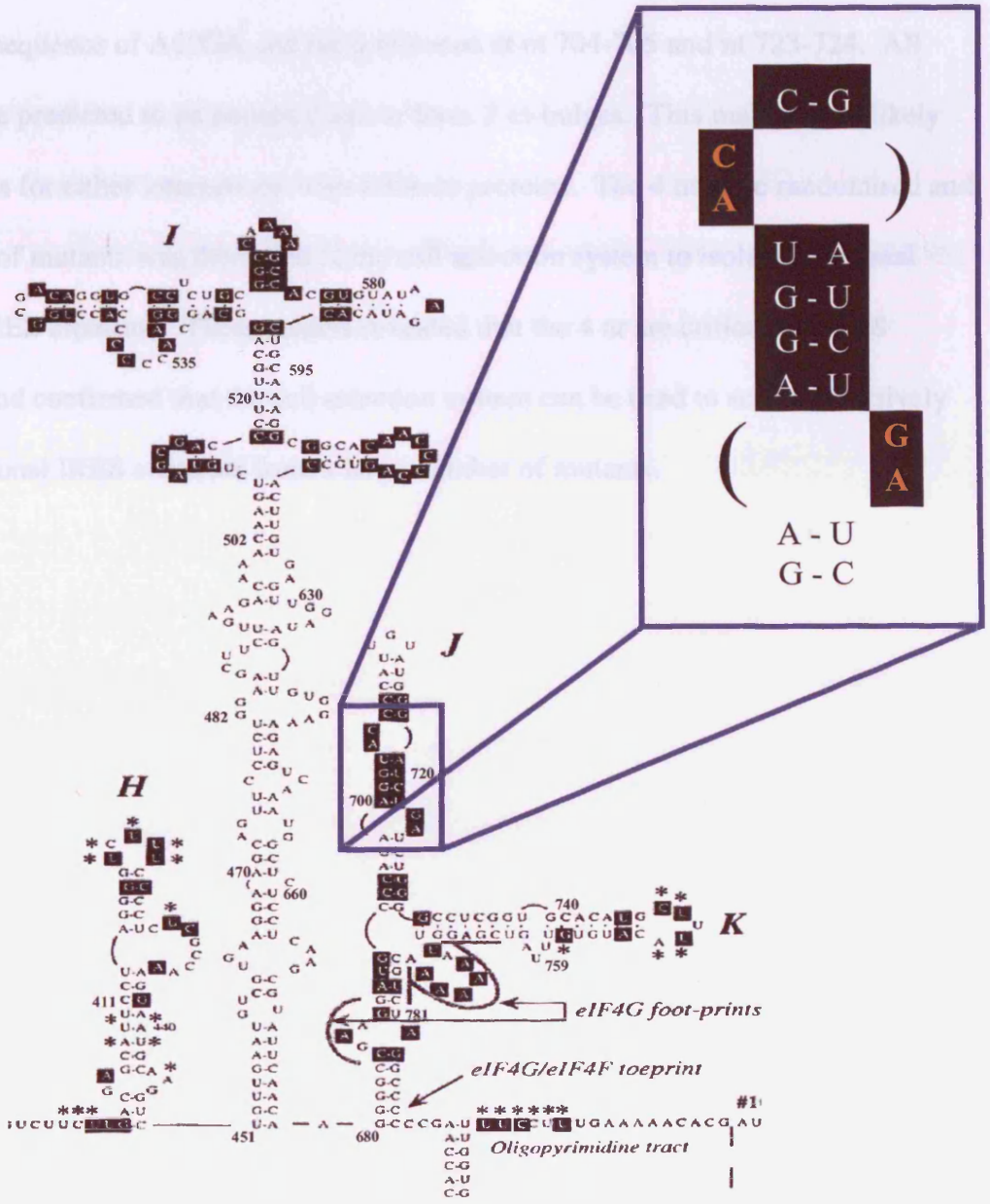
I
H
J
K
C - G
C A
U - A
G - U
G - C
A - U
G A
A - U
G - C
eIF4G foot-prints
eIF4G/eIF4F toeprint
Oligopyrimidine tract

As mentioned before only a small proportion of conserved nt have been investigated (e.g. Lopez de Quinto & Martinez-Salas, 1997, Hoffmann & Palmenberg, 1995). Consequently, it was decided to investigate 4 conserved bases within the J-domain that lie close to the eIF4GI binding site (shown in Figure 8). These nucleotides have the sequence of AC/GA and are positioned at nt 704-705 and nt 723-724. All four nt are predicted to be unpaired and to form 2 nt-bulges. This makes them likely candidates for either interactions with RNA or proteins. The 4 nt were randomised and this pool of mutants was then used in the cell selection system to isolate functional mutant IRES elements. These studies revealed that the 4 nt are critical for IRES activity and confirmed that the cell selection system can be used to screen effectively for functional IRES elements from a large number of mutants.

3.2 Methods

3.2.1 Generation of a Pool of J Domain Mutants

The 4 bases at nt 704-705 and 723-724 were randomised using overlap PCR with complementary degenerate primers as shown schematically in Figure 9. The plasmid pSKEMCRB (Drew & Belsham, 1994), which contains the EMCV IRES cDNA, was used as a template in two separate PCR reactions. In the first reaction, the degenerate primer 5' dAAGGTNNCCCATTGTATGGGATCTNNTCTGGGGCCT 3' (forward) was used with a M13 primer (reverse, Promega) and in the second reaction the degenerate primer 5' dCCAGANNAGATCCCATACAATGGGNNACCTTCTG GG 3' (reverse) was used with a T7 primer (forward, Stratagene). The products (240 bp and 500 bp respectively) were purified using a low melting point agarose gel and GFX kit (Amersham Biosciences). The degenerate primers used were complementary to each other and therefore the two products obtained from the first round of PCR were used as templates in an overlap PCR with the T7 and M13 primers. This generated a 725 bp product which was phenol extracted and digested with *Eco*RI and *Bam*HI to produce a 550 bp fragment which was gel purified as before. This fragment was subsequently ligated into a pGUS/RXB/HOOK vector (Robertson *et al.*, 1999) similarly digested with *Eco*RI and *Bam*HI. Over 800 colonies were produced. A selection of these colonies (28 in total) were screened by restriction digests and all had the correct structure. The remaining colonies were pooled into two groups, grown in *E. coli* and the pooled plasmid DNA was isolated.

Figure 9: Overlap PCR with complementary degenerate primers was used to randomise 4 nt within the J domain of the EMCV IRES. The first two PCRs used the template DNA pSKEMCRB which contains the EMCV IRES cDNA (Drew & Belsham, 1994). In PCR 1, a M13 reverse primer was used with a degenerate forward primer. In PCR 2, the primers used were a T7 forward primer and a degenerate reverse primer which is complementary to the forward degenerate primer. Both PCR products were purified and then used as templates in an overlap PCR (PCR 3) with the T7 forward primer and M13 reverse primers. The resulting PCR product was digested with *Eco*RI and *Bam*HI to release a fragment corresponding to the full-length EMCV IRES containing mutations at the 4 nt targeted.

Figure 9

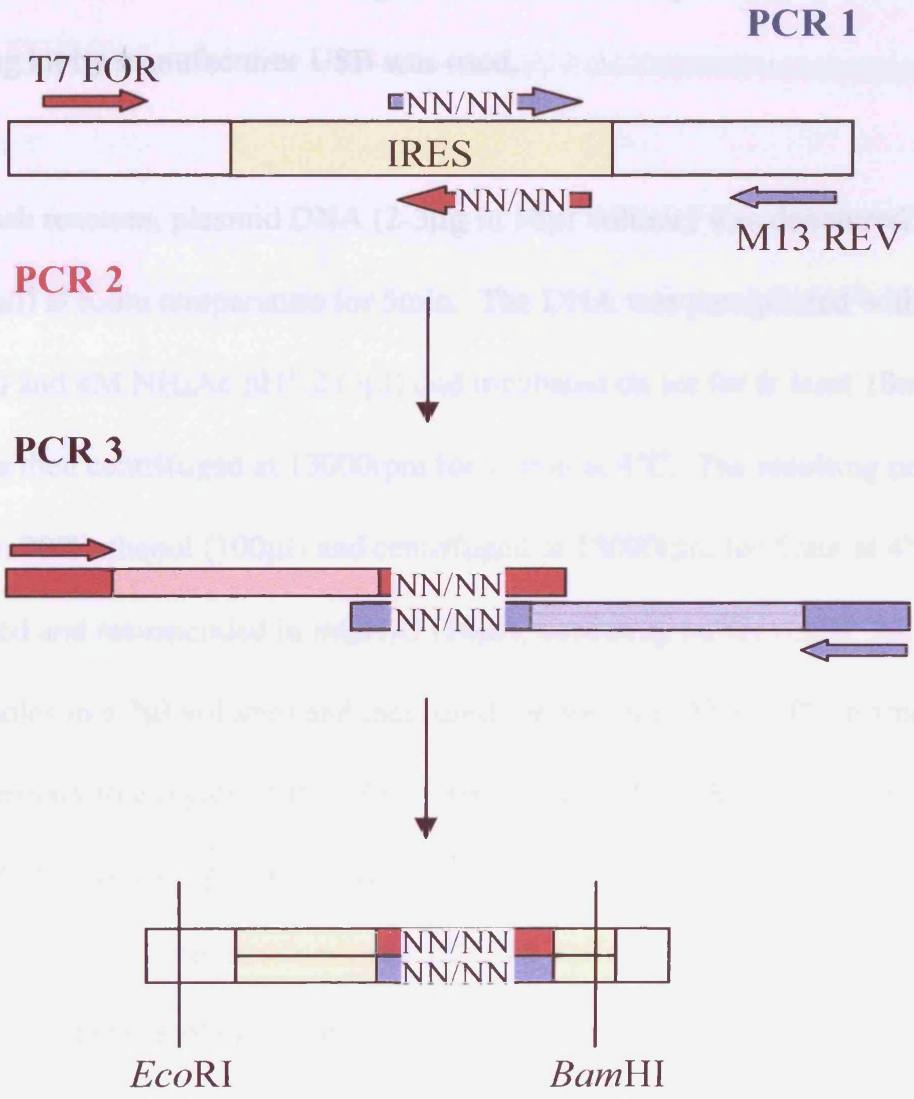
PCR 1
T7 FOR
NN/NN
IRES
NN/NN
M13 REV
PCR 2
PCR 3
NN/NN
NN/NN
NN/NN
NN/NN
EcoRI
BamHI

3.2.2 Sequencing to Confirm a Degenerate Set of Sequences within the Pool of Mutants

The pool of J domain mutants generated was sequenced to confirm that randomisation of bases had occurred at all 4 nt using [^{35}S]-labelling and the dideoxy-mediated chain termination method (Sanger, 1977; modified by Kristensen, 1988). The T7 Sequencing kit by manufacturer USB was used.

For each reaction, plasmid DNA (2-3μg in 18μl volume) was denatured using 2M NaOH (2μl) at room temperature for 5min. The DNA was precipitated with 100% ethanol (75μl) and 4M NH_4Ac pH5.2 (3μl) and incubated on ice for at least 10min. The DNA was then centrifuged at 13000rpm for 10min at 4°C. The resulting pellet was washed in 70% ethanol (100μl) and centrifuged at 13000rpm for 5min at 4°C. The pellet was dried and resuspended in mQH_2O (10μl), annealing buffer (USB, 2μl), primer (20pmoles in a 2μl volume) and incubated for 30min at 37°C. The primer used was complementary to a region in the HOOK sequence (5' GTCACCAGTGGAAC CTG 3'). Then the following mix was added: 2μl diluted T7 polymerase (USB, 5 units in 1:4 dilution using manufacturer's enzyme dilution buffer), 'A' labelling mix (USB, 3μl) and [^{35}S] dATPαS label (1μl, 5μCi/μl). The reactions were incubated for 5min at room temperature. This reaction mix was then split into 4 tubes and the appropriate termination mix was added (USB, 2.5μl of either A, C, G or T). The tubes were incubated for 5min at 37°C and then the stop solution (USB, 5μl) was added. The samples were heated at 75°C for 3min and loaded onto a 6% acrylamide/8M urea gel (1.5μl reaction mix per well). TBE running buffer was used (1x, final concentrations

100mM Tris, 100mM Boric acid and 50mM EDTA) and the gel was run at 75V for 30min. After this time the buffer in the lower chamber was replaced with a buffer composed of 2 parts 1xTBE and 1 part 3M NaAc and the gel was run for a further 2hr.

3.2.3 HOOK Cell Selection System

The pool of GUS/HOOK vectors containing the J-loop mutants was transfected into COS-7 cells (35mm dishes, approximately 75% confluent) which had previously been infected with a recombinant vaccinia virus called vTF7-3 (Fuerst *et al.*, 1986). This virus expresses T7 RNA polymerase and facilitates transient expression of the dicistronic GUS/HOOK transcripts. The transfection and the transient expression assay are briefly described here but a more detailed description can be found in Chapter 2. The plasmid DNA was transfected into the COS cells using Lipofectin and Optimem (8µl and 192µl, respectively, both Invitrogen). Different dilutions of DNA were used as specified in the Results, Section 3.3.2. At 1 hr prior to transfection, the cells were infected with vTF7-3 (previously titrated to give maximal expression of reporter gene). After 4-6hr of incubation at 37°C (in a 5% CO_2 incubator), DMEM media with Hepes containing 10% FCS was added (2ml). Approximately 20 hours later, the cells were harvested and the cell selection procedure was carried out.

For cell selection, the cells were harvested in 3mM EDTA/ Ca^{2+} and Mg^{2+}- free PBS (137mM NaCl, 2.7mM KCl, 10mM Na_2HPO_4, 2mM KH_2PO_4 final concentrations, 0.5ml). The intact cells were spun down, resuspended in serum-free DMEM (100µl) with anti-myc antibody 9E10 (0.2µl, Santa Cruz Biotech) and then incubated on ice for 45min. The cells were washed twice in DMEM with 1% FCS

(0.5ml), resuspended in DMEM/1% FCS (400µl) and incubated with washed sheep anti-mouse IgG-coated Dynal beads (5µl, Dynal) for 45min at 4°C with constant mixing. The magnetic beads with bound cells were isolated using a magnetic particle concentrator (MPC, Dynal). These selected cells were washed twice with serum-free DMEM (0.5ml) to generate the selected cell population.

3.2.4 RNA Extraction from Selected Cell Population

The RNA from selected cells was extracted using Trizol (0.5ml, Invitrogen). The samples were incubated for 5min at room temperature and a chloroform extraction was carried out by adding 100µl chloroform, incubating at room temp for 3min and centrifuging at 14000rpm for 15min. The upper, aqueous phase was removed and isopropanol (250µl) and glycogen (20µg) were added. These samples were incubated at room temperature for 10min and centifuged at 14000rpm for 10min. The pellet of RNA was washed with 75% ethanol (0.5ml) and then air-dried for 5min. The pellet was resuspended in nuclease-free H_2O (20µl, Promega).

3.2.5 RT-PCR of IRES Elements Recovered After Cell Selection

Before RT-PCR was carried out, DNA template contamination in the extracted RNA was removed by treating with DNase (using RQ1 RNase-free DNase, Promega). The RNA solution (10µl) was added to 10x RQ1 DNase buffer (5µl), RQ1 DNase (1µl) and the reaction volume was made up to 50µl with mQH_2O. The reactions were incubated at 37°C for 15min and then the RNA was purified using a phenol/

chloroform extraction and ethanol precipitation. The RNA pellet was resuspended in nuclease-free H_2O (10µl, Promega).

Subsequently, reverse transcription was carried out. DNase-treated RNA (5µl) was added to random hexamers (100ng, Roche) and the reaction volume was made up to 10µl with mQH_2O. These samples were incubated at 70°C for 5min to denature any secondary structure in the RNA and then cooled at room temperature for 10min to allow primer annealing. This mixture was then added to reverse transcription reactions containing Moloney Murine Leukemia Virus Reverse Transcriptase (M-MLV RT) (200units, Invitrogen), M-MLV RT 5x buffer (4µl, Invitrogen), BSA (final concentration 0.1mg/ml, Promega), DTT (final concentration 10mM, Invitrogen) and dNTPs (final concentration 0.5mM each, Promega). These reactions were incubated at room temperature for 5min and then at 37°C for 30-60min.

A PCR was carried out using 5µl of the cDNA as template DNA and the primers 5' CTGCACTCAATGTACACCGA 3' (forward) and 5' GACGAACCCA GTGCATTCC 3' (reverse) which anneal within the GUS and HOOK sequences respectively. The DNA polymerase used was *Taq* (Roche) and the reactions were set up as described in Chapter 2. An annealing temperature of 58°C was used. In order to determine the efficiency of the DNase step, PCR was carried out on samples either with or without the addition of DNase and/or reverse transcriptase. If the DNase step had been effective, reactions carried out on samples that had been DNase treated but not reversed transcribed would not generate a product. These controls were carried out to ensure that the product generated from the RT-PCR and used for cloning had been

derived from the RNA source only and had not resulted from any DNA contamination. The PCR reactions were analysed by agarose gel electrophoresis.

The expected fragment of approximately 1000 bp was generated only in an RT-dependent fashion (see below) and this was then digested with *Bam*HI and *Eco*RI to produce a 550 bp product which corresponds to the EMCV IRES cDNA. This product was gel purified and ligated into similarly digested pGUS/RXB/HOOK vector. The ligations were transformed into competent *E. coli* cells (DH5α). The plasmid DNA from a number of individual colonies was extracted (40 mini-preps in total) for protein expression analysis. The remaining colonies were pooled and this pool was used in a further round of cell selection. Plasmids containing the cDNA of mutants of interest were amplified in *E.coli* and midi-preps were carried out for use in sequencing reactions and protein expression analysis.

3.2.6 Sequencing of IRES Elements Recovered After Cell Selection

After cell selection and screening, individual IRES elements were sequenced using an automated sequencer, the ALFexpress DNA Sequencer (Amersham Biosciences). The method used is described in detail in Chapter 2 (Section 2.14). GUS/HOOK vectors containing the IRES cDNA were used in sequence reactions containing a Cy5-labeled primer (MWG-Biotech) which was either complementary to a region in the HOOK sequence (5' GTCACCAGTGGAACCTG 3') or complementary to a region in the GUS sequence (5' GGGAGGCAAACAATGAA TCA 3'). The sequencing reactions were set up using the AutoRead Sequencing kit (Amersham

Biosciences). The entire sequence of the IRES was determined to check if any second site mutations were present.

3.2.7 Protein Expression Analysis

The *in vitro* activity of individual J-loop mutants was investigated using TNT reactions as described in Chapter 2 (Section 2.13). Briefly, 10µl reactions containing T7 Quick Coupled Transcription/ Translation master mix (Promega) and ^{35}S-Methionine (10µCi) were programmed with 0.5µg of DNA and allowed to proceed for 1hr at 30°C. An aliquot (3µl) was then analysed using SDS-PAGE (10%) and autoradiography. Phosphoimager screening (Personal molecular imager FX/ BIO-Rad) was used in conjunction with Quantity One software for quantification of the proteins produced.

To confirm the activity of specific IRES mutants within cells, mutants were transiently expressed within BHK-38 cells using a recombinant vaccinia virus as described in Section 3.2.3. Cell selection was then carried out as described in Section 3.2.3 except that protein extracts (rather than RNA extracts as described in Section 3.2.4) were taken from the selected cells. These protein extracts were prepared using buffer C (50mM Tris pH 8.0, 0.12M NaCl, 0.5% NP40, 50µl). Total cell extracts were also obtained from cells prior to cell selection. The level of specific proteins in these extracts was determined using SDS-PAGE and Western blot analysis. The following antibodies were used for immunoblotting: mouse anti-c-myc monoclonal antibody (9E10) (1:1000, Santa Cruz Biotech), rabbit anti-GUS (1:5000, 5 Prime → 3 Prime, Inc) and rabbit anti-actin (1:1000, Sigma).

3.2.8 Construction of Point Mutants

It was decided to generate all the possible mutants containing just one nt different from the wt sequence of AC/GA since several such mutants had been recovered which demonstrated significant activity. Out of the 12 possible sequences, 5 had already been isolated and the remaining 7 sequences (namely GC/GA, AG/GA, AU/GA, AC/CA, AC/UA, AC/GC and AC/GU) were generated using overlap PCR as described in Section 3.2.1. One difference to the protocol in Section 3.2.1 was that instead of using the complementary degenerate primers for the mutagenesis, primers with a specific sequence at the four nt targeted were used and these are detailed in Table 4. Additionally, *Pfu* DNA polymerase (Promega, 1.5 units) was used instead of *Taq* as *Pfu* has a proof-reading activity and should therefore reduce the chance of secondary mutations occurring. The PCR reactions were set up as described in Section 2.2 and an annealing temperature of 52°C was used. The final PCR product (of 725bp) was phenol extracted and digested with *Eco*RI and *Bam*HI. The 550bp fragment generated was purified using a low melting point agarose gel and GFX kit (Amersham Biosciences). It was then ligated into a pGUS/RXB/HOOK vector also digested with *Eco*RI and *Bam*HI and this plasmid was amplified in *E.coli* (DH5α). A selection of the resulting colonies were screened by restriction digests to ensure the plasmid had the correct structure. Midi-preps of the plasmid DNA were then carried out and the activity of these mutants was investigated using protein expression analyses. The entire sequence of the IRES was checked using the automated ALFexpress DNA Sequencer (Amersham Biosciences) to confirm the structure of the plasmid was correct and that no secondary mutations were present.

Sequence of Mutant	Sequence of Primer
GC/GA (For)	5' AAGGT**GC**CCCATTGTATGGGATCT**GA**TCTGGGGCCT 3'
(Rev)	5' CCAGA**TC**AGATCCCATACAATGGGG**C**ACCTTCTGGG 3'
AG/GA (For)	5' AAGGT**AG**CCCATTGTATGGGATCT**GA**TCTGGGGCCT 3'
(Rev)	5' CC**A**GA**TC**AGATCCCATACAATGGG**CT**ACCTTCTGGG 3'
AU/GA (For)	5' AAGGTA**T**CCCATTGTATGGGATCT**GA**TCTGGGGCCT 3'
(Rev)	5' CCAGA**TC**AGATCCCATACAATGGG**AT**ACCTTCTGGG 3'
AC/CA (For)	5' AAGGTA**CC**CCATTGTATGGGATCT**CA**TCTGGGGCCT 3'
(Rev)	5' CCAGA**TG**AGATCCCATACAATGGGG**T**ACCTTCTGGG 3'
AC/UA (For)	5' AAGGTA**CC**CCATTGTATGGGATCT**TA**TCTGGGGCCT 3'
(Rev)	5' CCAGA**TA**AGATCCCATACAATGGGG**T**ACCTTCTGGG 3'
AC/GC (For)	5' AAGGTA**CC**CCATTGTATGGGATCT**GC**TCTGGGGCCT 3'
(Rev)	5' CCAGA**GC**AGGATCCCATACAATGGGG**T**ACCTTCTGGG 3'
AC/GU (For)	5' AAGGTA**CC**CCATTGTATGGGATCT**GT**TCTGGGGCCT 3'
(Rev)	5' CCAGA**AC**AGATCCCATACAATGGGG**T**ACCTTCTGGG 3'

Table 4: Sequences of primers used to generate point mutants within the J domain of the EMCV IRES. The mutant sequence shown in bold corresponds to the sequence generated at nt 704-705 and 723-724 within the J domain of the EMCV IRES. The forward and reverse primers are indicated as For and Rev, respectively

3.3 Results

The objective of this work was to determine the importance of 4 conserved, unpaired nucleotides within domain J at positions 704-705 and 723-724 (shown in Figure 8) by using a cell selection system for functional IRES elements previously developed in our laboratory (Mulder *et al.*, 1998; Robertson *et al.*, 1999). The location of these 4 nucleotides is in close proximity to the eIF4GI binding site.

3.3.1 Generation of IRES Elements with Mutations in the J Domain

To generate a pool of EMCV IRES elements with randomised bases at nucleotides 704-705 and 723-724, overlap PCR with degenerate primers was carried out. These IRES elements were then cloned into the pGUS/RXB/HOOK vector. After transformation, over 800 colonies were produced and these were grouped together to form two pools. The pool to be used in subsequent experiments was sequenced to confirm there was randomisation of bases at the four nucleotides targeted for mutagenesis. Figure 10 shows that there are bands of equal intensity for each base at the 4 nt targeted for mutagenesis in contrast to the surrounding sequence, which is unique. This suggests that a highly degenerate pool of plasmids had been generated.

3.3.2 Modification of Cell Selection System for Functional IRES Elements

In previous uses of the cell selection system, functional IRES elements were efficiently isolated but a relatively high background of non-functional IRES elements

Figure 10: The pool of EMCV IRES elements containing mutations within the J-loop were sequenced using [^{35}S]-α-dATP sequencing (with a reverse primer complementary to the HOOK ORF) and autoradiography. The four nucleotides that have been mutated are labeled N and these show bands of equal intensity for each base. This is in contrast to the surrounding sequence, which is unique.

Figure 10

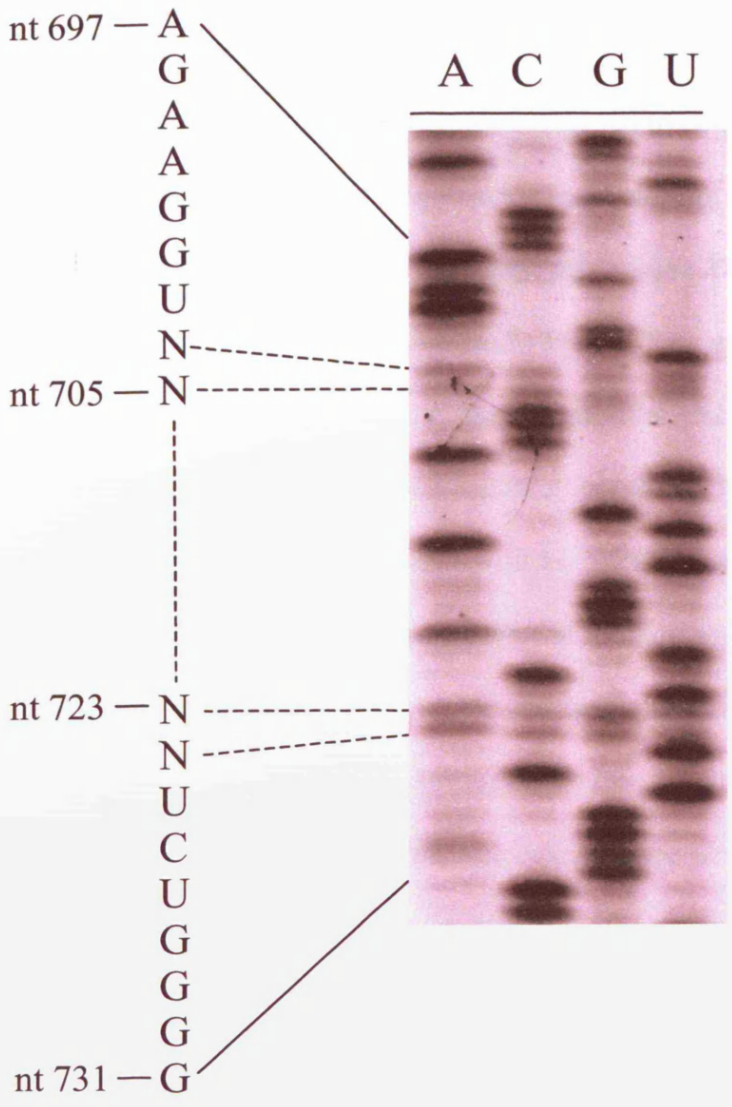

was also detected (Robertson *et al.*, 1999; Robertson, 1999). One possible reason for this background was co-transfection of plasmids. The fact that co-transfection can occur is well known and is often exploited when it is desirable to co-transfect two or more plasmids (e.g. Mulder *et al.*, 1998). However, in this case, co-transfection could lead to selection of a cell containing both a functional and non-functional IRES element. Another reason for the high background could have been that plasmid DNA adhered to the outside of a cell during transfection and this led to contamination of the plasmid DNA isolated from selected cells. Previously, in an attempt to limit this problem, the plasmid DNA was linearised by digestion at a unique *Xho*I site downstream of the HOOK sequence (Robertson *et al.*, 1999). This meant that if the linearised molecules remained on the outside of the cell after transfection, they would not be readily transformed into *E.coli*. *Xho*I digestion of the plasmid DNA increased the proportion of functional IRES elements recovered from 10% to 20% but it also affected expression of HOOK within transfected cells. In this present study, two modifications were made to the cell selection system in an attempt to alleviate these problems and preliminary experiments were carried out to investigate if they were feasible as described below. It should be noted, however, that the pool of J domain mutants used in these preliminary experiments differs from the one used in the subsequent cell selection experiments. This is because the initial pool of mutants used was later determined to have significant wild-type contamination (Robertson, 1999).

To avoid co-transfection occurring, lower dilutions of DNA were used in the transfections. Previously, 2.5μg of plasmid DNA had been used in all DNA transfections. The transfection reagent used (Lipofectin) is a cationic lipid reagent. It acts by approximately 5 lipid molecules associating with one DNA molecule and

carrying it into the cell. Therefore, decreasing the amount of DNA used should decrease the level of co-transfection. To test this initially, cell selection was carried out in COS-7 cells using 4 different amounts of DNA (0.5μg, 100ng, 20ng and 4ng). The proportion of cells being selected per dish of cells was investigated using SDS-PAGE of selected cell extracts followed by immunoblotting or coomassie-blue staining (Figure 11). Immunoblotting of the levels of actin within selected cell extracts and the coomassie-blue staining of selected cell extracts both showed that a low but detectable level of cell selection occurred when as little as 20 ng of DNA was transfected. This is not surprising as the transient expression system used is very efficient (Fuerst *et al.*, 1986). Furthermore, the level of protein present in the selected cell extract decreased when less DNA was used in the transfection for both pGUS/FMD/HOOK (containing the wild-type FMDV IRES) and for the pool of J-loop mutants. This suggests that the number of cells selected per dish of cells decreased when less DNA was used in the transfection and therefore co-transfection should have been reduced.

The second problem of plasmid DNA adhering to the outside of a cell during transfection was then addressed. The total mRNA was extracted from the selected cells instead of plasmid DNA to ensure that all the IRES elements recovered had been expressed within the selected cells. To confirm that RNA extraction would work, an experiment was set up in which 4 different amounts of DNA (0.5μg, 100ng, 20ng and 4ng) were used during cell transfection. Cell selection was then carried out and the total RNA was extracted from the resulting selected cell population. These RNA samples were DNase-treated and then treated with reverse transcriptase (RT) to produce cDNA of the recovered IRES elements. PCR was carried out using this cDNA and primers complementary to the GUS and HOOK sequences. Reactions were also

Figure 11: Cell selection carried out after transfection of cells with different amounts of plasmid DNA. COS-7 cells, previously infected with vTF7-3, were transfected with the amount of plasmid DNA indicated. Cell selection was then carried out and protein extracts were taken from the selected cell population. These extracts were analysed using SDS-PAGE followed by either coomassie-blue staining (panel A) or immunoblotting to detect the level of actin present (panel B). This shows that cell selection occurred when as little as 20 ng of DNA was transfected.

The plasmid pGUS/FMD/HOOK contains the wt FMDV IRES cDNA. pGUS/Jpool/ HOOK denotes a pool of plasmids containing the cDNA of EMCV IRES elements containing mutations at nt 704-705 and 723-724.

Figure 11

A:

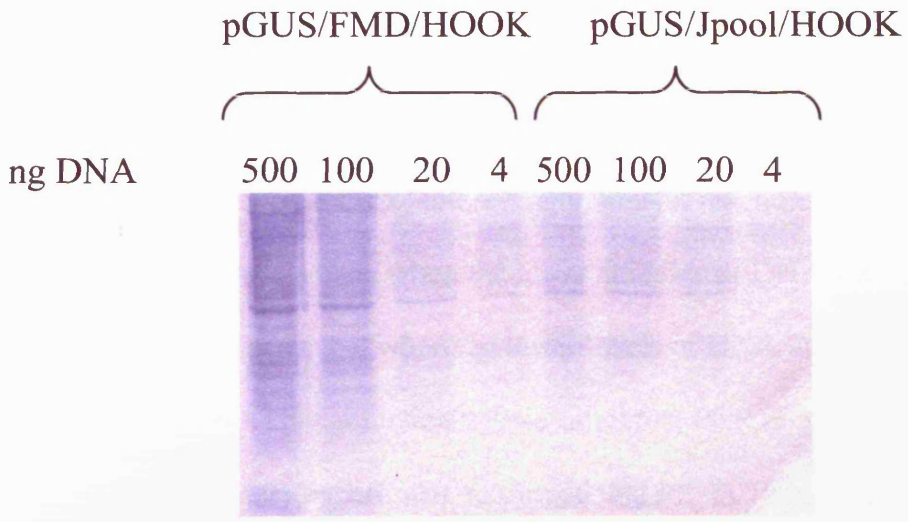
pGUS/FMD/HOOK
pGUS/Jpool/HOOK
ng DNA
500 100 20 4 500 100 20 4

B:

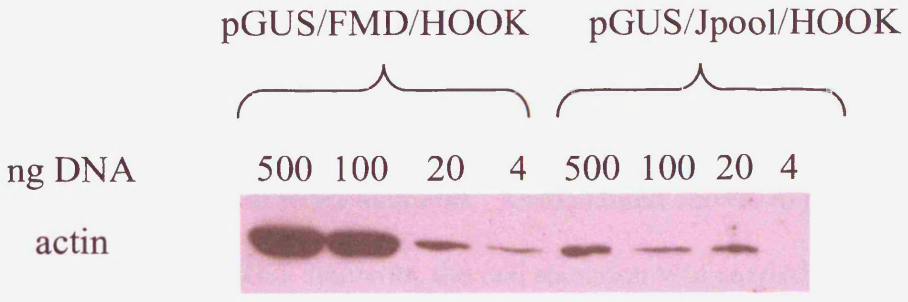
pGUS/FMD/HOOK
pGUS/Jpool/HOOK
ng DNA
500 100 20 4 500 100 20 4
actin

set up in which PCR was carried out with RNA not treated with DNase and/or RT. These control reactions confirmed that all DNA contamination had been removed completely by the DNase step. Figure 12 shows that even with the lowest amount of DNA (4ng), RT-PCR was very efficient and a clear band of the expected size (approximately 1000bp) was seen. Reactions including DNase but no RT did not generate a band indicating that the DNase step had indeed been complete and removed all trace of any template DNA. Reactions omitting DNase and RT produced strong bands when both 0.5μg and 100ng were used in the transfections. This product will have been generated from a DNA source. Interestingly though, reactions omitting DNase and RT failed to produce a band when the lower amounts of DNA such as 20ng and 4ng were used. This indicates that when the lower levels of DNA were used in transfection, the level of DNA contamination was so small that PCR amplification fails. Therefore, this preliminary experiment confirmed that RT-PCR could be easily used to recover IRES elements expressed within selected cells.

3.3.3 Cell Selection of EMCV IRES Elements with Mutations in the J Domain

The pool of EMCV IRES elements containing mutations within the J-loop as described in Section 3.3.1 was transfected into COS-7 cells and cell selection was carried out to isolate functional IRES elements. As explained above, to reduce selection of non-functional IRES elements, the cell selection was carried out after transfection of cells with different dilutions of DNA (2.5μg, 500ng, 100ng and 20ng). The RNA was then extracted from selected cells and RT-PCR was performed. No PCR products were generated in reactions containing no RT, which confirms that all DNA contamination was successfully removed, and therefore that the product

Figure 12: Cell selection was carried on cells transfected with different amounts of pGUS/poolJ/HOOK plasmid DNA. The total RNA was extracted from the selected cell population and either treated with DNase and/or RT. PCR reactions were then carried out with primers complementary to the GUS and HOOK sequences. The PCR products were analyzed using agarose gel electrophoresis. Note, no product was seen for reactions including DNase but no RT which indicates that the DNase step had indeed been complete and all traces of template DNA had been removed.

Figure 12

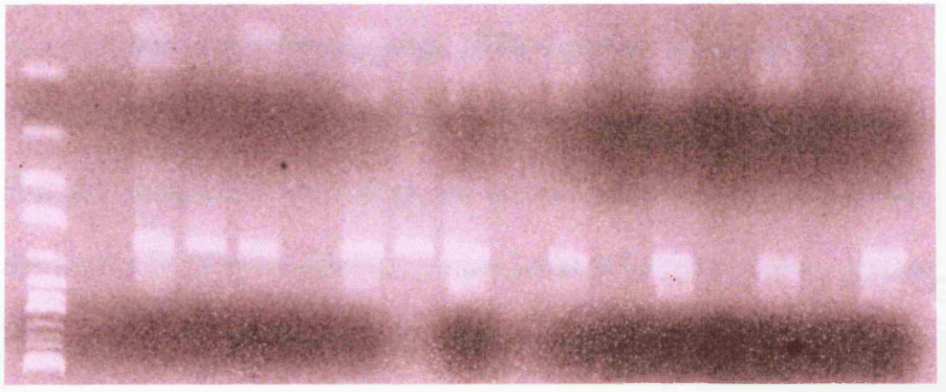

DNase	M	+	+	−	−	+	+	−	−	+	+	−	−	+	+	−	−
RT		−	+	−	+	−	+	−	+	−	+	−	+	−	+	−	+
DNA used		0.5µg				100ng				20ng				4ng			

generated has been derived only from an RNA source. The IRES elements recovered were cloned back into dicistronic GUS/HOOK vectors and amplified in *E.coli.* After cloning, around 500 colonies were generated and plasmid DNA was isolated from individual colonies.

The plasmid DNA from 40 individual colonies was isolated and the *in vitro* activity of the IRES elements was tested using coupled transcription/translation reactions (TNTs). For these screening purposes, IRES elements recovered after transfection with lower levels of DNA were used (the majority of IRESes screened were isolated from the transfection with 20 ng and the rest were from the 100ng and 500 ng DNA transfections). The remaining colonies (over 400) were pooled together and maxi-preped to generate a second pool of mutants, that was used in a further round of cell selection. From these two rounds of cell selection and previous work (utilizing a pool of mutants which was abandoned due to significant wild-type contamination, Robertson, 1999), a large number of mutant IRES elements were isolated. These show a large range of activities.

3.3.4 Identification of Functional IRES Elements with Mutations in the J Domain

A total of 7 different IRES mutants were isolated which were functional and these are listed in Table 5. The TNT assays (shown in Figure 13) showed that some sequences were more efficient at mediating IRES activity than others but they all produced a higher level of HOOK than the negative control pGUS/RXB/HOOK which contained no IRES between the two cistrons. The ratio of HOOK: GUS produced in the TNT reactions was quantified using a phosphoimager screen and Quantity One

	Sequence at nt 704, 705/ 723, 724	Second site mutation	No. of times isolated
Cycle 1	AC/GA (wt)		3
	AA/GA		1
	AC/GG		1
Cycle 2	AC/GA (wt)		2
	GC/GA	557 C → U	1
	AA/GA		1
From same pool	CC/GA		1
	UC/GA		1
Others	GC/GA	537 C → U	1
	AC/AA		1
	AC/GG		1
	UA/GA		1

Table 5: Sequences of mutant IRES elements recovered which demonstrate significant activity *in vitro*. These mutants were recovered from two rounds of cell selection and also from cell selection using a different pool of J domain mutants which was later abandoned due to significant wild-type contamination (Robertson, 1999). The entire length of the IRES elements was sequenced and any secondary mutations found are indicated.

Figure 13: A number of EMCV IRES J domain mutants recovered showed significant IRES activity *in vitro*. Dicistronic GUS/HOOK vectors containing the J domain mutants were used in TNT reactions as described in Methods. The proteins produced were analysed using SDS-PAGE and the autoradiograph is shown here. The sequences of the mutants at the 4 nt targeted for mutagenesis are shown with the mutated base/s shown in blue.

A GUS/HOOK vector containing the wt EMCV IRES was included as a positive control. RXB is the plasmid GUS/RXB/HOOK which did not contain an IRES element between the two cistrons. A second negative control was included which is a non-functional J domain mutant with the sequence GC/CU.

The ratio of HOOK:GUS translated for each construct was quantified using a phosphoimager and Quantity One software. The value obtained was multiplied by 1000 to produce the value shown here.

* This mutant contains a second site mutation at nt 537 in domain I (C → U)

This mutant contains a second site mutation at nt 557 in domain I (C → U)

Figure 13

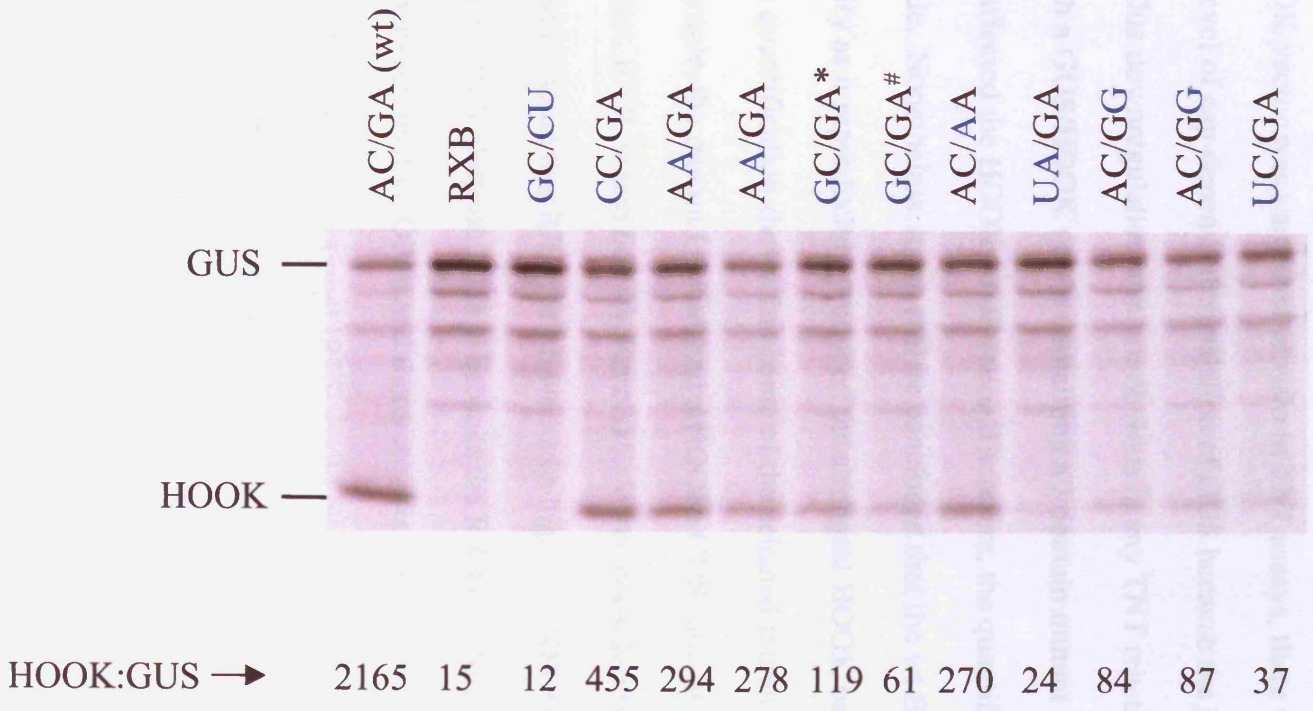
AC/GA (wt)
RXB
GC/CU
CC/GA
AA/GA
AA/GA
GC/GA*
GC/GA#
AC/AA
UA/GA
AC/GG
AC/GG
UC/GA
GUS
HOOK
HOOK:GUS
2165 15 12 455 294 278 119 61 270 24 84 87 37

software. The value obtained was multiplied by 1000 (shown in Figure 13). A simple comparison shows that the wild-type IRES was much more efficient than any of the mutants obtained (giving a HOOK: GUS ratio of 2165 compared to the most active mutant which has a value of 455). Nevertheless, the scenario is complicated by the fact that the translation of GUS and HOOK compete for translation factors. When the GUS/EMC/HOOK vector was translated *in vitro* in TNT assays, there was a distinct decrease in the level of cap-dependent translation of GUS because the EMCV IRES is very efficient. This downregulation was not obvious in any TNT reactions programmed with a GUS/HOOK vector containing a J domain mutant IRES element but it may have affected the HOOK: GUS ratio. Therefore, the quantification values act only as a guide. Nonetheless, it can still be concluded that the wt EMCV IRES had the highest activity as it reproducibly produced the strongest HOOK band in the TNTs. Additionally, the quantification shows that some of the selected mutants had very low activity. For example, the mutant UC/GA had a HOOK: GUS ratio of 37 compared to the negative control, RXB, which had a value of 15. When considering these values, however, it should be noted that RXB may have had a higher HOOK:GUS ratio than for a non-functional IRES element. This is because the RXB construct has a short linker sequence between the two ORFs and therefore it is possible that reinitiation may have occurred *in vitro*. A non-functional IRES would have a highly structured region of 450 nt between the 2 ORFs making reinitiation very unlikely and indeed several IRES elements isolated (described in Section 3.3.5) expressed a lower amount of HOOK protein than the RXB control.

The vast majority of the active sequences (6 out of 7) had only one nucleotide different from the wild-type sequence of AC/GA. The mutant UA/GA was the only

mutant found which had 2nt different from the wt sequence and yet was still functional (albeit to a very low extent, giving a HOOK:GUS ratio of 24). The sequences of AA/GA, GC/GA and AC/GG were all found in duplicate. This suggests that only a small proportion of the pool of J-loop mutants were functional. As expected, the wild-type sequence was also isolated a number of times. Within the functional sequences isolated were mutants with substitutions at all 4 positions. However, this is too small a group to reach any conclusions as to whether a mutation at one nt had more effect than another and this was investigated further (see below).

A complication to the analysis of the results was the presence of second site point mutations. These were generated during the PCR step due to the low fidelity of *Taq* polymerase. There were two positive IRES elements with the sequence GC/GA but they had different second site mutations and varied in activity. The mutant with the higher activity had a second site mutation at nt 537 in stem-loop I (C mutated to U). This substitution is present in the IRES from strain EMCV-B (strain EMCV-R was used in this study) and is therefore unlikely to have had much effect on activity. Second site mutations are of interest since if the first mutation is at a nucleotide important for interactions, a second compensatory mutation may occur which could restore the activity of the mutant back to that of wt. However, in both previous and the current study (Robertson *et al.*, 1999), second site mutations have decreased the activity further. Indeed a third mutant IRES was isolated with the mutant sequence GC/GA but this mutant was non-functional. It was found to contain a different second site mutation (the G at nt 730 at the J/K domain boundary was substituted for an A) which must have abolished IRES activity. In later work (refer to Figure 17 and 18) a

GC/GA mutant was generated which did not contain any second site mutation and this was clearly functional.

The functional J-loop mutant IRES elements were transfected into BHK cells and cell selection was carried out to confirm their activity within cells. The HOOK and GUS levels were analysed from both total cell extracts and selected cell extracts (i.e. before and after cell selection) using SDS-PAGE and immunoblotting (see Figure 14). The levels of actin were also investigated in the selected cell extracts (SCE) as actin is an abundant cellular protein and therefore acts as a marker of cell selection. All the mutants tested mediated sufficient levels of HOOK to allow cell selection as all have clear bands for HOOK, GUS and actin in the immunoblots of SCE. This is in contrast to the negative control RXB, which did not cause cell selection to occur and there was no detectable HOOK or actin in the SCE. Even though some of the mutants (namely AC/GG and UC/GA) mediated a rather low level of translation of HOOK, they were all clearly selected within the system. This confirms the sensitivity of the system as observed previously (Robertson *et al.*, 1999 and Robertson, 1999). It should be noted that the mutant with two nucleotides different from the wt sequence, UA/GA, was not included in this set of mutants. This is because in the TNT assay it mediated very low production of HOOK and it was therefore decided to include it in the set of J-loop mutants with low or no activity. A low level of GUS was detected within SCE from cells transfected with RXB. This was consistently observed in these experiments and previously (Mulder *et al.*, 1998; Robertson *et al.*, 1999) but clearly no significant cell selection occurred because there was no detectable HOOK or actin protein in the same extract. Instead it suggests that GUS is a "sticky" protein which was retained non-

Figure 14: Cell selection was carried out to investigate the IRES activity within cells for specific J domain mutants which showed significant activity *in vitro*. Plasmids encoding the dicistronic GUS/HOOK mRNAs containing the J domain mutant IRESes (2.5μg) were transfected individually into BHK cells. Cell selection was carried out after approximately 20hr. SDS-PAGE and Western blot analysis was used to detect the GUS, HOOK and actin levels in the selected cell protein extracts and total cell protein extracts. The nt which differ from the sequence of the wt IRES are shown in blue. Actin is an abundant cellular protein and therefore acts as a marker for cell selection. The level of GUS in the total cell extracts is indicative of transfection efficiency.

* This mutant contains a second site mutation at nt 537 in domain I (C → U)

This mutant contains a second site mutation at nt 557 in domain I (C → U)

Figure 14

A- Selected cell extracts:

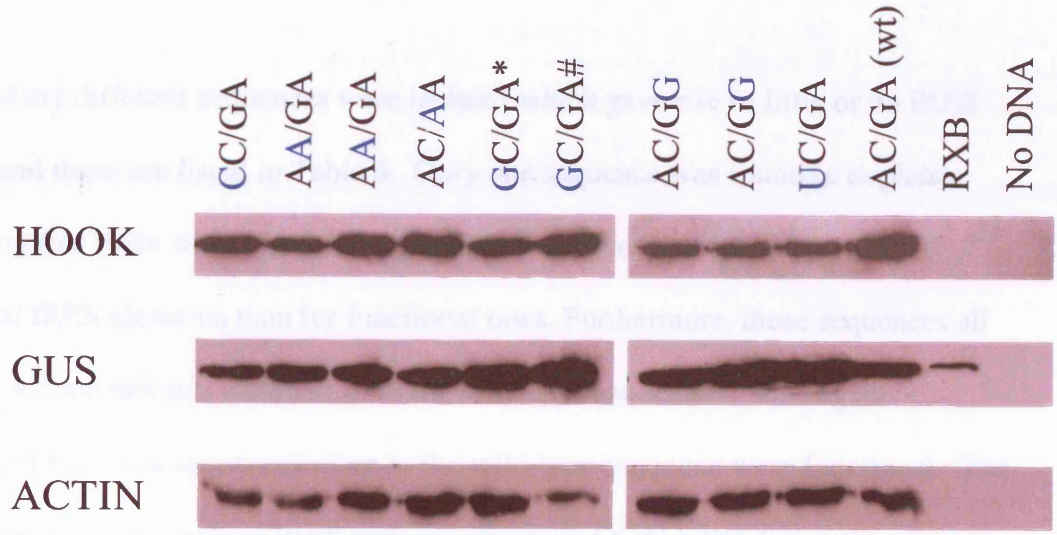

B- Total cell extracts

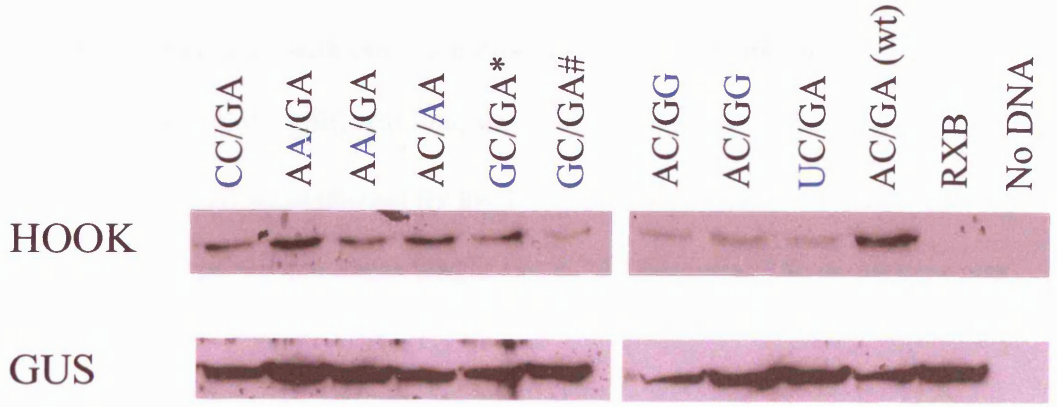

specifically on the magnetic beads. Fortunately, this level of GUS was significantly lower than that from genuine cell selection of functional IRES elements.

3.3.5 Identification of IRES Elements with Mutations in the J Domain which have Little or No Activity

Many different sequences were isolated which gave rise to little or no IRES activity and these are listed in Table 6. Only one sequence was found in duplicate suggesting that there were many more possible sequences that gave rise to non-functional IRES elements than for functional ones. Furthermore, these sequences all had 2, 3 or 4 nucleotides different from the wild-type sequences. This again emphasizes that only sequences close to the wild-type sequence were functional. The only exception was a mutant IRES with the sequence GC/GA but this also contained a second site mutation (G730→A). As mentioned previously, a GC/GA mutant was generated without any secondary mutations and this was clearly functional. Analysis of all the functional and non-functional IRES elements recovered from the same pool of mutants demonstrated that, with one exception, each base was identified at each position. This confirms that significant randomisation of bases had occurred within this pool of J-loop mutants as suggested by the [^{35}S]- sequencing (shown in Figure 10). However, this does not prove that every single one of the potential 256 sequences was generated.

The *in vitro* activity for the majority of these sequences is shown in Figure 15. As mentioned previously, several of these sequences (e.g. GC/CU) appeared to express a lower level amount of HOOK than the RXB control. The chance of reinitiation

	Sequence at nt 704, 705/ 723, 724	Second site mutations	No. of times isolated
Cycle 1	AA/GU		1
Cycle 2	CG/CC	564 G → A	1
From same pool	GC/CU		1
	GA/UA	771 A → G	1
	CC/AG	730 G → A	1
	GC/GA	730 G → A	1
Other	UG/GA		1
	GU/GA		1
	UG/GG		1
	AC/AG		1
	CA/GA		1
	UC/AA		1
	GC/CU		1
	CA/GC	806 G → A	1
	UA/GC		1
	UA/UG		1
	CU/GA	515 G→ A	1
	UC/GG		1

Table 6: The sequences of mutant IRES elements recovered which show low or no activity *in vitro*. The entire length of the IRES elements was sequenced and any secondary mutations found are indicated. The 'other' IRES elements were isolated from previous cell selection experiments using a different pool of J domain mutants which was later abandoned due to significant wild-type contamination (Robertson, 1999).

Figure 15: A large number of J domain mutants have low or no activity *in vitro*. Dicistronic GUS/HOOK vectors containing the J domain mutants were used in TNT reactions. The proteins produced were analysed using SDS-PAGE and autoradiography. The sequences of these mutants at the 4 nt targeted for mutagenesis are shown with the mutated bases shown in blue.

^ This mutant contains a second site mutation at nt 564 in domain I (G → A)

Figure 15

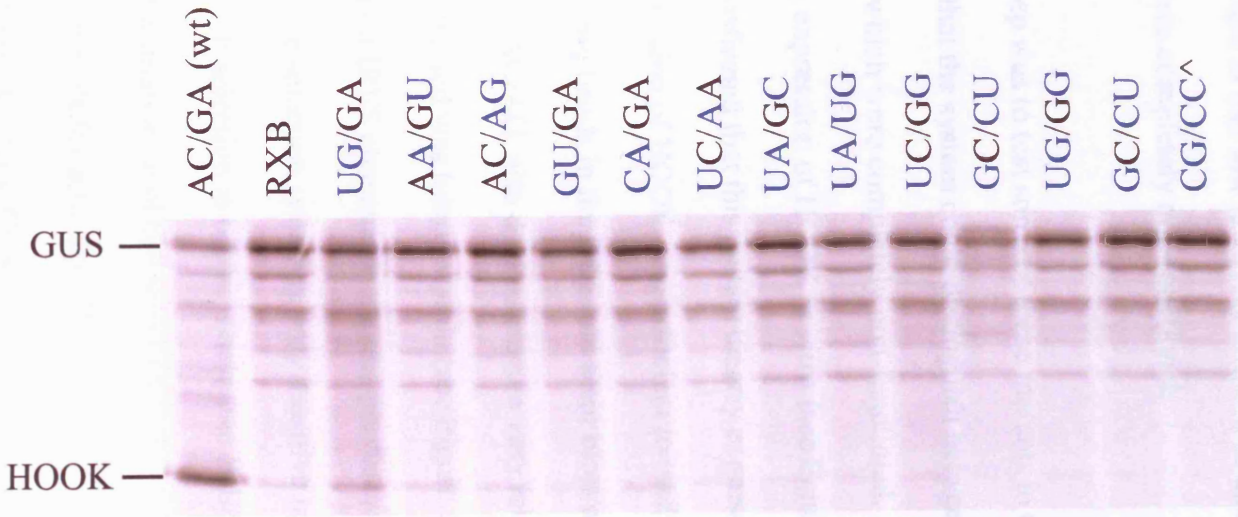
AC/GA (wt)
RXB
UG/GA
AA/GU
AC/AG
GU/GA
CA/GA
UC/AA
UA/GC
UA/UG
UC/GG
GC/CU
UG/GG
GC/CU
CG/CC^
GUS
HOOK

occurring was reduced for the non-functional IRES elements since these constructs contain a long, highly structured region between the 2 ORFs, unlike the RXB construct. Consequently, a construct containing a non-functional IRES represents a more rigorous negative control. It should be noted that all these mutants mediated very low levels of HOOK expression and at this low level it is difficult to discriminate if mutants had slight activity or were completely non-functional.

The next step was to test some of these mutants in the cell selection system and this demonstrated that the system could distinguish between IRES elements with low activity and those which were completely non-functional. The mutant UA/GA mediated very low expression of HOOK *in vitro* (see Figure 13) but after cell selection, immunoblotting confirmed that this mutant clearly expressed HOOK (shown in Figure 16). This low expression of HOOK was sufficient to mediate cell selection (as indicated by the strong bands in the GUS and actin blots of SCE). Two other mutants, namely UG/GA and AC/AG, also demonstrated a very low activity within cells and the level of HOOK expressed was faintly visible (see Figure 16). However, as shown for the functional mutant IRES elements tested and previous work (Robertson *et al.*, 1999; Robertson, 1999), the selection system is very sensitive and a low expression of HOOK was sufficient for cell selection to occur. These two IRES elements were barely functional and yet a small level of cell selection had occurred as both gave rise to faint bands in the western blots for actin and GUS of SCE. The remaining IRES elements tested, namely AA/GU, GU/GA, GC/CU and CG/CC[1] were completely non-functional and no cell selection was observed.

1- This mutant contains a second site mutation at nt 564 (G → A)

Figure 16: Cell selection was carried out to test the *in vivo* activity of several J domain mutants which showed little or no activity *in vitro*. Plasmids encoding the dicistronic GUS/HOOK mRNAs containing the J domain mutant IRESes (2.5μg) were transfected into BHK cells. Cell selection was carried out. Immunoblotting was used to detect the GUS, HOOK and actin levels in selected cell protein extracts and total cell protein extracts. The nt which differ from the sequence of the wt IRES are shown in blue.

^ This mutant contains a second site mutation at nt 564 (G → A)

Figure 16

A- Selected cell extracts:

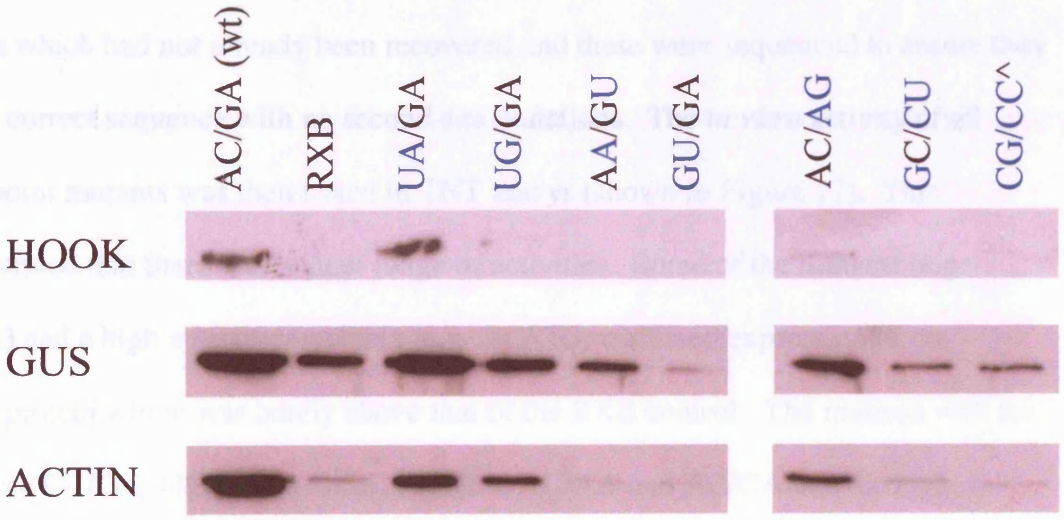

B- Total cell extracts:

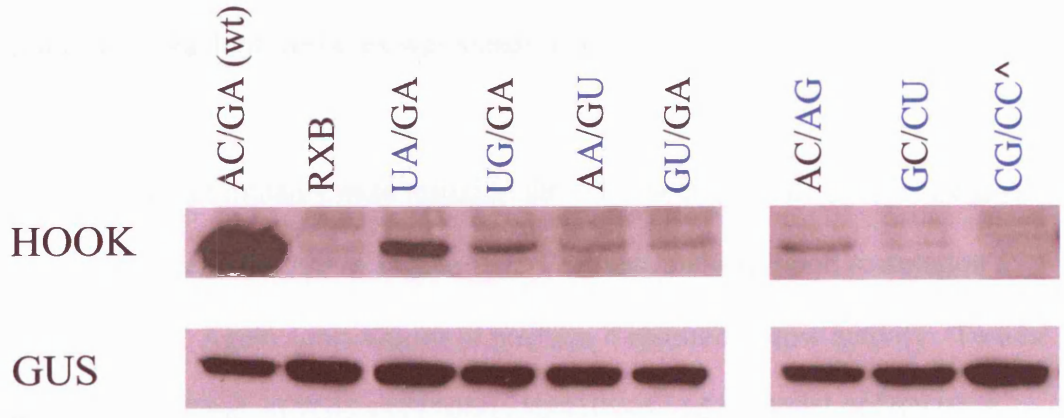

3.3.6 The Activity of Single Point Mutants

The vast majority of functional IRES mutants recovered had only one nucleotide different from the wild-type sequence and therefore it was decided to investigate if all mutants with one substitution from the wild-type sequence were functional. PCR was used to specifically generate each of the remaining single point mutants which had not already been recovered and these were sequenced to ensure they had the correct sequence with no second site mutations. The *in vitro* activity of all single point mutants was then tested in TNT assays (shown in Figure 17). This demonstrated that there was a large range of activities. Some of the mutants (e.g. GC/GA) had a high activity but others (e.g. AC/GU) mediated expression of the HOOK protein which was barely above that of the RXB control. The mutants with the sequences CC/GA, GC/GA, AA/GA, AG/GA, AC/AA and AC/CA had the highest activities. Overall, it is clear that the position of the substitution did have an effect on activity. Mutations at position 3 showed the least effect, as all three of these mutants were clearly active. This is in contrast to the three mutants with a substitution at position 4 which each demonstrated a very low activity. Interestingly the least activity was observed when each of the bases was substituted by a U residue.

The single point mutants were tested in the cell selection system to investigate their activity within cells (shown in Figure 18). This data showed good correlation to their activity *in vitro*. Again substitutions at position 4 resulted in low activity. Two of these mutants AC/GC and AC/GU were barely functional and the level of HOOK expressed was only faintly visible.

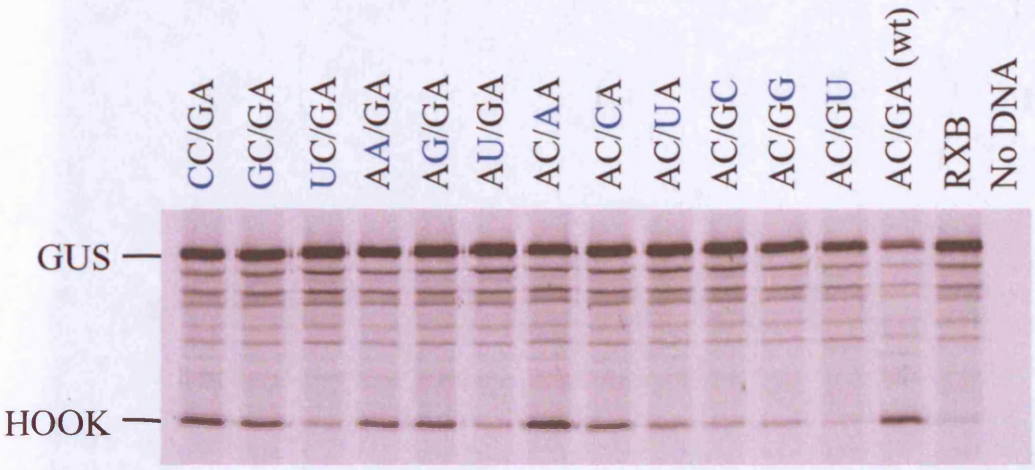

Figure 17: The *in vitro* activity of single-point J domain mutants was investigated. Dicistronic GUS/HOOK vectors containing the J domain mutants were used in TNT reactions. This figure shows an autoradiograph of the radioactively labeled proteins produced. RXB is the plasmid pGUS/RXB/HOOK which acts as a negative control as it contained no IRES between the GUS and HOOK ORFs. The mutated nt are shown in blue.

Figure 18: Cell selection of J domain mutants containing single point mutations. Plasmids (2.5μg), encoding dicistronic GUS/HOOK mRNAs containing the mutant IRES within the intercistronic space, were transfected into BHK cells. Cell selection was then carried out and protein extracts were taken from both the total cell and selected cell population. Immunoblotting analysis was used to detect the GUS, HOOK and actin levels in these extracts. The nt which differ from the sequence of the wt IRES are shown in blue.

Figure 18

A- Selected Cell Extracts:

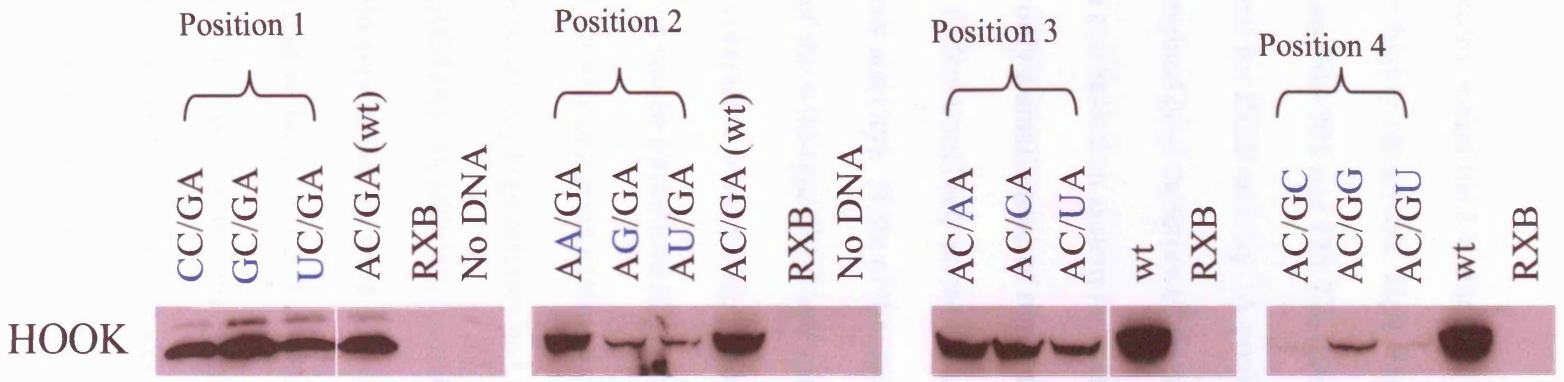

B-Total Cell Extracts:

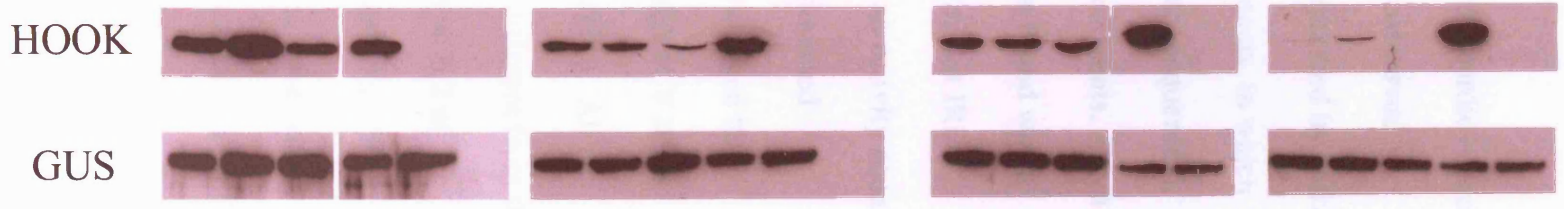

3.4 Discussion

Many nucleotides within the J-K domains of IRES elements from cardioviruses and aphthoviruses are highly conserved. Here it is shown that 4 such conserved nucleotides at positions 704-705 and 723-724 (using the numbering described by Duke *et al.*, 1992) are critical for IRES activity. A pool of EMCV IRES mutants, in which these 4 nt were randomised (and therefore containing up to 256 different sequences), was analysed using a cell selection system to isolate functional IRES elements. From these investigations, only a small group of mutant IRES elements were found which retained any activity (9 functional sequences were isolated including mutant IRES elements with very low activity). None of the mutants recovered had an activity equal to or more than that of the wild-type IRES and many had severely diminished activities. This is in contrast to other mutagenesis experiments which showed that several point mutations can be introduced at various positions into the EMCV IRES without affecting the activity to a great extent (van der Velden *et al.*, 1995). All the mutants isolated with relatively high activity had only one nucleotide different from the wild-type sequence (AC/GA). In addition, a small number of mutants with 2 nt different from the wild-type sequence were recovered which had low activity. The remainder of the mutants isolated with 2, 3 or 4 nucleotide substitutions were non-functional. In addition, a number of mutants were recovered which possessed second site mutations and these additional mutations reduced IRES activity further. In particular, a substitution at a conserved nt at the J-K boundary (nt 730, G→A) severely decreased IRES activity.

To analyse if all mutants with one nucleotide different from the wt sequence were functional, a set of single point mutants was generated. This revealed that some single point mutants did in fact have relatively low IRES activity. Furthermore, the position of the substitution had an effect on activity. In particular, substitutions at position 4, of the 4 nt targeted for mutagenesis, dramatically diminished IRES activity. In comparison, all IRES mutants with substitutions at position 1 retained significant activity. The least activity for the single point mutants was observed when a U residue was substituted at each position. It is unclear why the presence of a U residue had such a dramatic effect on IRES activity when several of the points mutants which contained a substitution of the other pyrimidine, C, demonstrated a much higher activity.

It has been demonstrated that these 4 conserved nt are critical for internal initiation but their specific role remains unknown. Their role is considered in detail in Chapter 4 but, in brief, there are 3 possibilities. The first of these is that the sequence AC/GA is important for maintaining the secondary structure of the IRES element. Inspection of the predicted secondary structure of the J-K domains (shown in Figure 8) shows that these 4 nt are present as unpaired two-nucleotide bulges and surrounded by a high level of base-pairing. Therefore, it would seem unlikely that thermodynamics would favour a change in secondary structure. The other two possibilities are that these nt are involved in either RNA-RNA interactions required for the maintenance of the tertiary structure of the IRES or in functional protein interactions. The fact that the nt are unpaired makes both of these options probable. As mentioned previously, eIF4GI binds close to these nt. Indeed, Kolupaeva *et al.* (1998) identified that the A at nt 724 is protected during a chemical protection assay of the EMCV IRES incubated with eIF4GI. This is the nt at position 4 within the J-loop mutant pool and it is

substitutions at this nt which have the most profound effect on IRES activity. Furthermore, the same research group recently reported that the A residue at nt 704 (i.e. position 1 of the 4 nt targeted for mutagenesis) was also protected from chemical modification by eIF4GI (Kolupaeva *et al.*, 2002). Consequently, it was decided to investigate if there was a correlation between the activity of J-loop mutants and their ability to bind eIF4GI. This was done using a bead-IRES-protein binding assay (Stassinopoulos & Belsham, 2001) and is described in Chapter 4.

The selection system has been previously used to analyse a large pool of mutants in the GNRA motif (Robertson *et al.*, 1999). Both applications of the system have demonstrated that it represents a convenient and effective way of investigating the importance of particular nucleotides in relation to IRES function. It also confirmed that the system is very sensitive, as a low expression of HOOK at the cell surface is sufficient for cell selection to occur. Moreover, it has been shown that the system is useful at distinguishing between non-functional IRES elements and IRES elements with a low activity. However, within both applications, a relatively high background of non-functional IRES elements was observed. Several modifications were made in an attempt to reduce this background. The first of these modifications was to extract the RNA rather than DNA from selected cells which means that all the IRES elements recovered had been expressed within the selected cells. Therefore, it can be deduced that the background of non-functional IRES elements still observed cannot have resulted from contamination of plasmids adhering to the outside of cells during transfection. Consequently, the low level of enrichment seen must result from co-transfection of plasmids. Attempts were made to reduce the level of co-transfection occurring but these seem to have had limited success.

Since this selection system was first developed, two other systems have been set up to screen for sequences which function as IRES elements within cells (Owens *et al.*, 2001; Venkatesan & Dasgupta, 2001). Both these systems utilised dicistronic constructs encoding 2 different fluorescent proteins. Cells, containing constructs in which both cistrons were expressed, were selected using fluorescent-activated cell sorting. Additionally, both systems were used to analyse a large library of random synthetic sequences of either 9nt or 18nt (Owens *et al.*, 2001) or 50nt (Venkatesan & Dasgupta, 2001) for IRES function. However, these systems used different methods for delivering the dicistronic plasmids/constructs into cells. Owens and colleagues used a retroviral vector to express the dicistronic constructs within mammalian cells. Bacterial protoplast fusion was utilised by Venkatesan and Dasgupta for delivery of a library of bicistronic plasmids into mammalian cells. Bacterial protoplast-fusion has the advantage that it results in near-clonal delivery of plasmids into cells (Tan & Frankel, 1998) and a relatively high level of enrichment was seen in the selection system used by Venkatesan and Dasgupta. Interestingly, they also carried out preliminary experiments to compare using the selection system following delivery of plasmids into cells by either protoplast fusion or by transfection. They used a pool of IRES elements containing mostly weak IRES elements and few very active IRES elements (using a ratio of 10^4 known weak IRES elements to 1 known strong IRES element). Significantly more enrichment of functional IRES elements was observed when protoplast fusion was used rather than transfection. For future applications of the HOOK selection system, it would be interesting to investigate using other methods of delivering the dicistronic GUS/HOOK vectors into cells and see if the level of enrichment gained in the system could be improved. It is very possible that using

bacterial protoplast fusion as a near-clonal method of delivering plasmids into cells within the HOOK selection system could alleviate the problem of a high background. However, despite this problem, the HOOK selection system clearly allows sufficient enrichment to facilitate identification of functional IRES elements.

CHAPTER 4

Protein Interactions with EMCV IRES Elements containing Mutations within Domain J

4.1 Introduction and Aims

As described in Chapter 3, four conserved nucleotides within domain J of the EMCV IRES (nt 704-705 and 723-724) have been identified as essential for IRES activity. The next step was to investigate the actual function of these nt and determine if they were involved in IRES:protein interactions. The EMCV IRES has been shown to require the canonical translation factors eIF2, eIF3, eIF4A and eIF4G to form 48S preinitiation complexes in an *in vitro* assay (Pestova *et al.*, 1996a; Pestova *et al.*, 1996b). The middle third of factor eIF4GI (amino acids 635-1039) contains an RNA binding domain (Pestova *et al.*, 1996a; Marcotrigiano *et al.*, 2001) and has been shown to bind directly to the EMCV IRES element (Pestova *et al.*, 1996a; Kolupaeva *et al.*, 1998). Therefore, it acts to recruit 40S ribosome subunits to the IRES sequence and allow internal initiation to occur. A second function of this binding is to enable eIF4A to be recruited to the IRES element which is also essential for IRES activity (Pause *et al.*, 1994b; Svitkin *et al.*, 2001a).

The binding site for eIF4GI is now known to lie within the J-K region for cardio- and aphthovirus IRES elements (Kolupaeva *et al.*, 1998; Lopez de Quinto & Martinez-Salas, 2000; Saleh *et al.*, 2001; Stassinopoulos & Belsham, 2001). The first

study involved chemical and enzymatic protection assays of the EMCV IRES incubated with eIF4GI and this suggested that eIF4GI interacted with the oligo(A) loop situated at the junction between the J and K domains (Kolupaeva *et al.*, 1998). However, mutagenesis studies revealed that the structural context of this loop was also critical for eIF4GI binding (Kolupaeva *et al.*, 1998). In addition, several other nucleotides within the J and K domains are also protected by eIF4GI in chemical/ enzymatic probing including the A at position 704 and the A at position 724 (Kolupaeva *et al.*, 1998; Kolupaeva *et al.*, 2002). The results reported in Chapter 3 show that many mutations at nt 704, 705, 723 and/ or 724 within the EMCV IRES resulted in a significant loss of IRES activity and interestingly IRES elements containing a substitution at position 724 alone demonstrated a very low activity. Recently, strong evidence has been presented that confirms the interaction of eIF4G to the FMDV IRES elements is functionally relevant *in vivo* (Lopez de Quinto & Martinez-Salas, 2000). Therefore, it was decided to investigate if the low activity of several of the J domain mutants could be explained by a reduced ability to bind eIF4G compared to the wild-type IRES.

A bead-IRES-protein binding assay was developed in our laboratory to investigate protein interactions to the FMDV IRES (Stassinopoulos & Belsham, 2001). The system utilises polyadenylated IRES elements which are immobilised on oligo-dT magnetic beads. This bead: IRES complex is then incubated in rrl and following this, the proteins bound to the IRES are analysed (the system is shown diagrammatically in Figure 19). It was used to demonstrate that eIF4G, eIF4A and eIF4B bind to the 3' end of the FMDV IRES. This work confirmed the findings of other studies which used UV cross-linking assays (Meyer *et al.*, 1995; Lopez de Quinto & Martinez-Salas, 2000;

Figure 19: Bead-IRES-protein binding assay. An RNA molecule corresponding to the EMCV IRES attached to a 30nt-long poly(A) tail was immobilised to oligo dT-coated magnetic beads. The bead-IRES complex was then incubated with rrl for 1 hr. After this time, the proteins bound to the IRES-bead complex were analysed using SDS-PAGE and immunoblotting. The levels of specific proteins in the depleted lysate could also be analysed.

Figure 19

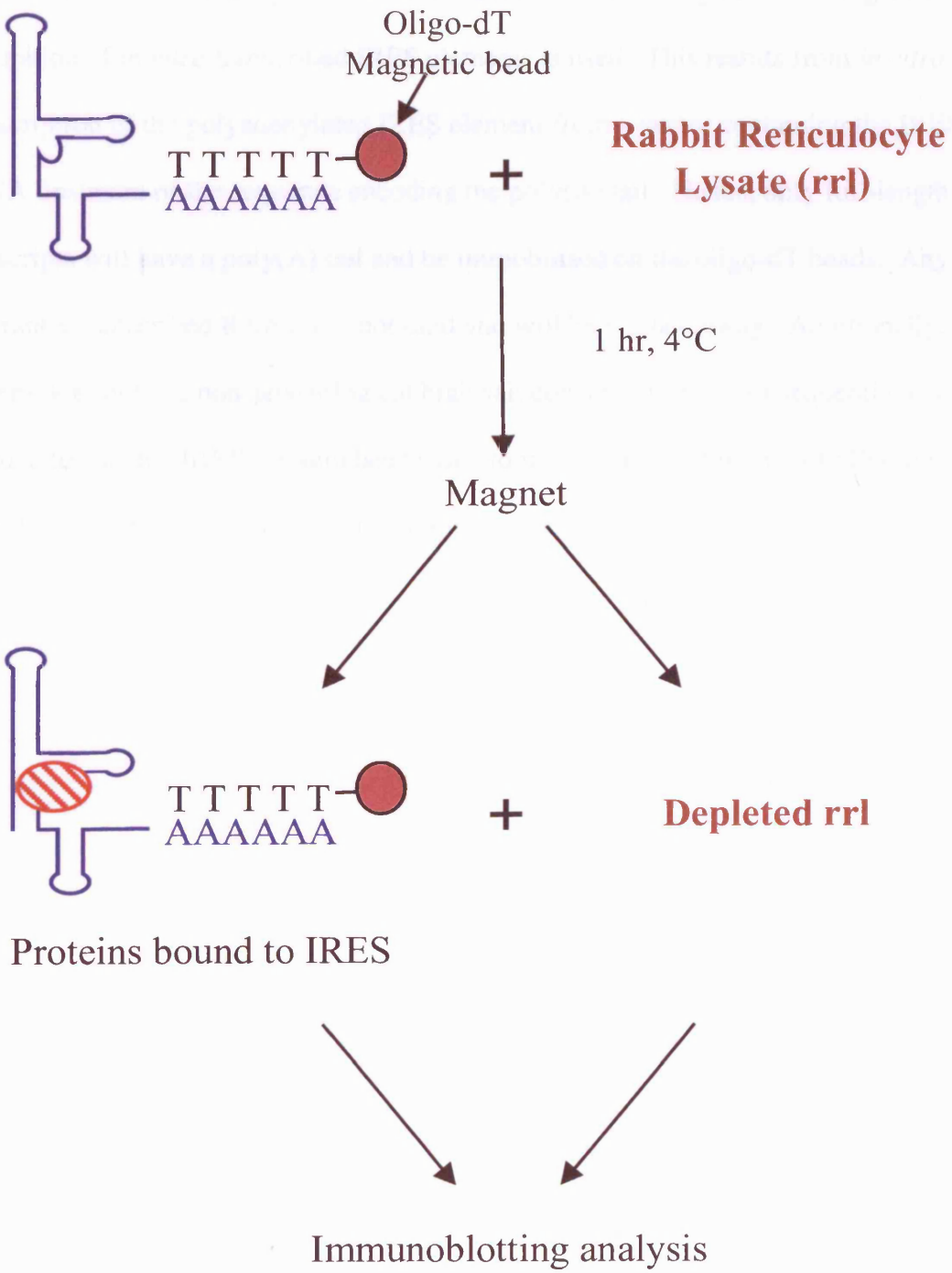
Oligo-dT
Magnetic bead
T T T T T
AAAAAA
+
Rabbit Reticulocyte Lysate (rrl)
1 hr, 4°C
Magnet
T T T T T
AAAAAA
+
Depleted rrl
Proteins bound to IRES
Immunoblotting analysis

Saleh *et al.*, 2001; Lopez de Quinto *et al.*, 2001). Furthermore, the effect of the depletion of IRES-binding proteins from rrl on IRES activity was investigated using functional assays of the FMDV IRES activity within depleted lysates. This showed that eIF4G depletion from the rrl significantly inhibited FMDV IRES-mediated translation. The bead assay offers several advantages including that a homogenous population of *in vitro* transcribed IRES elements is used. This results from *in vitro* transcription of the polyadenylated IRES element from a vector containing the IRES cDNA upstream of the sequence encoding the poly(A) tail. Hence, only full-length transcripts will have a poly(A) tail and be immobilised on the oligo-dT beads. Any aberrantly transcribed RNAs will not bind and will be washed away. Additionally, the system does not use non-physiological high salt concentrations. Consequently, it was decided to use this IRES: protein bead assay to investigate the binding of eIF4GI to EMCV IRES elements which contain mutations within the J domain.

4.2 Methods

4.2.1 Construction of pSP64poly(A) Plasmids

A fragment of the EMCV cDNA encoding domains J to M of the IRES was cloned into the pSP64poly(A) vector to facilitate *in vitro* transcription of an RNA corresponding to the 3' section of the IRES with a 30-nt long poly(A) tail linked at the 3' end. The cDNAs of five IRES elements containing mutations within the J domain were cloned into pSP64poly(A) and these are listed in Table 7. To facilitate this cloning, PCR was performed on GUS/HOOK vectors containing the cDNAs of the J domain mutants. This PCR introduced a *Hind*III site just upstream of the cDNA corresponding to the start of the J domain of the IRES. The PCR was carried out (as described in Section 2.2) using an annealing temperature of 50°C and the proof-reading enzyme, *Pfu* (Promega, 1.5 units). The primers used were 5' GTATAAGCTTAGGGG CTGAAGGATGCC 3' (forward, complementary to the start of the J domain) and 5' GGAATGCACTGGGTTCGTC 3' (reverse, complementary to the HOOK region). The PCR generated a 355bp product. A separate PCR was carried out to generate a product containing the wt EMCV IRES cDNA. In this reaction, the template SKEMCRB (Drew & Belsham, 1994) was used with the primers 5' GTATAAGCTTA GGGGCTGAAGGATGCC 3' (forward) and M13 (Promega, reverse). This produced an approximately 250bp product.

The PCR products were purified using a low melting point agarose gel and GFX kit (Amersham Biosciences) and resuspended in 50µl mQ H_2O. These products were treated with *Taq* DNA polymerase which added an A residue to the 3'

J Domain EMCV IRES Mutants Sequence at nt 704, 705/ 723, 724	Activity*
AC/GA (wt)	++++
A**A**/GA	++
A**A**/G**U** #	+/–
AC/**AG**	+
AC/G**U**	+/–
GC/**CU**	–

Table 7: The EMCV IRES elements containing mutations within the J domain (at conserved nt 704-705 and 723, 724) which were used in the IRES: protein binding assay. The nt highlighted differ from the wt sequence. The relative activities shown correspond to the activity of the respective IRES elements both *in vitro* (in TNT assays) and in transient expression assays within cells as reported in Chapter 3.

* These activities relate to: ++++ wt IRES activity; ++ clearly functional but reduced activity compared to wt IRES; + low IRES activity; +/– little or no activity or – clearly non-functional

This mutant contains a second site mutation at nt 741 (A → U)

ends of the PCR product and allow the PCR products to be cloned into a T-vector which has a 3' terminal T residue. Reactions were set up with 4µl purified PCR product, 10x *Taq* buffer containing $MgCl_2$ (1µl, Roche), dATPs (final concentration 0.2mM), *Taq* polymerse (5 units, Roche) and made up to a final volume of 10µl with mQ H_2O. The reactions were incubated at 70°C for 30min. This product was then ligated directly into the T-Easy vector (Promega). This cloning step allowed more efficient cleavage of the PCR products by the restriction enzyme *Hind*III which has a very low cleavage efficiency when the restriction site has short overhangs. After transformation, vectors containing inserts were selected by screening on indicator X-gal LB plates (LB agar plates containing 0.5mM IPTG and 80µg/ml X-gal). If an insert is present it will disrupt the B-galactosidase gene within the vector and therefore the resulting colony will be white not blue on X-gal LB plates. These plasmids were then digested with both *Hind*III and *Bam*HI to generate a 144 bp fragment encoding domains J,K, L and M (nt 679-823 using the numbering system of Duke *et al.*, 1992). This fragment was ligated into similarly digested pSP64Poly(A) (Promega) and transformed into competent *E. coli* cells (DH5α). Resulting colonies were screened using restriction enzyme digestion to confirm the insert was present. Midi-prep DNA was then purified. The sequence was verified using an automated ALFexpress DNA Sequencer (as described in Section 2.14). A Cy5-labeled primer complementary to the SP64poly(A) vector (5' TAGGCTTGTACATATTGTCG 3') was used.

4.2.2 *In Vitro* Transcription

The plasmids derived from pSP64Poly(A) were linearised with *Eco*RI and the

resulting DNAs were purified using phenol extraction followed by ethanol precipitation. A pSP64poly(A) plasmid containing the full-length FMDV IRES (nt 371-803) in anti-sense orientation (named F-, Stassinopoulos & Belsham, 2001) was also linearised. These linearized plasmids were used as templates for *in vitro* transcription. The RNA transcripts were produced according to the manufacturer's instructions (SP6 Megascript, Ambion). Briefly, reactions were set up containing 1μg linear template DNA, ATP, CTP, GTP and UTP (final concentrations 5mM each), 10x reaction buffer (2μl), SP6 RNA polymerase mix (2μl) and made up to a final volume of 20μl. An overnight incubation at 37°C was used. An aliquot for each RNA (1μl) was run on a 1% TBE gel (final concentrations 100mM Tris, 100mM Boric acid and 50mM EDTA) and viewed under UV illumination to confirm the reaction had worked. The RNA product was approximately 175nt for all the samples (composed of 144nt IRES fragment and a 30nt-long poly(A) tail). The RNAs were purified using phenol/ chloroform/ isopropanol extraction and resuspended in nuclease-free H_2O (25μl, Promega). Spectrophotometry (λ_{260}) was used to determine the concentration of the RNAs using the equation: OD_{260} x dilution factor x 40 = μg/ml RNA.

4.2.3 Bead-IRES-Protein Binding Assay

4.2.3a Analysis of eIF4GI Binding to the J Domain EMCV IRES Mutants

Oligo-dT Dynabeads (0.5ml, Dynal) were captured using a magnetic particle concentrator (MPC, Dynal) and the supernatant was removed. Note, for all steps involving the MPC, the beads were placed in the MPC for at least 30s. The beads were washed with 0.5xSSC (75mM NaCl, 7.5 mM Tri-sodium citrate to pH 7.0, 0.5ml) and

twice with binding buffer (10mM Tris pH 7.5, 100mM KCl, 2mM $MgCl_2$, 200µl) using the MPC. They were resuspended in 50µl binding buffer. An excess of *in vitro* transcribed RNA transcripts (5µg) was incubated with the washed beads at 4°C for 30min with constant mixing. Using the MPC, the unbound RNA was removed and 20µl was run on a 1% TBE gel to confirm an excess of RNA had been used. The beads were washed twice with binding buffer (200µl). Nuclease-treated rabbit reticulocyte lysate mix (50µl, Promega) was added to the beads and incubated at 4°C for 60min with constant mixing. Using the MPC, the beads were captured and the depleted rrl was removed. The bead-IRES-protein complexes were washed twice in binding buffer (200µl) and resuspended in SDS-sample buffer (80µl). To dissociate the bound proteins from the beads, the SDS-buffer/ bead mix was incubated at 4°C for 10min on a rotating wheel. The SDS-buffer was removed using the MPC and then heated at 95°C for 5min. The used beads were discarded. The level of eIF4GI bound to the IRES elements was analysed by 7% SDS-PAGE, followed by western blotting. The immunoblotting was carried out as described in Section 2.12 using an antibody raised against the C-terminal of eIF4GI (Li *et al.*, 2001a).

4.2.3b Analysis of eIF4A Binding to the J Domain EMCV IRES Mutants

The bead assay was carried out as above but with several notable differences. These are:

1) The bead: RNA complex was incubated with 25µl rrl and 5µg tRNA (Sigma) instead of 50µl rrl.

2) After the 60min incubation of the beads with the rrl, the depleted lysate was removed and kept. Aliquots of the depleted rrl (1μl) were added to SDS-sample buffer and the remainder was stored at –70°C.

3) Immunoblotting analysis was carried out using 10% SDS-PAGE and an antibody raised against the N-terminus of eIF4AI (Li *et al.*, 2001a).

Results

4.3.1 Analysis of eIF4GI Binding to EMCV IRES Elements Containing Mutations within the J Domain

Mutations at nt 704-705 and nt 723-724 within domain J of the EMCV IRES can have a pronounced effect on IRES activity as demonstrated in Chapter 3. A selection of J domain mutants showing a wide range in activities was used (shown in Table 7) to investigate if the interaction of eIF4GI with the EMCV IRES were affected by these mutations. Fragments of EMCV cDNA corresponding to the J, K, L and M domains of the IRES of five J domain mutants and the wt EMCV IRES were cloned in the SP64poly(A) vector. These vectors were linearised with *Eco*RI and then transcribed *in vitro* to generate RNAs corresponding to domains J to M of the EMCV IRES linked at their 3' termini to a 30 nt poly(A) tail. The poly(A) tail enables the IRES fragments to be immobilised on oligo-dT magnetic beads. It also ensures that full-length transcripts are exclusively immobilised as only full length transcripts will have a poly(A) tail. The solution containing unbound RNA was analysed using electrophoresis to ensure an excess of RNA was used (see Figure 20, panel A).

The bead- IRES complexes were then incubated with nuclease-treated rrl (50μl) and the level of eIF4GI bound to the IRES elements was analysed (Figure 20, panel B). This experiment was carried out in duplicate and identical results were obtained. As expected, the wt EMCV IRES bound eIF4GI strongly. This was in contrast to the J domain mutants. The mutant containing the sequence of AA/GA at the 4 nt targeted for mutagenesis bound the highest amount of eIF4GI compared to the

Figure 20: Bead-IRES-protein binding assay to analyze the level of eIF4GI bound to EMCV IRES elements containing mutations within the J domain. RNAs (5μg) corresponding to nt 679-823 of the EMCV IRES linked to a 30nt-poly(A) tail, were immobilized onto oligo-dT Dynabeads. The unbound RNA was removed and electrophoresis of an aliquot of the unbound RNA (20μl) confirmed an excess of RNA had been incubated with the beads (panel A). The bead-IRES complexes were then incubated with 50μl of rrl. After this time, the depleted lysate was removed and the proteins bound to the beads were eluted in 80μl SDS-sample buffer. The level of eIF4GI bound to the IRES elements was analyzed using SDS-PAGE (6%) and immunoblotting (panel B).

F- is an RNA containing the full-length FMDV IRES in the anti-sense orientation. An aliquot of non-depleted rrl (1μl rrl in SDS-sample buffer) was included as a positive control for immunoblotting.

This mutant contains a second site mutation at nt 741 (A → U)

Figure 20

A


AA/GA
AA/GU #
AC/AG
AC/GU
GC/CU
AC/GA (wt)
F–
Excess RNA

B

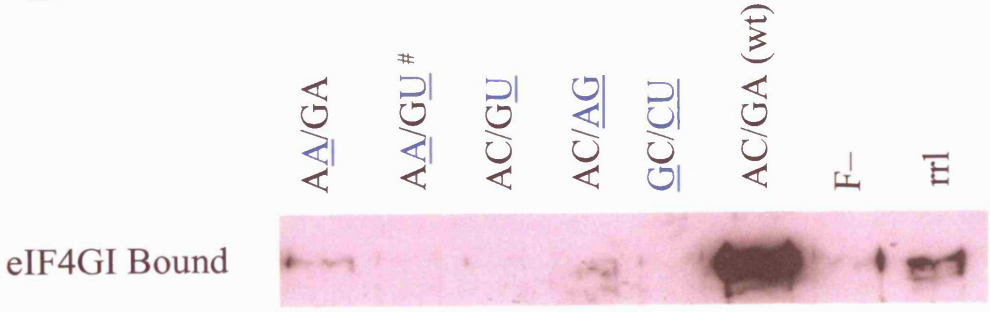
AA/GA
AA/GU #
AC/GU
AC/AG
GC/CU
AC/GA (wt)
F–
rrl
eIF4GI Bound

other mutants. However, although it did bind eIF4GI, it was to a much lesser extent than the wt IRES. This mutant IRES element is known to have a significant activity (much higher than the other J domain mutants tested in this assay) but it does have a lower activity than the wt IRES. For example, phosphoimager quantification of the IRES-mediated translation of proteins in TNT assays suggest the sequence AA/GA results in an IRES element which is approximately 7-fold less active that the wt IRES (see Chapter 3, Figure 13). Additionally, this IRES element was clearly functional within cells but, again, to a lesser extent than the wt IRES (see Figures 14 and 18). Therefore, there is a clear correlation between the activity of the J domain mutant IRES elements and their ability to bind eIF4GI. The remaining J domain mutant IRES elements tested either bound very low or no eIF4GI as none was detected in this assay. It should be noted that mutant AA/GU contains a second site mutation (nt 741 A→U) which may have affected the binding of eIF4GI. The RNA F- is the full-length FMDV IRES in the anti-sense orientation and, as expected (Stassinopoulos & Belsham, 2001), this did not bind eIF4GI.

4.3.2 Analysis of eIF4A Binding to EMCV IRES Elements Containing Mutations within the J Domain

It was decided to investigate the level of eIF4A bound to the J domain mutant IRES elements as eIF4A and eIF4G are associated together in the complex eIF4F. The bead assay was repeated. As for the eIF4GI assay, the RNA left unbound after incubation of the RNA with the beads was analysed using electrophoresis to confirm an excess of RNA had been incubated with the oligo-dT magnetic beads (see Figure 21, panel A). The bead-IRES complexes were then incubated with 20μl of nuclease-

Figure 21: Bead-IRES-protein binding assay to analyze the level of eIF4A bound to EMCV IRES elements containing mutations within the J domain. RNAs (5μg) corresponding to nt 679-823 of the EMCV IRES linked to a 30nt-poly(A) tail, were immobilized onto oligo-dT Dynabeads. The unbound RNA was removed and agarose gel electrophoresis of an aliquot of the unbound RNA (20μl) confirmed an excess of RNA had been incubated with the beads (panel A). The bead-IRES complexes were then incubated with 20μl of rrl and 5μg tRNA. After this time, the depleted lysate was removed and the proteins bound to the beads were eluted in 80μl SDS-sample buffer. The level of eIF4A bound to the IRES elements was analyzed using SDS-PAGE (10%) and immunoblotting (panel B).

F- is an RNA containing the full-length FMDV IRES in the anti-sense orientation. An aliquot of non-depleted rrl (1μl rrl in SDS-sample buffer) was included as a positive control for immunoblotting.

This mutant contains a second site mutation at nt 741 (A → U)

Figure 21

A

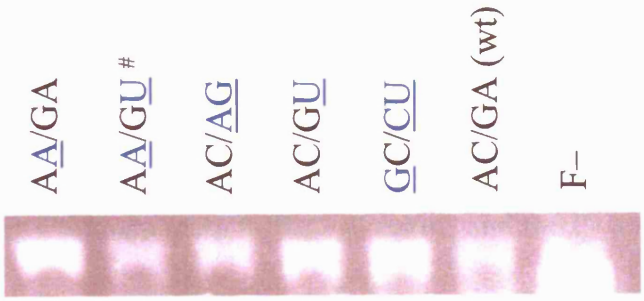
AA/GA
AA/GU #
AC/AG
AC/GU
GC/CU
AC/GA (wt)
F–

B

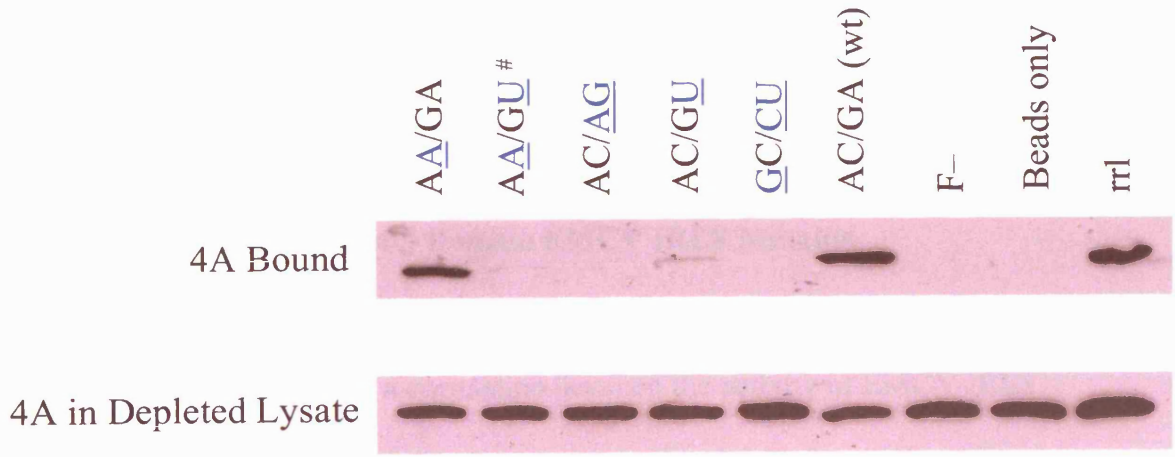
AA/GA
AA/GU #
AC/AG
AC/GU
GC/CU
AC/GA (wt)
F–
Beads only
rrl
4A Bound
4A in Depleted Lysate

treated rrl with added competitor RNA (tRNA, 5μg) to prevent any non-specific binding of eIF4A to the IRES. Immunoblotting analysis of eIF4A bound to the IRES:bead complexes revealed that the wt IRES strongly bound eIF4A (see Figure 21, Panel B). Additionally, the mutant containing the sequence AA/GA showed significant binding of eIF4A. It should be noted that the difference in binding affinity of the wt IRES and the mutant AA/GA for eIF4A appeared to be less than the difference in their affinities for eIF4GI (as seen in Figure 20, Panel B). Therefore it seems that some eIF4A is binding to the mutant IRES containing the sequence AA/GA independently of eIF4G binding. The remaining J domain mutant IRES elements and the F- transcript did not bind eIF4A. This confirms that the interaction between eIF4A and the wt IRES (in addition to the interaction between the IRES containing the sequence AA/GA and eIF4A) is specific. Some depletion of eIF4A from the rrl could also be detected in the reactions containing transcripts for the wt IRES and the mutant AA/GA (see Figure 21, panel B). Therefore, as expected, this assay confirmed the pattern of binding seen for the eIF4GI-binding assay,

4.3.3 Secondary Structure of J Domain EMCV IRES Mutants

It is clear that there is a correlation between the activity of EMCV IRES containing mutations at these four conserved nt within J domain and the ability of eIF4GI to bind to the mutants. However, it also possible that these mutations may affect the secondary structure of the J and K domains. Sequence prediction studies have shown that these 4 nt are present as unpaired two-nucleotide bulges and are surrounded by a high level of base-pairing (Duke *et al.*, 1992; Palmenberg & Sgro, 1997). It would seem that thermodynamics are unlikely to favour a change in structure

Figure 22: Predicted secondary structure of the J and K domains of the EMCV IRES mutants using the mfold program, version 3.1 (Zuker *et al.*, 1999; Mathews *et al.*, 1999). The name of the mutants shown corresponds to the sequence at nt 704, 705/ 723, 724 in domain J. The purple asterisks mark the position of nt 704 and 705. The green asterisks highlight nt 723 and 724.

The mutant AA/GU contains a secondary mutation at nt 741 (A→U)

Figure 22

AC/GA (wt)

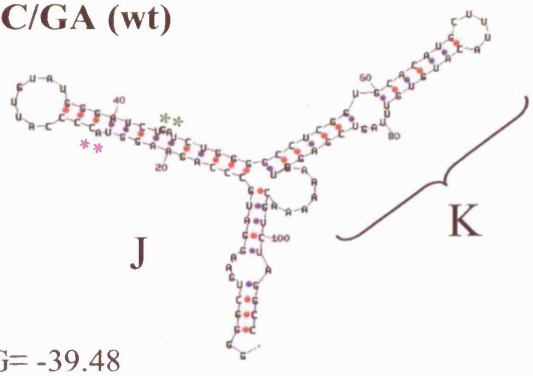

dG= -39.48

AA/GA

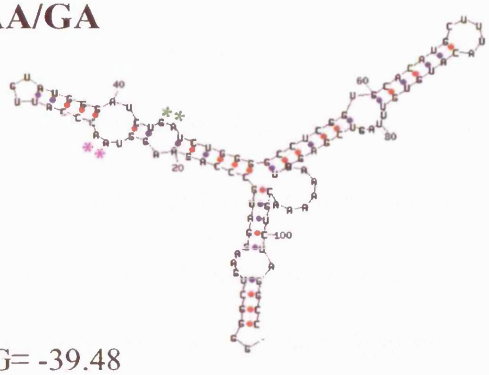

dG= -39.48

AA/GU

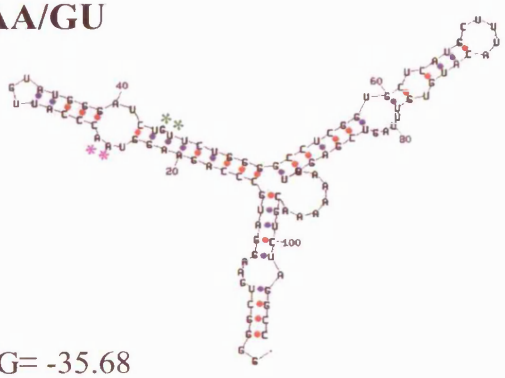

dG= -35.68

AC/AG

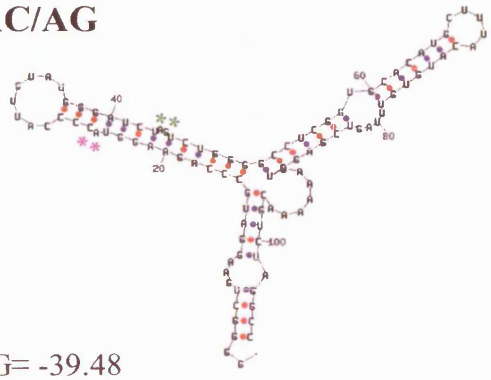

dG= -39.48

AC/GU

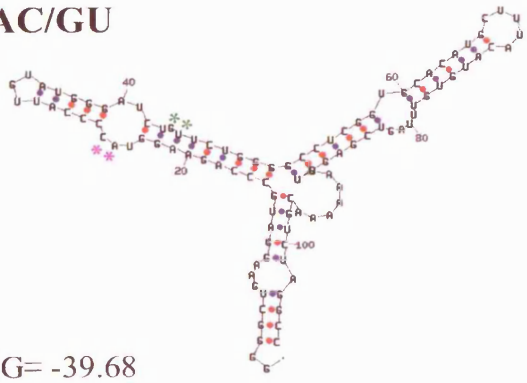

dG= -39.68

GC/CU

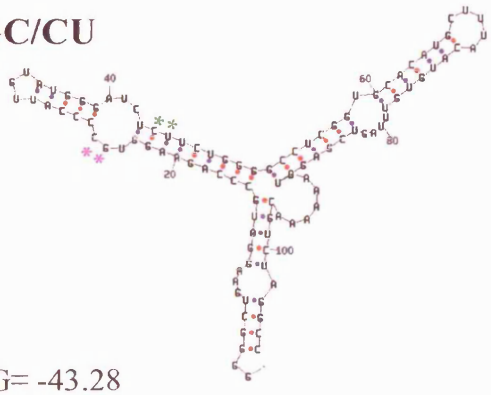

dG= -43.28

but for confirmation of this, it was decided to investigate the secondary structure of the J domain mutants using the RNA-folding prediction program, mfold version 3.1 (Zuker *et al.*, 1999; Mathews *et al.*, 1999). The results of this (shown in Figure 22) show that some very localised changes in secondary structure do occur within the stem of domain J. Note, the secondary mutation within the mutant containing the sequence AA/GU (of nt 741 A→U) does result in a slight change in secondary structure. Nonetheless, all the changes in secondary structure observed for the mutants are minor and do not change the basic Y-shape of the J and K domains. It is interesting to note that the secondary structure of the wt IRES was identical to the severely deficient mutant containing the sequence AC/AG, using this sequence prediction method. Furthermore, the functional mutant containing the motif AA/GA which can bind eIF4GI and eIF4A (albeit to a lesser extent than wt) shows the biggest change in secondary structure. These observations suggest that the small changes in the predicted secondary structure do not correlate to IRES activity and may not be significant.

4.4 Discussion

It has been shown that the conserved sequence at nt 704, 705, 723 and 724 within the J domain of the EMCV IRES is involved in the binding of eIF4GI. This was demonstrated by a clear correlation between the activity of IRES elements containing mutations within the J domain and the ability of the respective IRES elements to bind eIF4GI. It is interesting to recall (from Chapter 3) that no J domain mutant was isolated which had an activity equal to or more than the wt IRES. Hence, it is possible that the optimal binding of eIF4GI to the EMCV IRES occurs with the wt sequence of AC/GA at these nt. However, it should be noted that although the majority of sequences were generated, there is no guarantee that every possible sequence was analysed during cell selection. Furthermore, it is also feasible that other interactions (e.g. RNA: RNA interactions) could be involved in determining the activity of the J domain mutants but this will be discussed in detail below. The level of eIF4A bound to the J domain mutants followed the same pattern of binding as that observed with eIF4GI. This was expected because the two factors are associated with each other in the complex eIF4F. It is thought that eIF4A binds to the IRES indirectly through its interaction with eIF4G. This hypothesis is supported by previous experiments using the IRES-protein binding assay described here. It was found that eIF4A could not bind to the full-length FMDV IRES in eIF4G-depleted lysates (Stassinopoulos, 2000). The association of eIF4A with eIF4G is known to strongly stimulate eIF4G binding to the IRES (Lomakin *et al.*, 2000) and eIF4A is essential for IRES-mediated translation (Pause *et al.*, 1994b; Svitkin *et al.*, 2001a). The X-ray structure of the central portion of eIF4G has recently been determined and mutagenesis studies have revealed that the binding sites for eIF4A and IRES are adjacent and partially overlapping to each other

(Marcotrigiano *et al.*, 2001). This may explain why the binding of eIF4A and the IRES to eIF4G are linked.

The combination of using the cell selection system and the protein-IRES assay proved a powerful way to show a functional relevance for the binding of eIF4GI to the IRES *in vivo*. Since this work was commenced, another study has reported the same requirement of eIF4GI binding to the FMDV IRES for IRES activity (Lopez de Quinto and Martinez-Salas, 2000). In this case, the nucleotides 686 and 687 (sequence AA) were identified as being involved in the interaction of the IRES with eIF4GI. Like the nt investigated in our study, these nt are predicted to be unpaired and form a 2nt bulge. It would be interesting to analyse if these nt are also involved in binding eIF4GI to the EMCV IRES as one of the two nt is conserved among all cardio- and aphthovirus IRES elements and it is likely that eIF4G interacts with several nt distributed throughout the J domain. If so, it would be of significance to investigate the involvement of each of the different nt. So far, it has been shown that modification of just one nucleotide in the J domain is sufficient to abolish eIF4GI binding and IRES activity.

Recently, the interaction of the functional homolog of eIF4GI, called eIF4GII, with the EMCV IRES has been shown to be essential for IRES activity (Lopez de Quinto *et al.*, 2001). Identical to eIF4GI, eIF4GII binds to nucleotides 686 and 687 within domain J and mutations at these nt abolish eIF4GII binding and IRES activity. This suggests that both homologs bind to similar sequences and indeed there is 88% sequence identity between the central region of eIF4GI and eIF4GII (nt 754-1003) which contains the IRES binding site (Marcotrigiano *et al.*, 2001). Furthermore, residues shown to be critical for IRES binding are conserved between the two eIF4Gs.

Considering these facts, it seems likely that binding of eIF4GII to the J domain mutant IRES elements will also be affected to a similar extent as eIF4GI binding. The J domain mutants which do not bind eIF4GI are unlikely to bind eIF4GII as they have low IRES activity. Nonetheless, it remains to be determined if mutations could arise within the IRES which would lead to preferential binding of one of the two homologs.

It is also important to consider the effect of mutations on the secondary and tertiary structure of the IRES element. The predicted secondary structure of the different J domain mutants using the mfold program suggested that although small localised changes may have occurred, these do not correlate to changes in IRES activity or eIF4GI binding. However, these predicted secondary structures may not be wholly accurate and indeed there are small differences between the wt IRES secondary structure obtained from mfold and that obtained by Duke and colleagues in 1992. One such difference is that nt 705 is base-paired in the mfold prediction of the wt IRES which is of course relevant as nt 705 is one of the nt targeted for mutagenesis. In an attempt to resolve if changes in secondary structure had occurred within the mutant IRES elements, constructs were given to Graham Conn, UMIST, for analysis using RNA melting curves. Preliminary data shows that the mutants containing the sequences AA/GA and AC/AG at the 4nt targeted for mutagenesis gave rise to similar profiles as the wt IRES within the RNA melt experiments (data not shown). This indicates that the secondary structure for these three IRES elements is very similar. The conditions used resembled the conditions of the bead assay (i.e. 120mM KCl and 1mM $MgCl_2$). Unlike, the mfold structure predictions, the RNA melt profiles strongly suggested that significant alterations in secondary structure had occurred within the mutants containing the sequences AA/GU, AC/GU and GC/CU. The most divergent

profile was observed for the mutant containing the sequence AA/GU but this is likely to be due to a second site mutation at nt 741 (A→U). Therefore, it is possible that some of the mutations within the J domain (analysed in Chapters 3 and 4) may give rise to differences in secondary structure. The effect of this on eIF4GI binding has not been addressed directly in this study. However, from the preliminary RNA melting experiments it can be deduced that the mutant containing the sequence AC/AG has similar secondary structure to the wt IRES and yet it cannot bind eIF4GI. This suggests that factors other than secondary structure alterations influence eIF4G binding to the IRES element.

Furthermore, it would also be interesting to investigate the effect of the J domain mutations on the tertiary structure of the IRES. Unfortunately, little is known about the EMCV IRES tertiary structure. Studies on the FMDV IRES have indicated that RNA: RNA interactions do occur between domains (Ramos & Martinez-Salas, 1999; Beales *et al.*, 2001). Of course, both the secondary and tertiary structure of the IRES element could affect protein interactions. This is known to be the case for the interaction of the ribosomal protein S9 and eIF3 with the HCV IRES (Odreman-Macchioli *et al.*, 2000). It is possible that the IRES-protein binding assay used here could be modified to investigate interactions of the various domains of the EMCV IRES and to determine if the mutations within the J domain affect these. This could be performed by immobilising a specific domain of the IRES on oligo-dT beads, incubating with radioactively labelled fragments of the IRES and using autoradiography to investigate if any interaction occurred. So far, the bead assay has been used to investigate mainly IRES to protein interactions but it should prove useful in a wide range of applications.

CHAPTER 5

The Use of the Hepatitis C Virus IRES Element within the HOOK Cell Selection System

5.1 Introduction and Aims

Hepatitis C virus (HCV) belongs to the genus *Hepaciviruses* within the *Flaviviridae* family. This virus is widespread with an estimated 2% prevalence worldwide. Most people affected (approximately 70%) suffer from chronic infections. Interferon α and ribavirin are used to treat HCV but unfortunately these are not effective against several strains of HCV and an alternative is required. HCV is similar to picornaviruses in several aspects. It has a small positive sense RNA genome of approximately 9500nt which has both a 5' and 3' untranslated region with a single large ORF which encodes a polyprotein (refer to Figure 23, Panel A). Further, there is an IRES element present within the 5'UTR. However, there are also several significant differences between HCV and picornaviruses. One example of this is that the IRES elements from these viruses are significantly different. The HCV IRES is much smaller than the picornavirus IRES elements as it is just over 300nt long. Furthermore, its secondary structure and function are very different. The HCV IRES (shown in Figure 23, Panel B) is made up from 3 stem-loop structures (domains II to IV) and a pseudoknot which is critical for activity (Wang *et al.*, 1995). There is an additional stem-loop (domain I) upstream (nt 1-40 of the 5' UTR) but this is thought to be

Figure 23: Panel A shows the genome of HCV (ssRNA, about 9kb). There is one large ORF which encodes a polyprotein which is proteolytically cleaved by both cellular proteases and two virally-encoded proteases to produce the mature viral proteins. The structural proteins including the core protein (C) are shown in blue. The non-structural proteins are shown in orange. The 5' UTR contains an IRES element. The 3' UTR is involved in replication.

Panel B is an outline of the secondary structure of the HCV IRES. It is composed of 4 domains but the necessity of domain I remains unclear. There is a pseudoknot structure upstream of the initiator AUG.

Figure 23

A

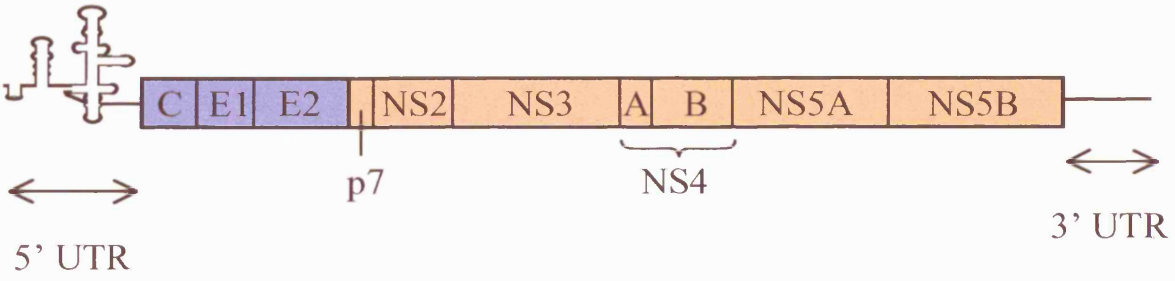
C
E1
E2
NS2
NS3
A
B
NS5A
NS5B
p7
NS4
5' UTR
3' UTR

B

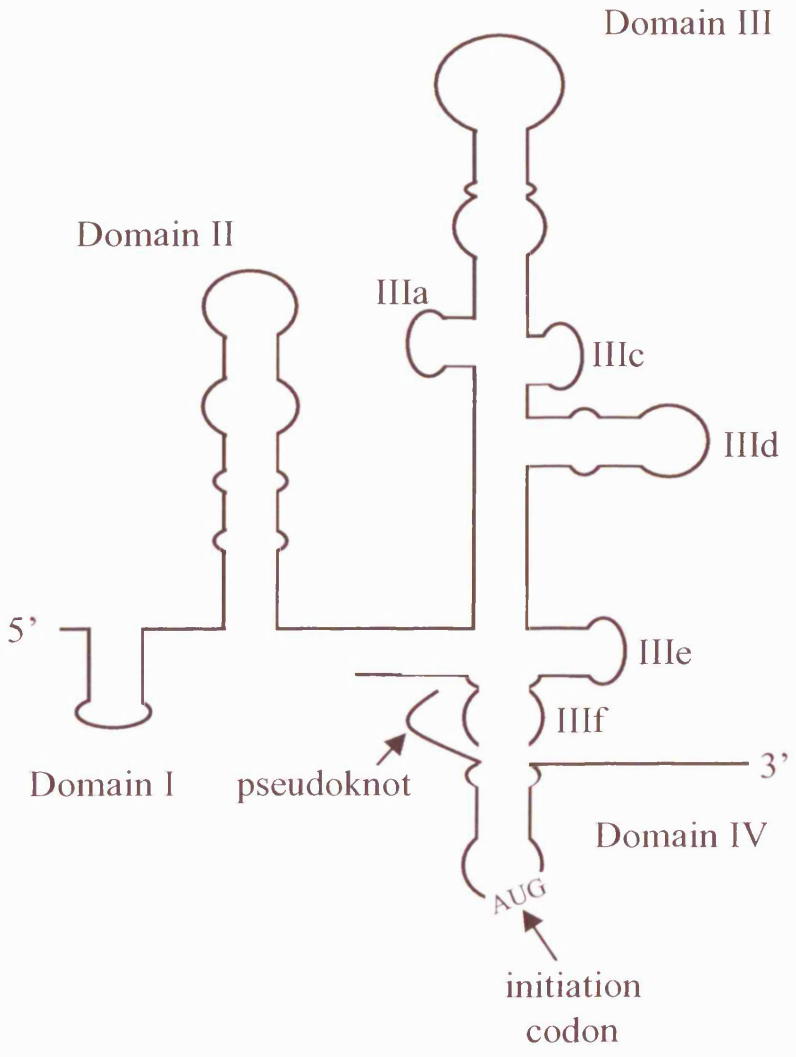
Domain III
Domain II
IIIa
IIIc
IIId
5'
IIIe
IIIf
3'
Domain I
pseudoknot
Domain IV
AUG
initiation
codon

unnecessary for the activity of the IRES (Rijnbrand *et al.*, 1995; Honda *et al.*, 1996; Reynolds *et al.*, 1996). There is also a significant body of research which suggests that downstream sequences (i.e. part of the coding sequence) are required for efficient IRES-driven translation (Reynolds *et al.*, 1995; Honda *et al.*, 1996; Lu & Wimmer, 1996). The effect of including part of the coding sequence varied depending on the reporter gene used and is now believed to be due to a requirement for a lack of secondary structure immediately downstream of the initiation site (Rijnbrand *et al.*, 2001). This means that the specific sequence of the viral coding sequence is unimportant and explains why some reporter genes which contain little secondary structure are translated efficiently from the HCV IRES with no need for viral sequence downstream of the initiator codon.

Another interesting feature of the HCV IRES is that it can recruit 40S ribosomal subunits directly (Pestova *et al.*, 1998b). 43S preinitiation complexes can be formed *in vitro* without the presence of eIF3, eIF4A, eIF4B or eIF4F. Indeed, translation initiation for HCV is unaffected by dominant negative mutants of eIF4A unlike cap-dependent or picornavirus IRES-driven translation (Pause *et al.*, 1994b; Pestova *et al.*, 1998b; Svitkin *et al.*, 2001a). Initially, HCV IRES-driven translation was considered to occur in a similar manner to translation of prokaryotic RNA as the small ribosome binds directly to prokaryotic RNA through base-pairing to the Shine-Dalgarno sequence. However, now it appears that the 40S subunit binds at multiple points in the IRES and that the tertiary structure of the HCV IRES is critical for binding (Kolupaeva *et al.*, 2000; Kieft *et al.*, 2001). Cryo-EM reconstructions of the HCV IRES bound to the 40S subunit (at approximately 20Å resolution) reveal that binding of the IRES induces a conformational change in the ribosomal subunit (Spahn

et al., 2001a). Other proteins have been shown to bind to the HCV IRES such as hnRNP L (heterogeneous nuclear ribonucleoprotein L), PTB and La but are not required for formation of 48S preinitiation complexes *in vitro* (Hahm *et al.*, 1998; Ali & Siddiqui, 1995; Ali & Siddiqui, 1997; Pestova *et al.*, 1998b). The factor eIF3 binds to the IRES and stimulates formation of 48S preinitiation complexes (Pestova *et al.*, 1998b; Sizova *et al.*, 1998). Furthermore, it is essential for assembly of 80S complexes (Pestova *et al.*, 1998b).

A cell selection system used to identify functional IRES elements is described in detail in Chapter 3. To recap this system allows selection of transfected cells expressing mRNAs containing a functional IRES element. If a functional IRES element is present there will be expression of a protein that is targeted to the plasma membrane and hence displays a cell surface epitope which allows selection of the cell. This system has now been used for several applications (Mulder *et al.*, 1998; Robertson *et al.*, 1999). However, all uses of the system have involved IRES elements from picornaviruses only. It was decided to investigate if the system could also be used to select functional HCV IRES elements. If this trial was successful it would facilitate thorough mutational analysis of the HCV IRES as the system can screen large numbers of mutants for sequences which give rise to functional IRES elements. Fortunately, it was found that HCV IRES elements of differing lengths and from a range of genotypes were all suitable for use in the selection system.

5.2 Methods

Bicistronic GUS/HOOK vectors containing IRES elements from different HCV genotypes and different lengths of the HCV 5'UTR (see Figure 24 for details) were kindly provided by Sven Enterlein and Prof. David Rowlands, University of Leeds.

Protein expression analysis was then carried out as described in Section 3.2.7 to assay the activity of the differing IRES elements both *in vitro* and within the HOOK cell selection system.

5.3 Results

Four different GUS/HOOK constructs were constructed at the University of Leeds which contained different portions of the HCV sequence from genotype 1b inserted between the two cistrons. The minimal defined IRES element lies within nt 40-344 but it was decided to investigate if nt 1-40 and 344-388 had any stimulatory effect on IRES activity within the context of this particular reporter system. This is because previous reports have generated different 5' and 3' boundaries for the HCV IRES element (Wang *et al.*, 1993; Fukushi *et al.*, 1994; Reynolds *et al*, 1995; Rijnbrand *et al.*, 1995; Lu & Wimmer, 1996; Laporte *et al.*, 2000). Furthermore, constructs were tested which contained HCV IRES elements from different genotypes

Figure 24: Portions of the HCV IRES were cloned into GUS/HOOK vectors which will express the dicistronic constructs shown. The area shown in red is the HCV 5'UTR. The HCV IRES lies within nucleotides 40-344 of the 5'UTR but nucleotides 1-40 and 344-380 have been reported to stimulate IRES activity in some cases. Constructs 1b1 to 1b4 contain different portions of the 5'UTR from genotype 1b. The remaining constructs contain the 5'UTR from other genotypes of HCV (2b, 3a, 4a, 5a and 6a) and are named accordingly. The HCV polyprotein ORF starts at nt 344 so translation of constructs 1b2, 1b3, 2b, 3a, 4a, 5a and 6a will produce a fusion protein of the HOOK protein and part of the HCV core protein.

Figure 24

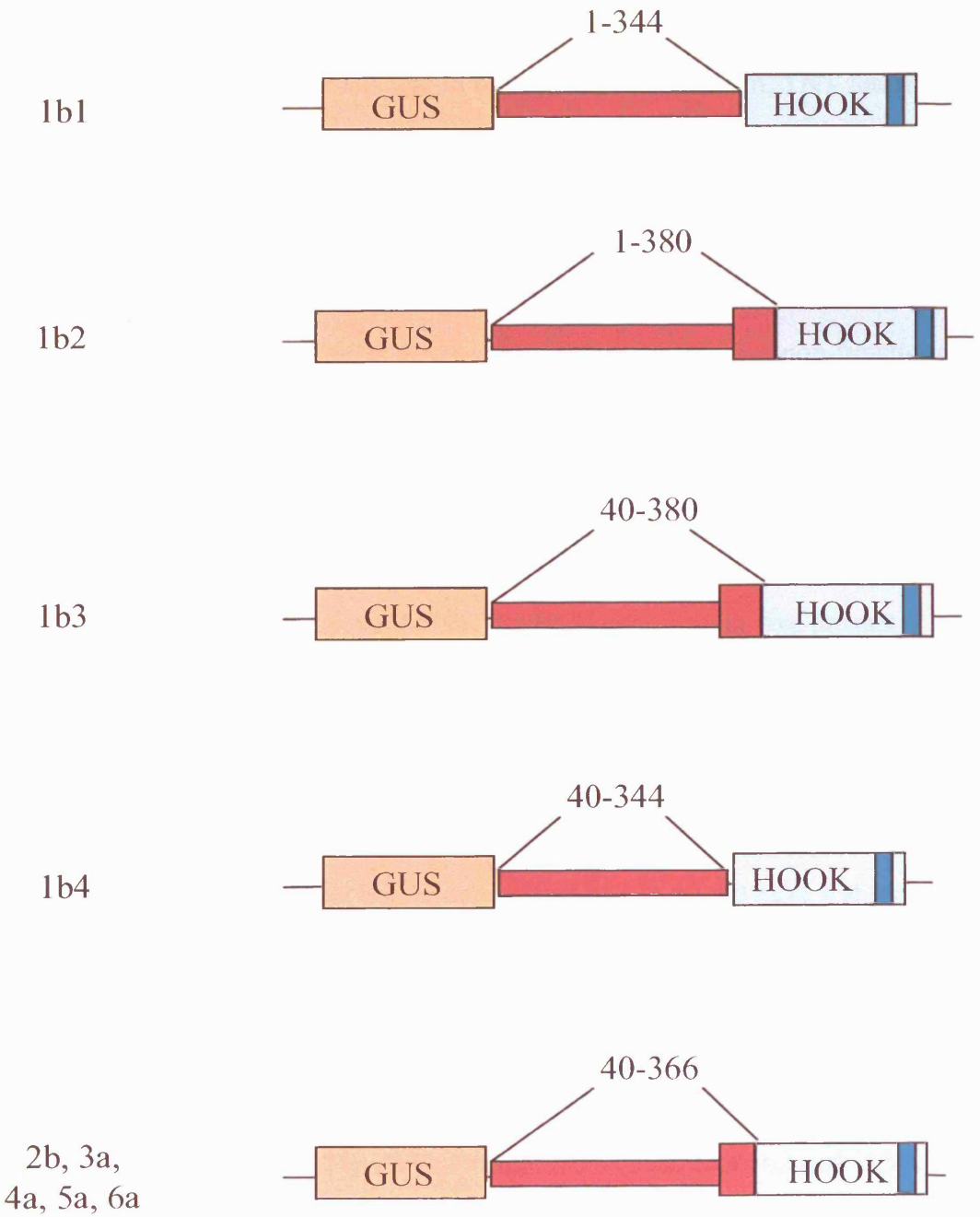
1b1
1-344
GUS
HOOK
1b2
1-380
GUS
HOOK
1b3
40-380
GUS
HOOK
1b4
40-344
GUS
HOOK
2b, 3a,
4a, 5a, 6a
40-366
GUS
HOOK

as these are known to vary significantly in their activity both *in vitro* and within cells (Buratti *et al.*, 1997; Collier *et al.*, 1998).

5.3.1 *In Vitro* Activity of the HCV IRES Constructs

Before testing the constructs within the cell selection system, TNT reactions were carried out to investigate the relative activities of the different constructs *in vitro*. Figure 25 shows that there was a large difference between the translational efficiencies of these constructs. Interestingly, construct 1b4, which contains the minimal defined length of the HCV IRES element (nt 40-344 from genotype 1b), was non-functional in this assay and no expression of HOOK was observed. Construct 1b1 was also non-functional which suggests that the first 40 nt of the 5'UTR did not significantly stimulate the activity of the IRES element. However, HCV IRES activity was strongly stimulated if part of the coding sequence for the HCV core protein was present immediately downstream of the IRES (shown by constructs 1b2 and 1b3 compared to 1b1 and 1b4). The highest activity of the HCV IRES was observed for construct 1b2, which contains nucleotides 1 to 380 and appeared to be as efficient as the wild-type EMCV IRES. This indicates that the sequence from nt 1 to 40 did have a stimulatory effect when in the context of the 40-380nt sequence. Constructs 1b2, 1b3, 2b, 3a, 4a, 5a and 6a contain part of the HCV coding sequence immediately upstream of the HOOK ORF and therefore a fusion protein of HOOK and part of the HCV core protein was seen for these constructs. The fusion protein from constructs 1b2 and 1b3 was larger than for the others as more HCV coding sequence was included in these two constructs. These differences in the size of the HOOK protein are clearly visible (in Figure 25). As expected, the HCV IRES elements from different genotypes showed

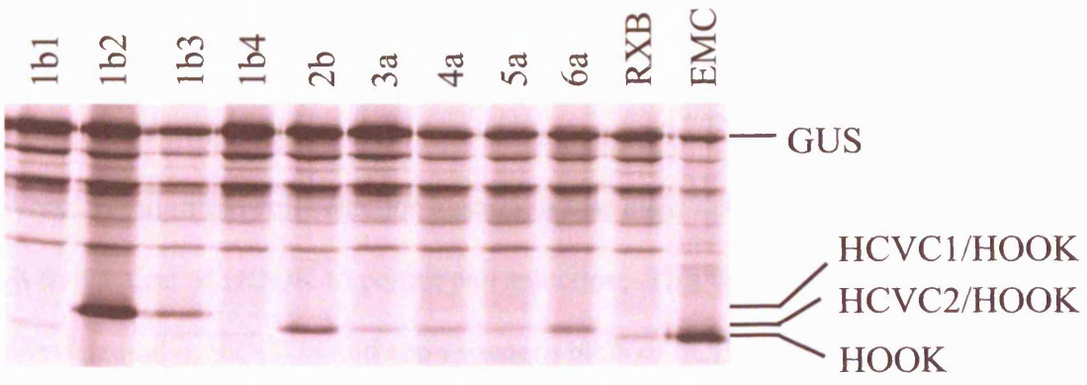

Figure 25: *In vitro* activity of the different HCV IRES constructs (as detailed in Figure 24). The GUS/HOOK plasmids were used to program TNT reactions and the proteins produced were analysed using SDS-PAGE and autoradiography. EMC is a GUS/HOOK vector containing the wt EMCV IRES. RXB is the plasmid GUS/RXB/HOOK which contains no IRES between the two cistrons. HCVC1/HOOK and HCVC2/HOOK are fusion proteins formed from part of the HCV core protein and the HOOK protein.

different activities. The IRES elements from genotypes 1b, 2b and 6a demonstrated the highest efficiency, in contrast to those from strains 3a, 4a and 5a which had either very low or no activity. The genotype 1b had the greatest activity when the sequences flanking the IRES were included in the construct.

5.3.2 Analysis of the Use of the HCV IRES in the Cell Selection System

When tested in the cell selection system, it was clear that all the constructs led to enough translation of HOOK to permit cell selection. This was evident from the clear bands detected in the GUS and actin western blots of SCE for the constructs containing the HCV IRES compared to the negative control RXB (shown in Figure 26, panel A). This is surprising considering many constructs had low or no activity in the TNT assays but may reflect some disparity between the *in vitro* and *in vivo* activity of the HCV IRES. Moreover, it is already known that the selection system is very sensitive and cells will be selected even if only a low level of HOOK is produced (Robertson *et al.*, 1999 and also refer to Chapter 3). Constructs 1b1, 1b3, 1b4, 3a and 4a all mediated low expression of HOOK with very faint bands detected in the HOOK SCE western blots. It should be mentioned that the constructs containing the IRES elements from genotype 5a and 6a and the EMCV IRES, all gave far stronger bands on the actin blot than for the other samples. This was due to a disparity in transfer efficiency in the western blots. A repeat experiment confirmed that these 3 constructs gave rise to bands of a similar intensity in the actin blot as the other constructs tested (except, of course, the negative control RXB and the control experiment containing no DNA which both gave no signal in the repeat experiment). Although all the HCV IRES elements mediated sufficient expression of HOOK to lead to cell selection,

Figure 26: The GUS/HCV IRES/HOOK constructs were tested in the cell selection system. BHK cells were transfected with plasmid DNA and cell selection was carried out. Immunoblotting was used to detect the levels of GUS, HOOK and actin in the selected cell extracts and total cell extracts. Actin acts as a marker for cell selection and the level of GUS in the total cell extracts indicates the efficiency of transfection.

Figure 26

A- Selected Cell Extracts:

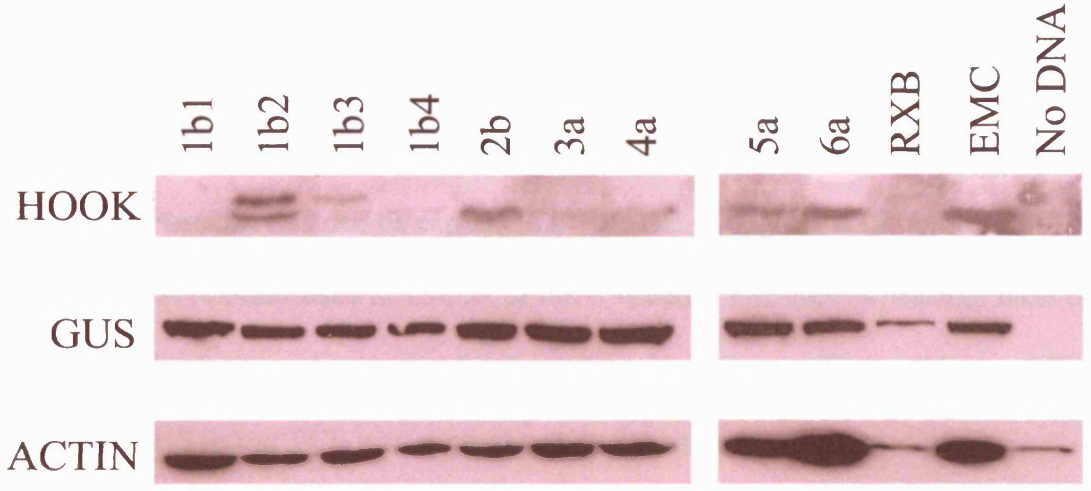

B- Total Cell Extracts:

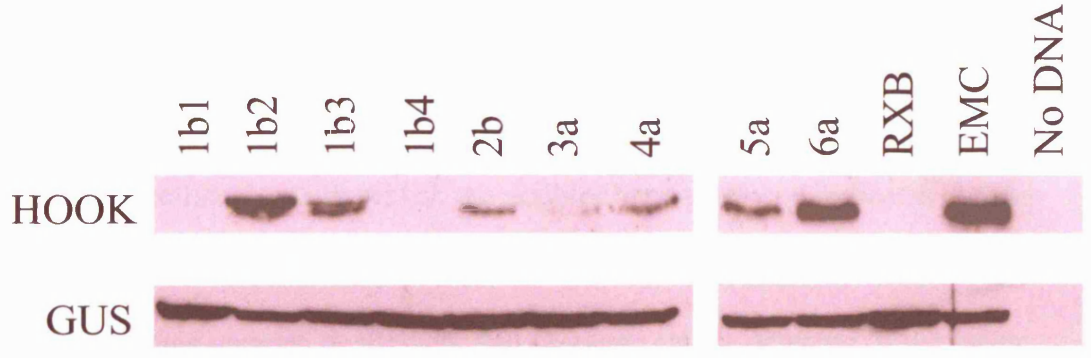

differences in HOOK expression was seen between the different genotypes (as was observed in the *in vitro* assay). The genotype 1b appeared to have the greatest activity. Previous reports have observed the IRES from genotype 2b to be more active than the IRES from 1b (Kamoshita *et al.*, 1997; Collier *et al.*, 1998). However, it should be remembered that in our assay a longer portion of the HCV 5'UTR was included in the 1b2 construct than for the other HCV IRES elements tested and these flanking sequences clearly enhance IRES activity. It is surprising that the IRES belonging to genotype 6a is so active as it was suggested to be the least efficient within cells (Collier *et al.*, 1998). Possibly this can be explained by the use of slightly different lengths of the HCV 5'UTR (Collier used nt 18-357 of the 5'UTR). The HOOK western blots of TCE confirm the pattern of activities for the different genotypes (Figure 26, panel B). The level of GUS in the TCE was approximately the same for each construct, indicating the efficiency of transfection was approximately equal.

An interesting feature is the presence of a doublet HOOK band for constructs 1b2 and 1b3. As mentioned before, these constructs both contain 36 nt of the HCV coding sequence and therefore will produce a fusion protein of the HCV core protein and HOOK. Before this investigation, it was unknown whether the fusion of additional sequences to the N-termini of the HOOK protein would affect expression of the c-myc epitope at the cell surface. However, the doublet band produced indicates that the fusion protein is actually cleaved within the cell and targeting of the c-myc epitope to the cell membrane appears unaffected. No cleavage can be detected of the fusion protein resulting from translation of constructs 2b, 3a, 4a, 5a or 6a. This could be due to the difference in size between the uncleaved and cleaved HOOK is too small to allow clear resolution of them by mini-gel SDS-PAGE. Alternatively, this smaller

fusion protein may remain uncleaved. Whatever the case, it appears that expression of a fusion protein of HOOK does not affect targeting of the c-myc epitope to the cell surface and cells containing a functional HCV IRES elements were successfully selected for.

Like the *in vitro* data, the 1b2 construct containing nt 1-380 of the 5'UTR was the most active of the HCV IRES elements tested giving the highest expression of HOOK within cells. This confirms previous suggestions that part of the coding sequence immediately downstream of the IRES can stimulate IRES activity significantly (Reynolds *et al.*, 1995; Honda *et al.*, 1996 and Lu & Wimmer, 1996). Several research groups suggest the first 40 nt are not involved in IRES activity (e.g. Rijnbrand *et al.*, 1995; Honda *et al.*, 1996 and Reynolds *et al.*, 1996) but it appears that nt 1-40 do stimulate IRES-mediated expression of HOOK. This stimulation has also been observed in a few other cases (Fukushi *et al.*, 1994; Laporte *et al.*, 2000). All these findings indicate that the HCV IRES can be used in the HOOK cell selection system.

5.3.3 Secondary Structure in HOOK Coding Sequence

As shown above, the sequences flanking the minimal defined HCV IRES element of nt 40-344 increased activity of the IRES when the HOOK reporter gene was used. Differences in the length of the IRES required for maximum activity have been noted when different reporter genes have been used (Rijnbrand *et al.*, 2001). These differences have even been noted for other viral IRES elements such as the EMCV IRES (Hennecke *et al.*, 2001). In the case of HCV, these differences are believed to be

Figure 27: RNA-folding predictions using mfold program, version 3.1 (Zuker *et al.*, 1999; Mathews *et al.*, 1999).

Panel A shows the folding of the HCV 5'UTR nt 331-380.

Panel B shows nt 331-344 of the HCV IRES coupled to the first part of the HOOK RNA transcript (approximately 45nt).

The location of the initiation codon (and the 3' boundary of the IRES) is highlighted in a red box.

Figure 27

A: HCV 5' UTR (nt 331-389)

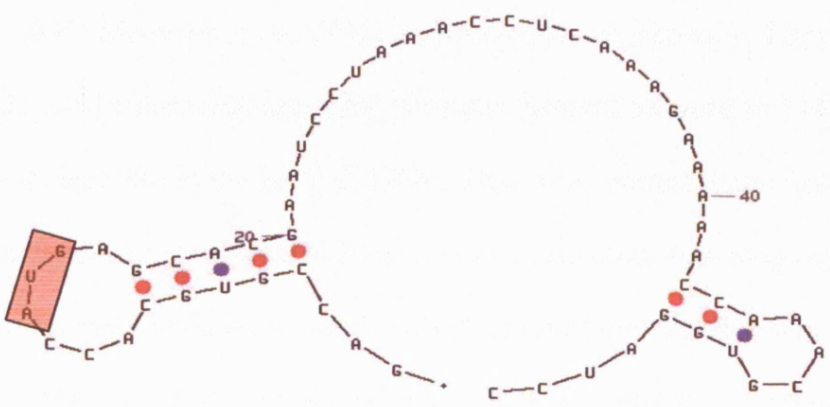

dG= -8.8

B: HCV 5'UTR nt 331-344 and part of HOOK RNA transcript

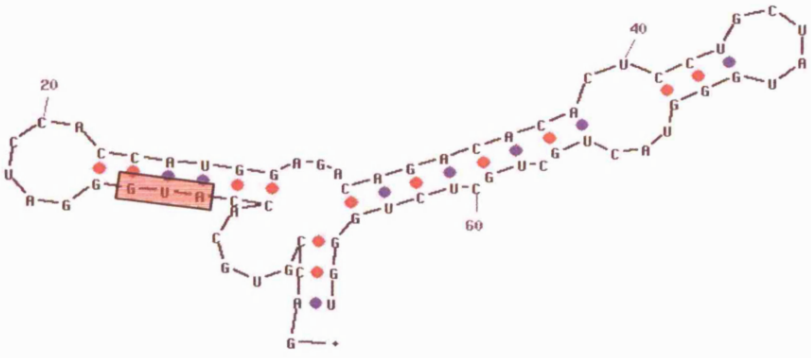

dG= -17.1

due to a requirement for a lack of secondary structure immediately downstream of the initiation site (Rijnbrand *et al.*, 2001). The presence of secondary structure is not thought to affect ribosome binding but is believed to be required for a subsequent event which has to occur before peptide synthesis can proceed. Consequently it was decided to investigate if any secondary structure was present within the first part of the HOOK coding sequence. The mfold structure prediction program, version 3.1., was used (Zuker *et al.*, 1999; Mathews *et al.*, 1999) and the results are shown in Figure 27. As expected, there is no substantial secondary structure present between nt 344 (from the initiation codon) and 380 of the HCV 5' UTR. This is in contrast to the first portion of the HOOK ORF which is predicted to form a more substantial stem loop structure. Hairpin structures positioned immediately downstream of the initiation codon are known to inhibit IRES activity (Rijnbrand *et al.*, 2001) and this may explain why HCV coding sequence immediately downstream of the IRES stimulates translation of HOOK.

5.4 Discussion

Research into HCV was hampered for many years by a lack of either a small animal model or a tissue culture system. Infectious full-length cDNAs were made available but RNA (from virus replication) could only be recovered when these were injected into primates (Kolykhalov *et al.*, 1997; Yanagi *et al.*, 1997). Recently significant advances have been made which include a small animal model (Mercer *et al.*, 2001) and a subgenomic selectable replicon which is functional within cell culture (Lohmann *et al.*, 1999; Blight *et al.*, 2000). The replicon system has limitations however, which include that it only genotype 1a and 1b can be used. Thus, it was desirable to investigate whether the HCV IRES could be used within a selection system previously developed in our laboratory (Mulder *et al.*, 1998; Robertson *et al.*, 1999) which identified functional IRES elements. This system would allow study of the translational efficiency of the HCV IRES independently of replication.

One potential problem of using the HCV IRES within the selection system was that part of the HCV protein-coding sequence would have to be included downstream of the HCV IRES within the bicistronic GUS/HOOK vectors to stimulate IRES activity. This would result in expression of a fusion protein formed from part of the HCV core protein and the HOOK protein. It was unknown whether this fusion protein would affect targeting of the c-myc epitope to the cell surface within the cell selection system. Consequently, several constructs were tested which contained different lengths of the HCV 5'UTR and IRES elements from different HCV genotypes. An *in vitro* assay showed that the minimal defined IRES element from HCV genotype 1b (i.e. containing no HCV coding sequence) was non-functional. In

addition, the IRES element from several HCV genotypes which contained 12nt of HCV coding sequence were non-functional in the assay. However, the activity of these constructs was significantly higher within BHK cells and all the HCV IRES constructs expressed a sufficient level of HOOK to permit cell selection. The difference between the activity of the HCV IRES elements *in vitro* and within cells may be due to the differences in temperature. The TNT assays were carried out at 30°C but the cultured cells were incubated at 37°C. Possibly the lower temperature of 30°C affected the secondary structure of the IRES element in the *in vitro* assay.

Nonetheless, it was consistently shown that the activity of the 1b HCV IRES both within cells and *in vitro* was greatly enhanced by the presence of the first 40 nt in the 5'UTR and also the first 36 nt of the HCV coding sequence (as an additional effect). This was in agreement with the findings of others (Reynolds *et al.*, 1995; Honda *et al.*, 1996; Lu & Wimmer, 1996; Laporte *et al.*, 2000). The HCV 1b construct containing nt 1-380 of the HCV sequence efficiently expressed a fusion protein of HOOK but fortunately this did not affect targeting of the c-myc epitope to the cell surface and cell selection occurred unhampered. It was interesting to observe that this fusion protein was actually cleaved by cellular proteases to release the mature HOOK protein which was then expressed at the cell surface.

Consequently, it can be concluded that the HCV IRES from several genotypes can be used within the cell selection system. This is a great advantage as this system allows screening of large numbers of mutant IRES elements to select sequences which give rise to functional IRES elements. Indeed, since this work was carried out, advances have been made by Sven Enterlein and others at the University of Leeds

(Enterlein, 2001). The selection system has now been adapted for use within transformed hepatocytes (HuH-7 cells) to more accurately represent the natural environment for HCV translation. Furthermore, studies have been commenced to study nt 266-269 (sequence GGGU) within the terminal loop of subdomain IIId using the selection system. This particular region was chosen as it is clear from previous mutational studies that subdomain IIId (along with other regions in domain III) are essential for IRES activity (Kieft *et al.*, 1999). Furthermore, the tertiary structure of this region has been elucidated by NMR (Klinck *et al.*, 2000). The 4 nucleotides at position 266-269 in the HCV IRES from genotype 1b2 were randomised by overlap PCR and the resulting pool of mutants was screened using the cell selection system. This work remains to be completed but it has identified a functional sequence of UGUA. It is surprising that this sequence gives rise to a functional IRES element as a previous study showed that each of the 3 Gs are essential for activity (Jubin *et al.*, 2000). However, this study analyzed a relatively small combination of mutations and the great advantage of the selection system is that it can screen through a pool of mutants containing up to 256 possible sequences. This allows a thorough investigation. To conclude, the work reported here has successfully prepared the way for future mutational study of the HCV IRES.

CHAPTER 6

Functional Analysis of Swine Vesicular Disease Virus 2A Protease: Residue 20 is a Critical Virulence Determinant

6.1 Introduction and Aims

Swine Vesicular Disease Virus (SVDV) is a member of the genus *Enterovirus* within the family *Picornaviridae*. It has a close serological relationship to another enterovirus, Coxsackie B5 (Graves, 1973; Inoue *et al.*, 1989; Zhang *et al.*, 1999). SVDV causes an infectious disease in pigs which induces the formation of vesicles on the feet, legs, mouth and tongue. It is vital to control SVDV as the lesions produced are clinically indistinguishable from those caused by FMDV.

The 2A protein of entero- and rhinoviruses is a protease of about 17kDa. It belongs to the trypsin-like subgroup of serine proteases but is unusual in that the active site nucleophile is a cysteine not serine. There are several activities associated with the 2A protease. The first is that it mediates the primary cleavage event within the viral polyprotein (Toyoda *et al.*, 1986). This cleavage occurs in *cis* at the N-terminus of 2A. Consequently, the structural proteins are separated from the proteins involved in replication. The 2A protease also induces the cleavage of eIF4G within entero- and rhinovirus infected cells which causes a rapid inhibition of host cell protein synthesis (Krausslich *et al.*, 1987). This cleavage separates the N-terminal part of eIF4G, containing the eIF4E-binding site, from the middle portion of eIF4G (Lamphear *et al.*,

1995). This inhibits cap-dependent translation and results in a rapid inhibition of host cell protein synthesis. However, translation of the viral RNA is unaffected by eIF4G cleavage. The cardio- and aphthovirus IRES elements have been shown to be capable of recruiting the 40S ribosomal subunits with just the middle portion of eIF4G (Pestova *et al.*, 1996a) and it is very possible that the entero- and rhinovirus IRES elements are similar in this respect. Additionally, the 2A protease has been reported to stimulate the activity of IRES elements belonging to entero- and rhinovirus both *in vitro* and *in vivo* (Borman *et al.*, 1995; Borman *et al.*, 1997; Roberts *et al.*, 1998). This stimulation could be a direct result of 2A inducing cleavage of eIF4G and thereby reducing competition for translation factors. However, there is some evidence that suggests eIF4G cleavage and IRES activation are not directly linked (Hambidge & Sarnow, 1992; Roberts *et al.*, 1998)

Previous studies within our laboratory investigated the role of residue 20 within 2A in determining SVDV virulence. This work originated from research into an avirulent and virulent strain of SVDV. The avirulent strain, called H/3'76, was first characterised in 1980 (Kodama *et al.*, 1980a). Unlike the virulent strain (J1'73), this virus shows low pathogenicity when innoculated into pigs and has a small-plaque phenotype when grown in tissue culture (although its overall titre is similar to the virulent strain) (Kodama *et al.*, 1980b; Kanno *et al.*, 1998). Generating full-length infectious clones for both H/3'76 (called 00) and J1'73 (called J1), which showed identical behaviour to their parental viruses (Kanno *et al.*, 1998), made it possible to determine the region of the SVDV genome responsible for virulence. This region lies within the coding sequence and encompasses the sequences encoding the C-terminus of 1C, all of 1D and the N-terminus of 2A (nt 2233 to 3368) (Kanno *et al.*, 1999). Within

this region there are eight nt differences between strains J1 and 00 which will result in amino acid change. One of these changes is situated within 1C, six lie within 1D and there is one substitution within the protease 2A. It was the substitution within the 2A protease that was found to be critical for virulence. Targeted-mutagenesis revealed that altering residue 20 of the J1 2A protease from an arginine to an isoleucine (which is present within strain 00) changed the phenotype of the virus to small-plaque (Kanno *et al.*, 1999). Substitutions within strain 00 at both residue 20 in 2A and at residue 132 within 1D conferred a large plaque phenotype and virulence in pigs indicating that these two residues are important in determining virulence.

Characterisation of the SVDV 2A protease from the two strains demonstrated that a substitution at residue 20 had little effect on the efficiency of cleavage at the 1D/2A junction but was important in determining the level of eIF4G cleavage and IRES activation mediated by the protease (Sakoda *et al.*, 2001). A single amino acid change of an isoleucine to an arginine at residue 20 within the avirulent-strain 2A protease resulted in a protein which behaved like the virulent-strain 2A protease in that an increased amount of eIF4G cleavage and IRES activation were detected. The catalytic triad of the SVDV 2A protease consists of a histidine at residue 21, aspartic acid at residue 39 and cysteine at residue 110. Therefore, residue 20 is adjacent to the catalytic amino acid histidine and may affect substrate recognition by the protease. The aim of this study was to further investigate the importance of residue 20. Residue 20 in the J1 strain 2A protease was substituted for each of the 20 amino acids and the activities of these mutant 2A proteases were characterised.

6.2 Methods

6.2.1 Plasmids

The plasmids used were provided by Toru Inoue from the National Institute of Animal Health, Japan. These are illustrated in Figure 28. Basically, pGEM3Z plasmids were used which contain an insert consisting of the coding region of 1D-2A derived from the virulent J1 strain with a myc-tag at the N-terminus of 1D (Sakoda *et al.*, 2001). Residue 20 within the 2A coding sequence was altered using mutagenesis to each of the 20 amino acids (encoded by the codons listed in Table 8).

The plasmids pGEM3Z/J1Δ, pGEM3Z/J1, pGEM-CAT/CB4/LUC and pGEM-CAT/SVDJ(+)/LUC have all been described previously (Roberts *et al.*, 1998; Sakoda *et al.*, 2001). Plasmid pGEM3Z/J1Δ contains an in-frame deletion which removes the 1D/2A junction and renders the 2A protease inactive. Plasmid pGEM-CAT/CB4/LUC contains the IRES element from the enterovirus coxsackie B4 virus placed between a chloramphenicol acetyl transferase (CAT) ORF and a luciferase (LUC) ORF. pGEM-CAT/SVDJ(+)/LUC is identical except it contains the IRES element from the J1 strain of SVDV.

6.2.2 Protein Expression Analysis

The efficiency of cleavage at the 1D/2A junction of the mutant 2A proteases was investigated *in vitro* using TNTs (primarily as described in Section 2.13). The reactions contained T7 Quick Coupled Transcription/ Translation lysate (Promega,

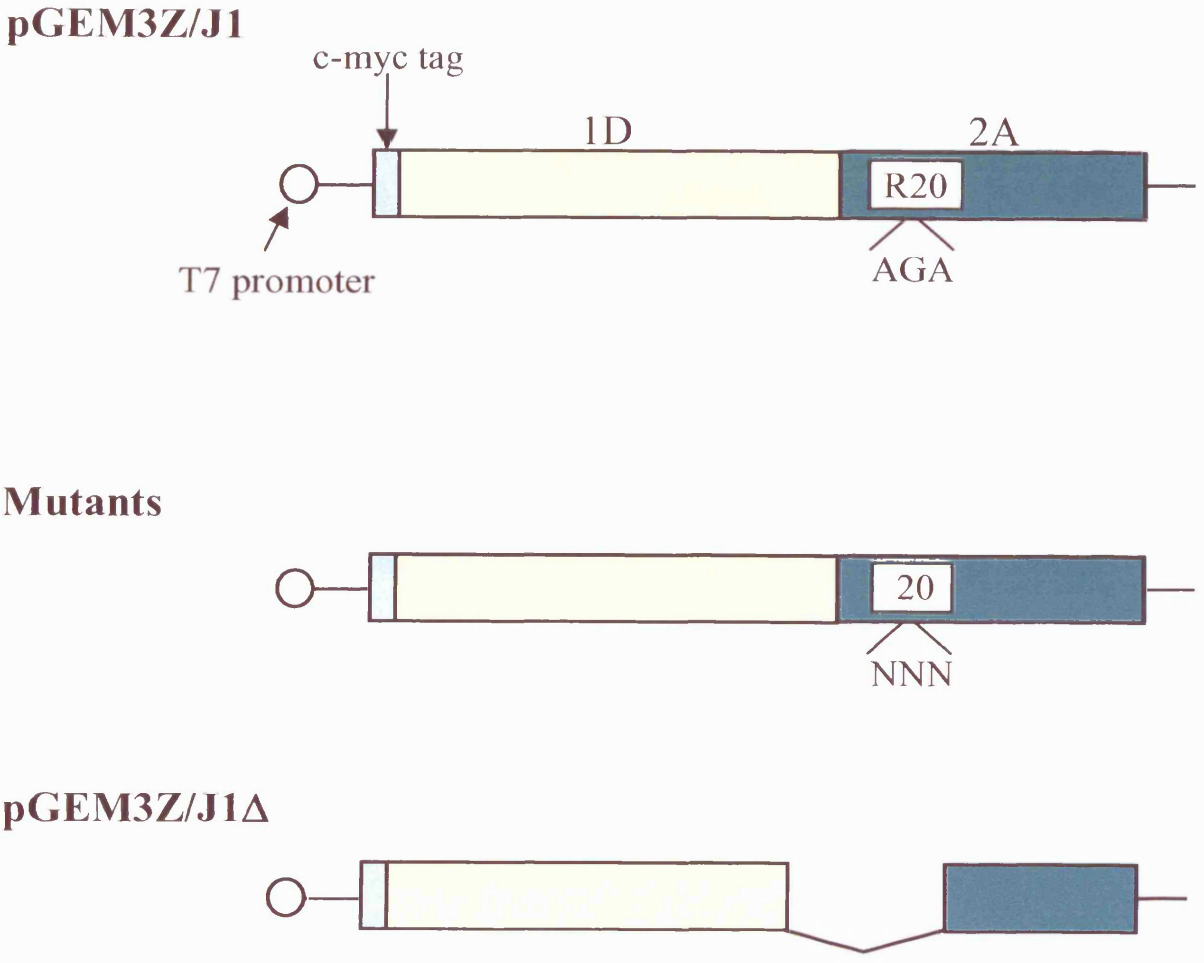

Figure 28: The SVDV plasmids used. The coding region of 1D/2A derived from the virulent SVDV strain J1 was cloned into the pGEM-3Z plasmid. A c-myc epitope tag is present at the N-terminus of 1D. For the 2A mutants, residue 20 was substituted for each of the 20 amino acids or a stop codon.

Code	Amino Acid	Nature of side-group	Codon
G	Glycine (Gly)	Aliphatic	GGC
A	Alanine (Ala)	aliphatic	GCT
V	Valine (Val)	aliphatic	GTG
L	Leucine (Leu)	aliphatic	CTG
I	Isoleucine (Ile)	aliphatic	ATT
S	Serine (Ser)	uncharged, contains –OH group	TCA
T	Threonine (Thr)	uncharged, contains –OH group	ACC
D	Aspartic acid (Asp)	acidic	GAT
E	Glutamic acid (Glu)	acidic	GAA
N	Asparagine (Asn)	uncharged, polar	AAT
Q	Glutamine (Gln)	uncharged, polar	CAG
F	Phenylalanine (Phe)	aromatic	TTT
Y	Tyrosine (Tyr)	aromatic, contains –OH group	TAT
K	Lysine (Lys)	basic	AAA
R	Arginine (Arg)	basic	CGC
W	Tryptophan (Trp)	aromatic, contains –NH group	TGG
H	Histidine (His)	basic	CAC
C	Cysteine (Cys)	uncharged, contains sulphur	TGC
M	Methionine (Met)	uncharged, contains sulphur	ATG
P	Proline (Pro)	aliphatic, cyclic	CCC
*	Termination codon	n/a	TGA

Table 8: The 20 amino acids and the nature of their side chains. The codons used to encode residue 20 in the SVDV 2A proteases are also shown.

6.5μl), 0.5μg plasmid DNA, [^{35}S]-Methionine (10μCi) and were made up to a final volume of 10μl with mQ H_2O. The reactions were incubated at 30°C. Aliquots (3μl) were removed after a 2hr incubation for analysis by SDS-PAGE (12%) and autoradiography. Phosphoimager screening (Personal molecular imager FX/ BIO-Rad) was used in conjunction with Quantity One software for quantification of the radioactive proteins.

Transient expression assays were performed (as described in Section 2.10) to investigate the efficiency of cleavage at the 1D/2A junction within cells and also the cleavage of eIF4GI by the mutant 2A proteases. Briefly, BHK-38 cells were infected with a recombinant vaccinia virus called vTF7-3 (Fuerst *et al.*, 1986) and transfected with plasmid DNA (2.5μg) using Lipofectin and Optimem (8μl and 192μl, respectively, both Invitrogen). After 4-6hr of incubation at 37°C (in a 5% CO_2 incubator), DMEM media with Hepes containing 10% FCS was added (2ml). After 20hr, the cells were harvested and cell extracts were prepared using buffer C (50mM Tris pH 8.0, 0.12M NaCl, 0.5% NP40, 400μl). The levels of specific proteins in these extracts were investigated using SDS-PAGE and western blot analysis (10% SDS-PAGE for anti-c-myc blots or 6% for anti-eIF4GI blots). The following antibodies were used for immunoblotting: mouse anti-c-myc monoclonal antibody (9E10) (1:500, Santa Cruz Biotech or 1:1000, Roche) and sheep anti-eIF4GI (C-terminal region) (1:1000, Li *et al.*, 2001a).

The transient expression assays above were also performed to investigate IRES activation by the mutant 2A proteases. In these experiments, the plasmid DNA (0.5μg) was co-transfected with 2μg of the reporter plasmid, pGEM-CAT/CB4/LUC or pGEM-

CAT/SVDJ(+)/LUC. After 20hr cell extracts were prepared using buffer C (400µl). The level of CAT and LUC present in these extracts was analyzed using SDS-PAGE (10%) and Western blot analysis. The following antibodies were used for immunoblotting: rabbit anti-CAT (1:3000, 5 Prime → 3 Prime, Inc) and rabbit anti-LUC (1:1000, Promega). In addition to this, the luciferase enzyme activity was measured (as described in Section 2.11) to more sensitively determine the level of LUC expression.

6.3 Results

The work reported below was carried out in collaboration with Toru Inoue from the National Institute of Animal Health, Japan.

The constructs used are derivatives of the pGEM3Z-vector containing inserts encoding a c-myc epitope tag immediately upstream of the 1D-2A proteins from the virulent SVDV strain, J1 (whose expression is under the control of a T7 promoter). Residue 20 in the 2A sequence was substituted for each of the 20 amino acids. These constructs will henceforth be denoted by the letter code for the amino acid present at residue 20 (Table 8 shows the single letter codes for amino acids). A construct was also made in which residue 20 was substituted for a stop codon.

6.3.1 Ability of the Mutant 2A Proteases to Cleave the 1D/2A Junction *in Vitro*

The 1D-2A proteins were expressed *in vitro* by programming TNT reactions with each of the plasmids. The TNT reactions were allowed to proceed for two hours and then the radioactively labelled proteins were analysed using SDS-PAGE and autoradiography (shown in Figure 29). This was an effective assay for investigating how efficient the mutant 2A proteases (expressed as 1D-2A) were at cleaving the 1D/2A junction *in vitro*. A range in the ratio of cleaved 1D to uncleaved 1D-2A was observed for the 2A mutants (shown in Figure 29, panel A). The experiment was repeated 3 times and a similar pattern of results was observed each time. The ratio of uncleaved 1D-2A to cleaved 1D was quantified (using a phosphoimager and Quantity

Figure 29: The expression of the mutant 2A proteases *in vitro* and their ability to cleave 1D-2A. The plasmids encoding the 1D/2A proteins were used to program TNT reactions. The reactions were allowed to proceed for 2hr and then the proteins were analysed using SDS-PAGE (12%) and autoradiography.

Panel B is a longer exposure of the same gel as shown on panel A and this allows the mature 2A protein produced to be more visible.

Figure 29

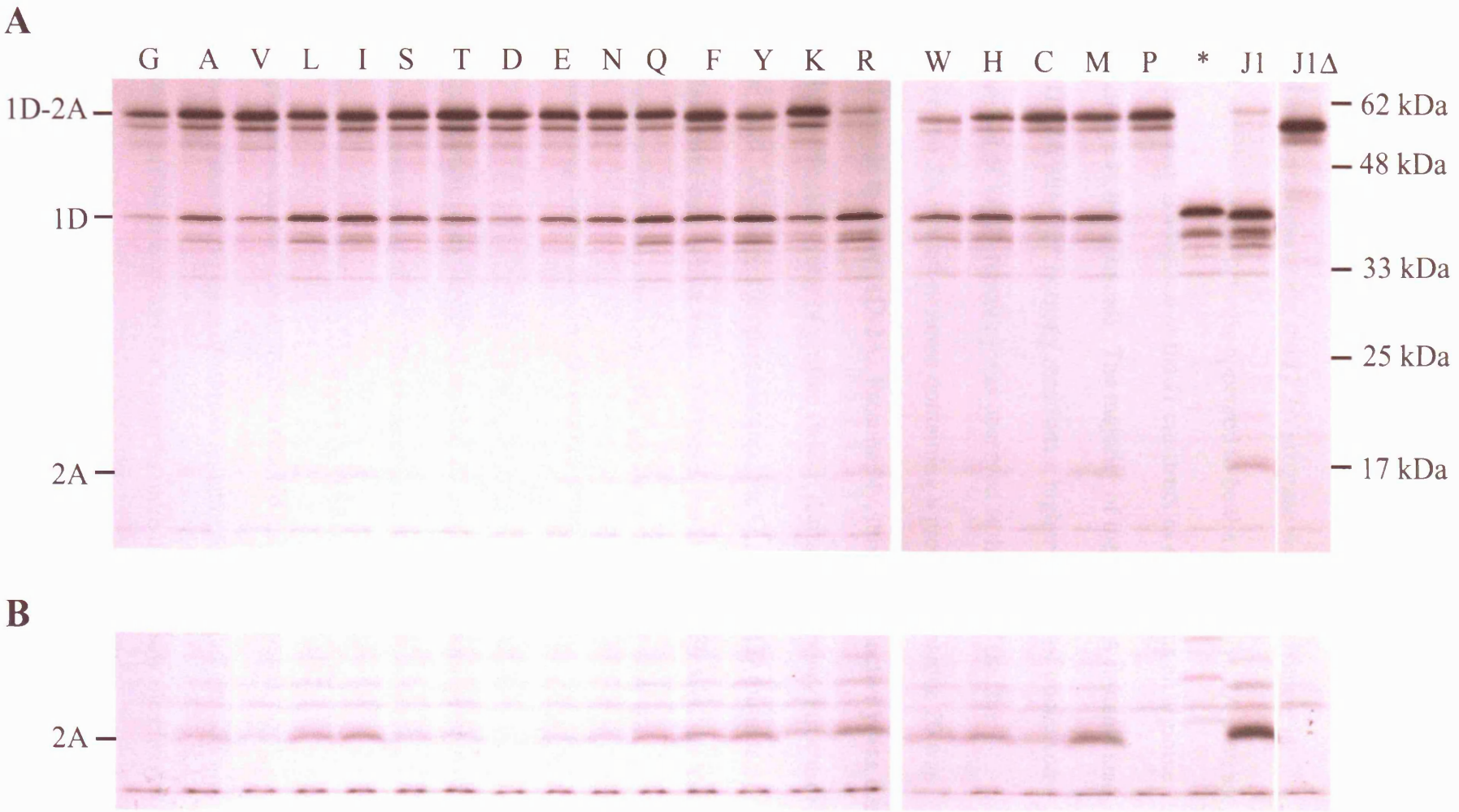
A
G A V L I S T D E N Q F Y K R W H C M P * J1 J1Δ
1D-2A
1D
2A
62 kDa
48 kDa
33 kDa
25 kDa
17 kDa
B
2A

One software) and the mean value obtained for the three experiments is shown in Figure 30.

As expected from previous work, the J1 2A protease was very efficient at cleaving the 1D/2A junction and it actually appeared to be the most active 2A protease in this assay. (The R mutant is identical to the J1 construct as it contains an arginine residue at position 20 in a J1 background). The majority of the other 2A mutants also efficiently cleaved 1D-2A although in many reactions a higher amount of uncleaved 1D-2A (compared to that of the J1 reaction) was observed at the end of the 2hr incubation. However, the 2A mutant protease containing a proline at residue 20 was totally defective and unable to cleave 1D-2A. Presumably, this lack of activity was due to the presence of the cyclic side group of proline (which disrupts secondary structure) close to the catalytic triad. A group of 4 other mutants, the G. V, T and D mutants, were also less efficient proteases in this assay. Of these, the D mutant cleaved the least 1D-2A and gave a ratio of 1D-2A to cleaved 1D of about 11, compared with the remaining 15 mutants which have a 1D-2A: 1D ratio of under 5.

The mutant containing a stop codon at residue 20 produced a fusion protein of the 1D and the first 19 amino acids of 2A. This was observed to be a slightly larger size than the cleaved 1D protein in Figure 29, Panel A. The control plasmid J1Δ produced a 1D-2A protein with the 1D/2A junction deleted and, as expected, no cleavage was observed. Panel B of Figure 29 shows an autoradiograph of the bottom portion of the gel which had been exposed for longer to more clearly show the cleaved 2A protein. As expected, no cleaved 2A was observed for the P mutant, the stop mutant or the J1Δ control.

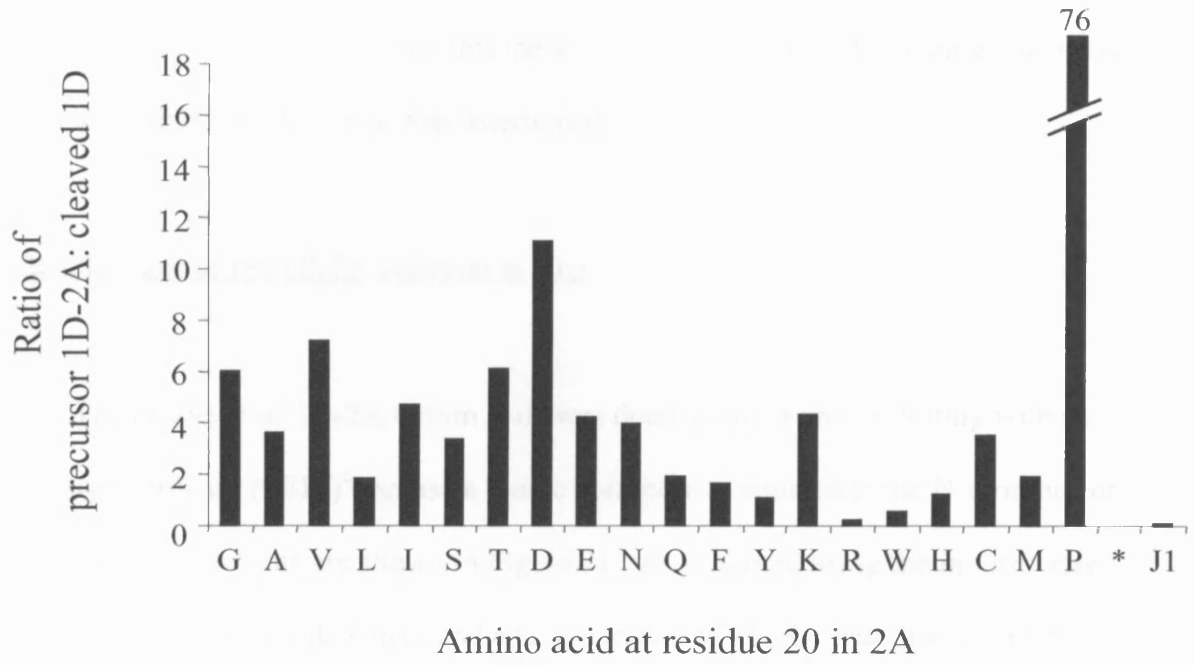

Figure 30: Quantification of the ratio of uncleaved ID-2A to cleaved 1D detected in the *in vitro* TNT reactions shown in Figure 29. The ratio was calculated using a phosphoimager and Quantity One software. The mean values from three separate experiments are shown.

6.3.2 Activity of the Mutant 2A Proteases within Cells

The plasmids were transfected into BHK cells infected with the recombinant vaccinia virus, vTF7-3 (Fuerst *et al.*, 1986). This achieved transient expression of the 1D-2A proteins within cells. From this the ability of the mutant 2A proteases to cleave 1D-2A and eIF4GI within cells was determined.

6.3.2a Cleavage of the 1D/2A Junction *in vivo*

The cleavage of 1D-2A within cells was detected by immunoblotting with an anti-c-myc antibody (9E10) because a c-myc epitope was situated at the N-terminus of 1D. These western blots are shown in Figure 31. As observed using the *in vitro* assay, the P mutant was clearly defective and a large amount of 1D-2A was produced but no cleaved 1D was detected. The remaining mutants were all efficient at cleaving 1D-2A and no uncleaved 1D-2A was detectable for any of them (i.e. the cleavage of 1D-2A has gone to completion). The levels of cleaved 1D do, however, vary. For instance, the mutants G, V and D have strong bands corresponding to the cleaved c-myc tagged 1D protein in the western blots. This is in contrast to the faint bands detected for cleaved 1D in the expression assays of J1 and for the mutants containing Y, K, W or H at residue 20. This is likely to be due to this latter group of mutants efficiently inducing eIF4G cleavage and hence shutting off their own expression. eIF4GI cleavage inhibits cap-dependent translation and the mRNAs expressed in the vaccinia system are capped. Previous experiments with the 2A proteases from the J1 strain and the avirulent 00 strain showed a similar pattern (Sakoda *et al.*, 2001). Expression of the J1 2A protease induced efficient cleavage of eIF4GI within cells and this correlated

Figure 31: Expression of the 1D-2A proteins within cells. The plasmids were transfected into BHK cells infected with vTF7-3. The cells were harvested after 20hr. SDS-PAGE (10%) and western blot analysis with an anti-c-myc antibody was used to analyze the levels of uncleaved 1D-2A and cleaved 1D within the cellular extracts (as a c-myc epitope is present at the N-terminus of 1D).

Figure 31

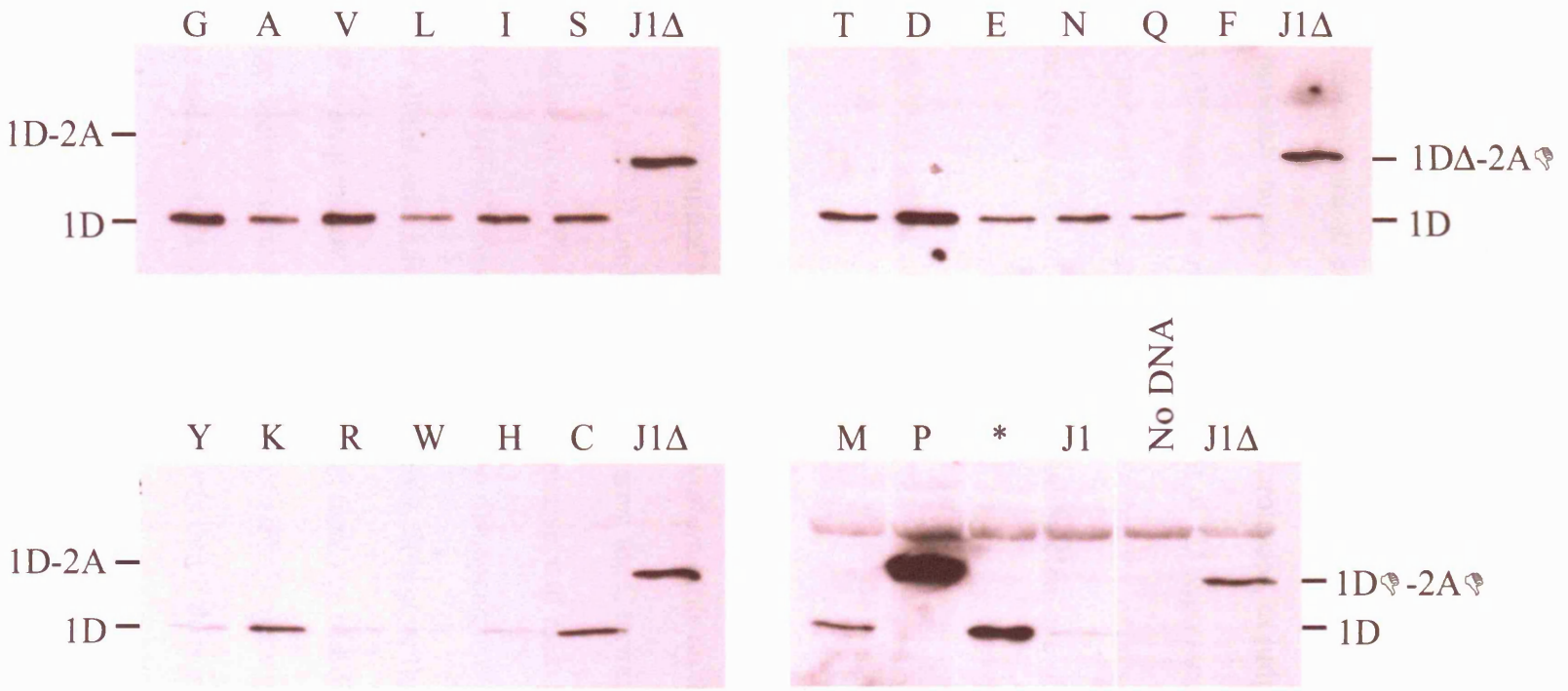
G A V L I S J1Δ
T D E N Q F J1Δ
1D-2A
1D
1DΔ-2A
1D
Y K R W H C J1Δ
M P * J1 No DNA J1Δ
1D-2A
1D
1D -2A
1D

well with little or no detectable 1D (or 1D-2A). The 2A protease from the 00 strain, however, was not very effective at inducing eIF4GI cleavage and this correlated with a much higher expression of 1D. Consistent with this, the present study shows that the constructs encoding a non-functional 2A protease (i.e. the P mutant, the stop codon mutant and the J1Δ control) are all efficiently expressed. In addition to this, there is a general correlation between the activities of the 2A proteases, as judged from the efficiency of 1D-2A cleavage *in vitro*, to the amount of 1D expressed in this assay. Mutants which were very efficient at cleaving 1D-2A *in vitro* expressed less 1D within cells, presumably due to being more efficient at inducing cleavage of eIF4GI.

6.3.2b Cleavage of eIF4G1 within cells by 2A Mutants

To investigate if the above hypothesis was correct, the cleavage of eIF4GI cleavage occurring was determined by performing western blots on the same extracts but probing with an anti-eIF4GI antibody (raised against the C terminal part of eIF4GI). These blots are shown Figure 32. The appearance of cleavage products of eIF4GI is an indicator of eIF4GI cleavage rather than disappearance of intact eIF4GI as it is possible that not all the cells have been transfected. It is clear that all the 2A mutants except the P or stop mutant induced efficient cleavage of eIF4GI. No significant differences were detected in the amount of eIF4GI cleavage induced by the other 19 2A mutants and a disadvantage of this assay is that it does not permit quantification of the kinetics of the cleavage. It is clear that by the time of cell harvesting about the same level of eIF4GI cleavage had occurred for all the 2A mutants (with the exception of the P mutant) but the kinetics of this cleavage may well have differed. Indeed, this is suggested from the differences in expression of 1D (or 1D-2A)

Figure 32: The level of eIF4GI cleavage induced by the mutant 2A proteases. The 1D-2A plasmids were transfected into BHK cells infected with vTF7-3 and cellular extracts were taken after 20hr. The cleavage of eIF4GI within the cells was investigated using SDS-PAGE (6%) and immunoblotting with an antibody raised against the C-terminal region of eIF4GI. Full-length eIF4GI and the cleavage products of eIF4GI are labelled.

Figure 32

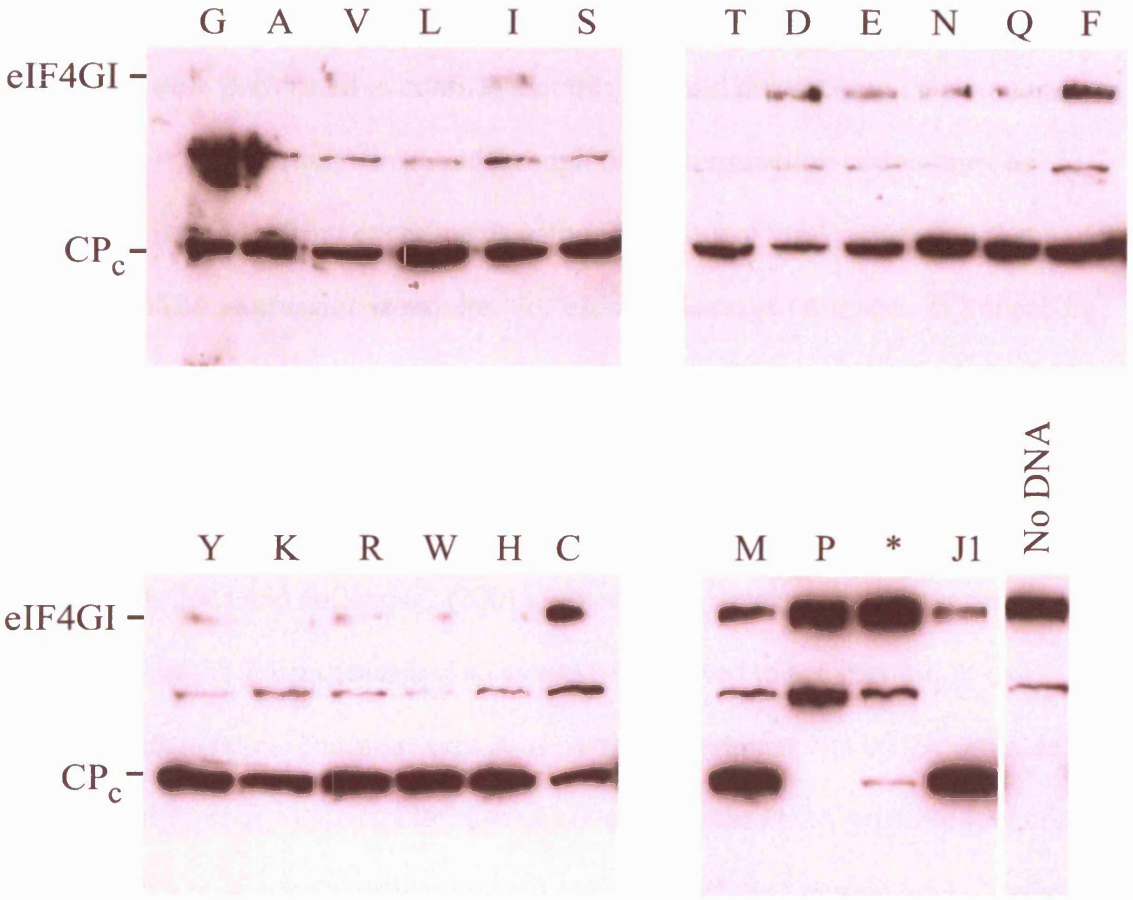

detected (as discussed above). It seems likely that if the kinetics of the eIF4G cleavage were slower, more 1D would be expressed as the inhibition of cap-dependent translation would occur later. This could explain why higher levels of 1D were seen for mutants such as G, D and V which do not appear to be as active as some of the remainder 2A proteases such as J1 or mutants Y, K, W or H.

There are two more interesting points that arise from this experiment. The first is that the stop codon mutant clearly induced a small amount of eIF4GI cleavage. Experiments were performed to confirm that this plasmid did not contain a contaminant and therefore it appears that some read through of the termination codon must be occurring. It is known from experiments using inhibitors of viral replication that a very low amount of 2A expression is required for eIF4GI cleavage (Bonneau & Sonenberg, 1987; Gradi *et al.*, 1998b). Therefore, a very small level of read through could be occurring to cause the low level of eIF4G cleavage detected. The second observation is that the mutant I behaved differently to the 2A protease from the 00 strain as observed by Sakoda and colleagues (2001). These two proteases both have an I residue at position 20 of the 2A protease and so would be expected to act very similarly. However, in an identical transient expression assay experiment, the 00 2A protease was clearly less efficient at inducing cleavage of eIF4G than the J1 2A protease (Sakoda *et al.*, 2001). This is obviously different to the behaviour of the I mutant which induced a level of eIF4G cleavage which could not be differentiated in this assay from the J1 protease. This suggests that other amino acid differences between the 00 and J1 1D-2A region may also be important for the activity of the 2A protease.

6.3.3 IRES Activation by the Mutant 2A Proteases

To investigate the level of IRES stimulation induced by the mutant 2A proteases, the 1D-2A plasmids were co-transfected with the reporter plasmid pGEM-CAT/CB4/LUC into vTF7-3 infected BHK cells. This plasmid encodes a dicistronic CAT/LUC mRNA in which the enterovirus coxsackie B4 IRES is positioned in the intergenic region. Therefore, expression of CAT is cap-dependent whilst expression of LUC is mediated by the IRES element. The level of LUC expressed was measured using the sensitive luciferase enzyme assay. The mean values of 3 separate experiments are shown in Figure 33. The level of LUC expressed when pGEM-CAT/CB4/LUC alone was transfected into cells was set to a value of 100%. As expected the P mutant and the J1Δ control did not stimulate the activity of the IRES. The remaining mutants again showed a range of activities. The pattern of activation was similar to that observed for the 1D/2A cleavage activity *in vitro*. For instance the D mutant (after the P mutant) shows the lowest amount of IRES activation. The IRES activity was only stimulated about 2-fold by this mutant which is about the same level of activation seen for the stop mutant. Presumably, the low level of IRES activation by the stop mutant is due to read through of the stop codon as detected in the eIF4G cleavage assay. Additionally, mutants G, V and T only stimulated IRES activity by about 3-fold. Mutants I, E and K induced about a 4-fold enhancement of IRES activity, while the remaining 2A mutants appear to have a slightly higher activity, bringing about a 5-6 fold increase. The pattern of results seen was very similar to the results obtained when the same co-transfection experiment was carried out with a reporter plasmid containing the SVDV IRES, pGEM-CAT/SVDJ(+)/LUC (shown in Figure 34).

Figure 33: The level of IRES activation mediated by the mutant 2A proteases. The 1D-2A plasmids were co-transfected with the reporter plasmid pGEM-CAT/CB4/LUC (containing the coxsackie B4 IRES) into vTF7-3 infected BHK cells. Cellular extracts were prepared after 20hr and the LUC enzyme activity was measured. The values shown are the means ± standard deviations for 3 independent experiments. The level of LUC expressed when the reporter plasmid was transfected into cells alone (denoted above by the symbol -) was set to a value of 100% and the other results are shown as a % of this control.

Figure 33

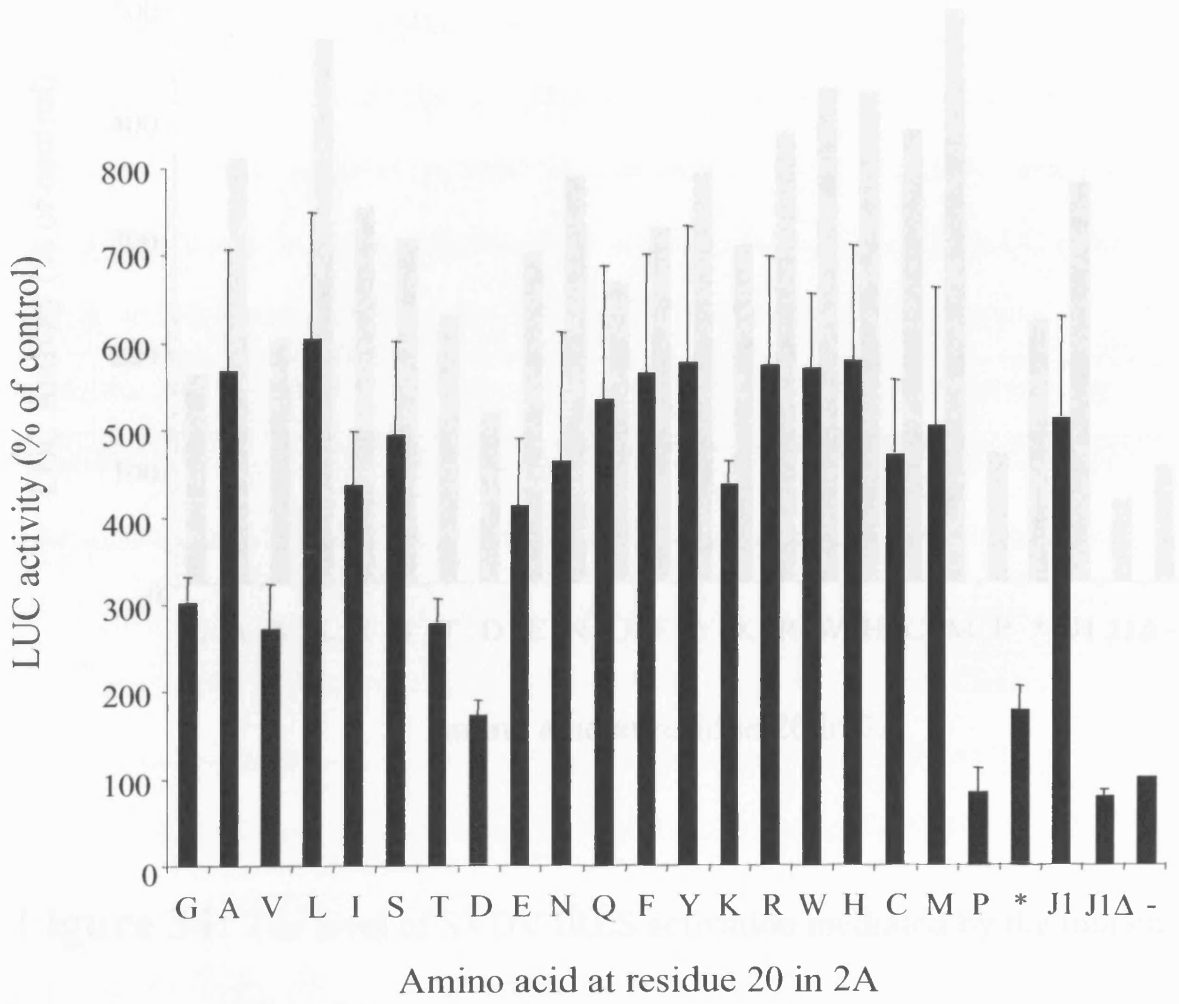
LUC activity (% of control)
800
700
600
500
400
300
200
100
0
G A V L I S T D E N Q F Y K R W H C M P * J1 J1Δ -
Amino acid at residue 20 in 2A

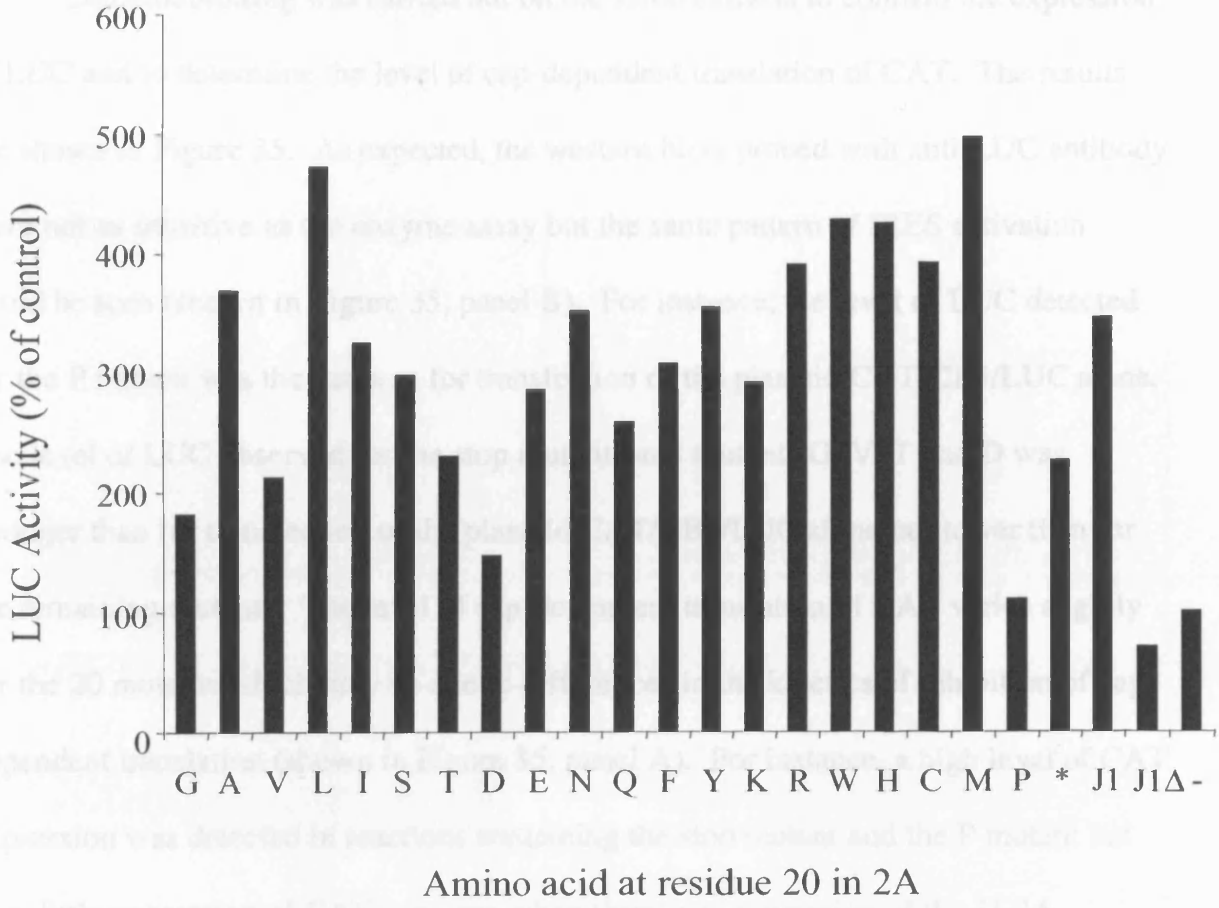

Figure 34: The level of SVDV IRES activation mediated by the mutant 2A proteases. The 1D-2A plasmids were co-transfected with the reporter plasmid pGEM-CAT/SVDJ(+)/LUC (containing the SVDV J1 IRES) into vTF7-3 infected BHK cells. Cellular extracts were taken after 20hr and the LUC enzyme activity was measured. The LUC activity observed when pGEM-CAT/SVDVJ(+)/LUC alone was transfected into cells (denoted above by the symbol -) was set to a value of 100% and the other results are shown as a % of this control.

Immunoblotting was carried out on the same extracts to confirm the expression of LUC and to determine the level of cap-dependent translation of CAT. The results are shown in Figure 35. As expected, the western blots probed with anti-LUC antibody were not as sensitive as the enzyme assay but the same pattern of IRES activation could be seen (shown in Figure 35, panel B). For instance, the level of LUC detected for the P mutant was the same as for transfection of the plasmid CAT/CB4/LUC alone. The level of LUC observed for the stop mutants and mutants G, V, T and D was stronger than for transfection of the plasmid CAT/CB4/LUC alone but lower than for the remaining mutants. The level of cap-dependent translation of CAT varies slightly for the 20 mutants which may be due to differences in the kinetics of inhibition of cap-dependent translation (shown in Figure 35, panel A). For instance, a high level of CAT expression was detected in reactions containing the stop mutant and the P mutant but very little expression of CAT was seen when there was expression of the J1 2A protease or the M mutant. Nevertheless, the levels of CAT for the different 2A protease mutants did not vary as much as the levels of 1D in the transient expression assay shown in Figure 31. There are two possible reasons for this. The first is that Western blot analysis detects the amount of protein accumulated by the time of cell harvesting and CAT is a relatively stable protein. Therefore, immunoblotting analysis of CAT may not be a very sensitive measure of the kinetics of eIF4GI cleavage and of how long cap-dependent translation was allowed to proceed. In addition, within the transient expression assay (described in Section 6.3.2a), a localised effect may be occurring. Newly translated 2A proteins may cleave eIF4G molecules close by the actively-translating ribosomes and hence make the inhibition of cap-dependent translation of 1D-2A more pronounced.

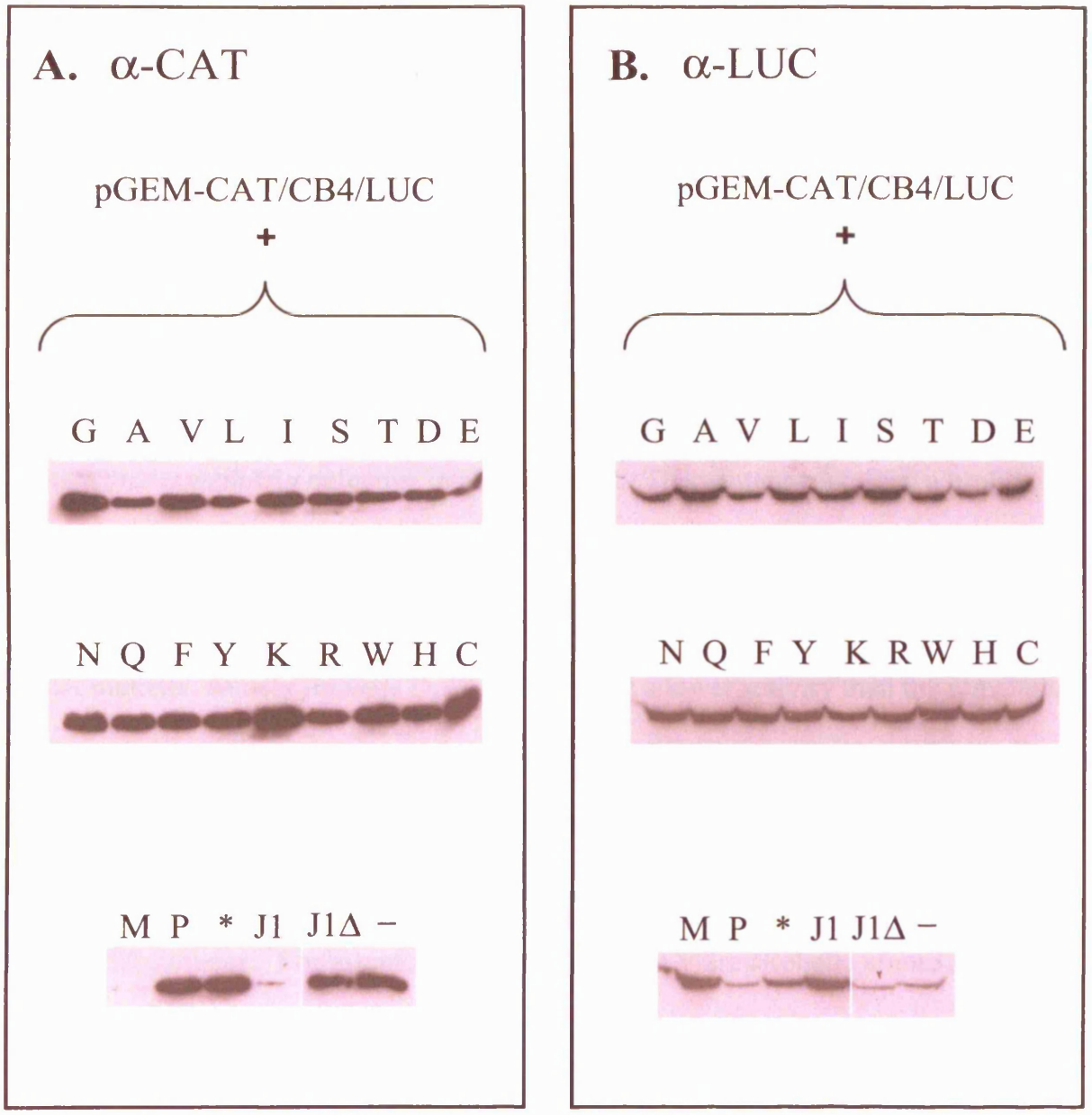

Figure 35: SDS-PAGE (10%) and immunoblotting was carried out on the same cellular extracts as in Figure 33 to investigate the level of cap-dependent translation of CAT (Panel A) and confirm the expression of LUC (Panel B).

6.4 Discussion

Previous studies have indicated that residue 20 within the SVDV 2A protease is critical for determining virus virulence (Kanno *et al.*, 1999). Further investigation has shown that residue 20 affects the ability of the protease to inhibit cellular translation and stimulate IRES-mediated translation of the viral RNA (Sakoda *et al.*, 2001). The work reported here investigated the effect of substituting residue 20 for each of the 20 amino acids. These mutant 2A proteases showed a range of activities but only one mutant was completely defective in all the assays. This mutant contained a proline residue at position 20. Presumably the cyclic side-chain of proline affects the structure of the active site in some way and causes the protease to be non-functional. A subset of 2A mutants, namely mutants D, G, V and T had a lower activity than the remaining mutants in several assays. They were less efficient at both cleaving the 1D/2A junction and stimulating enterovirus IRES activity. No obvious connection could be made between the nature of the amino acid side-chain at residue 20 and the activity of the mutant 2A protease. For instance, the mutants G and V are aliphatic amino acids and yet substitution with other aliphatic amino acids such as A and L resulted in a more active protease. It remains unclear why this is so and the actual role of residue 20 is unclear. Recent studies have shown that the HRV 2A protease binds directly to eIF4GI at a site distinct from the cleavage site (Foeger *et al.*, 2002). The residues within the 2A protease responsible for this interaction have not yet been identified and it is possible that residue 20 in the SVDV 2A protease may have a role such as this.

The level of eIF4GI cleavage mediated by the mutants was assayed but unfortunately little difference was detected between all the mutants (with the exception

of the defective proline mutant). When the plasmids were expressed within cells, all the expressed 1D-2A was cleaved (except for the proline mutant) but the levels of cleaved 1D observed varied considerably. As suggested above, these differences in expression could indicate differences in the kinetics of eIF4G cleavage. This is feasible as the slower eIF4G is cleaved, the longer cap-dependent translation can carry on and therefore more protein can be expressed. In support of this hypothesis, there is a general correlation between the efficiency of the 2A protease to cleave the 1D/2A junction *in vitro* and the level of 1D expressed within cells. Nevertheless, it should be noted that differences in the level of transfection could also give rise to the varying levels of 1D protein observed. Future experiments would definitely benefit from including a control for the efficiency of transfection. For example, quantitative RT-PCR or Northern blots could be used to measure the level of mRNA expressed. In addition it would be an advantage to develop a better assay for eIF4G cleavage. One possibility would be to perform a time-course experiment using rrl TNT reactions programmed with the 1D-2A plasmids. The level of eIF4G cleavage would be investigated using immunoblotting.

There were two unexpected but interesting results. The first of these is that the I mutant did not behave like the 2A protease from the 00 strain of SVDV. These two proteases have an isoleucine at residue 20 but the I mutant has a J1 strain background in contrast to the 00 construct. The I mutant was much more efficient at inducing eIF4G cleavage and stimulating IRES activity than the 00 construct (as reported in Sakoda *et al.*, 2001). This suggests that other amino acid differences between the two proteases affect its activity. There are 8 amino acid differences between the 1D-2A region of J1 and 00. Two are situated within the 2A region at residue 20 and 126 but

residue 126 does not lie within the region of the ORF critical for virus virulence (which encompasses the C-terminus of 1C, all of 1D and the N-terminus of 2A). Out of the six amino acid substitutions within region 1D, residue 132 has been shown to be involved in virus virulence (Kanno *et al.*, 1999). Therefore, these data suggest there is a possibility that the protein 1D affects the activity of the 2A protease but this requires further investigation.

The second point of interest is that the stop mutant behaved differently from expected. This mutant contains a termination codon at residue 20 and therefore a non-functional, truncated 2A protein will be translated. However, expression of the construct within cells resulted in a low level of eIF4GI cleavage and also of low level IRES activation. It seems likely that a very small amount of read through of the stop codon by ribosomes is occurring to produce small amounts of full-length 2A. Previously it was demonstrated that only a low level of 2A expression is required for eIF4G cleavage *in vivo* (Bonneau & Sonenberg, 1987; Gradi *et al.*, 1998b). This could mean that the transient expression system here could be adapted for use to investigate termination read through *in vivo*. This would be useful as premature translation termination has been linked to many inherited diseases and therefore is a target for treatment of these diseases (for a review see Maquat, 2000). Furthermore, a pathway exists within mammalian cells by which mRNAs containing a premature stop codon within a coding sequence are targeted for degradation (see Maquat, 2000). This complicates experiments studying termination read through within cells. Fortunately, transient expression of the stop mutant construct in the vTF7-3 system leads to significant expression of the truncated 1D-2A protein (presumably the pathway does not occur in vaccinia-infected cells since transcription is cytoplasmic). However,

before establishing this assay it would be necessary to confirm that the eIF4G cleavage seen was indeed due to termination read through.

Residue 20 of the SVDV 2A protease is a critical determinant of virus virulence (Kanno *et al.*, 1999) but the work presented here shows that amino acid substitutions at residue 20 did not drastically affect the activities of the 2A protease with the exception of a proline substitution. However, several 2A mutants had a lower activity than the I mutant (the amino acid present at residue 20 of the avirulent strain 00 2A protease). Consequently it would be of great interest to introduce several of these substitutions within full-length viral cDNA and assay the virulence of the resulting viruses. Previous studies have reported a link between the efficiency of translation of picornavirus RNA and virus virulence. For example, mutations within the PV IRES element are known to affect neurovirulence (Minor, 1992). Investigation of temperature-sensitive, attenuated PV mutants containing mutations within the IRES showed that revertant mutants could be isolated which still contained the IRES mutation but also had an additional mutation within the 2A protease (Macadam *et al.*, 1994; Rowe *et al.*, 2000). Therefore, the 2A protease clearly has an affect on virus virulence through its indirect involvement in translation of picornavirus RNA. One possible effect of the viral 2A protease could be to stop the anti-viral response of the host cell (via cleavage of eIF4G). It is known that FMDV lacking the leader coding region is avirulent in cattle and pigs. When inoculated into cattle a localised response is seen but the virus cannot spread systemically (Brown *et al.*, 1996). When tested in tissue culture it was shown that the leaderless virus could not suppress translation of host interferon α and β (Chinsangaram *et al.*, 1999).

CHAPTER 7

Discussion and Conclusions

The aim of this study was to investigate certain aspects of picornavirus RNA translation, including analysis of the mechanism of IRES-mediated translation and the indirect effect of the enterovirus 2A protease on viral translation. Specifically, the functional role of certain conserved nucleotides within the EMCV IRES and their interaction with cellular translation initiation factors was examined. Separately, the role of residue 20 within the SVDV 2A protease was investigated as it had had previously been identified as a virulence determinant (Kanno *et al.*, 1999).

The main conclusions reached from the studies into the EMCV IRES are as follows. Nucleotides 704-705 and 723-724 within the J domain of the EMCV IRES, which are conserved among all cardio- and aphthoviruses, are essential for IRES activity. Furthermore, the mutations at these four nucleotides influence binding of eIF4GI (and consequently eIF4A) to the IRES. There was a clear correlation between the activity of the J domain mutant and its ability to bind eIF4GI. Prior to the start of this project, it was known that eIF4G (or at least the middle portion of eIF4G) was required, in addition to the factors eIF4A, eIF2 and eIF3, for ribosome recruitment to the IRES *in vitro* (Pestova *et al.*, 1996a; Pestova *et al.*, 1996b). Chemical/ enzymatic protection assays of the EMCV IRES incubated with eIF4GI indicated that eIF4GI bound to the J-K domains of the IRES (Kolupaeva *et al.*, 1998). The data presented here provides evidence that the binding of eIF4GI to the IRES is functionally relevant

both *in vitro* and *in vivo*. In support of this, Lopez de Quinto & Martinez-Salas, (2000) identified two nucleotides in the J domain of the FMDV IRES which are essential for IRES activity due to their involvement in eIF4GI binding. These two nucleotides are nearby to the four nucleotides investigated here but are closer to the base of stem-loop J (nt 686 and 687).

The characterisation of the J domain mutants was facilitated by two systems previously developed in the laboratory. The first of these is a cell selection system which allows identification of functional IRES elements. It was used to select functional mutants from a pool of EMCV IRES mutants containing up to 256 possible sequences. The second system used was a bead-IRES-protein binding assay which allowed analysis of the proteins interacting with the IRES. Within the bead assay, polyadenylated IRES elements were immobilised on oligo-dT magnetic beads and incubated in rrl. Following this, proteins bound to the IRES could be analysed. The combination of these systems provided a powerful tool to identify nucleotides which are critical for IRES activity and involved in protein interactions. Both systems have been used predominantly to investigate aspects of picornavirus RNA translation but could also be adapted for use in other areas. For example, the data presented in Chapter 5 demonstrated that the HCV IRES element was suitable for use within the cell selection system. This is particularly useful since the analysis of HCV *in vivo* is limited as full-length HCV cDNA clones are only infectious when injected into primates (Kolykhalov *et al.*, 1997; Yanagi *et al.*, 1997). A subgenomic selectable replicon has been set up which allows analysis of HCV replication within cultured cells but only genotypes 1a and 1b can be used in this system (Lohmann *et al.*, 1999; Blight *et al.*, 2000). In contrast, the IRES elements from many different HCV genotypes were

shown to be suitable for use in the cell selection system. Therefore, this system can facilitate thorough mutagenesis studies on the HCV IRES. There are many questions which remain unanswered about the protein interactions of the HCV IRES. One example of this is that eIF3 is essential for assembly of 80S complexes during HCV IRES-mediated translation but its actual role remains unclear (Pestova *et al.*, 1998b). It would be interesting to mutate several nucleotides within the IRES which have been suggested to interact with either eIF3 or the 40S ribosomal subunit and hence determine the importance of these nucleotides to IRES function. One possible target is loop IIIb as several conserved nucleotides within this region have been identified to interact with eIF3 (Sizova *et al.*, 1998; Collier *et al.*, 2002). Although mutational analysis has been carried out on relevant nucleotides within this domain, only a small number of mutant sequences have been investigated (Collier *et al.*, 2002).

It is also possible that the HOOK cell selection system could be modified for analysis of cellular IRES elements. Many aspects of translation initiation directed by cellular IRES elements are unclear. The cell selection system could define sequences within the IRES that are necessary for activity and thus provide clues as to the mechanism by which cellular IRES elements recruit ribosomes. Modifications to the existing system would, however, need to be implemented. One modification would be to change the cell line used to one in which the cellular IRES elements have high activity. For example, the two cell types used in this study were BHK-38 and COS-7 cells but the c-myc IRES has low activity in cells derived from murine origin and COS-7 cells (Stoneley *et al.*, 2000a). Also, the vTF7-3 transient expression system could not be used since transcription is cytoplasmic and some cellular IRES elements have been reported to require a nuclear event before they are active (Stoneley *et al.*, 2000a).

However, the plasmids also contain a CMV promoter and therefore this promoter could be used to transiently express the dicistronic constructs within cells. As mentioned before, the specificity of the cell selection system is likely to be enhanced if co-transfection of plasmids can be eliminated. One possible way to do this is to use protoplast fusion as a means of delivering the DNA into the cells (Tan & Frankel, 1998).

The IRES-bead assay is a useful tool for investigating protein to IRES interactions as shown here by the investigation of the J domain mutants to bind eIF4GI. Moreover, it may be possible to adapt the assay to examine RNA: RNA interactions within the picornavirus IRES. It is known that tertiary interactions occur within the FMDV IRES (Ramos & Martinez-Salas, 1999; Beales *et al.*, 2001) but little attempt has been made to define the tertiary structure of any of the picornavirus IRES elements. This is an area which needs to be explored in the future as the tertiary structure of the IRES is likely to determine protein interactions. Also it may confirm the role of *trans*-acting factors such as PTB which bind to multiple regions of the IRES and are thought to stabilise the tertiary structure of the IRES. The IRES-bead assay could be used to at least show which domains of the EMCV IRES have the potential to interact with each other. A more thorough analysis would require NMR analysis and crystal structure determination. Structural studies on the HCV IRES are much more advanced. The tertiary structure of several functionally relevant regions of the IRES have been determined by both NMR and cystallography (Klinck *et al.*, 2000; Collier *et al.*, 2002; Kieft *et al.*, 2002). As shown in this study and by many other lines of evidence, the J-K domain of the EMCV IRES represents a functional domain as it interacts with eIF4GI/ and eIF4GII (Kolupaeva *et al.*, 1998; Lopez de Quinto & Martinez-Salas,

2000; Saleh *et al.*, 2001; Stassinopoulos & Belsham, 2001; Lopez de Quinto *et al.*, 2001). Therefore, it would be interesting to look at the tertiary structure of these domains in particular by crytallography. This is a more realistic target at this point in time than determining the three-dimensional structure of the entire IRES element. It could also provide a target for structure-based drug design.

The latter part of this study investigated the role of residue 20 within the SVDV 2A protease which has been revealed to be a virulence determinant. In this study, residue 20 was changed to each of the 20 amino acids. The conclusions reached from this are that amino acid substitutions at residue 20 are reasonably well tolerated with the exception of proline. Slight differences were seen in the ability of the mutant 2A proteases to cleave the 1D/2A junction within the viral polyprotein and to activate IRES activity (with the exception of the proline mutant). It is also possible that this residue affects the ability of the 2A protease, to some extent, to induce eIF4GI cleavage but this has yet to be confirmed. Surprisingly, no correlation was observed between the nature of the amino acid at residue 20 and the activity of the mutant 2A. The role of residue 20 remains unclear but it may be involved in substrate recognition.

The understanding of the mechanism by which the entero- and rhinovirus 2A proteases operate remains sketchy. Two key issues need resolving. The first is whether cleavage of eIF4G is direct. *In vitro* cleavage assays have revealed that it is possible for the 2A protease to cleave eIF4GI directly (Lamphear *et al.*, 1993; Liebig *et al.*, 1993; Haghighat *et al.*, 1996) but there is controversy about whether this actually occurs *in vivo*. For instance, there is evidence that the activity within PV-infected cells that cleaves eIF4GI has been reported to be distinct from the 2A protease (Lloyd *et al.*,

1986; Bovee *et al.*, 1998a). Furthermore, the concentration of 2A protease required for efficient cleavage of eIF4GI *in vitro* is thought to be higher than that present *in vivo* (Bovee *et al.*, 1998b). Therefore, maybe the 2A protease activates a latent cellular protease but such a substrate for 2A has not yet been identified. Recent experiments have separated two cellular activities within PV-infected cells which, in addition to the 2A protease, cleave eIF4GI (Zamora *et al.*, 2002). During PV-infection, eIF4GI was cleaved at two distinct sites. Interestingly, these cellular activities could be detected within uninfected cells under certain conditions, e.g. apoptosis. The second issue that requires clarification is whether eIF4G cleavage by the 2A protease is directly linked to IRES activation. Several lines of evidence suggest this is not the case. For example, the PV 2A protease has been shown to stimulate IRES activity at a time when there was little inhibition of host cell protein synthesis (Hambidge & Sarnow, 1992). Additionally, another inhibitor of cap-dependent translation, 4E-BP2, had no effect on IRES activity suggesting that the IRES stimulation is not due simply to loss of competition for translation factors (Roberts *et al.*, 1998). It is possible that the 2A protease modifies another cellular protein which in turn activates the activity of the viral IRES. Again the identity of this substrate for 2A is unknown. The results of the study into the SVDV 2A mutants confirm that an active protease is required for IRES activation.

It is becoming increasing clear in the field of picornavirus RNA translation that the efficiency of translation is closely linked to virus tropism. Cell tropism has been shown to be affected by mutations within the IRES. For example, the Sabin vaccine strains of PV all contain mutations within domain V which contribute to the attenuated phenotype (Minor, 1992). Additionally, the substitution of the FMDV IRES within

the genome of the cardiovirus TMEV (GDVII strain) resulted in an attenuated virus within murine brain cells (Pilipenko *et al.*, 2000). Ultimately, it is the protein requirements of an IRES element that will determine its activity within different cell types and affect virus tropism. Additionally, the studies into the SVDV 2A proteases and also into a leaderless FMDV virus, highlight that the indirect effect of the viral proteases on viral translation can influence virus virulence (Chinsangaram *et al.*, 1999; Kanno *et al.*, 1999). This is confirmed by the fact that mutations within the PV IRES which conferred a temperature-sensitive phenotype were compensated by mutations within the 2A protein (Macadam *et al.*, 1994).

The fact that virus tropism is linked to the proteins which are required for IRES activity makes it essential to characterise the protein interactions of all the different picornavirus IRES elements. One issue that needs addressing is that many of the studies conducted on IRES-interacting proteins have been performed *in vitro*. Therefore, a lot of the interactions have yet to be proved functionally relevant within cells. Two such examples of this are La and PTB. *In vitro*, La has been shown to stimulate PV IRES activity (Meerovitch *et al.*, 1993; Svitkin *et al.*, 1994) and PTB has been shown to stimulate the activity of the FMDV, HRV and PV IRES elements (Borman *et al.*, 1993; Niepmann *et al.*, 1997; Hunt & Jackson, 1999; Pilipenko *et al.*, 2000). It is unclear if La and PTB stimulate IRES activity *in vivo* as viral translation occurs in the cytoplasm but both these proteins are predominantly nuclear. During PV infection, cleavage of La occurs which results in a truncated La protein accumulating in the cytoplasm (Shiroki *et al.*, 1999). This may explain how La is recruited to the PV IRES but the functional role of this truncated La protein *in vivo* still requires

clarification. As of yet, there is no explanation of how nuclear-distributed PTB protein interacts with the PV IRES.

Another subject which requires clarification is the role of eIF4G and eIF4A in translation mediated by the PV and HRV IRES elements. Dominant negative mutants of eIF4A have been shown to inhibit PV and HRV translation (although to a lesser extent than the EMCV and FMDV IRES elements) (Svitkin *et al.*, 2001a). Nevertheless, there is still no direct evidence that eIF4G (or cleaved eIF4G) interacts with the entero- and rhinovirus IRES elements *in vitro* or *in vivo*. Hopefully, the recently discovered RNA interference technology will aid research into IRES-interacting proteins in the near future since this technique can knock down the expression of specific proteins within cultured cells.

REFERENCES

Acharya, R *et al.* (1989). The 3-dimensional structure of foot-and-mouth-disease virus at 2.9-Å resolution. Nature **337**(6209): 709-716.

Agol, VI *et al.* (1998). Two types of death of poliovirus-infected cells: caspase involvement in the apoptosis but not cytopathic effect. Virology **252**(2): 343-353.

Agol, VI *et al.* (2000). Competing death programs in poliovirus-infected cells: commitment switch in the middle of the infectious cycle. Journal of Virology **74**(12): 5534-5541.

Agrawal, RK *et al.* (1998). Visualization of elongation factor G on the *Escherichia coli* 70S ribosome: The mechanism of translocation. Proceedings of the National Academy of Sciences of the United States of America **95**(11): 6134-6138.

Agrawal, RK *et al.* (2000). Visualization of tRNA movements on the *Escherichia coli* 70S ribosome during the elongation cycle. Journal of Cell Biology **150**(3): 447-459.

Ali, N & Siddiqui, A (1995). Interaction of polypyrimidine tract-binding protein with the 5'-noncoding region of the hepatitis-C virus-RNA genome and its functional requirement in internal initiation of translation. Journal of Virology **69**(10): 6367-6375.

Ali, N & Siddiqui, A (1997). The La antigen binds 5' noncoding region of the hepatitis C virus RNA in the context of the initiator AUG codon and stimulates internal ribosome entry site-mediated translation. Proceedings of the National Academy of Sciences of the United States of America **94**(6): 2249-2254.

Ali, N *et al.* (2000). Human La antigen is required for the hepatitis C virus internal ribosome entry site-mediated translation. Journal of Biological Chemistry **275**(36): 27531-27540.

Ali, IK *et al.* (2001a). Truncated initiation factor eIF4G lacking an eIF4E binding site can support capped mRNA translation. EMBO Journal **20**(15): 4233-4242.

Ali, IK *et al.* (2001b). Activity of the hepatitis A virus IRES requires association between the cap-binding translation initiation factor (eIF4E) and eIF4G. Journal of Virology **75**(17): 7854-7863.

Alonso, MA & Carrasco, L (1981). Reversion by hypotonic medium of the shutoff of protein-synthesis induced by encephalomyocarditis virus. Journal of Virology **37**(2): 535-540.

Altmann, M *et al.* (1989). The mammalian translation initiation factor 4E substitutes for its yeast homologue *in vivo*. Journal of Biological Chemistry **264**: 12145-12147.

Andersen, GR & Nyborg, J (2001). Structural studies of eukaryotic elongation factors. The ribosome. Cold Spring Harbor, N. Y., Cold Spring Harbor Laboratory Press: 425-439

Andino, R *et al.* (1990). A functional ribonucleoprotein complex forms around the 5' end of poliovirus RNA. Cell **63**(2): 369-380.

Andino, R *et al.* (1993). Poliovirus RNA-synthesis utilizes an RNP complex formed around the 5'-end of viral-RNA. EMBO Journal **12**(9): 3587-3598.

Arnold, E *et al.* (1987). Implications of the picornavirus capsid structure for polyprotein processing. Proceedings of the National Academy of Sciences of the United States of America **84**(1): 21-25.

Asano, K *et al.* (1999). Conserved bipartite motifs in yeast eIF5 and eIF2B epsilon, GTPase-activating and GDP-GTP exchange factors in translation initiation, mediate binding to their common substrate eIF2. EMBO Journal **18**(6): 1673-1688.

Asano, K *et al.* (2000). A multifactor complex of eukaryotic initiation factors, eIE1, eIF2, eIF3, eIF5, and initiator tRNA(Met) is an important translation initiation intermediate *in vivo*. Genes & Development **14**(19): 2534-2546.

Bablanian, R *et al.* (1991). Mechanism of selective translation of vaccinia virus messenger-RNAs - differential role of poly(A) and initiation-factors in the translation of viral and cellular messenger-RNAs. Journal of Virology **65**(8): 4449-4460.

Back, SH *et al.*, (2002). Translation of polioviral mRNA is inhibited by cleavage of polypyrimidine tract-binding proteins executed by polioviral 3C(pro). Journal of Virology **76**(5): 2529-2542

Bandyopadhyay, A & Maitra, U (1999). Cloning and characterization of the p42 subunit of mammalian translation initiation factor 3 (eIF3): demonstration that eIF3 interacts with eIF5 in mammalian cells. Nucleic Acids Research **27**(5): 1331-1337.

Barco, A *et al.* (2000). Poliovirus protease 3C(pro) kills cells by apoptosis. Virology **266**(2): 352-360.

Barton, DJ *et al.* (1999). Translating ribosomes inhibit poliovirus negative-strand RNA synthesis. Journal of Virology **73**(12): 10104-10112.

Barton, DJ *et al.* (2001). 5 'cloverleaf in poliovirus RNA is a *cis*-acting replication element required for negative-strand synthesis. EMBO Journal **20**(6): 1439-1448.

Battiste, JL *et al.* (2000). The eIF1A solution structure reveals a large RNA-binding surface important for scanning function. Molecular Cell **5**(1): 109-119.

Bazan, JF & Fletterick, RJ (1988). Viral cysteine proteases are homologous to the trypsin-like family of serine proteases - structural and functional implications. Proceedings of the National Academy of Sciences of the United States of America **85**(21): 7872-7876.

Beales, LP *et al.* (2001). The internal ribosome entry site (IRES) of hepatitis C virus visualized by electron microscopy. RNA **7**(5): 661-670.

Belnap, DM *et al.* (2000). Molecular tectonic model of virus structural transitions: the putative cell entry states of poliovirus. Journal of Virology **74**(3): 1342-1354.

Belov, GA *et al.* (2000). Early alteration of nucleocytoplasmic traffic induced by some RNA viruses. Virology **275**(2): 244-248.

Belsham, GJ (1992). Dual initiation sites of protein-synthesis on foot-and-mouth-disease virus-RNA are selected following internal entry and scanning of ribosomes *in vivo*. EMBO Journal **11**(3): 1105-1110.

Belsham, GJ & Jackson, RJ (2000). Translation initiation on picornavirus RNA. Translational control of gene expression. Sonenberg, N *et al.* (ed.) Cold Spring Harbor, N. Y., Cold Spring Harbor Laboratory Press: 869-900.

Belsham, GJ *et al.* (2000). Foot-and-mouth disease virus 3C protease induces cleavage of translation initiation factors eIF4A and eIF4G within infected cells. Journal of Virology **74**(1): 272-280.

Benz, JH, *et al.* (1999). Crystal structure of the ATPase domain of translation initiation factor 4A from *Saccharomyces cerevisiae* - the prototype of the DEAD box protein family. Structure with Folding & Design **7**(6): 671-679.

Bergamini, GT *et al.* (2000). Picornavirus IRESes and the poly(A) tail jointly promote cap- independent translation in a mammalian cell-free system. RNA **6**(12): 1781-1790.

Bergelson, JM *et al.* (1997). Isolation of a common receptor for coxsackie B viruses and adenoviruses 2 and 5. Science **275**(5304): 1320-1323.

Berinstein, A *et al.* (1995). Antibodies to the vitronectin receptor (integrin alpha(V)beta(3)) inhibit binding and infection of foot-and-mouth-disease virus to cultured-cells. Journal of Virology **69**(4): 2664-2666.

Berlioz, C & Darlix, JL (1995). An internal ribosomal entry mechanism promotes translation of murine leukemia-virus gag polyprotein precursors. Journal of Virology **69**(4): 2214-2222.

Bernstein, JO *et al.* (1997). PDGF2/c-sis mRNA leader contains a differentiation-linked internal ribosomal entry site (D-IRES). Journal of Biological Chemistry **272**(14): 9356-9362.

Bienz, KD *et al.* (1983). Intracellular-distribution of poliovirus proteins and the induction of virus-specific cytoplasmic structures. Virology **131**(1): 39-48.

Black, TL *et al.* (1989). The cellular 68,000-Mr protein-kinase is highly autophosphorylated and activated yet significantly degraded during poliovirus infection - implications for translational regulation. Journal of Virology **63**(5): 2244-2251.

Blight, KJ *et al.* (2000). Efficient initiation of HCV RNA replication in cell culture. Science **290**(5498): 1972-1974.

Blyn, LB *et al.* (1996). Poly(rC) binding protein 2 binds to stem-loop IV of the poliovirus RNA 5' noncoding region: Identification by automated liquid chromatography tandem mass spectrometry. Proceedings of the National Academy of Sciences of the United States of America **93**(20): 11115-11120.

Blyn, LB *et al.* (1997). Requirement of Poly(rC) binding protein 2 for translation of poliovirus RNA. Journal of Virology **71**(8): 6243-6246.

Bonneau, AM & Sonenberg, N (1987). Proteolysis of the p220 component of the cap-binding protein complex is not sufficient for complete inhibition of host-cell protein-synthesis after poliovirus infection. Journal of Virology **61**(4): 986-991.

Borman, A *et al.* (1993). The involvement of a spliceosome component in internal initiation of human rhinovirus RNA translation. Journal of General Virology **74**: 1775-1788.

Borman, AM *et al.* (1994). Sequences within the poliovirus internal ribosome entry segment control viral-RNA synthesis. EMBO Journal **13**(13): 3149-3157.

Borman, AM *et al.* (1995). Picornavirus internal ribosome entry segments - comparison of translation efficiency and the requirements for optimal internal initiation of translation *in-vitro*. Nucleic Acids Research **23**(18): 3656-3663.

Borman, AM & Kean, KM (1997). Intact eukaryotic initiation factor 4G is required for hepatitis A virus internal initiation of translation. Virology **237**(1): 129-136.

Borman, AM *et al.* (1997). Comparison of picornaviral IRES-driven internal initiation of translation in cultured cells of different origins. Nucleic Acids Research **25**(5): 925-932.

Borman, AM *et al.* (2001). Detailed analysis of the requirements of hepatitis A virus internal ribosome entry segment for the eukaryotic initiation factor complex eIF4F. Journal of Virology **75**(17): 7864-7871.

Bovee, ML *et al.* (1998a). The predominant eIF4G-specific cleavage activity in poliovirus- infected HeLa cells is distinct from 2A protease. Virology **245**(2): 229-240.

Bovee, ML *et al.* (1998b). Direct cleavage of eIF4G by poliovirus 2A protease is inefficient *in vitro*. Virology **245**(2): 241-249.

Brown, BA & Ehrenfeld, E (1979). Translation of poliovirus RNA *in vitro*: changes in cleavage pattern and initiation sites by ribosomal salt wash. Virology **97**: 396-405.

Brown, CM *et al.* (1990). Sequence-analysis suggests that tetra-nucleotides signal the termination of protein-synthesis in eukaryotes. Nucleic Acids Research **18**(21): 6339-6345.

Brown, EA *et al.* (1991). The 5' nontranslated region of hepatitis-A virus-RNA - secondary structure and elements required for translation *in vitro*. Journal of Virology **65**(11): 5828-5838.

Brown, EA *et al.* (1992). Secondary structure of the 5' nontranslated regions of hepatitis-C virus and pestivirus genomic RNAs. Nucleic Acids Research **20**(19): 5041-5045.

Brown, EA *et al.* (1994). *In-vitro* characterization of an internal ribosomal entry site (IRES) present within the 5' nontranslated region of hepatitis A virus-RNA - comparison with the IRES of encephalomyocarditis virus. Journal of Virology **68**(2): 1066-1074.

Brown, CC *et al.* (1996). Pathogenesis of wild-type and leaderless foot-and-mouth disease virus in cattle. Journal of Virology **70**(8): 5638-5641.

Buratti, E *et al.* (1997). *In vivo* translational efficiency of different hepatitis C virus 5'-UTRs. FEBS Letters **411**(2-3): 275-280.

Buratti, E *et al.* (1998). Functional analysis of the interaction between HCV 5 'UTR and putative subunits of eukaryotic translation initiation factor elF3. Nucleic Acids Research **26**(13): 3179-3187.

Burroughs, JND *et al.* (1971). Further evidence for multiple proteins in the foot-and-mouth disease virus particle. Journal of General Virology **13**: 73-84.

Carrasco, L & Smith, AE (1976). Sodium ions and the shut-off of host cell protein synthesis by picornavirus. Nature **264**: 807.

Carthy, CM *et al.* (1998). Caspase activation and specific cleavage of substrates after coxsackievirus B3-induced cytopathic effect in HeLa cells. Journal of Virology **72**(9): 7669-7675.

Caruthers, JM *et al.* (2000). Crystal structure of yeast initiation factor 4A, a DEAD-box RNA helicase. Proceedings of the National Academy of Sciences of the United States of America **97**(24): 13080-13085.

Caskey, CT *et al.* (1971). Hydrolysis of fMet-tRNA by peptidyl transferase. Proceedings of the National Academy of Sciences of the United States of America **68**(12): 3163-3167.

Cate, JH *et al.* (1996). Crystal structure of a group I ribozyme domain: Principles of RNA packing. Science **273**(5282): 1678-1685.

Chakrabarti, A & Maitra, U (1991). Function of eukaryotic initiation factor-5 in the formation of an 80-S ribosomal polypeptide-chain initiation complex. Journal of Biological Chemistry **266**(21): 14039-14045.

Chappell, SA *et al.* (2000a). A 9-nt segment of a cellular mRNA can function as an internal ribosome entry site (IRES) and when present in linked multiple copies greatly

enhances IRES activity. Proceedings of the National Academy of Sciences of the United States of America **97**(4): 1536-1541.

Chappell, SA *et al.* (2000b). A mutation in the c-myc-IRES leads to enhanced internal ribosome entry in multiple myeloma: A novel mechanism of oncogene de-regulation. Oncogene **19**(38): 4437-4440.

Chaudhuri, JD *et al.* (1999). Distinct functions of eukaryotic translation initiation factors eIF1A and eIF3 in the formation of the 40 S ribosomal preinitiation complex. Journal of Biological Chemistry **274**(25): 17975-17980.

Chinsangaram, J *et al.* (1999). Ability of foot-and-mouth disease virus to form plaques in cell culture is associated with suppression of alpha/beta interferon. Journal of Virology **73**(12): 9891-9898.

Cho, MW *et al.* (1994). Membrane rearrangement and vesicle induction by recombinant poliovirus 2C and 2BC in human-cells. Virology **202**(1): 129-145.

Choi, SK *et al.* (2000). Physical and functional interaction between the eukaryotic orthologs of prokaryotic translation initiation factors IF1 and IF2. Molecular and Cellular Biology **20**(19): 7183-7191.

Clark, ME *et al.* (1993). Direct cleavage of human TATA-binding protein by poliovirus protease 3C *in vivo* and *in vitro*. Molecular and Cellular Biology **13**(2): 1232-1237.

Coldwell, MJ *et al.* (2000). Initiation of Apaf-1 translation by internal ribosome entry. Oncogene **19**(7): 899-905.

Collier, AJ *et al.* (1998). Translation efficiencies of the 5 ' untranslated region from representatives of the six major genotypes of hepatitis C virus using a novel bicistronic reporter assay system. Journal of General Virology **79**: 2359-2366.

Collier, AJ *et al.* (2002). A conserved RNA structure within the HCV IRES eIF3-binding site. Nature Structural Biology **9**(5): 375-380.

Conroy, SC *et al.* (1990). Characterization of the 46,000-dalton subunit of eIF-4F. Archives of Biochemistry and Biophysics **282**(2): 363-371.

Cornelis, S *et al.* (2000). Identification and characterization of a novel cell cycle-regulated internal ribosome entry site. Molecular Cell **5**(4): 597-605.

Costa, M & Michel, F (1995). Frequent use of the same tertiary motif by self-folding RNAs. EMBO Journal **14**(6): 1276-1285.

Craig, AWB *et al.* (1998). Interaction of polyadenylate-binding protein with the eIF4G homologue PAIP enhances translation. Nature **392**(6675): 520-523.

Curran, J *et al.* (1998). Translational gymnastics on the Sendai virus P/C mRNA. Seminars in Virology **8**(4): 351-357.

Curry, S *et al.* (1995). Viral-RNA modulates the acid sensitivity of foot-and-mouth-disease virus capsids. Journal of Virology **69**(1): 430-438.

Czaplinski, K *et al.* (1998). The surveillance complex interacts with the translation release factors to enhance termination and degrade aberrant mRNAs. Genes & Development **12**(11): 1665-1677.

De Gregorio, E *et al.* (1998). Translational activation of uncapped mRNAs by the central part of human eIF4G is 5 'end-dependent. RNA **4**(7): 828-836.

Devaney, MA *et al.* (1988). Leader protein of foot-and-mouth-disease virus is required for cleavage of the p220 component of the cap-binding protein complex. Journal of Virology **62**(11): 4407-4409.

Doedens, JR & Kirkegaard, K (1995). Inhibition of cellular protein secretion by poliovirus proteins 2B and 3A. EMBO Journal **14**(5): 894-907.

Dolph, PJ *et al.* (1990). Translation by the adenovirus tripartite leader - elements which determine independence from cap-binding protein complex. Journal of Virology **64**(6): 2669-2677.

Domier, LL *et al.* (2000). Sequence requirements for translation initiation of *Rhopalosiphum padi* virus ORF2. Virology **268**(2): 264-271.

Dominguez, DI *et al.* (1998). Ribosome shunting in cauliflower mosaic virus - Identification of an essential, and sufficient structural element. Journal of Biological Chemistry **273**(6): 3669-3678.

Donnelly, MLL *et al.* (1997). The cleavage activities of aphthovirus and cardiovirus 2A proteins. Journal of General Virology **78**: 13-21.

Dorner, AJ *et al.* (1984). *In vitro* translation of poliovirus RNA - utilization of internal initiation sites in reticulocyte lysate. Journal of Virology **50**(2): 507-514.

Drew, J & Belsham, GJ (1994). *Trans* complementation by RNA of defective foot-and-mouth- disease virus internal ribosome entry site elements. Journal of Virology **68**(2): 697-703.

Duke, GM *et al.* (1992). Sequence and structural elements that contribute to efficient encephalomyocarditis virus-RNA translation. Journal of Virology **66**(3): 1602-1609.

Duncan, R *et al.* (1987). Regulated phosphorylation and low abundance of HeLa-cell initiation-factor eIF-4F suggest a role in translational control - Heat-shock effects on eIF-4F. Journal of Biological Chemistry **262**(1): 380-388.

Ehrenberg, M & Tenson, T (2002). A new beginning of the end of translation. Nature Structural Biology **9**(2): 85-87.

Enterlein, S. (2001). Studies on selectable reporter for hepatitis C virus internal ribosome entry site function, Thesis (MRes)-University of Leeds

Etchison, D *et al.* (1982). Inhibition of HeLa-cell protein-synthesis following poliovirus infection correlates with the proteolysis of a 220,000-dalton polypeptide associated with eukaryotic initiation factor-3 and a cap binding-protein complex. Journal of Biological Chemistry **257**(24): 4806-4810.

Etchison, D & Fout, S (1985). Human rhinovirus-14 infection of HeLa-cells results in the proteolytic cleavage of the p220 cap-binding complex subunit and inactivates globin messenger-RNA translation *in vitro*. Journal of Virology **54**(2): 634-638.

Fadden, P *et al.* (1997). Identification of phosphorylation sites in the translational regulator, PHAS-I, that are controlled by insulin and rapamycin in rat adipocytes. Journal of Biological Chemistry **272**(15): 10240-10247.

Feduchi, E *et al.* (1995). Effects of poliovirus 2A(pro) on vaccinia virus gene expression. European Journal of Biochemistry **234**(3): 849-854.

Fernandez, J *et al.* (2001). Internal ribosome entry site-mediated translation of a mammalian mRNA is regulated by amino acid availability. Journal of Biological Chemistry **276**(15): 12285-12291.

Fletcher, CM *et al.* (1999). Structure and interactions of the translation initiation factor eIF1. EMBO Journal **18**(9): 2631-2637.

Foeger, N *et al.* (2002). Recognition of eukaryotic initiation factor 4G isoforms by picornaviral proteinases. Journal of Biological Chemistry **277**(46): 44300-44309.

Fouillot, N *et al.* (1993). Translation of the hepatitis-B virus P-gene by ribosomal scanning as an alternative to internal initiation. Journal of Virology **67**(8): 4886-4895.

Freistroffer, DV *et al.* (1997). Release factor RF3 in *E-coli* accelerates the dissociation of release factors RF1 and RF2 from the ribosome in a GTP-dependent manner. EMBO Journal **16**(13): 4126-4133.

Freistroffer, DV *et al.* (2000). The accuracy of codon recognition by polypeptide release factors. Proceedings of the National Academy of Sciences of the United States of America **97**(5): 2046-2051.

Fuerst, TR *et al.* (1986). Eukaryotic transient-expression system based on recombinant vaccinia virus that synthesizes bacteriophage-T7 RNA-polymerase. Proceedings of the National Academy of Sciences of the United States of America **83**(21): 8122-8126.

Fukushi, S *et al.* (1994). Complete 5' noncoding region is necessary for the efficient internal initiation of hepatitis-C virus-RNA. Biochemical and Biophysical Research Communications **199**(2): 425-432.

Futterer, J *et al.* (1993). Nonlinear ribosome migration on cauliflower mosaic virus-35S RNA. Cell **73**(4): 789-802.

Gallie, DR (1991). The cap and poly(A) tail function synergistically to regulate messenger-RNA translational efficiency. Genes & Development **5**(11): 2108-2116.

Gamarnik, AV & Andino, R (1997). Two functional complexes formed by KH domain containing proteins with the 5' noncoding region of poliovirus RNA. RNA **3**(8): 882-892.

Gamarnik, AV & Andino, R (1998). Switch from translation to RNA replication in a positive- stranded RNA virus. Genes & Development **12**(15): 2293-2304.

Gamarnik, AV & Andino, R (2000). Interactions of viral protein 3CD and poly(rC) binding protein with the 5 'untranslated region of the poliovirus genome. Journal of Virology **74**(5): 2219-2226.

Gan, WN & Rhoads, RE (1996). Internal initiation of translation directed by the 5'-untranslated region of the mRNA for eIF4G, a factor involved in the picornavirus-induced switch from cap-dependent to internal initiation. Journal of Biological Chemistry **271**(2): 623-626.

Gan, WN *et al.* (1998). Functional characterization of the internal ribosome entry site of eIF4G mRNA. Journal of Biological Chemistry **273**(9): 5006-5012.

Gerber, K *et al.* (2001). Biochemical and genetic studies of the initiation of human rhinovirus 2 RNA replication: Identification of a *cis*-replicating element in the coding sequence of 2A(pro). Journal of Virology **75**(22): 10979-10990.

Gingras, AC *et al.* (1996). Activation of the translational suppressor 4E-BP1 following infection with encephalomyocarditis virus and poliovirus. Proceedings of the National Academy of Sciences of the United States of America **93**(11): 5578-5583.

Gingras, AC *et al.* (1999). eIF4 initiation factors: Effectors of mRNA recruitment to ribosome and regulators of translation. Annual Review of Biochemistry **68**: 913-963

Glaser, W & Skern, T (2000). Extremely efficient cleavage of eIF4G by picornaviral proteinases L and 2A in vitro. FEBS Letters **480**(2-3): 151-155.

Glass, MJ & Summers, DF (1993). Identification of a *trans*-acting activity from liver that stimulates hepatitis-A Virus translation *in vitro*. Virology **193**(2): 1047-1050.

Goldstaub, D *et al.* (2000). Poliovirus 2A protease induces apoptotic cell death. Molecular and Cellular Biology **20**(4): 1271-1277.

Goodfellow, I *et al.* (2000). Identification of a *cis*-acting replication element within the poliovirus coding region. Journal of Virology **74**(10): 4590-4600.

Gorbalenya, AE *et al.* (1991). Putative papain-related thiol proteases of positive-strand RNA viruses - identification of rubivirus and aphthovirus proteases and delineation of a

novel conserved domain associated with proteases of rubivirus, alpha- and coronaviruses. FEBS Letters **288**(1-2): 201-205.

Goss, DJ *et al.* (1988). Effects of eukaryotic initiation factor-iii on eukaryotic ribosomal-subunit equilibrium and kinetics. Biochemistry **27**(5): 1489-1494.

Goyer, C *et al.* (1993). Tif4631 and Tif4632 - 2 yeast genes encoding the high-molecular-weight subunits of the cap-binding protein complex (eukaryotic initiation factor-4F) contain an RNA recognition motif-like sequence and carry out an essential function. Molecular and Cellular Biology **13**(8): 4860-4874.

Gradi, A *et al.* (1998a). A novel functional human eukaryotic translation initiation factor 4G. Molecular and Cellular Biology **18**(1): 334-342.

Gradi, A *et al.* (1998b). Proteolysis of human eukaryotic translation initiation factor eIF4GII, but not eIF4GI, coincides with the shutoff of host protein synthesis after poliovirus infection. Proceedings of the National Academy of Sciences of the United States of America **95**(19): 11089-11094.

Grant, CM & Hinnebusch, AG (1994). Effect of sequence context at stop codons on efficiency of reinitiation in GCN4 translational control. Molecular and Cellular Biology **14**(1): 606-618.

Graves, JH (1973). Serological relationship of swine vesicular disease virus and Coxsackie B5 virus. Nature **245**(5424): 314-315.

Green, R & Noller, HF (1997). Ribosomes and translation. Annual Review of Biochemistry **66**: 679-716.

Greve, JM *et al.* (1989). The major human rhinovirus receptor Is ICAM-1. Cell **56**(5): 839-847.

Grifo, JA *et al.* (1983). New initiation-factor activity required for globin messenger-RNA translation. Journal of Biological Chemistry **258**(9): 5804-5810.

Guarne, A *et al.* (1998). Structure of the foot-and-mouth disease virus leader protease: a papain-like fold adapted for self-processing and eIF4G recognition. EMBO Journal **17**(24): 7469-7479.

Gustin, KE & Sarnow, P (2001). Effects of poliovirus infection on nucleo-cytoplasmic trafficking and nuclear pore complex composition. EMBO Journal **20**(1-2): 240-249.

Haghighat, A *et al.* (1995). Repression of cap-dependent translation by 4E-binding protein-1 - competition with p220 for binding to eukaryotic initiation factor-4E. EMBO Journal **14**(22): 5701-5709.

Haghighat, A *et al.* (1996). The eIF4G-eIF4E complex is the target for direct cleavage by the rhinovirus 2A proteinase. Journal of Virology **70**(12): 8444-8450.

Haghighat, A & Sonenberg, N (1997). eIF4G dramatically enhances the binding of eIF4E to the mRNA 5'-cap structure. Journal of Biological Chemistry **272**(35): 21677-21680.

Hahm, B *et al.* (1998). Polypyrimidine tract-binding protein interacts with HnRNP L. FEBS Letters **425**(3): 401-406.

Hambidge, SJ & Sarnow, P (1992). Translational enhancement of the poliovirus 5' noncoding region mediated by virus-encoded polypeptide-2A. Proceedings of the National Academy of Sciences of the United States of America **89**(21): 10272-10276.

Han, BG & Zhang, JT (2002). Regulation of gene expression by internal ribosome entry sites or cryptic promoters: the eIF4G story. Molecular and Cellular Biology **22**(21): 7372-7384.

Hassett, DE *et al.* (1997). Analysis of a temperature-sensitive vaccinia virus mutant in the viral mRNA capping enzyme isolated by clustered charge-to- alanine mutagenesis and transient dominant selection. Virology **238**(2): 391-409.

Hayashi, S *et al.* (2000). Increase in cap- and IRES-dependent protein synthesis by overproduction of translation initiation factor eIF4G. Biochemical and Biophysical Research Communications **277**(1): 117-123.

Heesom, KJ *et al.* (1998). Insulin-stimulated kinase from rat fat cells that phosphorylates initiation factor 4E-binding protein 1 on the rapamycin-insensitive site (serine-111). Biochemical Journal **336**: 39-48.

Hellen, CUT *et al.* (1994a). The cellular polypeptide p57 (pyrimidine tract-binding protein) binds to multiple sites in the poliovirus 5' nontranslated region. Journal of Virology **68**(2): 941-950.

Hellen, CUT *et al.* (1994b). Effect of mutations downstream of the internal ribosome entry site on initiation of poliovirus protein-synthesis. Journal of Virology **68**(10): 6312-6322.

Hemmings-Mieszczak, MG *et al.* (1998). Regulation of CaMV 35 S RNA translation is mediated by a stable hairpin in the leader. RNA **4**(1): 101-111.

Henis-Korenblit, S *et al.* (2000). A novel form of DAP5 protein accumulates in apoptotic cells as a result of caspase cleavage and internal ribosome entry site-mediated translation. Molecular and Cellular Biology **20**(2): 496-506.

Henis-Korenblit, S *et al.* (2002). The caspase-cleaved DAP5 protein supports internal ribosome entry site-mediated translation of death proteins. Proceedings of the National Academy of Sciences of the United States of America **99**(8): 5400-5405.

Hennecke, M *et al.* (2001). Composition and arrangement of genes define the strength of IRES-driven translation in bicistronic mRNAs. Nucleic Acids Research **29**(16): 3327-3334

Herold, J & Andino, R (2001). Poliovirus RNA replication requires genome circularization through a protein-protein bridge. Molecular Cell **7**(3): 581-591.

Hershey, JW & Merrick, WC (2000). Pathway and mechanism of initiation of protein synthesis. Translational control of gene expression. Sonenberg, N *et al.* (ed.) Cold Spring Harbor, N. Y., Cold Spring Harbor Laboratory Press.

Hindiyeh, M *et al.* (1999). Poliovirus mutants at histidine 195 of VP2 do not cleave VP0 into VP2 and VP4. Journal of Virology **73**(11): 9072-9079.

Hinnebusch, AG (1997). Translational regulation of yeast GCN4 - A window on factors that control initiator-tRNA binding to the ribosome. Journal of Biological Chemistry **272**(35): 21661-21664.

Hoffman, MA & Palmenberg, AC (1995). Mutational analysis of the J-K stem-loop region of the encephalomyocarditis virus IRES. Journal of Virology **69**(7): 4399-4406.

Hogle, JM *et al.* (1985). 3-dimensional structure of poliovirus at 2.9 Å resolution. Science **229**(4720): 1358-1365.

Holcik, M & Korneluk, RJ (2000). Functional characterization of the X-linked inhibitor of apoptosis (XIAP) internal ribosome entry site element: Role of La autoantigen in XIAP translation. Molecular and Cellular Biology **20**(13): 4648-4657.

Holcik, M *et al.* (2000). Translational upregulation of X-linked inhibitor of apoptosis (XIAP) increases resistance to radiation induced cell death. Oncogene **19**(36): 4174-4177.

Holzmann, K *et al.* (2000). A human common nuclear matrix protein homologous to eukaryotic translation initiation factor 4A. Biochemical and Biophysical Research Communications **267**(1): 339-344.

Honda, M *et al.* (1996). Structural requirements for initiation of translation by internal ribosome entry within genome-length hepatitis C virus RNA. Virology **222**(1): 31-42.

Honda, M *et al.* (1999). A phylogenetically conserved stem-loop structure at the 5 ' border of the internal ribosome entry site of hepatitis C virus is required for cap-independent viral translation. Journal of Virology **73**(2): 1165-1174.

Hoshino, S *et al.* (1999a). Novel function of the eukaryotic polypeptide-chain releasing factor 3 (eRF3/GSPT) in the mRNA degradation pathway. Biochemistry-Moscow **64**(12): 1367-1372.

Hoshino, S *et al.* (1999b). The eukaryotic polypeptide chain releasing factor (eRF3/GSPT) carrying the translation termination signal to the 3 '-poly(A) tail of mRNA - Direct association of eRF3/GSPT with polyadenylate-binding protein. Journal of Biological Chemistry **274**(24): 16677-16680.

Hu, MC *et al.* (1999). rRNA-complementarity in the 5 ' untranslated region of mRNA specifying the Gtx homeodomain protein: Evidence that base- pairing to 18S rRNA

affects translational efficiency. Proceedings of the National Academy of Sciences of the United States of America **96**(4): 1339-1344.

Huez, I *et al.* (1998). Two independent internal ribosome entry sites are involved in translation initiation of vascular endothelial growth factor mRNA. Molecular and Cellular Biology **18**(11): 6178-6190.

Hunt, SL *et al.* (1999). unr, a cellular cytoplasmic RNA-binding protein with five cold-shock domains, is required for internal initiation of translation of human rhinovirus RNA. Genes & Development **13**(4): 437-448.

Hunt, SL & Jackson, RJ (1999). Polypyrimidine-tract binding protein (PTB) is necessary, but not sufficient, for efficient internal initiation of translation of human rhinovirus-2 RNA. RNA **5**(3): 344-359.

Hwang, WL & Su, TS (1998). Translational regulation of hepatitis B virus polymerase gene by termination-reinitiation of an upstream minicistron in a length-dependent manner. Journal of General Virology **79**: 2181-2189.

Imataka, H & Sonenberg, N (1997). Human eukaryotic translation initiation factor 4G (eIF4G) possesses two separate and independent binding sites for eIF4A. Molecular and Cellular Biology **17**(12): 6940-6947.

Imataka, H *et al.* (1997). A new translational regulator with homology to eukaryotic translation initiation factor 4G. EMBO Journal **16**(4): 817-825.

Imataka, H *et al.* (1998). A newly identified N-terminal amino acid sequence of human eIF4G binds poly(A)-binding protein and functions in poly(A)-dependent translation. EMBO Journal **17**(24): 7480-7489.

Inoue, T *et al.* (1989). The complete nucleotide-sequence of swine vesicular disease virus. Journal of General Virology **70**: 919-934.

Ito, K *et al.* (2000). A tripeptide 'anticodon' deciphers stop codons in messenger RNA. Nature **403**(6770): 680-684.

Jackson, T *et al.* (2000). The epithelial integrin alpha v beta 6 is a receptor for foot-and-mouth disease virus. Journal of Virology **74**(11): 4949-4956.

Jackson, T *et al.* (2002). Integrin alpha v beta 1 is a receptor for foot-and-mouth disease virus. Journal of Virology **76**(3): 935-941.

Jaramillo, M *et al.* (1991). RNA unwinding in translation - assembly of helicase complex intermediates comprising eukaryotic initiation-factors eIF-4F and eIF-4B. Molecular and Cellular Biology **11**(12): 5992-5997.

Jelachich, ML & Lipton, HL (1999). Restricted Theiler's murine encephalomyelitis virus infection in murine macrophages induces apoptosis. Journal of General Virology **80**: 1701-1705.

Jen, G & Thach, RE (1982). Inhibition of host translation in encephalomyocarditis virus- infected L-cells - a novel mechanism. Journal of Virology **43**(1): 250-261.

Jia, XY *et al.* (1993). Primary cleavage of the HAV capsid protein-precursor in the middle of the proposed 2A coding region. Virology **193**(1): 515-519.

Joachims, M *et al.* (1999). Cleavage of poly(A)-binding protein by enterovirus proteases concurrent with inhibition of translation *in vitro*. Journal of Virology **73**(1): 718-727.

Johannes, G & Sarnow, P (1998). Cap-independent polysomal association of natural mRNAs encoding c-myc, BiP, and eIF4G conferred by internal ribosome entry sites. RNA **4**(12): 1500-1513.

Johannes, G *et al.* (1999). Identification of eukaryotic mRNAs that are translated at reduced cap binding complex eIF4F concentrations using a cDNA microarray. Proceedings of the National Academy of Sciences of the United States of America **96**(23): 13118-13123.

Johnson, ER & McKay, DB (1999). Crystallographic structure of the amino terminal domain of yeast initiation factor 4A, a representative DEAD-box RNA helicase. RNA **5**(12): 1526-1534.

Jubin, R *et al.* (2000). Hepatitis C virus internal ribosome entry site (IRES) stem loop IIId contains a phylogenetically conserved GGG triplet essential for translation and IRES folding. Journal of Virology **74**(22): 10430-10437.

Kaku, Y *et al.* (2002). Unique characteristics of a picornavirus internal ribosome entry site from the porcine teschovirus-1 talfan. Journal of Virology **76**(22): 11721-11728.

Kaminski, A *et al.* (1990). Initiation of encephalomyocarditis virus-RNA translation - the authentic initiation site is not selected by a scanning mechanism. EMBO Journal **9**(11): 3753-3759.

Kaminski, A *et al.* (1994). Translation of encephalomyocarditis virus-RNA - parameters influencing the selection of the internal initiation site. EMBO Journal **13**(7): 1673-1681.

Kaminski, A *et al.* (1995). Direct evidence that polypyrimidine tract binding protein (PTB) is essential for internal initiation of translation of encephalomyocarditis virus RNA. RNA **1**(9): 924-938.

Kaminski, A & Jackson, RJ (1998). The polypyrimidine tract binding protein (PTB) requirement for internal initiation of translation of cardiovirus RNAs is conditional rather than absolute. RNA **4**(6): 626-638.

Kamoshita, N *et al.* (1997). Genetic analysis of internal ribosomal entry site on hepatitis C virus RNA: Implication for involvement of the highly ordered structure and cell type-specific *trans* acting factors. Virology **233**(1): 9-18.

Kanamori, Y & Nakashima, N (2001). A tertiary structure model of the internal ribosome entry site (IRES) for methionine-independent initiation of translation. RNA **7**(2): 266-274.

Kanno, T *et al.* (1998). Viruses produced from complementary DNA of virulent and avirulent strains of swine vesicular disease viruses retain the *in vivo* and *in vitro* characteristics of the parental strain. Archives of Virology **143**(6): 1055-1062.

Kanno, T *et al.* (1999). Mapping the genetic determinants of pathogenicity and plaque phenotype in swine vesicular disease virus. Journal of Virology **73**(4): 2710-2716.

Karimi, R *et al.* (1999). Novel roles for classical factors at the interface between translation termination and initiation. Molecular Cell **3**(5): 601-609.

Kerekatte, V *et al.* (1999). Cleavage of poly(A)-binding protein by coxsackievirus 2A protease *in vitro* and *in vivo*: Another mechanism for host protein synthesis shutoff? Journal of Virology **73**(1): 709-717.

Kieft, JS *et al.* (2001). Mechanism of ribosome recruitment by hepatitis C IRES RNA. RNA **7**(2): 194-206.

Kieft, JS *et al.* (2002). Crystal structure of an RNA tertiary domain essential to HCV IRES-mediated translation initiation. Nature Structural Biology **9**(5): 370-374.

Kim, YK *et al.* (2000). Polypyrimidine tract-binding protein inhibits translation of BiP mRNA. Journal of Molecular Biology **304**(2): 119-133.

Kim, YK *et al.* (2001). La autoantigen enhances translation of BiP mRNA. Nucleic Acids Research **29**(24): 5009-5016.

Kirchweger, R *et al.* (1994). Foot-and-mouth-disease virus leader proteinase - purification of the Lb form and determination of its cleavage site on eIF4-Gamma. Journal of Virology **68**(9): 5677-5684.

Kleijn, M *et al.* (1996). Phosphorylation state of the cap-binding protein eIF4E during viral infection. Virology **217**(2): 486-494.

Klinck, R *et al.* (2000). A potential RNA drug target in the hepatitis C virus internal ribosomal entry site. RNA **6**(10): 1423-1431.

Klinger, MHF *et al.* (2001). Perinuclear accumulation of hepatitis A virus proteins, RNA, and particles and ultrastructural alterations in infected cells. Archives of Virology **146**(12): 2291-2307.

Kodama, M *et al.* (1980a). Swine vesicular disease viruses isolated from healthy pigs in non-epizootic period. I. Isolation and identification. National Institute of Animal Health Quarterly **20**(1): 1-10.

Kodama, M *et al.* (1980b). Swine vesicular disease viruses isolated from healthy pigs in non-epizootic period. II. Vesicular formation and virus multiplication in

experimentally inoculated pigs. National Institute of Animal Health Quarterly **20**(4): 123-130.

Kolupaeva, VG *et al.* (1996). Structural analysis of the interaction of the pyrimidine tract-binding protein with the internal ribosomal entry site of encephalomyocarditis virus and foot-and-mouth disease virus RNAs. RNA **2**(12): 1199-1212.

Kolupaeva, VG *et al.* (1998). Translation eukaryotic initiation factor 4G recognizes a specific structural element within the internal ribosome entry site of encephalomyocarditis virus RNA. Journal of Biological Chemistry **273**(29): 18599-18604.

Kolupaeva, VG *et al.* (2000). An enzymatic footprinting analysis of the interaction of 40S ribosomal subunits with the internal ribosomal entry site of hepatitis C virus. Journal of Virology **74**(14): 6242-6250.

Kolupaeva, VG *et al.*, (2002). Personal communication.

Kolykhalov, AA *et al.* (1997). Transmission of hepatitis C by intrahepatic inoculation with transcribed RNA. Science **277**(5325): 570-574.

Kozak, M (1987a). An analysis of 5'-noncoding sequences from 699 vertebrate messenger-RNAs. Nucleic Acids Research **15**(20): 8125-8148.

Kozak, M (1987b). Effects of intercistronic length on the efficiency of reinitiation by eukaryotic ribosomes. Molecular and Cellular Biology **7**(10): 3438-3445.

Kozak, M (1989). The scanning model for translation - an update. Journal of Cell Biology **108**(2): 229-241.

Kozak, M (1991a). Effects of long 5' leader sequences on initiation by eukaryotic ribosomes *in vitro*. Gene Expression **1**(2): 117-125.

Kozak, M (1991b). A short leader sequence impairs the fidelity of initiation by eukaryotic ribosomes. Gene Expression **1**(2): 111-115.

Kozak, M (1999). Initiation of translation in prokaryotes and eukaryotes. Gene **234**(2): 187-208.

Kozak, M (2001a). New ways of initiating translation in eukaryotes? Molecular and Cellular Biology **21**(6): 1899-1907.

Kozak, M (2001b). Constraints on reinitiation of translation in mammals. Nucleic Acids Research **29**(24): 5226-5232.

Krausslich, HG *et al.* (1987). Poliovirus proteinase-2A induces cleavage of eukaryotic initiation factor-4F polypeptide-p220. Journal of Virology **61**(9): 2711-2718.

Kristensen, T *et al.* (1988). T7 DNA polymerase in automated dideoxy sequencing. Nucleic Acids Research **16**(8): 3487-3496.

Kruger, M *et al.* (2000). Identification of eIF2B gamma and eIF2 gamma as cofactors of hepatitis C virus internal ribosome entry site-mediated translation using a functional genomics approach. Proceedings of the National Academy of Sciences of the United States of America **97**(19): 8566-8571.

Kuhn, R *et al.* (1990). Functional-analysis of the internal translation initiation site of foot-and-mouth-disease virus. Journal of Virology **64**(10): 4625-4631.

Kuo, RL *et al.* (2002). Infection with enterovirus 71 or expression of its 2A protease induces apoptotic cell death Journal of General Virology **83**: 1367-1376.

Kuyumcu-Martinez, NM *et al.* (2002). Efficient cleavage of ribosome-associated poly(A)-binding protein by enterovirus 3C protease. Journal of Virology **76**(5): 2062-2074.

Kyrpides, NC & Woese, CR (1998). Universally conserved translation initiation factors. Proceedings of the National Academy of Sciences of the United States of America **95**(1): 224-228.

Laemmli, UK (1970). Cleavage of structural proteins during the assembly of the head of bacteriophage T4. Nature **227**(259): 680-685.

Lamphear, BJ *et al.* (1993). Mapping the cleavage site in protein-synthesis initiation factor-eIF-4-Gamma of the 2A proteases from human coxsackievirus and rhinovirus. Journal of Biological Chemistry **268**(26): 19200-19203.

Lamphear, BJ *et al.* (1995). Mapping of functional domains in eukaryotic protein-synthesis initiation-factor 4G (eIF4G) with picornaviral proteases - implications for cap-dependent and cap-independent translational initiation. Journal of Biological Chemistry **270**(37): 21975-21983.

Laporte, J *et al.* (2000). Comparative analysis of translation efficiencies of hepatitis C virus 5 'untranslated regions among intraindividual quasispecies present in chronic infection: Opposite behaviors depending on cell type. Journal of Virology **74**(22): 10827-10833.

Laurino, MP *et al.* (1999). The beta subunit of eukaryotic translation initiation factor 2 binds mRNA through the lysine repeats and a region comprising the C-2-C-2 motif. Molecular and Cellular Biology **19**(1): 173-181.

Lawson, TG *et al.* (1986). Influence of 5' proximal secondary structure on the translational efficiency of eukaryotic messenger-RNAs and on their interaction with initiation-factors. Journal of Biological Chemistry **261**(30): 13979-13989.

Le, SY & Maizel, JV (1997). A common RNA structural motif involved in the internal initiation of translation of cellular mRNAs. Nucleic Acids Research **25**(2): 362-369.

Li, QY *et al.* (1999). Eukaryotic translation initiation factor 4AIII (eTF4AIII) is functionally distinct from eIF4AI and eIF4AII. Molecular and Cellular Biology **19**(11): 7336-7346.

Li, W *et al.* (2001a). Eukaryotic initiation factors 4A (eIF4A) and 4G (eIF4G) mutually interact in a 1 : 1 ratio *in vivo*. Journal of Biological Chemistry **276**(31): 29111-29115.

Li, W *et al.* (2001b). Cleavage of translation initiation factor 4AI (eIF4AI) but not eIF4AII by foot-and-mouth disease virus 3C protease: identification of the eIF4AI cleavage site. FEBS Letters **507**(1): 1-5.

Liebig, H. D., E. Ziegler, *et al.* (1993). Purification of 2 picornaviral-2A proteinases - interaction with eIF4-gamma and influence on *in-vitro* translation. Biochemistry **32**(29): 7581-7588.

Liebig, HD *et al.* (2002). A thermosensitive mutant of HRV2 2A proteinase: evidence for direct cleavage of eIF4GI and eIF4GII. Febs Letters **523**(1-3): 53-57.

Lin, CG & Lo, SJ (1992). Evidence for involvement of a ribosomal leaky scanning mechanism in the translation of the hepatitis-B virus pol-gene from the viral pregenome RNA. Virology **188**(1): 342-352.

Lloyd, RE *et al.* (1986). Cleavage of the cap binding-protein complex polypeptide p20 is not effected by the 2nd poliovirus protease 2A. Virology **150**(1): 299-303.

Lobert, PE *et al.* (1999). A coding RNA sequence acts as a replication signal in cardioviruses. Proceedings of the National Academy of Sciences of the United States of America **96**(20): 11560-11565.

Lohmann, V *et al.* (1999). Replication of subgenomic hepatitis C virus RNAs in a hepatoma cell line. Science **285**(5424): 110-113.

Lomakin, IB *et al.* (2000). Physical association of eukaryotic initiation factor 4G (eIF4G) with eIF4A strongly enhances binding of elF4G to the internal ribosomal entry site of encephalomyocarditis virus and is required for internal initiation of translation. Molecular and Cellular Biology **20**(16): 6019-6029.

Lopez de Quinto, S & Martinez-Salas, E (1997). Conserved structural motifs located in distal loops of aphthovirus internal ribosome entry site domain 3 are required for internal initiation of translation. Journal of Virology **71**(5): 4171-4175.

Lopez de Quinto, S & Martinez-Salas, E (1999). Involvement of the aphthovirus RNA region located between the two functional AUGs in start codon selection. Virology **255**(2): 324-336.

Lopez de Quinto, S & Martinez-Salas, E (2000). Interaction of the eIF4G initiation factor with the aphthovirus IRES is essential for internal translation initiation *in vivo*. RNA **6**(10): 1380-1392.

Lopez de Quinto, S *et al.* (2001). IRES interaction with translation initiation factors: Functional characterization of novel RNA contacts with eIF3, eIF4B, and eIF4GII. RNA **7**(9): 1213-1226.

Lopez de Quinto, S *et al.* (2002). IRES-driven translation is stimulated separately by the FMDV 3 '-NCR and poly(A) sequences. Nucleic Acids Research **30**(20): 4398-4405.

Lu, HH & Wimmer, E (1996). Poliovirus chimeras replicating under the translational control of genetic elements of hepatitis C virus reveal unusual properties of the internal ribosomal entry site of hepatitis C virus. Proceedings of the National Academy of Sciences of the United States of America **93**(4): 1412-1417.

Luo, M *et al.* (1987). The atomic-structure of mengo-virus at 3.0-Å resolution. Science **235**(4785): 182-191.

Luukkonen, BGM *et al.* (1995). Efficiency of reinitiation of translation on human-immunodeficiency-virus type-1 messenger-RNAs Is determined by the length of the upstream open reading frame and by intercistronic distance. Journal of Virology **69**(7): 4086-4094.

Lyons, T *et al.* (2001). Poliovirus 5 '-terminal cloverleaf RNA is required in *cis* for VPg uridylylation and the initiation of negative-strand RNA synthesis. Journal of Virology **75**(22): 10696-10708.

Macadam, AJ *et al.* (1994). Role for poliovirus protease 2A in cap independent translation. EMBO Journal **13**(4): 924-927.

Mader, S *et al.* (1995). The translation initiation-factor eIF-4E binds to a common motif shared by the translation factor eIF-4-gamma and the translational repressors 4E-binding proteins. Molecular and Cellular Biology **15**(9): 4990-4997.

Maquat, LE (2000). Nonsense-mediated RNA decay in mammalian cells: a splicing-dependent means to down-regulate the levels of mRNAs that prematuely terminate translation. Translational control of gene expression. Sonenberg, N *et al.* (ed.) Cold Spring Harbor, N. Y., Cold Spring Harbor Laboratory Press: 849-868

Marcotrigiano, J *et al.* (1997). Co-crystal structure of the messenger RNA 5' cap-binding protein (eIF4E) bound to 7-methyl-GDP. Cell **89**(6): 951-961.

Marcotrigiano, J *et al.* (2001). A conserved HEAT domain within eIF4G directs assembly of the translation initiation machinery. Molecular Cell **7**(1): 193-203.

Mason, PW *et al.* (2002). Identification and characterization of a *cis*-acting replication element (cre) adjacent to the internal ribosome entry site of foot-and-mouth disease virus. Journal of Virology **76**(19): 9686-9694.

Mathews, DH *et al.* (1999). Expanded sequence dependence of thermodynamic parameters improves prediction of RNA secondary structure. Journal of Molecular Biology **288**: 911-940.

Matsuo, H *et al.* (1997). Structure of translation factor eIF4E bound to m(7)GDP and interaction with 4E-binding protein. Nature Structural Biology **4**(9): 717-724.

McCarthy, JE (2000). Translation initiation: Insect virus RNAs rewrite the rule book. Current Biology **10**(19): R715-R717.

McCaughan, KK *et al.* (1995). Translational Termination Efficiency in Mammals Is Influenced by the Base Following the Stop Codon. Proceedings of the National Academy of Sciences of the United States of America **92**(12): 5431-5435.

McKnight, KL & Lemon, SM (1998). The rhinovirus type 14 genome contains an internally located RNA structure that is required for viral replication. RNA **4**(12): 1569-1584.

Meerovitch, K *et al.* (1993). La autoantigen enhances and corrects aberrant translation of poliovirus RNA in reticulocyte lysate. Journal of Virology **67**(7): 3798-3807.

Mendelsohn, CL *et al.* (1989). Cellular receptor for poliovirus - molecular-cloning, nucleotide-sequence, and expression of a new member of the immunoglobulin superfamily. Cell **56**(5): 855-865.

Mercer, DF *et al.* (2001). Hepatitis C virus replication in mice with chimeric human livers. Nature Medicine **7**(8): 927-933.

Merrick, WC (1992). Mechanism and regulation of eukaryotic protein-synthesis. Microbiological Reviews **56**(2): 291-315.

Merrick, WC & Nyborg, J (2000). The protein biosynthesis elongation cycle. Translational control of gene expression. Sonenberg, N *et al.* (ed.). Cold Spring Harbor, N. Y., Cold Spring Harbor Laboratory Press: 89-126

Methot, N *et al.* (1996). A region rich in aspartic acid, arginine, tyrosine, and glycine (DRYG) mediates eukaryotic initiation factor 4B (eIF4B) self- association and interaction with eIF3. Molecular and Cellular Biology **16**(10): 5328-5334.

Meyer, K *et al.* (1995). Interaction of eukaryotic initiation-factor eIF-4B with a picornavirus internal translation initiation site. Journal of Virology **69**(5): 2819-2824.

Michel, YM *et al.* (2001). Eukaryotic initiation factor 4G-poly(A) binding protein interaction is required for poly(A) tail-mediated stimulation of picornavirus internal ribosome entry segment-driven translation but not for X-mediated stimulation of hepatitis C virus translation. Molecular and Cellular Biology **21**(13): 4097-4109.

Miller, LC *et al.* (2001). Role of the cytoplasmic domain of the beta-subunit of integrin alpha v beta 6 in infection by foot-and-mouth disease virus. Journal of Virology **75**(9): 4158-4164.

Minich, WB *et al.* (1994). Chromatographic resolution of *in-vivo* phosphorylated and nonphosphorylated eukaryotic translation initiation-factor eIF-4E - Increased cap

affinity of the phosphorylated form. Proceedings of the National Academy of Sciences of the United States of America **91**(16): 7668-7672.

Minor, PD (1992). The molecular-biology of polio vaccines. Journal of General Virology **73**: 3065-3077.

Mitchell, SA *et al.* (2001). Protein factor requirements of the Apaf-1 internal ribosome entry segment: Roles of polypyrimidine tract binding protein and upstream of N-ras. Molecular and Cellular Biology **21**(10): 3364-3374.

Moore, NF *et al.* (1981). Processing of cricket paralysis virus-induced polypeptides in Drosophila cells - production of high molecular-weight polypeptides by treatment with iodoacetamide. Archives of Virology **68**(1): 1-8.

Morino, S *et al.* (2000). Eukaryotic translation initiation factor 4E (eIF4E) binding site and the middle one-third of eIF4GI constitute the core domain for cap-dependent translation, and the C-terminal one- third functions as a modulatory region. Molecular and Cellular Biology **20**(2): 468-477.

Mulder, J *et al.* (1998). Vaccinia virus protein synthesis has a low requirement for the intact translation initiation factor eIF4F, the cap-binding complex, within infected cells. Journal of Virology **72**(11): 8813-8819.

Munroe, D & Jacobson, A (1990). Messenger-RNA poly(A) tail, a 3'enhancer of translational initiation. Molecular and Cellular Biology **10**(7): 3441-3455.

Murray, KE *et al.* (2001). Poly(rC) binding proteins mediate poliovirus mRNA stability. RNA **7**(8): 1126-1141.

Nakamura, Y *et al.* (2001). Protein tRNA mimicry in translation termination. The ribosome. Cold Spring Harbor, N. Y., Cold Spring Harbor Laboratory Press.

Naranda, T *et al.* (1996). SUI1/p16 is required for the activity of eukaryotic translation initiation factor 3 in *Saccharomyces cerevisiae*. Molecular and Cellular Biology **16**(5): 2307-2313.

Nateri, AS *et al.* (2000). *In vivo* and *in vitro* identification of structural and sequence elements of the human parechovirus 5 'untranslated region required for internal initiation. Journal of Virology **74**(14): 6269-6277.

Neznanov, N *et al.* (2001). Poliovirus protein 3A inhibits tumor necrosis factor (TNF)-induced apoptosis by eliminating the TNF receptor from cell surface. Journal of Virology **75**(21): 10409-10420.

Nicholson, R *et al.* (1991). Structural and functional-analysis of the ribosome landing pad of poliovirus type-2 - *in vivo* translation studies. Journal of Virology **65**(11): 5886-5894.

Nielsen, PJ & Trachsel, H (1988). The mouse protein-synthesis initiation factor-4A gene family includes 2 related functional genes which are differentially expressed. EMBO Journal **7**(7): 2097-2105.

Niepmann, M *et al.* (1997). Functional involvement of polypyrimidine tract-binding protein in translation initiation complexes with the internal ribosome entry site of foot-and-mouth disease virus. Journal of Virology **71**(11): 8330-8339.

Nissen, P *et al.* (2000). The structural basis of ribosome activity in peptide bond synthesis. Science **289**(5481): 920-930.

Ochs, K *et al.* (2002). Interaction of translation initiation factor eIF4B with the poliovirus internal ribosome entry site. Journal of Virology **76**(5): 2113-2122.

Odreman-Macchioli, FE *et al.* (2000). Influence of correct secondary and tertiary RNA folding on the binding of cellular factors to the HCV IRES. Nucleic Acids Research **28**(4): 875-885.

Ohlmann, T *et al.* (1995). Proteolytic cleavage of initiation-factor eIF-gamma in the reticulocyte lysate inhibits translation of capped messenger- RNAs but enhances that of uncapped messenger-RNAs. Nucleic Acids Research **23**(3): 334-340.

Ohlmann, T., M. Rau, *et al.* (1996). The C-terminal domain of eukaryotic protein synthesis initiation factor (eIF) 4G is sufficient to support cap- independent translation in the absence of eIF4E. EMBO Journal **15**(6): 1371-1382.

Ohlmann, T *et al.* (2000). An internal ribosome entry segment promotes translation of the simian immunodeficiency virus genomic RNA. Journal of Biological Chemistry **275**(16): 11899-11906.

Oldfield, S *et al.* (1994). Use of monoclonal-antibodies to study the structure and function of eukaryotic protein-synthesis initiation-factor eIF-2B. European Journal of Biochemistry **221**(1): 399-410.

Oliveira, MA *et al.* (1993). The structure of human rhinovirus-16. Structure **1**(1): 51-68.

Owens, GC *et al.* (2001). Identification of two short internal ribosome entry sites selected from libraries of random oligonucleotides. Proceedings of the National Academy of Sciences of the United States of America **98**(4): 1471-1476.

Palmenberg, AC & Sgro, JY (1997). Topological organization of picornaviral genomes: Statistical prediction of RNA structural signals. Seminars in Virology **8**(3): 231-241.

Parsley, TB *et al.* (1997). Poly (rC) binding protein 2 forms a ternary complex with the 5'-terminal sequences of poliovirus RNA and the viral 3CD proteinase. RNA **3**(10): 1124-1134.

Paul, AV *et al.* (1998). Protein-primed RNA synthesis by purified poliovirus RNA polymerase. Nature **393**(6682): 280-284.

Paul, AV *et al.* (2000). Identification of an RNA hairpin in poliovirus RNA that serves as the primary template in the *in vitro* uridylylation of VPg. Journal of Virology **74**(22): 10359-10370.

Paulin, FE *et al.* (1996). Aberrant translational control of the c-myc gene in multiple myeloma. Oncogene **13**(3): 505-513.

Paulin, FE *et al.* (1998). A single nucleotide change in the c-myc internal ribosome entry segment leads to enhanced binding of a group of protein factors. Nucleic Acids Research **26**(13): 3097-3103.

Pause, A & Sonenberg, N (1992). Mutational analysis of a DEAD box RNA helicase - the mammalian translation initiation-factor eIF-4A. EMBO Journal **11**(7): 2643-2654.

Pause, A *et al.* (1993). The HRIGRXXR region of the DEAD box RNA helicase eukaryotic translation initiation factor-4A is required for RNA-binding and ATP hydrolysis. Molecular and Cellular Biology **13**(11): 6789-6798.

Pause, A *et al.* (1994a). Insulin-dependent stimulation of protein-synthesis by phosphorylation of a regulator of 5'-cap function. Nature **371**(6500): 762-767.

Pause, A *et al.* (1994b). Dominant-negative mutants of mammalian translation initiation- factor eIF-4A define a critical role for eIF-4F in cap- dependent and cap-independent initiation of translation. EMBO Journal **13**(5): 1205-1215.

Pavlov, MY *et al.* (1997). Fast recycling of *Escherichia coli* ribosomes requires both ribosome recycling factor (RRF) and release factor RF3. EMBO Journal **16**(13): 4134-4141.

Pestova, TV *et al.* (1991). Translation of poliovirus RNA - role of an essential *cis*-acting oligopyrimidine element within the 5' nontranslated region and involvement of a cellular 57-kilodalton protein. Journal of Virology **65**(11): 6194-6204.

Pestova, TV *et al.* (1994). A conserved AUG triplet in the 5' nontranslated region of poliovirus can function as an initiation codon *in-vitro* and *in-vivo*. Virology **204**(2): 729-737.

Pestova, TV *et al.* (1996a). Functional dissection of eukaryotic initiation factor 4F: The 4A subunit and the central domain of the 4G subunit are sufficient to mediate internal entry of 43S preinitiation complexes. Molecular and Cellular Biology **16**(12): 6870-6878.

Pestova, TV *et al.* (1996b). Canonical eukaryotic initiation factors determine initiation of translation by internal ribosomal entry. Molecular and Cellular Biology **16**(12): 6859-6869.

Pestova, TV *et al.* (1998a). Eukaryotic ribosomes require initiation factors 1 and 1A to locate initiation codons. Nature **394**(6696): 854-859.

Pestova, TV *et al.* (1998b). A prokaryotic-like mode of cytoplasmic eukaryotic ribosome binding to the initiation codon during internal translation initiation of hepatitis C and classical swine fever virus RNAs. Genes & Development **12**(1): 67-83.

Pestova, TV *et al.* (2000). The joining of ribosomal subunits in eukaryotes requires eIF5B. Nature **403**(6767): 332-335.

Pilipenko, EV *et al.* (1989). Conservation of the secondary structure elements of the 5'-untranslated region of cardiovirus and aphthovirus RNAs. Nucleic Acids Research **17**(14): 5701-5711.

Pilipenko, EV *et al.* (2000). A cell cycle-dependent protein serves as a template-specific translation initiation factor. Genes & Development **14**(16): 2028-2045.

Pooggin, MM *et al.* (2001). Ribosome shunt is essential for infectivity of cauliflower mosaic virus. Proceedings of the National Academy of Sciences of the United States of America **98**(3): 886-891.

Poyry, TA *et al.* (2001). Construction of regulatable picornavirus IRESes as a test of current models of the mechanism of internal translation initiation. RNA **7**(5): 647-660.

Pyronnet, S *et al.* (1999). Human eukaryotic translation initiation factor 4G (eIF4G) recruits Mnk1 to phosphorylate eIF4E. EMBO Journal **18**(1): 270-279.

Pyronnet, S *et al.* (2000). A cell cycle-dependent internal ribosome entry site. Molecular Cell **5**(4): 607-616.

RajBhandary, UL (2000). More surprises in translation: Initiation without the initiator tRNA. Proceedings of the National Academy of Sciences of the United States of America **97**(4): 1325-1327.

Ramos, R & Martinez-Salas, E (1999). Long-range RNA interactions between structural domains of the aphthovirus internal ribosome entry site (IRES). RNA **5**(10): 1374-1383.

Reynolds, JE *et al.* (1995). Unique features of internal initiation of hepatitis-C virus-RNA translation. EMBO Journal **14**(23): 6010-6020.

Reynolds, JE *et al.* (1996). Internal initiation of translation of hepatitis C virus RNA: The ribosome entry site is at the authentic initiation codon. RNA **2**(9): 867-878.

Richter-Cook, NJ *et al.* (1998). Purification and characterization of a new eukaryotic protein translation factor - Eukaryotic initiation factor 4H. Journal of Biological Chemistry **273**(13): 7579-7587.

Rieder, E *et al.* (2000). Genetic and biochemical studies of poliovirus *cis*-acting replication element cre in relation to VPg uridylylation. Journal of Virology **74**(22): 10371-10380.

Rijnbrand, R *et al.* (1995). Almost the entire 5' non-translated region of hepatitis-C virus is required for cap-independent translation. FEBS Letters **365**(2-3): 115-119.

Rijnbrand, R *et al.* (2001). The influence of downstream protein-coding sequence on internal ribosome entry on hepatitis C virus and other flavivirus RNAs. RNA **7**(4): 585-597.

Roberts, LO & Belsham, GJ (1997). Complementation of defective picornavirus internal ribosome entry site (IRES) elements by the coexpression of fragments of the IRES. Virology **227**(1): 53-62.

Roberts, LO *et al.* (1998). Recognition of picornavirus internal ribosome entry sites within cells; influence of cellular and viral proteins. RNA **4**(5): 520-529.

Roberts, LO *et al.* (2000). Caspases are not involved in the cleavage of translation initiation factor elF4GI during picornavirus infection. Journal of General Virology **81**: 1703-1707.

Robertson, ME (1999). Structure-function analysis of a picornavirus IRES element. Thesis (Ph.D.)-University of Dundee.

Robertson, ME *et al.* (1999). A selection system for functional internal ribosome entry site (IRES) elements: Analysis of the requirement for a conserved GNRA tetraloop in the encephalomyocarditis virus IRES. RNA **5**(9): 1167-1179.

Rogers, GW *et al.* (1999). Biochemical and kinetic characterization of the RNA helicase activity of eukaryotic initiation factor 4A. Journal of Biological Chemistry **274**(18): 12236-12244.

Rohll, JB *et al.* (1995). The 3'-untranslated region of picornavirus RNA - features required for efficient genome replication. Journal of Virology **69**(12): 7835-7844.

Roll-Mecak, A *et al.* (2001). Engaging the ribosome: universal IFs of translation. Trends in Biochemical Sciences **26**(12): 705-709.

Rossmann, MG *et al.* (1985). Structure of a human common cold virus and functional-relationship to other picornaviruses. Nature **317**(6033): 145-153.

Rowe, A *et al.* (2000). Coding changes in the poliovirus protease 2A compensate for 5 ' NCR domain V disruptions in a cell-specific manner. Virology **269**(2): 284-293.

Rozen, F *et al.* (1990). Bidirectional RNA helicase activity of eukaryotic translation initiation factor-4A and factor-4F. Molecular and Cellular Biology **10**(3): 1134-1144.

Rust, RC *et al.* (2001). Cellular COPII proteins are involved in production of the vesicles that form the poliovirus replication complex. Journal of Virology **75**(20): 9808-9818.

Sachs, AB & Davis, RW (1989). The poly(A) binding-protein is required for poly(A) shortening and 60S ribosomal subunit-dependent translation initiation. Cell **58**(5): 857-867.

Sakoda, Y *et al.* (2001). An attenuating mutation in the 2A protease of swine vesicular disease virus, a picornavirus, regulates cap- and internal ribosome entry site-dependent protein synthesis. Journal of Virology **75**(22): 10643-10650.

Saleh, L *et al.* (2001). Functional interaction of translation initiation factor eIF4G with the foot-and-mouth disease virus internal ribosome entry site Journal of General Virology **82**: 757-763.

Sanger, F *et al.* (1977). DNA sequencing with chain-terminating inhibitors. Proceedings of the National Academy of Sciences of the United States of America **74**(12): 5463-5467.

Sangar, DV *et al.* (1987). All foot-and-mouth-disease virus serotypes initiate protein-synthesis at 2 separate AUGs. Nucleic Acids Research **15**(8): 3305-3315.

Sarnow, P *et al.* (1986). A poliovirus temperature-sensitive RNA-synthesis mutant located in a noncoding region of the genome. Proceedings of the National Academy of Sciences of the United States of America **83**(3): 571-575.

Sarnow, P (1989a). Role of 3'-end sequences in infectivity of poliovirus transcripts made *in vitro*. Journal of Virology **63**(1): 467-470.

Sarnow, P (1989b). Translation of glucose-regulated protein-78-immunoglobulin heavy-chain binding-protein messenger-RNA is increased in poliovirus-infected cells at a time when cap-dependent translation of cellular messenger-RNAs is inhibited. Proceedings of the National Academy of Sciences of the United States of America **86**(15): 5795-5799

Sasaki, J & Nakashima, N (1999). Translation initiation at the CUU codon is mediated by the internal ribosome entry site of an insect picorna-like virus *in vitro*. Journal of Virology **73**(2): 1219-1226.

Sasaki, J & Nakashima, N (2000). Methionine-independent initiation of translation in the capsid protein of an insect RNA virus. Proceedings of the National Academy of Sciences of the United States of America **97**(4): 1512-1515.

Schneider, RJ (1995). Cap-independent translation in adenovirus infected cells. Current Topics in Microbiology and Immunology. **203:** 117-129.

Schneider, RJ (2000). Adenovirus inhibition of cellular protein synthesis and preferential translation of viral mRNAs. Translational control of gene expression. Sonenberg, N *et al.* (ed.) Cold Spring harbor, N. Y., Cold Spring Harbor Laboratory Press: 901-914

Schultheiss, T *et al.* (1995). Polyprotein processing in echovirus 22: A first assessment. Biochemical and Biophysical Research Communications **217**(3): 1120-1127.

Sella, O *et al.* (1999). Differentiation-induced internal translation of c-sis mRNA: Analysis of the *cis* elements and their differentiation-linked binding to the hnRNP C protein. Molecular and Cellular Biology **19**(8): 5429-5440.

Selmer, M *et al.* (1999). Crystal structure of *Thermotoga maritima* ribosome recycling factor: A tRNA mimic. Science **286**(5448): 2349-2352.

Shafren, DR *et al.* (1997). Coxsackievirus A21 binds to decay-accelerating factor but requires intercellular adhesion molecule 1 for cell entry. Journal of Virology **71**(6): 4736-4743.

Shaughnessy, JD *et al.* (1997). cDNA cloning, expression analysis, and chromosomal localization of a gene with high homology to wheat eIF-(iso)4F and mammalian eIF-4G Genomics **39**(2): 192-197.

Shiroki, K *et al.* (1999). Intracellular redistribution of truncated La protein produced by poliovirus 3C(pro)-mediated cleavage. Journal of Virology **73**(3): 2193-2200.

Singh, LP *et al.* (1994). Phosphorylation of the guanine-nucleotide exchange factor and eukaryotic initiation-factor-2 by casein kinase-ii regulates guanine-nucleotide-binding and GDP/GTP exchange. Biochemistry **33**(31): 9152-9157.

Sizova, DV *et al.* (1998). Specific interaction of eukaryotic translation initiation factor 3 with the 5 ' nontranslated regions of hepatitis C virus and classical swine fever virus RNAs. Journal of Virology **72**(6): 4775-4782.

Sonenberg, N (1996). mRNA 5' cap-binding protein eIF4E and control of cell growth. Transcriptional control. Hershey, J et al. (ed.) Cold Spring Harbor, N. Y., Cold Spring Harbor Laboratory Press: 249-269.

Song, HW *et al.* (2000). The crystal structure of human eukaryotic release factor eRF1 - Mechanism of stop codon recognition and peptidyl-tRNA hydrolysis. Cell **100**(3): 311-321.

Spahn, CM *et al.* (2001a). Hepatitis C virus IRES RNA-induced changes in the conformation of the 40S ribosomal subunit. Science **291**(5510): 1959-1962.

Spahn, CM *et al.* (2001b). Structure of the 80S ribosome *from Saccharomyces cerevisiae* - tRNA-ribosome and subunit-subunit interactions. Cell **107**(3): 373-386.

Spector, DH & Baltimore, D (1974). Requirement of the 3'-terminal poly (adenylic acid) for the infectivity of poliovirus RNA. Proceedings of the National Academy of Sciences of the United States of America **71**: 2983.

Stark, H *et al.* (1997a). Arrangement of tRNAs in pre- and posttranslocational ribosomes revealed by electron cryomicroscopy. Cell **88**(1): 19-28.

Stark, H., M. V. Rodnina, *et al.* (1997b). Visualization of elongation factor Tu on the *Escherichia coli* ribosome. Nature **389**(6649): 403-406.

Stassinopoulos, IA (2000). Interactions of picornavirus internal ribosome entry sites with cellular proteins. Thesis (Ph.D.) - University of Sussex

Stassinopoulos, IA & Belsham, GJ (2001). A novel protein-RNA binding assay: Functional interactions of the foot-and-mouth disease virus internal ribosome entry site with cellular proteins. RNA **7**(1): 114-122.

Staunton, DE *et al.* (1989). A cell-adhesion molecule, ICAM-1, is the major surface-receptor for rhinoviruses. Cell **56**(5): 849-853.

Stein, I *et al.* (1998). Translation of vascular endothelial growth factor mRNA by internal ribosome entry: Implications for translation under hypoxia. Molecular and Cellular Biology **18**(6): 3112-3119.

Stone, DM *et al.* (1993). *Trans* complementation of cap-independent translation directed by poliovirus 5' noncoding region deletion mutants - evidence for RNA-RNA interactions. Journal of Virology **67**(10): 6215-6223.

Stoneley, M*et al.* (1998). c-myc 5 'untranslated region contains an internal ribosome entry segment. Oncogene **16**(3): 423-428.

Stoneley, M *et al.* (2000a). Analysis of the c-myc IRES; a potential role for cell-type specific trans-acting factors and the nuclear compartment. Nucleic Acids Research **28**(3): 687-694.

Stoneley, M *et al.* (2000b). c-myc protein synthesis is initiated from the internal ribosome entry segment during apoptosis. Molecular and Cellular Biology **20**(4): 1162-1169.

Suhy, DA *et al.* (2000). Remodeling the endoplasmic reticulum by poliovirus infection and by individual viral proteins: an autophagy-like origin for virus-induced vesicles. Journal of Virology **74**(19): 8953-8965.

Svitkin, YV *et al.* (1994). Internal translation initiation on poliovirus RNA - Further characterization of La function in poliovirus translation *in-vitro*. Journal of Virology **68**(3): 1544-1550.

Svitkin, YV *et al.* (2001a). The requirement for eukaryotic initiation factor 4A (eIF4A) in translation is in direct proportion to the degree of mRNA 5 ' secondary structure. RNA **7**(3): 382-394.

Svitkin, YV *et al.* (2001b). Poly(A)-binding protein interactions with eIF4G stimulates picornavirus IRES-dependent translations. RNA **7**(12): 1743-1752.

Tan, RY & Frankel, AD (1998). A novel glutamine-RNA interaction identified by screening libraries in mammalian cells. Proceedings of the National Academy of Sciences of the United States of America **95**(8): 4247-4252.

Tarun, SZ & Sachs, AB (1995). A common function for messenger-RNA-5' and messenger-RNA-3' ends in translation initiation in yeast. Genes & Development **9**(23): 2997-3007.

Teterina, NL *et al.* (1997). Induction of intracellular membrane rearrangements by HAV proteins 2C and 2BC. Virology **237**(1): 66-77.

Thomas, A *et al.* (1980). Mode of action of protein synthesis initiation factor eIF-1 from rabbit reticulocytes. FEBS Letters **116**(1): 67-71.

Tolskaya, EA *et al.* (1995). Apoptosis-inducing and apoptosis-preventing functions of poliovirus. Journal of Virology **69**(2): 1181-1189.

Toyoda, HM *et al.* (1986). A 2nd virus-encoded proteinase involved in proteolytic processing of poliovirus polyprotein. Cell **45**(5): 761-770.

van der Velden, A *et al.* (1995). Defective point mutants of the encephalomyocarditis virus internal ribosome entry site can be complemented in *trans*. Virology **214**(1): 82-90.

Venkatesan, A & Dasgupta, A (2001). Novel fluorescence-based screen to identify small synthetic internal ribosome entry site elements. Molecular and Cellular Biology **21**(8): 2826-2837.

Vestergaard, B *et al.* (2001). Bacterial polypeptide release factor RF2 is structurally distinct from eukaryotic eRF1. Molecular Cell **8**(6): 1375-1382.

von der Haar, T *et al.* (2000). Stabilization of eukaryotic initiation factor 4E binding to the mRNA 5 '-cap by domains of eIF4G. Journal of Biological Chemistry **275**(39): 30551-30555.

Walter, BL *et al.* (1999). Differential utilization of poly(rC) binding protein 2 in translation directed by picornavirus IRES elements. RNA **5**(12): 1570-1585.

Wang, CY *et al.* (1993). Translation of human hepatitis-C virus-RNA in cultured-cells is mediated by an internal ribosome-binding mechanism. Journal of Virology **67**(6): 3338-3344.

Wang, CY *et al.* (1995). An RNA pseudoknot Is an essential structural element of the internal ribosome entry site located within the hepatitis-C virus 5'-noncoding region. RNA **1**(5): 526-537.

Waskiewicz, AJ *et al.* (1999). Phosphorylation of the cap-binding protein eukaryotic translation initiation factor 4E by protein kinase Mnk1 *in vivo*. Molecular and Cellular Biology **19**(3): 1871-1880.

Welch, EM *et al.* (2000). Translation termination: it's not the end of the story. Translational control of gene expression. Sonenberg, N *et al.* (ed.) Cold Spring Harbor, N. Y., Cold Spring Harbor Laboratory Press: 467-486

Wells, SE, *et al.* (1998). Circularization of mRNA by eukaryotic translation initiation factors. Molecular Cell **2**(1): 135-140.

Welsh, GI & Proud, CG (1993). Glycogen-synthase kinase-3 is rapidly inactivated in response to insulin and phosphorylates eukaryotic initiation-factor eIF-2B. Biochemical Journal **294**: 625-629.

Weng, YM *et al.* (1996a). Genetic and biochemical characterization of mutations in the ATPase and helicase regions of the Upf1 protein. Molecular and Cellular Biology **16**(10): 5477-5490.

Weng, YM *et al.* (1996b). Identification and characterization of mutations in the UPF1 gene that affect nonsense suppression and the formation of the Upf protein complex but not mRNA turnover. Molecular and Cellular Biology **16**(10): 5491-5506.

Whetter, LE *et al.* (1994). Low efficiency of the 5' nontranslated region of hepatitis-A virus-RNA in directing cap-independent translation in permissive monkey kidney-cells. Journal of Virology **68**(8): 5253-5263.

Wilson, JE *et al.* (2000a). Naturally occurring dicistronic cricket paralysis virus RNA is regulated by two internal ribosome entry sites. Molecular and Cellular Biology **20**(14): 4990-4999.

Wilson, JE *et al.* (2000b). Initiation of protein synthesis from the A site of the ribosome. Cell **102**(4): 511-520.

Woolaway, KE *et al.* (2001). The 5 ' untranslated region of *Rhopalosiphum padi* virus contains an internal ribosome entry site which functions efficiently in mammalian, plant, and insect translation systems. Journal of Virology **75**(21): 10244-10249.

Xiang, WK *et al.* (1995). Interaction between the 5'-terminal cloverleaf and 3AB/3CD(pro) of poliovirus Is essential for RNA replication. Journal of Virology **69**(6): 3658-3667.

Yalamanchili, P *et al.* (1997). Inhibition of host cell transcription by poliovirus: Cleavage of transcription factor CREB by poliovirus-encoded protease 3C(pro). Journal of Virology **71**(2): 1220-1226.

Yamanaka, S *et al.* (1997). A novel translational repressor mRNA is edited extensively in livers containing tumors caused by the transgene expression of the apoB mRNA-editing enzyme. Genes & Development **11**(3): 321-333.

Yamashita, T *et al.* (1998). Complete nucleotide sequence and genetic organization of Aichi virus, a distinct member of the *Picornaviridae* associated with acute gastroenteritis in humans. Journal of Virology **72**(10): 8408-8412.

Yan, RQ *et al.* (1992). Amino-acid-sequence of the human protein-synthesis initiation factor eIF-4-gamma. Journal of Biological Chemistry **267**(32): 23226-23231.

Yanagi, M *et al.* (1997). Transcripts from a single full-length cDNA clone of hepatitis C virus are infectious when directly transfected into the liver of a chimpanzee. Proceedings of the National Academy of Sciences of the United States of America **94**(16): 8738-8743.

Yang, Q & Sarnow, P (1997). Location of the internal ribosome entry site in the 5' non-coding region of the immunoglobulin heavy-chain binding protein (BiP) mRNA: Evidence for specific RNA-protein interactions. Nucleic Acids Research **25**(14): 2800-2807.

Yueh, A & Schneider, RJ (1996). Selective translation initiation by ribosome jumping in adenovirus-infected and heat-shocked cells. Genes & Development **10**(12): 1557-1567.

Yueh, A & Schneider, RJ (2000). Translation by ribosome shunting on adenovirus and hsp70 mRNAs facilitated by complementarity to 18S rRNA. Genes & Development **14**(4): 414-421.

Yusupov, MM *et al.* (2001). Crystal structure of the ribosome at 5.5 angstrom resolution. Science **292**(5518): 883-896.

Zamora, M *et al.* (2002). Multiple eIF4GI-specific protease activities present in uninfected and poliovirus-infected cells. Journal of Virology **76**(1): 165-177.

Zavialov, AV *et al.* (2001). A posttermination ribosomal complex is the guanine nucleotide exchange factor for peptide release factor RF3. Cell **107**(1): 115-124.

Zhang, Y *et al.* (1994). A late adenovirus factor induces eIF-4E dephosphorylation and inhibition of cell protein-synthesis. Journal of Virology **68**(11): 7040-7050.

Zhang, G *et al.* (1999). Molecular evolution of swine vesicular disease virus. Journal of General Virology **80**: 639-651.

Zuker, M., D. H. Mathews, *et al.* (1999). Algorithms and thermodynamics for RNA secondary structure prediction: a practical guide. RNA Biochemistry and Biotechnology. J. Barciszewski and B. F. C. Clark. Kluwer, NATO ASI Series, Kluwer Academic Publishers: 11-43.